ISSN 1007-9327 (print)
ISSN 2219-2840 (online)

World Journal of *Gastroenterology*

World J Gastroenterol 2021 September 28; 27(36): 5989-6160

Published by Baishideng Publishing Group Inc

World Journal of Gastroenterology

Contents

Weekly Volume 27 Number 36 September 28, 2021

FRONTIER

REVIEW

MINIREVIEWS

ORIGINAL ARTICLE

Basic Study

Case Control Study

Retrospective Study

World Journal of Gastroenterology

Weekly Volume 27 Number 36 September 28, 2021

Contents

ABOUT COVER

Editorial Board Member of *World Journal of Gastroenterology*, Mark D Gorrell, BSc, PhD, Professor of Liver Science, Head, Liver Enzymes in Metabolism and Inflammation Program, Centenary Institute, Faculty of Medicine and Health, The University of Sydney, New South Wales 2006, Australia. m.gorrell@centenary.org.au

AIMS AND SCOPE

The primary aim of *World Journal of Gastroenterology* (*WJG*, *World J Gastroenterol*) is to provide scholars and readers from various fields of gastroenterology and hepatology with a platform to publish high-quality basic and clinical research articles and communicate their research findings online. *WJG* mainly publishes articles reporting research results and findings obtained in the field of gastroenterology and hepatology and covering a wide range of topics including gastroenterology, hepatology, gastrointestinal endoscopy, gastrointestinal surgery, gastrointestinal oncology, and pediatric gastroenterology.

INDEXING/ABSTRACTING

The *WJG* is now indexed in Current Contents®/Clinical Medicine, Science Citation Index Expanded (also known as SciSearch®), Journal Citation Reports®, Index Medicus, MEDLINE, PubMed, PubMed Central, and Scopus. The 2021 edition of Journal Citation Report® cites the 2020 impact factor (IF) for *WJG* as 5.742; Journal Citation Indicator: 0.79; IF without journal self cites: 5.590; 5-year IF: 5.044; Ranking: 28 among 92 journals in gastroenterology and hepatology; and Quartile category: Q2. The *WJG*'s CiteScore for 2020 is 6.9 and Scopus CiteScore rank 2020: Gastroenterology is 19/136.

RESPONSIBLE EDITORS FOR THIS ISSUE

Production Editor: *Jia-Hui Li*; **Production Department Director:** *Yu-Jie Ma*; **Editorial Office Director:** *Ze-Mao Gong*.

NAME OF JOURNAL
World Journal of Gastroenterology

ISSN
ISSN 1007-9327 (print) ISSN 2219-2840 (online)

LAUNCH DATE
October 1, 1995

FREQUENCY
Weekly

EDITORS-IN-CHIEF
Andrzej S Tarnawski, Subrata Ghosh

EDITORIAL BOARD MEMBERS
http://www.wjgnet.com/1007-9327/editorialboard.htm

PUBLICATION DATE
September 28, 2021

INSTRUCTIONS TO AUTHORS
https://www.wjgnet.com/bpg/gerinfo/204

GUIDELINES FOR ETHICS DOCUMENTS
https://www.wjgnet.com/bpg/GerInfo/287

GUIDELINES FOR NON-NATIVE SPEAKERS OF ENGLISH
https://www.wjgnet.com/bpg/gerinfo/240

PUBLICATION ETHICS
https://www.wjgnet.com/bpg/GerInfo/288

PUBLICATION MISCONDUCT
https://www.wjgnet.com/bpg/gerinfo/208

ARTICLE PROCESSING CHARGE
https://www.wjgnet.com/bpg/gerinfo/242

STEPS FOR SUBMITTING MANUSCRIPTS
https://www.wjgnet.com/bpg/GerInfo/239

ONLINE SUBMISSION
https://www.f6publishing.com

World Journal of Gastroenterology

Submit a Manuscript: https://www.f6publishing.com

World J Gastroenterol 2021 September 28; 27(36): 5989-6003

DOI: 10.3748/wjg.v27.i36.5989

ISSN 1007-9327 (print) ISSN 2219-2840 (online)

FRONTIER

Fluorescent cholangiography: An up-to-date overview twelve years after the first clinical application

Antonio Pesce, Gaetano Piccolo, Francesca Lecchi, Nicolò Fabbri, Michele Diana, Carlo Vittorio Feo

ORCID number: Antonio Pesce 0000-0002-7560-551X; Gaetano Piccolo 0000-0002-4942-7705; Francesca Lecchi 0000-0002-7568-4967; Nicolò Fabbri 0000-0001-7039-3717; Michele Diana 0000-0002-1390-8486; Carlo Vittorio Feo 0000-0003-0699-5689.

Author contributions: Pesce A and Piccolo G designed the research; Pesce A, Piccolo G, Fabbri N, and Lecchi F researched and wrote the manuscript; Diana M and Feo CV supervised the paper; all authors have read and approved the final manuscript.

Conflict-of-interest statement: The corresponding author declares that the manuscript has been submitted on behalf of all authors. All authors declare that they have no competing interests.

Antonio Pesce, Nicolò Fabbri, Carlo Vittorio Feo, Department of Surgery, Section of General Surgery, Ospedale del Delta, Azienda USL of Ferrara, University of Ferrara, Ferrara 44023, Italy

Gaetano Piccolo, Francesca Lecchi, Department of Health Sciences, University of Milan, Unit of Hepato-Bilio-Pancreatic and Digestive Surgery, San Paolo Hospital, Milano 20142, Italy

Michele Diana, Department of General, Digestive and Endocrine Surgery, University Hospital of Strasbourg, IRCAD, Research Institute Against Digestive Cancer, ICUBE lab, PHOTONICS for Health, University of Strasbourg, Strasbourg Cedex F-67091, France

Corresponding author: Antonio Pesce, MD, PhD, Research Fellow, Surgeon, Department of Surgery, Section of General Surgery, Ospedale del Delta, Azienda USL of Ferrara, University of Ferrara, Via Valle Oppio 2, Lagosanto (FE), Ferrara 44023, Italy. antonio.pesce@ausl.fe.it

Abstract

Laparoscopic cholecystectomy (LC) is one of the most frequently performed gastrointestinal surgeries worldwide. Bile duct injury (BDI) represents the most serious complication of LC, with an incidence of 0.3%-0.7%, resulting in significant perioperative morbidity and mortality, impaired quality of life, and high rates of subsequent medico-legal litigation. In most cases, the primary cause of BDI is the misinterpretation of biliary anatomy, leading to unexpected biliary lesions. Near-infrared fluorescent cholangiography is widely spreading in clinical practice to delineate biliary anatomy during LC in elective and emergency settings. The primary aim of this article was to perform an up-to-date overview of the evolution of this method 12 years after the first clinical application in 2009 and to highlight all advantages and current limitations according to the available scientific evidence.

Key Words: Laparoscopic cholecystectomy; Bile duct injury; Biliary anatomy; Fluorescent cholangiography; Indocyanine green

Core Tip: Fluorescence image-guided surgery is one of the most recent innovations in

Manuscript source: Invited manuscript

Specialty type: Gastroenterology and hepatology

Country/Territory of origin: Italy

Peer-review report's scientific quality classification

Grade A (Excellent): 0
Grade B (Very good): B, B, B, B
Grade C (Good): 0
Grade D (Fair): 0
Grade E (Poor): 0

Received: April 15, 2021
Peer-review started: April 15, 2021
First decision: July 1, 2021
Revised: July 10, 2021
Accepted: August 30, 2021
Article in press: August 30, 2021
Published online: September 28, 2021

P-Reviewer: Ghannam WM, Grosek J, Komatsu S, Wang SY
S-Editor: Wang LL
L-Editor: A
P-Editor: Xing YX

laparoscopic and robotic surgery. The visualization of biliary anatomy using fluorescence during surgery is becoming one of the most promising frontier approaches in minimally invasive surgery. This novel method is a powerful tool to detect biliary variants that could guide surgeons during dissection to prevent major bile duct lesions, and it has enormous potential to be considered the gold standard during all cholecystectomies. The up-to-date overview of this method confirms the efficacy of indocyanine green fluorescence cholangiography in detecting biliary anatomy, its importance as a teaching tool for young surgeons, and the effects on the reduction of conversion rate and bile duct injury, even if further considerable research remains necessary to optimize its use.

Citation: Pesce A, Piccolo G, Lecchi F, Fabbri N, Diana M, Feo CV. Fluorescent cholangiography: An up-to-date overview twelve years after the first clinical application. *World J Gastroenterol* 2021; 27(36): 5989-6003
URL: https://www.wjgnet.com/1007-9327/full/v27/i36/5989.htm
DOI: https://dx.doi.org/10.3748/wjg.v27.i36.5989

INTRODUCTION

Laparoscopic cholecystectomy (LC) is one of the most frequently performed gastrointestinal surgeries worldwide. Bile duct injury (BDI) represents the most serious complication of LC, with an incidence of 0.3% to 0.7%, resulting in significant perioperative morbidity and mortality, impaired quality of life, and high rates of subsequent medico-legal litigation[1,2]. In most cases, the primary cause of BDI is the misinterpretation of biliary anatomy, leading surgeons to unexpected biliary lesions (71%-97% of all cases)[3,4]. Various methods have been proposed and used to prevent iatrogenic biliary tract lesions[4]. Among them, near-infrared fluorescent cholangiography (NIRF-C) is widely spreading in clinical practice to delineate biliary anatomy during LC in elective and emergency settings. It is becoming one of the most popular and promising clinical applications in minimally invasive surgery[5,6]. In 2006, Stiles BM *et al*[7] first proposed fluorescent cholangiography in a mouse model by exploiting the unique auto fluorescent properties of bile for the intraoperative identification of the biliary anatomy in mice. The first application in humans was performed and described by *Ishizawa et al*[8] a few years later (2009). This classical method involves the intravenous injection of indocyanine green (ICG) dye before surgery. ICG binds to plasma proteins, with albumin as the principal carrier (95%), and is eliminated exclusively by the liver. The excitation of ICG by means of near-infrared light causes fluorescence, thereby delineating the anatomy of the biliary elements in real time. This innovative method was introduced as a means to prevent bile duct injuries during LC due to a better visualization of biliary anatomy during dissection. In 2015, we performed a systematic review of available studies by analyzing the efficacy of the novel technique in detecting bile duct structures during surgery. Detection rates of the biliary anatomy in 590 pooled patients were as follows: Cystic duct (CD) 96.2% (94.7%-97.7%), common hepatic duct (CHD) 78.1% (74.8%-81.4%), CD-CHD junction 72.0% (69.0%-75.0%), and common bile duct (CBD) 86.0% (83.3%-88.8%)[9]. Overall, these preliminary studies indicated that ICG fluorescence cholangiography is highly sensitive for the detection of extrahepatic biliary anatomy and may facilitate the prevention of bile duct injuries. Over the years, several single-center experiences from different countries[10-12] have been published regarding the usefulness of ICG fluorescence cholangiography in detecting biliary anatomy and analyzing patient outcomes after LC. The level of scientific evidence on ICG fluorescence cholangiography remains low. However, recent studies have significantly propelled the literature forward.

The primary aim of this article was to perform an up-to-date overview of the evolution of this method 12 years after its first clinical application and to highlight all the advantages and current limitations according to the available scientific literature.

TECHNIQUES

ICG administration can be performed in two different ways. The classical method described by Ishizawa T *et al*[8] in 2009 consists of the intravenous injection of ICG 30 min before surgery. Biliary visualization should be obtained prior to any dissection, during the dissection of the hepatocystic triangle, and after complete dissection according to the critical view of safety (CVS) method[13,14].This approach enables surgeons to check the biliary anatomy intraoperatively at any time. Recently, Dip F *et al*[15] summarized 10 important steps for the correct performance of fluorescent cholangiography during LC. The first two steps involve ICG intravenous administration and complete exposure of the hepatoduodenal ligament prior to any dissection. The primary objective of step 3 is the localization of the main biliary structures after the partial dissection of the hepatocystic triangle. Steps 4-7 are characterized by the identification of the CD, gallbladder-CD junction, CD-CHD junction, and CBD; step 8 is the identification of the cystic artery, in some cases by repeating ICG injection for fluorescent angiography to detect any anatomical arterial variations; step 9 is called "time-out", and it consists of the re-evaluation of the CVS before clipping and cutting any structures (as shown in Figures 1-2). After completing gallbladder removal, near-infrared (NIR) light should be turned on to identify any potential biliary leaks from the liver bed (step 10). At the current stage, there are two unresolved issues regarding NIRF-C, *i.e.*, the dose and the time required to obtain an optimal bile duct-to-liver fluorescence ratio >1. An elevated background liver signal may hinder the correct visualization of biliary anatomy. The dose and the time of administration of ICG are quite variable, as reported in the literature[16]. A recent study with data from the European Fluorescence Image-Guided Surgery (FIGS) registry[17] has shown a wide disparity in ICG dose and timing in NIRF-C across different European countries. Boogerd L *et al*[18] demonstrated that the highest bile duct-to-liver ratio was achieved 3 to 7 h after administration of 5 mg of ICG and 5 to 25 h after administration of 10 mg of ICG. Another study by Zarrinpar A *et al*[19] confirmed that a single dose of 0.25 mg/kg administered at least 45 min prior to visualization of the hepatocystic triangle facilitates intra-operative anatomical identification. Recently, Chen Q *et al*[20] demonstrated that the optimal effect of fluorescent cholangiography can be achieved by injecting 10 mg of ICG 10 to 12 h prior to surgery. Matsumura M *et al*[21] recommended the administration of 0.25 mg/kg ICG on the evening before surgery, as it may increase bile duct detectability in fluorescence cholangiography during LC. Based on our experience, we think that the administration of ICG 45 to 60 min before surgery is—from a logistical point of view - more practical since most patients are usually hospitalized on the same day as the surgical procedure. Indeed, the debate remains open, and a consensus conference may help the surgical community.

The direct injection of ICG into the gallbladder is a technique that allows overcoming the strong background signal in the liver. Liu YY *et al*[22] were the first to describe intracholecystic ICG administration during LC in a porcine model, proving the feasibility and usefulness of this technique to achieve adequate CVS. Few clinical studies of NIR cholecystocholangiography with direct ICG injection into the gallbladder were conducted, namely, two case reports, one case-control study, and a few prospective cohort studies, for a total of 80 patients, of whom 49 underwent surgery for symptomatic cholelithiasis and 31 for acute cholecystitis[22-26], as summarized in Table 1.

Liu YY *et al*[22] and Škrabec C *et al*[23] conducted the two widest studies, namely, a prospective cohort study of 46 patients and a case-control study including 20 patients, respectively. The authors described two different routes for intracholecystic ICG injection, *i.e.*, percutaneous transhepatic gallbladder drainage (trans-PTGBD) and intra-operative direct gallbladder puncture. A 1 mL amount of an ICG bile solution was used (ICG concentration = 0.025 mg/mL) made from a combination of 9 mL of bile mixed with 1 mL of a preparation of ICG and sterile water at a concentration of 0.25 mg/mL. NIR cholecystocholangiography with direct gallbladder injection was more successful in acute cholecystitis patients who underwent early or interval LC after the preliminary positioning of a PTGBD. Among all cases reported in the literature, only one patient required conversion to open cholecystectomy due to acute necrotic cholecystitis, which precluded safe laparoscopic dissection.

Intracholecystic ICG injection provides relevant advantages compared to intravenous NIR cholecystocholangiography, such as the real-time visualization of the biliary anatomy, including the gallbladder neck and Hartmann's pouch, which are safe landmarks to start the dissection. Additionally, the timing of ICG injection is irrelevant, and small dosages can be used.

Table 1 Cholecysto-cholangiography with direct intra-gallbladder indocyanine green injection

Ref.	Type of publication	No. of patients	No. of patients with gallbladder lithiasis	No. of patients with acute cholecystitis	Technique	Complication	Conversion to open surgery
Jao *et al* [26], 2020	Case series	2	0	2	2 trans-PTGBD cases	Lymphatic spillage	0
Nitta *et al* [24], 2020	Case report	1	0	1	1 case through DGBP	-	0
Škrabecet al [23], 2020	Case-controlled study	20	19	1	20 cases through DGBP	ICG bile leakage in 1 case; No progression of dye into the CD in 3 cases	1
Liu *et al* [22], 2017	Cohort study	46	21	25	18 trans-PTGBD cases; 28 cases through DGBP	ICG leakage in 5 cases	0
Graves *et al* [25], 2017	Cohort study	11	9	2	11 cases through DGBP	No progression of dye into the CD in 1 case	0

PTGBD: Percutaneous transhepatic gallbladder drainage; DGBP: Direct gallbladder puncture; ICG: Indocyanine green; CD: Cystic duct.

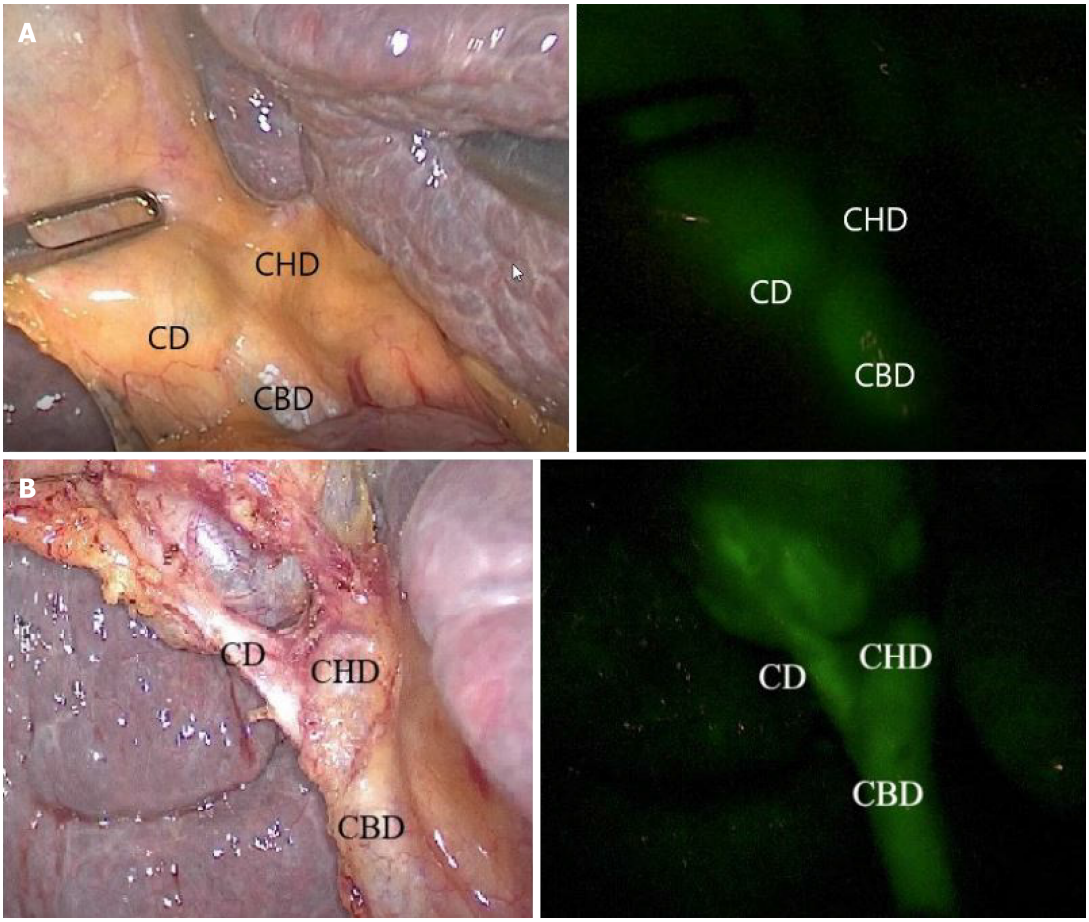

Figure 1 Intra-operative real-time identification of biliary structures in a cirrhotic patient, with visible light to the left and NIRF-C to the right. A: Pre-dissection visualization of biliary anatomy; B: After complete dissection. One can observe the posterior implantation of the cystic duct on the common hepatic duct. CD: Cystic duct; CHD: Common hepatic duct; CBD: Common bile duct.

The downside of direct ICG injection lies in the possibility of ICG bile leakage or lymph spillage during gallbladder dissection for acute cholecystitis, as ICG may enter through the necrotic gallbladder mucosa into the submucosal lymphatic drainage. In regard to the widest experiences reported in the literature[22,23], ICG bile leakage occurred in six patients in whom ICG was directly injected through a fine-needle puncture. Another limitation lies in the absence of progression of the dye into the CD

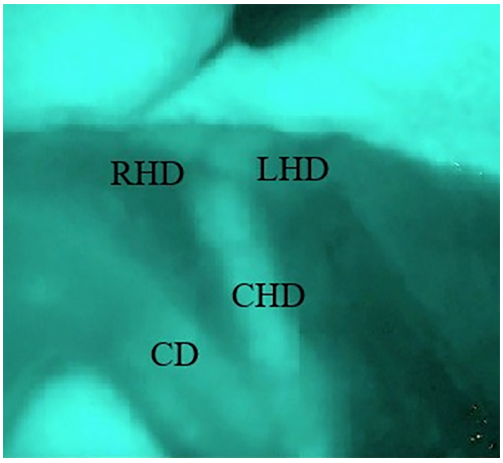

Figure 2 Classical extrahepatic biliary anatomy with identification of the right and left hepatic ducts using near-infrared fluorescent cholangiography. CD: Cystic duct; CHD: Common hepatic duct; RHD: Right hepatic duct; LHD: Left hepatic duct.

in cases of stone obstruction.

Based on the available data, we suggest that larger studies are necessary to validate the technique of intracholecystic ICG injection for NIR fluorescent cholangiography.

ICG FLUORESCENT CHOLANGIOGRAPHY IN PATIENTS WITH ACUTE CHOLECYSTITIS

Early LC is the gold standard treatment for patients with mild (grade I) and moderate (grade II) acute cholecystitis who have no response to initial (within 24 h) conservative treatment if performed within 72 h from the onset of symptoms according to 2018 Tokyo guidelines[27].

Fluorescent cholangiography may be very challenging in an emergency setting, when inflammation and adhesions at the hepatoduodenal ligament may impair the identification of biliary elements during dissection. Reaching the CVS may be particularly difficult in such situations[28].

In a recent meta-analysis, Dip F *et al*[29] suggested that using NIRF-C during elective cholecystectomy led to decreased BDI and conversion to open surgery compared to white light alone. However, there are limited data about its feasibility in an emergency setting. The identification of biliary structures may be challenging, especially in cases where there is an abundance of adhesions and severe inflammation of the gallbladder wall and surrounding tissues[9].

The literature contains four articles that provide data of patients who underwent LC for acute cholecystitis with NIR devices, *i.e.*, two cohort studies[30,31], one international European registry[17], and one randomized controlled trial (RCT)[32] are reported in Table 2.

In a large retrospective study involving 184 consecutive patients, Daskalaki E *et al* [31] reported the results of 24 patients who underwent robotic cholecystectomies (RCs) with ICG fluorescence for acute and gangrenous cholecystitis. The authors evaluated the detection rate of four biliary structures, *i.e.*, CD, CHD, CBD, and CD-CHD junction. In this subset of challenging surgical cases, the CD, CHD, CBD, and CD-CHD junction were successfully visualized in 91.6%, 79.1%, 79.1%, and 75% of cases, respectively.

Agnus V *et al*[17] reported data from the Euro-FIGS database, which enrolled 314 cases from 12 European surgical centers, including patients affected by symptomatic cholelithiasis (n = 248) and patients with acute cholecystitis (n = 58). A 5-point Likert scale was used to evaluate the quality of biliary anatomy visualization before and after the dissection of the hepatocystic triangle during LC with NIR devices. When the two groups (cholelithiasis *vs* acute cholecystitis) were compared, lower visualization quality scores were obtained in the CD group (2.76 ± 1.9 *vs* 3.54 ± 1.6, P = 0.001) and CD-CHD junction (2.43 ± 2 *vs* 3 ± 1.9, P = 0.04) before the preliminary dissection. The impact of variable inflammation on the visualization score of the biliary tree was also confirmed by means of multivariate linear regression analysis.

Table 2 Fluorescent cholangiography in patients with acute cholecystitis

Ref.	Type of publication	Procedure	No. of patients
Agnus *et al*[17], 2020	Euro-FIGS registry	LC	58
Dip *et al*[32], 2020	RCT	LC	44
Di Maggio *et al*[30], 2020	Prospective cohort study	LC	16
Daskalaki *et al*[31], 2014	Retrospective cohort study	RC	24
Yoshiya *et al*[33], 2019	Retrospective cohort study	LC after-PTGBD	130

FIGS: Fluorescence image-guided surgery; RCT: Randomized controlled trial; LC: Laparoscopic cholecystectomy; RC: Robotic cholecystectomy; PTGBD: Percutaneous transhepatic gallbladder drainage.

Similar data have been reported in a single-blinded randomized controlled trial[32] comparing the efficacy of NIR fluorescent cholangiography *vs* white light alone. The primary objective was the structure detection rate, defined as the total number of patients in whom a particular biliary structure was detected, both before and after dissection, in each study arm, divided by the total number of patients in each arm. The authors found that the degree of gallbladder inflammation was the most important variable, affecting the detection of CD and CBD before and after dissection, respectively, and of the CD-gallbladder junction only after dissection.

The usefulness of NIRF-C was also confirmed by Yoshiya S *et al*[33] during LC after PTGBD in patients with severe acute cholecystitis. The ICG fluorescence cholangiography group showed a significantly shorter operative time, a lower conversion rate, and a lower proportion of subtotal cholecystectomies[33].

NIR fluorescence cholangiography in emergency cholecystectomies is a safe and useful tool to prevent BDI during LC. However, the available data require further elaboration in randomized controlled studies in larger numbers of patients with acute cholecystitis undergoing LC with the aid of intra-operative fluorescent cholangiography.

DETECTION OF BILIARY VARIANTS USING ICG FLUORESCENCE

Various reports have underlined the importance of fluorescence image-guided cholecystectomy in detecting biliary variants. Fluorescent cholangiography allows the intraoperative identification of subvesical Luschka's ducts[34,35], aberrant bile ducts [36-38], anatomical CD variations[39], and gallbladder aberrations[40,41].

In specific studies, the diagnostic accuracy of NIRF-C in the evaluation of CD anatomy has been compared to that of magnetic resonance cholangiopancreatography (MRCP), which is the gold standard radiology diagnostic tool for the preoperative study of the biliary tree[42,43]. Pesce A *et al*[44] evaluated the ability of the two imaging methods to identify three selected features, namely, the insertion of CD, CD-CHD junction, and CD course. The level of insertion, course, and wall implantation of the CD were achieved by means of NIRF-C with diagnostic accuracy values of 65.2%, 78.3%, and 91.3%, respectively, in comparison with MRCP data.

In 2017, Diana M *et al*[45] prospectively evaluated the combination of three imaging modalities during robotic cholecystectomy, *i.e.*, virtual reality 3D modeling of MRCP, NIRF-C, and intraoperative cholangiogram (IOC). Surprisingly, expert hepatobiliary radiologists missed 5 out of 8 anatomical variants on preoperative MRCP, while surgeons were able to identify all variants through a virtual surgical exploration complemented with intraoperative fluorescent cholangiography.

In another observational study in 65 patients by Hiwatashi K *et al*[46], the authors found a statistically significant correlation between the delineation of CD using ICG cholangiography and preoperative MRCP.

Based on the current scientific literature (RCTs shown in Table 3), we strongly believe that NIRF-C is a useful tool to detect biliary variants that could guide surgeons during dissection to prevent any major bile duct lesions.

Table 3 Recruiting randomized controlled trials using indocyanine green fluorescence cholangiography

Study coordinator; NCT No.	Participating country	No. of patients	Period study	Published data	Main outcome	Controlled group	Dose indocyanine green	Dosing time	Conversion to open surgery	Bile duct injury
Dip *et al*[32]; NCT 02702843	United States	639	April 2016	*Ann Surg* 2020	Identification of biliary anatomy	White light	0.05 mg/kg	> 45 min prior to surgery	One patient for bleeding	No
Lehrskov *et al* [50]; NCT 02344654	Denmark	120	March 2015-August 2018	*Br J Surg* 2020	Visualization of the critical junction	Intraoperative cholangiogram	0.05 mg/kg	After intubation	No	No
van den Bos *et al*[61]; NCT 02558556	The Netherlands	308	January 2016	Ongoing	Time to achieve critical view of safety	White light	2.5 mg	After intubation	NA	NA
Koong *et al* [60] ; NCT04228835	Malaysia	63	March2017-July 2019	*Asian J Surg* 2021	Time to achieve critical view of safety	White light	2.5 mg	Before induction of anesthesia	No	No

NA: Not available.

FLUORESCENT CHOLANGIOGRAPHY *VS* STANDARD INTRAOPERATIVE CHOLANGIOGRAPHY

NIRF-C has been recognized as providing some advantages over conventional radiographic IOC, such as feasibility and safety, real-time visualization of biliary anatomy with safer dissection of the hepatocystic triangle, the lack of a learning curve, reduced X-ray exposure, and reduced costs and operative times[5,47-49]. In a Danish randomized controlled single-blind clinical trial[50], the authors compared NIRF-C *vs* IOC. They demonstrated that fluorescent cholangiography has the same capacity to identify the CVS, and is significantly faster and easier to perform than X-ray cholangiography[50]. In a recent meta-analysis by Lim SH *et al*[51], the authors concluded that there was no difference in the visualization of the CD, CBD, and CD-CBD junction using ICG fluorescence cholangiography compared to IOC. However, the ICG group reported increased rates of CHD visualization.

Dip F *et al*[52] analyzed medical costs and stated that the median cost of ICG fluorescence cholangiography was cheaper than that of IOC (13.97 ± 4.3 *vs* 778.43 ± 0.4 USD per patient, P = 0.0001).

Quaresima S *et al*[53] proposed that NIRF-C is a safe and effective procedure for the early recognition of anatomical biliary landmarks, with an important reduction in operative times compared to LC with intraoperative cholangiography.

In an article by Prevot F *et al*[54], the authors analyzed the ability to identify the CD, the CD-hepatic duct junction, and the CBD using fluorescence in comparison with standard IOC. The results of this study suggested that ICG fluorescence cholangiography is more effective than IOC in identifying the biliary tract after dissection.

In conclusion, we believe that there is considerable scientific evidence supporting the usefulness of NIRF-C with important advantages over conventional intraoperative cholangiography. NIRF-C represents a powerful real-time diagnostic tool for the detection of extrahepatic biliary anatomy during LC. Advantages and current limitations are summarized in Table 4.

FLUORESCENT CHOLANGIOGRAPHY IN OBESE PATIENTS

As reported in previous studies[9,31,55-57], the presence of dense adipose tissue surrounding the hepatocystic triangle may negatively affect the visualization of extrahepatic biliary tract using fluorescence. Obesity may represent a limitation of NIRF-C because NIR light has a penetration capability of only 5 to 10 mm[7-9]. In 2016, Dip F *et al*[58] conducted a prospective study to evaluate the accuracy of NIRF-C in obese *vs* non-obese patients. The results showed no difference in hepatic duct, CBD, or accessory duct detection rates between the two groups (P = 0.09, 0.16, and 0.66,

Table 4 Advantages and current limitations of fluorescent cholangiography in comparison to intraoperative cholangiogram and laparoscopic ultrasonography

Advantages	Limitations
Real-time visualization of biliary anatomy in elective and emergent settings	Limited in patients with specific conditions, such as overweight and obesity; it needs a preliminary dissection and exposure of the hepatocystic triangle
Safer dissection of the hepatocystic triangle	Limited scientific evidence in the setting of acute cholecystitis
Detection of biliary variants and biliary leaks	High variability about indocyanine green dose and dosing time
Implementing method in combination with adequate dissection and identification technique to achieve critical view of safety	Detection of bile duct stones
Feasibility and safety	Need for consensus conference and international guidelines
Reduced medical costs	
Time/faster	
Lack of X-ray exposure	
Simplicity and lack of learning curve	
Teaching tool for young surgeons	
Possibility to associate fluorescent angiography	
Strong potential to become a gold standard during all cholecystectomies	

respectively) before and after dissection of the hepatocystic triangle.

On the other hand, a German study[59] suggested that a BMI > 25 kg/m² and male sex significantly reduced the identification rate of CD before dissection of the hepatocystic triangle.

In a randomized controlled multicenter trial[32] comparing ICG *vs* white light alone, an increased BMI was associated with a reduced detection of most biliary structures in both groups, especially before dissection.

In general, our opinion is to use fluorescence to perform a complete dissection of the hepatocystic triangle in overweight and obese patients to obtain a good quality visualization of the biliary anatomy. In difficult cases where the surgeon is not able to clearly check the biliary anatomy, the surgeon should respect a sufficient thickness between the dissecting site and the main bile duct by working close to the gallbladder infundibulum to avoid unexpected biliary lesions. NIR imaging cannot be considered a substitute for good dissection and structure identification.

FLUORESCENT INCISIONLESS CHOLANGIOGRAPHY AS A TEACHING TOOL FOR YOUNG SURGEONS

It is well established that the risk of BDI correlates with the quality of the procedure performed, rather than the number of cases seen by the surgeon[1,2]. A clear identification of the biliary anatomy is crucial to perform a safe cholecystectomy and achieving CVS is now being taught as a key step of the operation to young surgeons[4,13]. In a recent randomized controlled trial[60], the time to achieve CVS from the gallbladder fundus retraction was measured by analyzing different levels of difficulty. The mean time, expressed in minutes, to achieve CVS was 22.3 ± 12.9 in the ICG-LC group (n = 30) and 22.8 ± 14.3 in the conventional LC group (P = 0.867). The authors concluded that fluorescent cholangiography may be a useful tool in difficult LC and in surgical training. A randomized controlled multicenter Dutch trial (FALCON trial) regarding the time to visualize CVS with NIRF-C compared to white light alone is still ongoing[61]. However, biliary structures are not always easily visualized laparoscopically. Fluorescence incisionless cholangiography may be a promising tool for training new surgeons in safe laparoscopic cholecystectomies by helping with biliary anatomy identification. To date, few studies have been conducted regarding the potential role of this technique in surgical training programs[62-64].

In 2016, Roy M *et al*[62] tested the ability of surgical students and residents to identify major biliary structures at NIR light. Participants were shown pictures taken at the same stage of hepatocystic triangle dissection in 10 cases of LC, first with NIR

light and then with Xenon white light. Both students and residents had a higher success rate of biliary tree identification with NIR fluorescence cholangiography. The authors also underlined the importance of NIRF-C to achieve appropriate intraoperative communication to guide residents, as it allows us to point out glowing structures in real time.

Similarly, in 2020, Rungsakulkij N *et al*[63] conducted a study to investigate the beneficial impact of fluorescence cholangiography on the ability of surgical residents to identify biliary structures. Participants were asked to identify the CD and artery, CBD and CHD in five LC videos, first without fluorescence, and then with NIRF-C. The results showed a higher misidentification rate among surgical residents in the without-FC modality than in the with-FC modality, proving the benefit of the technique among trainees.

In a study by Pesce A *et al*[47] on the usefulness of fluorescent cholangiography for biliary anatomy identification, surgical residents completed a survey on the perceived benefits of the technique. Responses were measured with a Likert scale. All participants agreed that NIRF-C facilitates the dissection of the hepatocystic triangle, hence being a useful adjuvant to training programs; 92% of respondents found the method easy to perform; 88% declared that it was effective in visualizing the biliary tree, and 84% found that the image quality was good. Consequently, residents consider the novel method a useful tool to visualize biliary anatomy and perform a safe dissection of the hepatocystic triangle, decreasing the risk of BDI.

From these experiences, it is safe to conclude that there is a large consensus regarding the beneficial role of NIRF-C in the training process of young surgeons. However, larger studies proving the benefits on the skills of surgical residents are required for the technique to be routinely performed in a teaching setting.

FLUORESCENT CHOLANGIOGRAPHY AND DETECTION OF BILIARY STONES

To date, there is no evidence that FC can effectively identify CBD stones by replacing IOC[64,65]. Intraoperative laparoscopic ultrasound (IOUS) could well represent a valid alternative to IOC in the detection of CBD stones[66,67]. Current limitations are related to the difficult learning curve and the lack of randomized controlled trials[66]. According to Daskalaki M *et al*[27], ICG fluorescence cholangiography can help to detect CD dilation and gallbladder stones (as shown in Figure 3), but it cannot rule out the presence of CBD stones. In a recent correspondence by Labil PL and Aroori S published in *Br J Surg*[65], the authors suggested performing an RCT comparing IOUS with X-ray and/or fluorescence cholangiography in LCto detect a difference in the rate of bile duct stone identification, as well as viewing the critical junction.

NIRF-C AND ROBOTIC CHOLECYSTECTOMY

Since the introduction of the robotic surgical platform in the 2000s, approximately 10% of all cholecystectomies are performed robotically[68] today. ICG technology was soon incorporated into the robotic platform, and the first case series involved patients who underwent single-incision or multiport robotic cholecystectomy (RC) with NIRF-C, as summarized in Table 5.

In a large retrospective cohort study including 184 patients, Daskalaki D *et al*[31] proved the feasibility of this technique. The four main biliary structures (CD, CHD, CD-CHD junction, CBD) were recognized using fluorescence imaging in 83% of cases. At least one structure was visualized in 99% of cases. Similar data have been reported by other authors[55,69-71].

Spinoglio G *et al*[70] showed that after dissection of the hepatocystic triangle, the visualization rates for each structure (CD, CHD, CD-CHD junction, CBD) increased to 97%. In addition, the rate of patients with two or three ducts visualized with NIR fluorescent cholangiography increased from 91% to 97% and from 86% to 95% before and after dissection, respectively.

In recent years, some authors compared data of patients who underwent robotic cholecystectomy with the use of ICG *vs* conventional LC[72,73]. In a retrospective cohort study, Sharma S *et al*[72] analyzed 287 consecutive cases, including 96 RCs and 191 LCs. The authors found a lower open conversion rate in the robotic cohort (2.1% *vs* 8.9% in LC), although this difference was not statistically significant.

Table 5 Studies reporting robotic cholecystectomy and near-infrared fluorescent cholangiography

Ref.	Type of publication	No. of patients	Technique	Incidence of conversion rate to open surgery (%)
Sharma *et al*[72], 2017	Retrospective cohort study	96	RC	2.1
Gangemi *et al*[73], 2017	Retrospective cohort study	676	RC	0.15
Maker *et al*[71], 2017	Cohort study	35	RC	NR
Daskalaki *et al*[31], 2014	Retrospective cohort study	184	RC	0.00
Spinoglio *et al*[70], 2013	Cohort study	45	SIRC	0.00
Buchs *et al*[55], 2013	Cohort study	23	SIRC	0.00
Buchs *et al*[69], 2012	Prospective cohort study	12	SIRC	0.00

RC: Robotic cholecystectomy; SIRC: Single-incision robotic cholecystectomy; NR: Not reported.

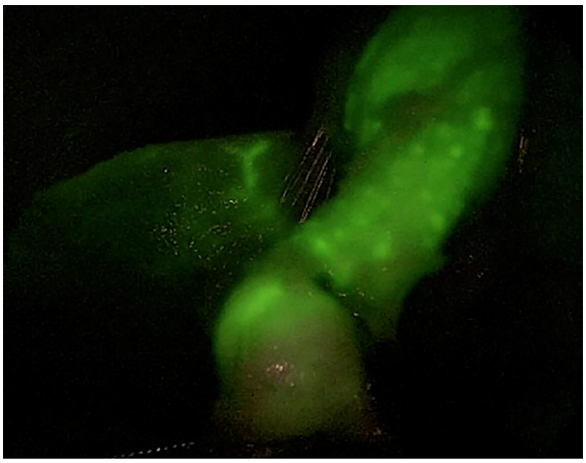

Figure 3 Identification of cystic duct stones by means of fluorescence.

Gangemi A *et al*[73] conducted a case-control study comparing the outcomes of ICG-aided RC *vs* LC at the University of Illinois (Chicago, United States). The authors reported a statistically significant difference between RC performed with the help of ICG and traditional LC in terms of the overall open conversion rate (0.15% *vs* 4.5%), open conversion rate in the acute setting (0.76% *vs* 9.57%), mean blood loss during surgery (14.37 mL *vs* 21.08 mL), and minor biliary injury rate (0.15% *vs* 1.04%). Additionally, a biliary tree anomaly was found in 2.07% of patients who underwent ICG-aided RC compared to 0.69% of patients who underwent LC with conventional intraoperative cholangiography.

Recently, Dip *et al*[29] conducted a meta-analysis evaluating whether NIFC with ICG could reduce conversion to open surgery and bile duct injuries during laparoscopic and robotic cholecystectomy. Patients who underwent ICG-aided RC showed a marked reduction in the rate of conversion to open surgery compared to RC without NIFC (weighted rate: 12/10.000 *vs* 322/10.000). Similar data were reported in the ICG-aided LC group (weighted rate: 23/10.000 *vs* 255/10.000). For BDI, a reduction was reported in the ICG-aided LC group compared to LC without NIFC (weighted rate: 23/10.000 *vs* 255/10.000), while no difference was noted regarding RC with and without NIFC. In conclusion, we believe that the use of NIRF-C may reduce the conversion rate in both minimally invasive procedures, laparoscopic and robotic cholecystectomy, while the reduction rate only exists in LC for BDI. However, further studies are required.

CONSENSUS CONFERENCES AND GUIDELINES

During the 4th International Congress of Fluorescence-Guided Surgery in Boca Raton, Florida in 2017, Dip F *et al*[74] conducted a pilot survey of 51 attending surgeons who

routinely performed laparoscopic cholecystectomies to identify their surgical practice and perceptions of intraoperative fluorescent cholangiography. Ten experts in ICG fluorescence-guided LC from North and South America, Europe, and Asia designed the survey for conference attendees. Seventy-eight percent of respondents underlined the importance for surgeons of having a noninvasive, simple, and reproducible diagnostic tool to identify the extrahepatic biliary anatomy in real time. In general, they recommended the routine use of NIRF-C during LC as a complimentary imaging technique, and 93.3% of them felt that the procedure would be useful in surgical training programs.

In a recent state-of-the-art consensus conference on the prevention of BDI during cholecystectomy published in *Annals of Surgery*[75], a pool of experts from five surgical societies (Society of Gastrointestinal and Endoscopic Surgeons, Americas Hepato-Pancreato-Biliary Association, International Hepato-Pancreato-Biliary Association, Society for Surgery of the Alimentary Tract, and European Association for Endoscopic Surgery) analyzed the scientific evidence among surgical practices to prevent bile duct injuries. At question 5B, *i.e.*, "Should intraoperative NIR biliary imaging with white light versus white light biliary imaging alone be used to limit the risk or severity of BDI during LC?", they answered the following question: We suggest that the use of NIR imaging may be considered an adjunct to white light alone to identify the biliary anatomy during cholecystectomy (conditional recommendation, very low certainty of evidence).

However, in a Delphi survey of 19 international experts in fluorescence-guided surgery attending a 1 d consensus meeting in Frankfurt, Germany in September 2019, fluorescence imaging was almost unanimously perceived to be both effective and safe across a broad range of clinical settings[76]. No specific recommendations were given for fluorescent cholangiography. Moreover, the safety of ICG dye has been underlined: the risk of adverse reactions to ICG injection, such as anaphylactic shock, is very small (approximately 0.003% at doses exceeding 0.5 mg/kg) according to the literature data [9,77].

CONCLUSION

The results of the current up-to-date overview confirmed the efficacy of ICG-fluorescence cholangiography in detecting biliary anatomy, its importance as a teaching tool for young surgeons, and the effects on the reduction of conversion rate and BDI, even if further considerable research remains necessary to optimize its use. This frontier method has enormous potential to become the gold standard during all cholecystectomies in elective and emergency settings due to its safety and limited costs. However, clear clinical guidelines are necessary for the surgical community.

REFERENCES

1 **Nuzzo G**, Giuliante F, Giovannini I, Ardito F, D'Acapito F, Vellone M, Murazio M, Capelli G. Bile duct injury during laparoscopic cholecystectomy: results of an Italian national survey on 56 591 cholecystectomies. *Arch Surg* 2005; **140**: 986-992 [PMID: 16230550 DOI: 10.1001/archsurg.140.10.986]

2 **Way LW**, Stewart L, Gantert W, Liu K, Lee CM, Whang K, Hunter JG. Causes and prevention of laparoscopic bile duct injuries: analysis of 252 cases from a human factors and cognitive psychology perspective. *Ann Surg* 2003; **237**: 460-469 [PMID: 12677139 DOI: 10.1097/01.SLA.0000060680.92690.E9]

3 **Pesce A**, Portale TR, Minutolo V, Scilletta R, Li Destri G, Puleo S. Bile duct injury during laparoscopic cholecystectomy without intraoperative cholangiography: a retrospective study on 1,100 selected patients. *Dig Surg* 2012; **29**: 310-314 [PMID: 22986956 DOI: 10.1159/000341660]

4 **Pesce A**, Palmucci S, La Greca G, Puleo S. Iatrogenic bile duct injury: impact and management challenges. *Clin Exp Gastroenterol* 2019; **12**: 121-128 [PMID: 30881079 DOI: 10.2147/CEG.S169492]

5 **Majlesara A**, Golriz M, Hafezi M, Saffari A, Stenau E, Maier-Hein L, Müller-Stich BP, Mehrabi A. Indocyanine green fluorescence imaging in hepatobiliary surgery. *Photodiagnosis Photodyn Ther* 2017; **17**: 208-215 [PMID: 28017834 DOI: 10.1016/j.pdpdt.2016.12.005]

6 **Baiocchi GL**, Diana M, Boni L. Indocyanine green-based fluorescence imaging in visceral and hepatobiliary and pancreatic surgery: State of the art and future directions. *World J Gastroenterol* 2018; **24**: 2921-2930 [PMID: 30038461 DOI: 10.3748/wjg.v24.i27.2921]

7 **Stiles BM**, Adusumilli PS, Bhargava A, Fong Y. Fluorescent cholangiography in a mouse model: an innovative method for improved laparoscopic identification of the biliary anatomy. *Surg Endosc*

2006; **20**: 1291-1295 [PMID: 16858526 DOI: 10.1007/s00464-005-0664-x]

8 **Ishizawa T**, Tamura S, Masuda K, Aoki T, Hasegawa K, Imamura H, Beck Y, Kokudo N. Intraoperative fluorescent cholangiography using indocyanine green: a biliary road map for safe surgery. *J Am Coll Surg* 2009; **208**: e1-e4 [PMID: 19228492 DOI: 10.1016/j.jamcollsurg.2008.09.024]

9 **Pesce A**, Piccolo G, La Greca G, Puleo S. Utility of fluorescent cholangiography during laparoscopic cholecystectomy: A systematic review. *World J Gastroenterol* 2015; **21**: 7877-7883 [PMID: 26167088 DOI: 10.3748/wjg.v21.i25.7877]

10 **Igami T**, Nojiri M, Shinohara K, Ebata T, Yokoyama Y, Sugawara G, Mizuno T, Yamaguchi J, Nagino M. Clinical value and pitfalls of fluorescent cholangiography during single-incision laparoscopic cholecystectomy. *Surg Today* 2016; **46**: 1443-1450 [PMID: 27002714 DOI: 10.1007/s00595-016-1330-8]

11 **Broderick RC**, Lee AM, Cheverie JN, Zhao B, Blitzer RR, Patel RJ, Soltero S, Sandler BJ, Jacobsen GR, Doucet JJ, Horgan S. Fluorescent cholangiography significantly improves patient outcomes for laparoscopic cholecystectomy. *Surg Endosc* 2020 [PMID: 33052527 DOI: 10.1007/s00464-020-08045-x]

12 **Bleszynski MS**, DeGirolamo KM, Meneghetti AT, Chiu CJ, Panton ON. Fluorescent Cholangiography in Laparoscopic Cholecystectomy: An Updated Canadian Experience. *Surg Innov* 2020; **27**: 38-43 [PMID: 31744398 DOI: 10.1177/1553350619885792]

13 **Strasberg SM**, Brunt LM. Rationale and use of the critical view of safety in laparoscopic cholecystectomy. *J Am Coll Surg* 2010; **211**: 132-138 [PMID: 20610259 DOI: 10.1016/j.jamcollsurg.2010.02.053]

14 **Ishizawa T**, Bandai Y, Ijichi M, Kaneko J, Hasegawa K, Kokudo N. Fluorescent cholangiography illuminating the biliary tree during laparoscopic cholecystectomy. *Br J Surg* 2010; **97**: 1369-1377 [PMID: 20623766 DOI: 10.1002/bjs.7125]

15 **Dip F**, Aleman R, Frieder JS, Gomez CO, Menzo EL, Szomstein S, Rosenthal RJ. Understanding intraoperative fluorescent cholangiography: ten steps for an effective and successful procedure. *Surg Endosc* 2021 [PMID: 33475844 DOI: 10.1007/s00464-020-08219-7]

16 **van den Bos J**, Wieringa FP, Bouvy ND, Stassen LPS. Optimizing the image of fluorescence cholangiography using ICG: a systematic review and ex vivo experiments. *Surg Endosc* 2018; **32**: 4820-4832 [PMID: 29777357 DOI: 10.1007/s00464-018-6233-x]

17 **Agnus V**, Pesce A, Boni L, Van Den Bos J, Morales-Conde S, Paganini AM, Quaresima S, Balla A, La Greca G, Plaudis H, Moretto G, Castagnola M, Santi C, Casali L, Tartamella L, Saadi A, Picchetto A, Arezzo A, Marescaux J, Diana M. Fluorescence-based cholangiography: preliminary results from the IHU-IRCAD-EAES EURO-FIGS registry. *Surg Endosc* 2020; **34**: 3888-3896 [PMID: 31591654 DOI: 10.1007/s00464-019-07157-3]

18 **Boogerd LSF**, Handgraaf HJM, Huurman VAL, Lam HD, Mieog JSD, van der Made WJ, van de Velde CJH, Vahrmeijer AL. The Best Approach for Laparoscopic Fluorescence Cholangiography: Overview of the Literature and Optimization of Dose and Dosing Time. *Surg Innov* 2017; **24**: 386-396 [PMID: 28457194 DOI: 10.1177/1553350617702311]

19 **Zarrinpar A**, Dutson EP, Mobley C, Busuttil RW, Lewis CE, Tillou A, Cheaito A, Hines OJ, Agopian VG, Hiyama DT. Intraoperative Laparoscopic Near-Infrared Fluorescence Cholangiography to Facilitate Anatomical Identification: When to Give Indocyanine Green and How Much. *Surg Innov* 2016; **23**: 360-365 [PMID: 26964557 DOI: 10.1177/1553350616637671]

20 **Chen Q**, Zhou R, Weng J, Lai Y, Liu H, Kuang J, Zhang S, Wu Z, Wang W, Gu W. Extrahepatic biliary tract visualization using near-infrared fluorescence imaging with indocyanine green: optimization of dose and dosing time. *Surg Endosc* 2020 [PMID: 33026517 DOI: 10.1007/s00464-020-08058-6]

21 **Matsumura M**, Kawaguchi Y, Kobayashi Y, Kobayashi K, Ishizawa T, Akamatsu N, Kaneko J, Arita J, Kokudo N, Hasegawa K. Indocyanine green administration a day before surgery may increase bile duct detectability on fluorescence cholangiography during laparoscopic cholecystectomy. *J Hepatobiliary Pancreat Sci* 2021; **28**: 202-210 [PMID: 33091224 DOI: 10.1002/jhbp.855]

22 **Liu YY**, Liao CH, Diana M, Wang SY, Kong SH, Yeh CN, Dallemagne B, Marescaux J, Yeh TS. Near-infrared cholecystocholangiography with direct intragallbladder indocyanine green injection: preliminary clinical results. *Surg Endosc* 2018; **32**: 1506-1514 [PMID: 28916859 DOI: 10.1007/s00464-017-5838-9]

23 **Gené Škrabec C**, Pardo Aranda F, Espín F, Cremades M, Navinés J, Zárate A, Cugat E. Fluorescent cholangiography with direct injection of indocyanine green (ICG) into the gallbladder: a safety method to outline biliary anatomy. *Langenbecks Arch Surg* 2020; **405**: 827-832 [PMID: 32827267 DOI: 10.1007/s00423-020-01967-z]

24 **Nitta T**, Kataoka J, Ohta M, Ueda Y, Senpuku S, Kurashima Y, Shimizu T, Ishibashi T. Laparoscopic cholecystectomy for cholecystitis using direct gallbladder indocyanine green injection fluorescence cholangiography: A case report. *Ann Med Surg (Lond)* 2020; **57**: 218-222 [PMID: 32793342 DOI: 10.1016/j.amsu.2020.07.057]

25 **Graves C**, Ely S, Idowu O, Newton C, Kim S. Direct Gallbladder Indocyanine Green Injection Fluorescence Cholangiography During Laparoscopic Cholecystectomy. *J Laparoendosc Adv Surg Tech A* 2017; **27**: 1069-1073 [PMID: 28574801 DOI: 10.1089/lap.2017.0070]

26 **Jao ML**, Wang YY, Wong HP, Bachhav S, Liu KC. Intracholecystic administration of indocyanine green for fluorescent cholangiography during laparoscopic cholecystectomy-A two-case report. *Int J*

Surg Case Rep 2020; **68**: 193-197 [PMID: 32172195 DOI: 10.1016/j.ijscr.2020.02.054]

27 **Okamoto K**, Suzuki K, Takada T, Strasberg SM, Asbun HJ, Endo I, Iwashita Y, Hibi T, Pitt HA, Umezawa A, Asai K, Han HS, Hwang TL, Mori Y, Yoon YS, Huang WS, Belli G, Dervenis C, Yokoe M, Kiriyama S, Itoi T, Jagannath P, Garden OJ, Miura F, Nakamura M, Horiguchi A, Wakabayashi G, Cherqui D, de Santibañes E, Shikata S, Noguchi Y, Ukai T, Higuchi R, Wada K, Honda G, Supe AN, Yoshida M, Mayumi T, Gouma DJ, Deziel DJ, Liau KH, Chen MF, Shibao K, Liu KH, Su CH, Chan ACW, Yoon DS, Choi IS, Jonas E, Chen XP, Fan ST, Ker CG, Giménez ME, Kitano S, Inomata M, Hirata K, Inui K, Sumiyama Y, Yamamoto M. Tokyo Guidelines 2018: flowchart for the management of acute cholecystitis. *J Hepatobiliary Pancreat Sci* 2018; **25**: 55-72 [PMID: 29045062 DOI: 10.1002/jhbp.516]

28 **Alander JT**, Kaartinen I, Laakso A, Pätilä T, Spillmann T, Tuchin VV, Venermo M, Välisuo P. A review of indocyanine green fluorescent imaging in surgery. *Int J Biomed Imaging* 2012; **2012**: 940585 [PMID: 22577366 DOI: 10.1155/2012/940585]

29 **Dip F**, Lo Menzo E, White KP, Rosenthal RJ. Does near-infrared fluorescent cholangiography with indocyanine green reduce bile duct injuries and conversions to open surgery during laparoscopic or robotic cholecystectomy? *Surgery* 2021; **169**: 859-867 [PMID: 33478756 DOI: 10.1016/j.surg.2020.12.008]

30 **Di Maggio F**, Hossain N, De Zanna A, Husain D, Bonomo L. Near-Infrared Fluorescence Cholangiography can be a Useful Adjunct during Emergency Cholecystectomies. *Surg Innov* 2020; 1553350620958562 [PMID: 32936054 DOI: 10.1177/1553350620958562]

31 **Daskalaki D**, Fernandes E, Wang X, Bianco FM, Elli EF, Ayloo S, Masrur M, Milone L, Giulianotti PC. Indocyanine green (ICG) fluorescent cholangiography during robotic cholecystectomy: results of 184 consecutive cases in a single institution. *Surg Innov* 2014; **21**: 615-621 [PMID: 24616013 DOI: 10.1177/1553350614524839]

32 **Dip F**, LoMenzo E, Sarotto L, Phillips E, Todeschini H, Nahmod M, Alle L, Schneider S, Kaja L, Boni L, Ferraina P, Carus T, Kokudo N, Ishizawa T, Walsh M, Simpfendorfer C, Mayank R, White K, Rosenthal RJ. Randomized Trial of Near-infrared Incisionless Fluorescent Cholangiography. *Ann Surg* 2019; **270**: 992-999 [PMID: 30614881 DOI: 10.1097/SLA.0000000000003178]

33 **Yoshiya S**, Minagawa R, Kamo K, Kasai M, Taketani K, Yukaya T, Kimura Y, Koga T, Kai M, Kajiyama K, Yoshizumi T. Usability of Intraoperative Fluorescence Imaging with Indocyanine Green During Laparoscopic Cholecystectomy After Percutaneous Transhepatic Gallbladder Drainage. *World J Surg* 2019; **43**: 127-133 [PMID: 30105635 DOI: 10.1007/s00268-018-4760-1]

34 **Kitamura H**, Tsuji T, Yamamoto D, Takahashi T, Kadoya S, Kurokawa M, Bando H. Efficiency of fluorescent cholangiography during laparoscopic cholecystectomy for subvesical bile ducts: A case report. *Int J Surg Case Rep* 2019; **57**: 194-196 [PMID: 30981075 DOI: 10.1016/j.ijscr.2019.03.042]

35 **Iwasaki T**, Takeyama Y, Yoshida Y, Kawaguchi K, Matsumoto M, Murase T, Kamei K, Takebe A, Matsumoto I, Nakai T. Identification of aberrant subvesical bile duct by using intraoperative fluorescent cholangiography: A case report. *Int J Surg Case Rep* 2019; **61**: 115-118 [PMID: 31357101 DOI: 10.1016/j.ijscr.2019.07.013]

36 **Tsuruda Y**, Okumura H, Setoyama T, Hiwatashi K, Minami K, Ando K, Wada M, Maenohara S, Natsugoe S. Laparoscopic cholecystectomy with aberrant bile duct detected by intraoperative fluorescent cholangiography concomitant with angiography: A case report. *Int J Surg Case Rep* 2018; **51**: 14-16 [PMID: 30130667 DOI: 10.1016/j.ijscr.2018.08.009]

37 **Bozzay J**, Vicente D, Jessie EM, Rodriguez CJ. Identification of Abnormal Biliary Anatomy Utilizing Real-Time Near-Infrared Cholangiography: A Report of Two Cases. *Case Rep Gastrointest Med* 2017; **2017**: 8628206 [PMID: 28536662 DOI: 10.1155/2017/8628206]

38 **Asai Y**, Igami T, Ebata T, Yokoyama Y, Mizuno T, Yamaguchi J, Onoe S, Watanabe N, Nagino M. Application of fluorescent cholangiography during single-incision laparoscopic cholecystectomy in the cystohepatic duct without preoperative diagnosis. *ANZ J Surg* 2021; **91**: 470-472 [PMID: 32681758 DOI: 10.1111/ans.16162]

39 **Kim NS**, Jin HY, Kim EY, Hong TH. Cystic duct variation detected by near-infrared fluorescent cholangiography during laparoscopic cholecystectomy. *Ann Surg Treat Res* 2017; **92**: 47-50 [PMID: 28090506 DOI: 10.4174/astr.2017.92.1.47]

40 **Naganuma S**, Ishida H, Konno K, Hamashima Y, Hoshino T, Naganuma H, Komatsuda T, Ohyama Y, Yamada N, Ishida J, Masamune O. Sonographic findings of anomalous position of the gallbladder. *Abdom Imaging* 1998; **23**: 67-72 [PMID: 9437066 DOI: 10.1007/s002619900287]

41 **Nojiri M**, Igami T, Toyoda Y, Ebata T, Yokoyama Y, Sugawara G, Mizuno T, Yamaguchi J, Nagino M. Application of fluorescent cholangiography during single-incision laparoscopic cholecystectomy for cholecystitis with a right-sided round ligament: Preliminary experience. *J Minim Access Surg* 2018; **14**: 244-246 [PMID: 29226884 DOI: 10.4103/jmas.JMAS_159_17]

42 **Shanmugam V**, Beattie GC, Yule SR, Reid W, Loudon MA. Is magnetic resonance cholangiopancreatography the new gold standard in biliary imaging? *Br J Radiol* 2005; **78**: 888-893 [PMID: 16177010 DOI: 10.1259/bjr/51075444]

43 **Griffin N**, Charles-Edwards G, Grant LA. Magnetic resonance cholangiopancreatography: the ABC of MRCP. *Insights Imaging* 2012; **3**: 11-21 [PMID: 22695995 DOI: 10.1007/s13244-011-0129-9]

44 **Pesce A**, La Greca G, Esposto Ultimo L, Basile A, Puleo S, Palmucci S. Effectiveness of near-infrared fluorescent cholangiography in the identification of cystic duct-common hepatic duct anatomy in comparison to magnetic resonance cholangio-pancreatography: a preliminary study. *Surg Endosc* 2020; **34**: 2715-2721 [PMID: 31598878 DOI: 10.1007/s00464-019-07158-2]

45 **Diana M**, Soler L, Agnus V, D'Urso A, Vix M, Dallemagne B, Faucher V, Roy C, Mutter D, Marescaux J, Pessaux P. Prospective Evaluation of Precision Multimodal Gallbladder Surgery Navigation: Virtual Reality, Near-infrared Fluorescence, and X-ray-based Intraoperative Cholangiography. *Ann Surg* 2017; **266**: 890-897 [PMID: 28742709 DOI: 10.1097/SLA.0000000000002400]

46 **Hiwatashi K**, Okumura H, Setoyama T, Ando K, Ogura Y, Aridome K, Maenohara S, Natsugoe S. Evaluation of laparoscopic cholecystectomy using indocyanine green cholangiography including cholecystitis: A retrospective study. *Medicine (Baltimore)* 2018; **97**: e11654 [PMID: 30045318 DOI: 10.1097/MD.0000000000011654]

47 **Pesce A**, Latteri S, Barchitta M, Portale TR, Di Stefano B, Agodi A, Russello D, Puleo S, La Greca G. Near-infrared fluorescent cholangiography - real-time visualization of the biliary tree during elective laparoscopic cholecystectomy. *HPB (Oxford)* 2018; **20**: 538-545 [PMID: 29292071 DOI: 10.1016/j.hpb.2017.11.013]

48 **Pesce A**, Diana M. Critical View of Safety During Laparoscopic Cholecystectomy: From the Surgeon's Eye to Fluorescent Vision. *Surg Innov* 2018; **25**: 197-198 [PMID: 29557253 DOI: 10.1177/1553350618763200]

49 **Dip FD**, Asbun D, Rosales-Velderrain A, Lo Menzo E, Simpfendorfer CH, Szomstein S, Rosenthal RJ. Cost analysis and effectiveness comparing the routine use of intraoperative fluorescent cholangiography with fluoroscopic cholangiogram in patients undergoing laparoscopic cholecystectomy. *Surg Endosc* 2014; **28**: 1838-1843 [PMID: 24414461 DOI: 10.1007/s00464-013-3394-5]

50 **Lehrskov LL**, Westen M, Larsen SS, Jensen AB, Kristensen BB, Bisgaard T. Fluorescence or X-ray cholangiography in elective laparoscopic cholecystectomy: a randomized clinical trial. *Br J Surg* 2020; **107**: 655-661 [PMID: 32057103 DOI: 10.1002/bjs.11510]

51 **Lim SH**, Tan HTA, Shelat VG. Comparison of indocyanine green dye fluorescent cholangiography with intra-operative cholangiography in laparoscopic cholecystectomy: a meta-analysis. *Surg Endosc* 2021; **35**: 1511-1520 [PMID: 33398590 DOI: 10.1007/s00464-020-08164-5]

52 **Dip F**, Roy M, Lo Menzo E, Simpfendorfer C, Szomstein S, Rosenthal RJ. Routine use of fluorescent incisionless cholangiography as a new imaging modality during laparoscopic cholecystectomy. *Surg Endosc* 2015; **29**: 1621-1626 [PMID: 25277476 DOI: 10.1007/s00464-014-3853-7]

53 **Quaresima S**, Balla A, Palmieri L, Seitaj A, Fingerhut A, Ursi P, Paganini AM. Routine near infra-red indocyanine green fluorescent cholangiography vs intraoperative cholangiography during laparoscopic cholecystectomy: a case-matched comparison. *Surg Endosc* 2020; **34**: 1959-1967 [PMID: 31309307 DOI: 10.1007/s00464-019-06970-0]

54 **Osayi SN**, Wendling MR, Drosdeck JM, Chaudhry UI, Perry KA, Noria SF, Mikami DJ, Needleman BJ, Muscarella P 2nd, Abdel-Rasoul M, Renton DB, Melvin WS, Hazey JW, Narula VK. Near-infrared fluorescent cholangiography facilitates identification of biliary anatomy during laparoscopic cholecystectomy. *Surg Endosc* 2015; **29**: 368-375 [PMID: 24986018 DOI: 10.1007/s00464-014-3677-5]

55 **Buchs NC**, Pugin F, Azagury DE, Jung M, Volonte F, Hagen ME, Morel P. Real-time near-infrared fluorescent cholangiography could shorten operative time during robotic single-site cholecystectomy. *Surg Endosc* 2013; **27**: 3897-3901 [PMID: 23670747 DOI: 10.1007/s00464-013-3005-5]

56 **Aoki T**, Murakami M, Yasuda D, Shimizu Y, Kusano T, Matsuda K, Niiya T, Kato H, Murai N, Otsuka K, Kusano M, Kato T. Intraoperative fluorescent imaging using indocyanine green for liver mapping and cholangiography. *J Hepatobiliary Pancreat Sci* 2010; **17**: 590-594 [PMID: 19844652 DOI: 10.1007/s00534-009-0197-0]

57 **Vlek SL**, van Dam DA, Rubinstein SM, de Lange-de Klerk ESM, Schoonmade LJ, Tuynman JB, Meijerink WJHJ, Ankersmit M. Biliary tract visualization using near-infrared imaging with indocyanine green during laparoscopic cholecystectomy: results of a systematic review. *Surg Endosc* 2017; **31**: 2731-2742 [PMID: 27844236 DOI: 10.1007/s00464-016-5318-7]

58 **Dip F**, Nguyen D, Montorfano L, Szretter Noste ME, Lo Menzo E, Simpfendorfer C, Szomstein S, Rosenthal R. Accuracy of Near Infrared-Guided Surgery in Morbidly Obese Subjects Undergoing Laparoscopic Cholecystectomy. *Obes Surg* 2016; **26**: 525-530 [PMID: 26224370 DOI: 10.1007/s11695-015-1781-9]

59 **Pax V**, Schneider-Koriath S, Scholz M, Wießner R, Ludwig K. [Fluorescence Cholangiography in Comparison to Radiographic Cholangiography During Laparoscopic Cholecystectomy]. *Zentralbl Chir* 2018; **143**: 35-41 [PMID: 29166696 DOI: 10.1055/s-0043-117495]

60 **Koong JK**, Ng GH, Ramayah K, Koh PS, Yoong BK. Early identification of the critical view of safety in laparoscopic cholecystectomy using indocyanine green fluorescence cholangiography: A randomised controlled study. *Asian J Surg* 2021; **44**: 537-543 [PMID: 33223453 DOI: 10.1016/j.asjsur.2020.11.002]

61 **van den Bos J**, Schols RM, Luyer MD, van Dam RM, Vahrmeijer AL, Meijerink WJ, Gobardhan PD, van Dam GM, Bouvy ND, Stassen LP. Near-infrared fluorescence cholangiography assisted laparoscopic cholecystectomy vs conventional laparoscopic cholecystectomy (FALCON trial): study protocol for a multicentre randomised controlled trial. *BMJ Open* 2016; **6**: e011668 [PMID: 27566635 DOI: 10.1136/bmjopen-2016-011668]

62 **Roy M**, Dip F, Nguyen D, Simpfendorfer CH, Menzo EL, Szomstein S, Rosenthal RJ. Fluorescent incisionless cholangiography as a teaching tool for identification of Calot's triangle. *Surg Endosc* 2017; **31**: 2483-2490 [PMID: 27778170 DOI: 10.1007/s00464-016-5250-x]

63 **Rungsakulkij N**, Thewmorakot S, Suragul W, Vassanasiri W, Tangtawee P, Muangkaew P, Mingphruedhi S, Aeesoa S. Fluorescence cholangiography enhances surgical residents' biliary delineation skill for laparoscopic cholecystectomies. *World J Gastrointest Surg* 2020; **12**: 93-103 [PMID: 32218892 DOI: 10.4240/wjgs.v12.i3.93]

64 **van de Graaf FW**, Zaïmi I, Stassen LPS, Lange JF. Safe laparoscopic cholecystectomy: A systematic review of bile duct injury prevention. *Int J Surg* 2018; **60**: 164-172 [PMID: 30439536 DOI: 10.1016/j.ijsu.2018.11.006]

65 **Labib PL**, Aroori S. Intraoperative ultrasound vs fluorescence and X-ray cholangiography for the identification of bile duct stones, biliary anatomy and bile duct injury during laparoscopic cholecystectomy: Time for a randomized controlled trial? *Br J Surg* 2020; **107**: e563 [PMID: 32841376 DOI: 10.1002/bjs.11862]

66 **Dili A**, Bertrand C. Laparoscopic ultrasonography as an alternative to intraoperative cholangiography during laparoscopic cholecystectomy. *World J Gastroenterol* 2017; **23**: 5438-5450 [PMID: 28839445 DOI: 10.3748/wjg.v23.i29.5438]

67 **Machi J**, Johnson JO, Deziel DJ, Soper NJ, Berber E, Siperstein A, Hata M, Patel A, Singh K, Arregui ME. The routine use of laparoscopic ultrasound decreases bile duct injury: a multicenter study. *Surg Endosc* 2009; **23**: 384-388 [PMID: 18528611 DOI: 10.1007/s00464-008-9985-x]

68 **Spinoglio G**, Lenti LM, Maglione V, Lucido FS, Priora F, Bianchi PP, Grosso F, Quarati R. Single-site robotic cholecystectomy (SSRC) versus single-incision laparoscopic cholecystectomy (SILC): comparison of learning curves. First European experience. *Surg Endosc* 2012; **26**: 1648-1655 [PMID: 22179472 DOI: 10.1007/s00464-011-2087-1]

69 **Buchs NC**, Hagen ME, Pugin F, Volonte F, Bucher P, Schiffer E, Morel P. Intra-operative fluorescent cholangiography using indocyanin green during robotic single site cholecystectomy. *Int J Med Robot* 2012; **8**: 436-440 [PMID: 22648637 DOI: 10.1002/rcs.1437]

70 **Spinoglio G**, Priora F, Bianchi PP, Lucido FS, Licciardello A, Maglione V, Grosso F, Quarati R, Ravazzoni F, Lenti LM. Real-time near-infrared (NIR) fluorescent cholangiography in single-site robotic cholecystectomy (SSRC): a single-institutional prospective study. *Surg Endosc* 2013; **27**: 2156-2162 [PMID: 23271272 DOI: 10.1007/s00464-012-2733-2]

71 **Maker AV**, Kunda N. A Technique to Define Extrahepatic Biliary Anatomy Using Robotic Near-Infrared Fluorescent Cholangiography. *J Gastrointest Surg* 2017; **21**: 1961-1962 [PMID: 28585107 DOI: 10.1007/s11605-017-3455-5]

72 **Sharma S**, Huang R, Hui S, Smith MC, Chung PJ, Schwartzman A, Sugiyama G. The utilization of fluorescent cholangiography during robotic cholecystectomy at an inner-city academic medical center. *J Robot Surg* 2018; **12**: 481-485 [PMID: 29181777 DOI: 10.1007/s11701-017-0769-y]

73 **Gangemi A**, Danilkowicz R, Elli FE, Bianco F, Masrur M, Giulianotti PC. Could ICG-aided robotic cholecystectomy reduce the rate of open conversion reported with laparoscopic approach? *J Robot Surg* 2017; **11**: 77-82 [PMID: 27435700 DOI: 10.1007/s11701-016-0624-6]

74 **Dip F**, Sarotto L, Roy M, Lee A, LoMenzo E, Walsh M, Carus T, Schneider S, Boni L, Ishizawa T, Kokudo N, White K, Rosenthal RJ. Incisionless fluorescent cholangiography (IFC): a pilot survey of surgeons on procedural familiarity, practices, and perceptions. *Surg Endosc* 2020; **34**: 675-685 [PMID: 31062156 DOI: 10.1007/s00464-019-06814-x]

75 **Brunt LM**, Deziel DJ, Telem DA, Strasberg SM, Aggarwal R, Asbun H, Bonjer J, McDonald M, Alseidi A, Ujiki M, Riall TS, Hammill C, Moulton CA, Pucher PH, Parks RW, Ansari MT, Connor S, Dirks RC, Anderson B, Altieri MS, Tsamalaidze L, Stefanidis D; and the Prevention of Bile Duct Injury Consensus Work Group. Safe Cholecystectomy Multi-society Practice Guideline and State of the Art Consensus Conference on Prevention of Bile Duct Injury During Cholecystectomy. *Ann Surg* 2020; **272**: 3-23 [PMID: 32404658 DOI: 10.1097/SLA.0000000000003791]

76 **Dip F**, Boni L, Bouvet M, Carus T, Diana M, Falco J, Gurtner GC, Ishizawa T, Kokudo N, Lo Menzo E, Low PS, Masia J, Muehrcke D, Papay FA, Pulitano C, Schneider-Koraith S, Sherwinter D, Spinoglio G, Stassen L, Urano Y, Vahrmeijer A, Vibert E, Warram J, Wexner SD, White K, Rosenthal RJ. Consensus Conference Statement on the General Use of Near-Infrared Fluorescence Imaging and Indocyanine Green Guided Surgery: Results of a Modified Delphi Study. *Ann Surg* 2020 [PMID: 33214476 DOI: 10.1097/SLA.0000000000004412]

77 **Benya R**, Quintana J, Brundage B. Adverse reactions to indocyanine green: a case report and a review of the literature. *Cathet Cardiovasc Diagn* 1989; **17**: 231-233 [PMID: 2670244 DOI: 10.1002/ccd.1810170410]

World Journal of Gastroenterology

Submit a Manuscript: https://www.f6publishing.com

World J Gastroenterol 2021 September 28; 27(36): 6004-6024

DOI: 10.3748/wjg.v27.i36.6004

ISSN 1007-9327 (print) ISSN 2219-2840 (online)

REVIEW

Histone methylation in pancreatic cancer and its clinical implications

Xing-Yu Liu, Chuan-Hao Guo, Zhi-Yuan Xi, Xin-Qi Xu, Qing-Yang Zhao, Li-Sha Li, Ying Wang

ORCID number: Xing-Yu Liu 0000-0001-5800-2787; Chuan-Hao Guo 0000-0001-5801-0453; Zhi-Yuan Xi 0000-0002-3747-3042; Xin-Qi Xu 0000-0002-7688-7619; Qing-Yang Zhao 0000-0002-0386-5507; Li-Sha Li 0000-0003-4048-5981; Ying Wang 0000-0003-1633-0007.

Author contributions: Liu XY, Guo CH, Xi ZY, Xu XQ, and Zhao QY drafted the manuscript and designed the tables; Li LS and Wang Y designed and revised the manuscript; All authors have read and approved the final manuscript.

Conflict-of-interest statement: The authors have no conflicts of interests or financial disclosures relevant to this manuscript.

Manuscript source: Invited manuscript

Xing-Yu Liu, Xin-Qi Xu, Qing-Yang Zhao, Ying Wang, The First Hospital of Jilin University, Jilin University, Changchun 130021, Jilin Province, China

Chuan-Hao Guo, Zhi-Yuan Xi, Li-Sha Li, The Key Laboratory of Pathobiology, Ministry of Education, College of Basic Medical Sciences, Jilin University, Changchun 130021, Jilin Province, China

Corresponding author: Ying Wang, MM, Technologist-In-Charge, The First Hospital of Jilin University, Jilin University, No. 126 Xinmin Street, Changchun 130021, Jilin Province, China. wangying_jy@jlu.edu.cn

Abstract

Pancreatic cancer (PC) is an aggressive human cancer. Appropriate methods for the diagnosis and treatment of PC have not been found at the genetic level, thus making epigenetics a promising research path in studies of PC. Histone methylation is one of the most complicated types of epigenetic modifications and has proved crucial in the development of PC. Histone methylation is a reversible process regulated by readers, writers, and erasers. Some writers and erasers can be recognized as potential biomarkers and candidate therapeutic targets in PC because of their unusual expression in PC cells compared with normal pancreatic cells. Based on the impact that writers have on the development of PC, some inhibitors of writers have been developed. However, few inhibitors of erasers have been developed and put to clinical use. Meanwhile, there is not enough research on the reader domains. Therefore, the study of erasers and readers is still a promising area. This review focuses on the regulatory mechanism of histone methylation, and the diagnosis and chemotherapy of PC based on it. The future of epigenetic modification in PC research is also discussed.

Key Words: Pancreatic cancer; Epigenetics; Histone modification; Methylation; Demethylation; Clinical application

Core Tip: Pancreatic cancer is a highly lethal malignancy of the digestive tract that is difficult to diagnose and treat. Histone methylation/demethylation equilibrium is altered in carcinogenesis, resulting in changes in chromatin structure and gene expression. Not only are histone methylation writers related to histone methylation

Specialty type: Gastroenterology and hepatology

Country/Territory of origin: China

Peer-review report's scientific quality classification
Grade A (Excellent): 0
Grade B (Very good): 0
Grade C (Good): C, C
Grade D (Fair): 0
Grade E (Poor): 0

Received: January 27, 2021
Peer-review started: January 27, 2021
First decision: February 25, 2021
Revised: March 12, 2021
Accepted: April 22, 2021
Article in press: April 22, 2021
Published online: September 28, 2021

P-Reviewer: Kobayashi S, Tada M
S-Editor: Gao CC
L-Editor: Filipodia
P-Editor: Li JH

erasers but histone methylation is also related to other epigenetic modifications. Therefore, histone methylation is addressed as a potentially important chemotherapy drug target.

Citation: Liu XY, Guo CH, Xi ZY, Xu XQ, Zhao QY, Li LS, Wang Y. Histone methylation in pancreatic cancer and its clinical implications. *World J Gastroenterol* 2021; 27(36): 6004-6024
URL: https://www.wjgnet.com/1007-9327/full/v27/i36/6004.htm
DOI: https://dx.doi.org/10.3748/wjg.v27.i36.6004

INTRODUCTION

Pancreatic cancer (PC) is a malignant tumor. The lack of adequate diagnostics for PC limits the efficacy of the few currently available treatment options. Current diagnostic methods include clinical biomarkers, imaging, biopsy, *etc.* To date, carcinoembryonic antigen 19 (CA-19) is the only PC clinical biomarker approved by the U.S. Food and Drug Administration[1], but the use of CA-19 is limited by its inadequate sensitivity and specificity[2,3]. Percutaneous biopsy can result in micrometastases in younger patients who receive surgery, so it is only appropriate for inoperable patients[4]. Current diagnostic methods are either inaccurate or limited. Conventional treatment methods for PC mainly include surgery, adjuvant chemotherapy, drug therapy, and radiation therapy[5]. Surgery remains the most important treatment, followed by adjuvant chemotherapy[5]. At present, only 15% to 20% patients can be surgically treated after diagnosis, and only 20% of the patients survive 5 years after receiving surgery[6,7]. Regarding chemotherapy, gemcitabine and other drugs have proved effective for advanced and metastatic PC, but the development of drug resistance has limited the effectiveness[8]. The survival rate of PC patients has not changed much in the past 40 years[8]. The robust molecular biomarkers need to be developed for diagnosis and targeted therapies.

Cancer development is a complex process involving both genetic and epigenetic changes. Genome instability, regulated by both genetic mutations and epigenetic modifications, contributes to tumor progression[9]. The concept of epigenetics itself is evolving with the increase of our knowledge of the molecular mechanism and regulation of gene expression. It is currently widely acknowledged that epigenetics is the study of alternations in gene expression patterns without changes in DNA sequences[10]. Epigenetic modifications include DNA methylation, histone modification and non-coding RNAs. Epigenetic modifications present a new direction for cancer prevention, clinical diagnosis, and drug development.

Histone modification is one of the most important and complicated epigenetic regulatory mechanisms and is crucial in PC. Histone modification affects chromatin structure, transcription, and DNA repair process[11]. Histone modification takes part in the regulation of chromatin architecture and specific loci regulation by recruiting cell-specific transcription factors and interacting with initiation and elongation factors [12]. Histone modification also regulates the transcription process by influencing RNA processing[12]. In terms of regulating chromatin structure, histone modification affects the higher-order chromatin structure by changing the interactions of histones with DNA, and/or by recruiting chromatin remodeling complexes indirectly[13-15].

Histone modifications include histone acetylation, methylation, phosphorylation, and ubiquitination. Histone methylation plays crucial roles in the development of PC. Therefore, this review focuses on histone methylation and its clinical applications.

HISTONE METHYLATION

Post-translational methylation in histone tails is a reversible dynamic chromatin modification. Methyl is dynamically added by methyltransferases-writers, removed by demethylase-erasers, and interpreted by effector proteins-readers[16]. Readers recognize specific sites and promote the recruitment of transcription factors or chromatin-associated protein complexes and bind to histones to enable the localization of enzymes to specific targets[17].

Histone methylation takes place on the residues of arginine, lysine, and histidine. According to the amino acid residues modified, there are arginine residue methyltransferases and lysine residue methyltransferases[18]. Histone arginine methylation is a universal post-translational modification, and aberrant histone arginine methylation is strongly associated with carcinogenesis and metastasis[19]. Arginine residues may be differentially methylated by different types of protein arginine N-methyltransferases (PRMTs)[19].

The maintenance of the balance between histone methylation and demethylation is fundamental to normal cellular development and function[20,21]. The break of the balance between histone methylation and demethylation results in oncogenesis and progression[21,22]. Corresponding to writers, erasers can be divided into arginine residue demethylases and lysine residue demethylases. However, current research on histone arginine residue demethylases is limited, so we only discuss lysine residue demethylases. Based on their mechanism of action, lysine demethylases (KDMs) are classified into two families: Flavin adenine dinucleotide (FAD)-dependent and Fe(II) and 2-oxoglutarate (2OG)-dependent[23-25].

The appropriate localization of histone methyltransferase and histone demethylase is dependent on the readers that can recognize histone modifications[26]. The reader can either be an independent polypeptide or a part of methyltransferase/demethylase [27-31]. Some reader domains such as chromodomain[32,33], Tudor domain[34], tryptophan-aspartic acid 40 (WD40) domain[35,36] and plant homeodomain (PHD) finger[37,38] are well known. These reader domains all have their own specific structure[32-38].

HISTONE METHYLATION WRITERS IN PC

Among histone methylation, arginine and lysine methylation are the most widely studied in PC[39]. Histone methylation is performed mainly by two types of writers: PRMTs and lysine methyltransferases (KMTs) (Table 1), with S-adenosyl-L-methionine (SAM) as the methyl donor[40].

PRMTs

PRMTs catalyze the transfer of a methyl group from SAM to a guanidino-nitrogen atom[41]. Three types of methylated arginine residues are found in mammalian cells: Asymmetric dimethyl-arginine (ADMA), symmetric dimethyl-arginine (SDMA) and monomethyl-arginine (MMA)[41]. Depending on their catalytic activity, PRMTs can be classified in three types[42]. Type I PRMTs are responsible for producing ADMA, whose methyl groups are linked to the same guanidino nitrogen atom. Type II PRMTs add the methyl groups on each of the guanidino nitrogen atom of arginine symmetrically, producing SDMA[42]. PRMT7 is the sole member of type III, exclusively catalyzing the formation of MMA[43]. PRMT1 and PRMT5 function in PC[44,45]. PRMT1 belongs to type I and PRMT5 belongs to type II[42].

PRMT1: PRMT1 is the founding member of the PRMT family, and PRMT1 can methylate histone H4 at arginine 3. This modification is associated with transcriptional activation[44]. Upregulation of PRMT1 is found in various cancer types[46-49]. PRMT1 is highly expressed in pancreatic ductal adenocarcinoma (PDAC) cells, and elevated PRMT1 levels predict a poor clinical outcome[44]. PRMT1 promotes PC cell growth *in vitro* and *in vivo*[44]. PRMT1 increases the β-catenin protein level in PC cells[44]. Overactivation of β-catenin signaling promotes the growth, migration, and metastasis of PC cells[50-52]. PRMT1 downregulation inhibits PC cell proliferation and invasion [53]. GLI family zinc finger 1 (Gli1) is a substrate of PRMT1 in PDAC. Methylation of Gli1 at R597 by PRMT1 promotes its transcriptional activity by enhancing the binding of Gli1 to the promoters of its target gene[54]. Interruption of Gli1 methylation attenuates oncogenic functions of Gli1 and sensitizes PDAC cells to gemcitabine treatment[54].

PRMT5: PRMT5 is a type II writer, responsible for symmetric demethylation[19,55]. PRMT5 regulates the expression of a wide spectrum of target genes by modifying the chromatin structure or transcriptional machinery[56]. Specifically, PRMT5 can catalyze the methylation of arginine 8 on histone H3 and arginine 3 on histone H4 (H4R3)[57]. High expression of PRMT5 has been observed in various cancers. PRMT5 expression improves cancer cell survival, proliferation, migration and metabolism while inhibiting cancer cell apoptosis[55]. PRMT5 expression is significantly upregulated in PC tissues[56]. PRMT5 promotes tumorigenesis and PC cell proliferation[45]. PRMT5

Table 1 Histone methyltransferases play a major role in pancreatic cancer

Family	Subfamily	Alias	Site	Function in pancreatic cancer
PRMTs	PRMT1	HRMT1L2, HMT2, ANM1	H4R3me2a	Increase the β-catenin protein level; Methylate Gli1 at R597[44,54]
	PRMT5	HRMT1L5, SKB1, HSL7	H3R2me2s	Silence the expression of the tumor suppressor FBW7; Promote EMT *via* activating EGFR/ AKT/β-catenin signaling[45,56,188,189]
KMTs	SMYD3	ZNFN3A1, ZMYND1	H4K5me3	Affect the PC progression by regulating MMP-2; Potentiate Ras signaling through methylation of MAP3K2[62,64]
	EZH2	KMT6, WVS, ENX-1	H3K27me3	Suppress miR-139-5p expression by upregulating H3K27me3; Repress the E-cadherin by tri-methylation of H3K27[78,190]

All current research on reprogramming histone methyltransferases that play a role in pancreatic cancer. EMT: Epithelial-mesenchymal transition; FBW7: F-Box and WD repeat domain containing 7; KMTs: Histone lysine methyltransferases; PC: Pancreatic cancer; PRMTs: Protein arginine N-methyltransferases.

promotes cell migration, invasion, and the epithelial-mesenchymal transition (EMT) *via* activating EGFR/AKT/β-catenin signaling in PC cells[45]. PRMT5 knockdown reduces glucose intake and lactate levels in PC cells[56]. PRMT5 can inhibit the expression of F-Box and WD repeat domain containing 7 (FBW7)[58,59]. PRMT5 inhibits FBW7 *via* suppression of *FBW7* gene promoter activity and elevation of cMyc stability, leading to tumorigenicity and aerobic glycolysis in PC cells[56]. PRMT5 induces the phosphorylation of epidermal growth factor receptor (EGFR) at Y1068 and Y1172[45]. Then PRMT5 activates phosphorylation of AKT and its downstream GSK3β [45].

KMTs

KMTs transfer one, two, or three methyl-groups to histone lysine residues[60]. KMTs are categorized into two protein families based on catalytic domain sequence similarity and structural organization[61]. Two major writers, SMYD3 (KMT3E) and EZH2 (KMT6), are related to PC[62,63]. SMYD3 is a member of SET and MYND-domain family[64]. EZH2 belongs to the polycomb family[61].

SMYD3: SMYD3 belongs to the SET and MYND-domain family. SMYD3 can promote the proliferation, migration, and invasion of many types of cancer[64]. SMYD3 is a protooncogene in liver, colon and breast tissue based on its high level of endogenous expression and cancer-related promoter polymorphism[65-70]. SMYD3 is upregulated in PC. SMYD3 is positively associated with caspase-3 and MMP-2 expression in PC tissues[62]. Active Src phosphorylates p300 in the nucleus, and then the complex binds to HMGA2 and SMYD3 genes. Therefore, HMGA2 and SMYD3 are regulated to promote PC cell migration and invasion[71].

EZH2: EZH2 is the enzymatic subunit of polycomb repressive complex 2 (PRC2), a complex that methylates lysine 27 of histone H3(H3K27) to promote transcriptional silencing[72]. High expression of EZH2 protein has been associated with several cancers[73-75]. EZH2 is overexpressed in PC[76]. FBW7 interacts with EZH2 and downregulates EZH2 *via* ubiquitination and degradation in PC cells[76]. Downregulation of FBW7 induces high EZH2 protein expression and promotes tumor progression in PC[76]. Long non-coding RNA (lncRNA) *BLACAT1* facilitates proliferation, migration, and aerobic glycolysis of PC cells by repressing *CDKN1C* *via* EZH2-induced histone H3 lysine 27 trimethylation (H3K27me3)[77]. EZH2 regulates the expression of miR-139-5p *via* H3K27me3, and the EZH2/miR-139-5p axis participates in the progression of PC, whereby downregulation of EZH2 and upregulation of miR-139-5p repress the EMT and lymph node metastasis of PC[78]. EZH2 can bind to the promoters of P15 and KLF2 to induce H3K27me3[79]. LncRNA *SNHG15* knockdown inhibits PC cell proliferation and tumorigenesis while inducing cell apoptosis, and the *SNHG15*-mediated oncogenic effect is partly by repressing P15 and KLF2 expression *via* EZH2-induced H3K27me3[79].

HISTONE METHYLATION ERASERS IN PC

The demethylation of arginine and lysine in histone tails is the two main forms of histone demethylation. Due to the large gaps in research on arginine demethylation, the main situation of KDMs in PC will be mainly described. KDMs can catalyze monomethyl, dimethyl or trimethyl labeling of histone lysine residues[12]. There is some evidence that occurrence, development, and therapy of PC are all related to KDMs[80,81] (Table 2).

KDM1

Flavin-dependent KDMs are a subfamily of amine oxidases that catalyze the selective posttranslational oxidative demethylation of methyl lysine side chains within substrates[82]. Two subtypes of KDMs, KDM1A and KDM1B, are related to PC[83,84]. They are expressed at high levels in PC tissues. To date, the expression patterns and physiological functions of KDM1A/LSD1 in PC have not been fully elucidated. KDM1A and hypoxia inducible factor-1α (HIF1α) are the interaction partners of the homeobox protein PROX1[85,86]. KDM1A acts synergistically with HIF1α in maintaining glycolysis[87]. Compared with KDM1A, KDM1B/LSD2 lacks a "tower domain" and has a zinc finger domain in the N-terminal region, which makes KDM1B endowed with different biochemical properties[24,25,88]. KDM1B is related to many important biological functions, including transcriptional regulation, genome imprinting, somatic cell reprogramming, DNA methylation, and signal transduction [89-92]. The downregulation of KDM1B can inhibit PC cell proliferation and promote PC cell apoptosis *in vitro*[93,94].

JmjC domain-containing protein family

JmjC domain-containing (JMJD) protein family is a type of Fe (II) and α-ketoglutarate-dependent dioxygenases. The JMJD protein family now consists of 33 members. There are 18 members with the ability to demethylate H3K4, H3K9, H3K27, H3K36, and H4K20[23,95-108].

KDM2B: KDM2B acts on H3K36 demethylation. KDM2B enhances the bypass of primary cell senescence by directly binding to tumor suppressor gene *CDKN2A* sites and demethylating histones, thereby guiding the recruitment of PRC2; thus, it plays an important role in cell cycle progression and senescence[109,110]. KDM2B regulates cell proliferation, migration, and angiogenesis[111-113]. KDM2B plays a crucial role in poorly differentiated PDAC, and there is an interaction between EZH2 and KDM2B [114].

KDM3A: KDM3A/JMJD1A, one member of the JMJD1 family, participates in transcriptional regulation by demethylating monomethyl or dimethyl H3K9[115,116]. Since cells are heterogeneous in early PDAC tissues, new progress has been made in the study of PDAC morphology, which is specifically manifested by the upregulation of *DCLK1* expression[117]. KDM3A plays a key role in the upregulation of *DCLK1* expression, and KDM3A expression inhibitors can inhibit the malignant properties of PDAC[118].

KDM4: The KDM4 subfamily consists of 12 demethylases including KDM4A, B, C, and D, which can catalyze the removal of inhibitory trimethyl marker of H3K9 and H3K36 related to transcription[98,119]. KDM4A, B, and D play a role in PC mainly. The interaction between regulatory factor X-associated protein RFXAP and KDM4A can disrupt DNA damage repair[120]. RFAXP is a key transcription factor for MHC II molecules[121,122]. It can bind to the promoter of *KDM4A* and induce its expression [120]. In PC, Fisetin can interact with RFXAP/KDM4A to inhibit PC tumor growth *in vivo* and cell proliferation *in vitro*[120]. In PC, KDM4B shows the ability to downregulate E-cadherin[123]. The high nuclear expression of KDM4D in the samples of pancreatic resection margins significantly and independently predicts an earlier recurrence in PC patients[124].

KDM5: KDM5 subfamily consists of four members, KDM5A, KDM5B, KDM5C, and KDM5D[125]. The role of KDM5 family in PC is not completely clear. KDM5A is associated with the development of PC[126]. KDM5A inhibits the expression of mitochondrial pyruvate carrier-1 (MPC-1) and controls the metabolites of pyruvate in mitochondria in PDAC[126]. Upregulation of MPC-1 seems to inhibit the development of cancer. Therefore, it can be inferred that KDM5A promotes the development of PDAC.

Table 2 Histone demethylase that plays a major role in pancreatic cancer

Family	Subfamily		Alias	Site	Function in pancreatic cancer
KDM1	KDM1A		LSD1	H3K4me1	Promote the occurrence of cancer[83]
	KDM1B		LSD2, AOF1	H3K4me2	Related to tumor tissue apoptosis[84]
Jumonji C	KDM2B		Ndy1, FBXL10, JHDM1B	H3K4me3, H3K36me2	Promote senescence of primary cells[109,110]
	KDM3A		JMJD1A, JHDM2A	H3K9me2 (preferential), H3K9me1	Regulate biological and pathological processes, including embryonic development, stem cell self-renewal and differentiation, genome integrity and tumorigenesis[191,192]
	KDM4 family	KDM4A	JMJD2A	H3K36me3, H3K9me3	Destruction of homologous recombination[120,138]
		KDM4B	JMJD2B	H3K9me3	Promote epithelial-mesenchymal transition[123]
		KDM4D	JMJD2D	H3K9me2/me3	Stimulates *in vitro* proliferation and cell survival, and plays a vital role in DNA double-strand break repair[193,194]
	KDM5A		JARID1A, RBBP2	H3K4me2	Promote the inhibition of active transcription and repair of DNA double-strand breaks[139,195]
	KDM6 family	KDM6A	UTX	H3K27me2/me3	The effect of KDM6A on PC tissue is currently unclear[196]
		KDM6B	JMJD3	H3K27me2/me3	Enhance the aggressiveness of cancer cells[176]
	PHD finger and zinc finger protein family	KDM7A	JHDM1D	H3K9me2, H3K27me2	May be related to the upregulation of E-cadherin gene expression[93]

All current research on reprogramming histone demethylases that play a role in pancreatic cancer. The table is sorted by family. PC: Pancreatic cancer; PHD: Plant homeodomain.

KDM6: KDM6 subfamily is mainly composed of KDM6A/UTX, its paralogs UTY and KDM6B[127]. They can demethylate the dimethyl and trimethyl groups of H3K27. They play important roles in the occurrence and development of many cancers. KDM6A/UTX has been the most frequently mutated epigenetic regulator in cancers including PC[128-133]. In addition, KDM6A also antagonizes PRC2-mediated H3K27 trimethylation catalyzed by EZH2, thereby regulating development[99,104,134]. KDM6A has not been found to function in PC tissues. Downregulation of KDM6B is widespread in many cancer cells[135,136]. Almost all pancreatic epithelial tissues have been detected *KRAS* gene mutations before they become cancerous[137]. KDM6B, which is located downstream of the *KRAS* gene, is upregulated in the pre-tumor phase of pancreatic intraepithelial tumors[138]. It is worth noting that the expression of KDM6B decreases with cancer development.

KDM7 (PHF and ZF protein subfamily): At present, the effect of KDM7 subfamily on PC has been seldom developed. According to relevant data, KDM7A may be related to the occurrence and development of PC[139].

READER DOMAIN IN WRITERS AND ERASERS

PHD fingers are central "readers" of histone post-translational modifications. They recognize specific histone modifications and bind to histone to ensure the different enzymes to locate in special targets[140,141]. They are structurally conserved, represented by the canonical C4HC2C/H sequence coordinating two zinc ions. They present in many chromatin-modifying proteins, such as demethylases or methyltransferases, or act as scaffolding proteins that can connect multi-subunit enzymatic complexes with a particular genomic region[30,140,141]. In this part, we will discuss how PHD fingers regulate histone methylation/demethylation and their binding substrates (Table 3).

Regulation of writers by PHD finger

KMT2A-E all have PHD fingers, but the number of PHD fingers in these proteins is different. KMT2A and KMT2B have four PHD fingers, while KMT2C has eight PHD fingers and KMT2D has seven PHD fingers, but KMT2E only has one PHD finger.

Table 3 Different enzymes and plant homeodomain finger domain

Type of enzyme	Name of enzyme	PHD domain	Histone substrates	Function
Histone demethylation enzyme	KDM1B/LSD2	PHD	H3K4me2	Unknown[25]
	KDM2A	PHD	H3K36me2/me1	Unknown[150]
	KDM4A-C	Two PHD	Unknown	Unknown[155,197]
	KDM5A	PHD1	Unmethylated H3K4 histone tail	PHD1 finger by H3 N-terminal tail peptides stabilizes binding of the substrate to the catalytic finger and improves the catalytic efficiency of demethylation[198,199]
		PHD2	Unmodified H3K4	Unknown[158]
		PHD3	H3K4me3	PHD3 finger can recruit substrate and it relates to demethylation propagation along nucleosomes *via* a positive-feedback regulatory mechanism[151,199]
	KDM5B	PHD1	H3K4me0	PHD1 finger recognizes the N-terminus of histone H3, provides an anchoring mechanism for KDM5B and PHD1-H3K4me0 is interaction is important for inhibition of migration[17]
		PHD2	Couldn't bind to histone	Unknown[17]
		PHD3	H3K4me3/H3K4me0	PHD3 finger detects H3K4me3, anchors at chromatin and spreads the transcriptionally inactive state
	KDM5C	PHD1	H3K4	PHD1 finger stabilizes the substrate peptide and helps to position the H3K4 in the JmjC finger exactly[162]
	PHF8(KDM7subfamily)	PHD1	Suppressive marks on H3K9me2/me3 and H3K27me2/me3 and H4k20me2/me3	PHD1 finger plays a significant role in PHF8 substrate recognition and helps to improve substrate affinity and specificity[164]
Histone methylation enzyme	KMT2A, KMT2B	PHD1	Unknown	PHD1 finger is necessary for a context-dependent regulation of holocomplex formation and implicated in tumor suppression[143]
		PHD2	Unknown	PHD2 finger shows the E3 ubiquitin ligase activity and involve in homo-dimerization[144,200]. Mutation in PHD2 will enhance transactivation ability and help to recruit target gene promoters
		PHD3	H3K4me3/me2	Unclear, one possibility is binding of H3K4me3 by PHD3 is necessary for the transcription-promoting effects of KMT2A/2B, another is to set a broad, methylated chromatin finger[145]
		PHD4	Unknown	PHD4 finger mediates intramolecular interactions between the N-terminal and C-terminal fragments of KMT2A with PHD1, and improves its stability[143]
	KMT2C	Eight PHD fingers	Unknown	These fingers help KMT2C to recruit to its target genes correctly[30,146]
	KMT2D	Seven PHD fingers	Unmodified histone H4 and asymmetrical H4R3me2	These fingers are essential for methyltransferase activity of KMT2D and KMT2D-mediated differentiation[201]
	KMT2E	PHD	H3K4me3	PHD finger binds to H3K4me3 specially and facilitates the recruitment of KMT2E to active transcription chromatin regions[148,149,202]

All current research on the regulation of writers and erasers by plant homeodomain domain. "Unknown" means that the corresponding literature was not mentioned. This table is sorted by types and subfamilies of enzymes. JmjC: Jumonji C; KMT: Histone lysine methyltransferase; PHD: Plant homeodomain.

There are 24 PHD fingers in KMT2A-E[142].

Regulation of KMT2A and KMT2B by PHD finger: KMT2A and KMT2B have similar domain architecture and both contain three consecutive PHD fingers, PHD1-3. These consecutive PHD fingers are followed by a bromodomain and the fourth PHD4 finger [142]. The precise function of PHD1 finger in KMT2A and KMT2B is unclear, but it can regulate the intramolecular interactions between N-terminal and C-terminal segments [143]. PHD1 fingers are necessary for holocomplex formation and are implicated in

tumor suppression[143]. PHD2 finger has an E3 ubiquitin ligase in the presence of the E2-conjugating enzyme CDC34[144]. Mutation of the PHD2 finger will cause increased transactivation ability of KMT2A and its recruitment to target genes[142], because of increased protein stability[144]. PHD3 finger binds to H3K4me3/me2, but the affinity between PHD3 finger and H3K4me2 is eight times lower than the affinity between PHD3 finger and H3K4me3[145]. Although PHD3 finger can recognize H3K4me3, the special function of KMT2A in transcriptional maintenance is unclear[145]. One possibility is that binding of H3K4me3 by PHD3 finger is necessary for the transcription-promoting effects of KMT2A, and another possibility is that newly deposited H3K4me3 mark helps KMT2A slide along the gene to set a broad, methylated chromatin domain[145]. The stability of KMT2A is dependent on its intramolecular interaction which is mediated *via* its PHD1 finger with PHD4 finger and the phenylalanine/tyrosine-rich domain of KMT2A[143]. Therefore, PHD4 finger in KMT2A can improve the stability of KMT2A in case of hydrolysis.

Regulation of KMT2C by PHD finger: KMT2C contains eight PHD fingers while KMT2D contains seven PHD fingers[142]. Although the function of PHD fingers in KMT2C is unclear, the functional extended PHD finger is important for KMT2C to be recruited to its target genes[146]. PHD4, PHD5, and PHD6 in KMT2D are tandem and these tandem PHDs can bind to unmethylated or asymmetrically demethylated H4 arginine3[147]. This connection is important for nucleosomal methylation activity and mediates stem cell differentiation by KMT2D[147]. But this binding ability is repressed by symmetrical demethylation on arginine-3 of histone H4 (H4R3me2s), because H4R3me2s can hinder the histone binding ability and catalytic activity in PHD4-6[142,147].

Regulation of KMT2E by PHD finger: The binding of KMT2E and histone is based on its single PHD finger which can bind to H3K4me3, and this special spatial structure of KMT2E makes it possible to recognize H3K4me3[148]. Although KMT2E can also bind to H3K4me2 and H3K4me1, the stability of binding of H3K4me2 and KMT2E is five times weaker than H3K4me3, while the stability of binding of H3K4me1 and KMT2E is sixteen times weaker than H3K4me3[148]. This can facilitate the recruitment of KMT2E to active transcription chromatin regions[148,149].

Regulation of erasers by PHD finger

PHD fingers can be found in KDMs[150,151]. These PHD fingers bind to the tail of H3 to enable the localization of enzymes to specific targets[152], and promote the recruitment of transcription factors or chromatin-associated protein complexes[17].

Regulation of KDM4 subfamily by PHD finger: PHD fingers can be found in KDM4 subfamily. KDM4A, KDM4B, and KDM4C have a catalytic histone demethylase domain, double PHD and Tudor domains, whereas KDM4D contains only a catalytic domain and lacks PHD and Tudor domains[153,154]. Although KDM4A-C have PHD fingers, the function of PHD fingers is unclear[155].

Regulation of KDM5 subfamily by PHD finger: KDM5 subfamily, including KDM5A-D, catalyze demethylation of the transcriptionally activating trimethylated and demethylated lysine-4 mark on H3[100,103,156,157]. KDM5A contains three PHD fingers (PHD1, PHD2, PHD3). Qualitative pull-down assays with isolated PHD1 domain of KDM5A show that it binds to unmodified H3K4 peptide[158]. The PHD1 finger preferentially recognizes unmethylated H3K4 histone tail, which is a KDM5A-mediated trimethylation products of H3K4 (H3K4me3) demethylation[151]. The function of PHD2 finger is unknown. PHD3 finger has been studied in the context of its fusion with nucleoporin NUP98 and it specifically binds to the H3K4me3, with a decrease in affinity for lower methylation states[17,158]. Since these preferred binding substrates are the products of KDM5A-mediated demethylation, a model in which demethylation can propagate along nucleosomes *via* a positive-feedback regulatory mechanism, has been put forward[151].

The KDM5B PHD1 finger can recognize the N-terminus of H3, which is unmodified or methylated at Lys9[17]. The KDM5B PHD2 finger cannot bind to histone. The KDM5B PHD3 finger prefers to bind to H3K4me3[17]. The PHD1 finger specifically binds to H3K4me0, and the PHD3 finger is selective for H3K4me3. A combination of two 'readers' capable of recognizing distinctive epigenetic marks is likely to impact KDM5B activity. Binding of PHD1 to H3K4me0 may provide an anchoring mechanism for KDM5B to sense H3K4me3 through PHD3 and slide along the H3K4me3-enriched promoters, demethylating nearby methylated H3K4 and further spreading the

transcriptionally inactive state of chromatin[17]. In addition, abrogation of H3 tail recognition by point mutation in the PHD1 domain of KDM5B decreases H3K4 demethylation in cells, resulting in the repression of tumor suppressor genes[159]. Therefore, the importance of interaction between PHD1 and H3 tail is proved.

Similarly, the PHD1 finger domain in KDM5C is close to the JmjC domain, and the linker of JmjC domain is 13 amino acids long and is expected to recognize and bind to H3K9me3[157,160]. Although the PHD1 domain is not necessary for the demethylase activity, it helps to recognize the substrate peptide[157,161]. The interaction between PHD1 domain and JmjC domain stabilizes the substrate peptide and the PHD1 domain can help precisely position H3K4 in the JmjC domain[162].

Regulation of KDM7 by PHD finger: PHF8 belongs to KDM7 subfamily and transcriptionally removes suppressive demethylation and monomethylation of lysine 9 and 27 on H3 and lysine 20 on H4[163]. PHF8 has a PHD finger which is closed to the catalytic domain. PHD finger in PHF8 plays a significant role in PHF8 substrate recognition, because it helps to improve substrate affinity and specificity[164]. PHF8 can be recruited to the promoters through the combination of its PHD finger and H3K4me2/3 during the cell cycle transition from G1 to S[107]. Although the functions of PHD fingers can be found in gastric cancer[165], breast cancer[166], colorectal cancer[167], lung cancer[168], *etc.*, the functions of PHD finger are still unclear in PC.

CLINICAL APPLICATION

Epigenetic genes play vital roles in maintaining structural stability and physiological functions of normal chromosomes and are deficient in some patients with PC, thereby serving as potential targets for correcting these deficiencies and precisely killing these aberrant PC cells[169]. The discovery of histone methyltransferases, demethylases and their active sites has provided new insights in the diagnosis and treatment of PC. The active sites and mechanism of the inhibitors in PC treatment are shown in Table 4.

Histone modifications define the previously unrecognized subsets of PC patients with different epigenetic states and therefore represent the prognostic and predictive biomarkers that can be used to guide clinical decisions, such as the use of fluorouracil chemotherapy[170]. H3K4me2, H3K9me2, or H3K18AC expressed at low levels are positively correlated with the poor prognosis of PC[170]. EZH2 expression is higher in PC cells than in normal cells; thus, EZH2 can be used as a potential biomarker for early diagnosis of PDAC[171]. High expression of KDM4D in benign cells near the edge of surgically resected PC tissues is predictive of early recurrence[124]. The discovery of epigenetic biomarkers can provide a great reference for early diagnosis, drug selection and surgery prognosis of PC.

SMYD3 is a candidate therapeutic target against PC, lung cancer and potentially other RAS-driven tumors[172]. In mice, complete loss of SMYD3 function with no apparent phenotype suggests that SMYD3 inhibitors, as chemotherapeutic agents, cause minimal collateral toxicity. The clinically used combination of Raf protein kinase or dual specificity threonine/tyrosine kinase inhibitors and SMYD3 inhibitors can reduce drug toxicity and suppress the development of drug resistance[172].

SMYD3 inhibitor piperidine-4-formamide-acetanilide compound, BCI-121, is a small molecule inhibitor that significantly inhibits proliferation in PC cell lines with high expression of SMYD3. BCI-121 and histone competitively bind to SMYD3; BCI-121 binds inside the lysine channel, which connects cofactor binding sites and histone peptide binding sites[173].

The PRMT5 inhibitor EZP015556 targets *MTAP* (a gene commonly lost in PC) negative tumors, which indicates that it is an effective treatment for a subpopulation of *MTAP* positive tumors. According to the individualized medication approach, the therapeutic response in different patient-derived organoids (PDOs), developed directly from patient tumor tissue is different. The PDO model is used to validate the effectiveness of PMRT5 inhibition as a potential treatment for PDAC[174]. EZH2 expression in PC cells is significantly higher than that in normal pancreatic duct cells and fibroblasts. 3-Deazaneplanocin A (DZNeP) regulates the expression of EZH2 and H3K27me3, synergically enhancing the anti-proliferative activity of gemcitabine and significantly increasing the apoptosis rate of cells[175]. DZNeP is an S-adenosine homocysteine hydrolase inhibitor. DZNeP also enhances the mRNA and protein expression of nucleoside transporter HENT1/HCNT1[175]. The combination of DZNeP and DZNeP/gemcitabine significantly reduces the growth volume of PDAC spheres in selective medium[175].

Table 4 Inhibitors for the treatment of pancreatic cancer

Drug type	Drug name	Active site	Mechanism	Effect	Targeting tumors
Relating to histone methyltransferase	SMYD3 inhibitor piperidine-4-formamide-acetylaniline compound (BCI-121)	It competes with histones to bind SMYD3, binding sites are formed within the SET and post-SET fingers and contained in a deep and narrow substrate binding cavity	BCI-121 is a competitive inhibitor significantly inhibits; SMYD3-substrate interaction and chromatin recruitment	It inhibits cancer cell growth and accumulates during the cell cycle S	High expression of SMYD3 protein in cancer cell lines (pancreatic cancer, lung, prostate and ovarian cancer)[173]
	PRMT5 inhibitor EZP015556	MTAP	-	It works for MTAP He and MTAP PDO	A negative tumor MTAP (a commonly lost gene in pancreatic cancer) [174]
	EZH2 inhibitor 3-Dazocycline A (DZNeP)	It regulates EZH2 and H3K27me3 protein expression	DZNeP inhibit the activity of S-adenosine-L-homocysteine (AdoHcy) hydrolase, which reversely hydrolyzes AdoHcy to adenosine and homocysteine, thereby inhibiting histone methylation	It synergistically enhanced antiproliferative activity of gemcitabine and significantly increased apoptosis rate	Pancreatic ductal carcinoma[175]
Relating to histone demethylase	BET inhibitor JQ1 related to KDM6A	Reducing activity and p63 levels of MYC pathways	GLI1 is the main target gene of the Hh pathway JQ1 reduces the mRNA and protein levels of primary human CAFs. TGF-β is an interstitial activator that JQ1 its induced response	Altered KMT2C (MLL3)-KDM6A (UTX)- PRC2 regulating axis	Pancreatic ductal carcinoma[169,176,177]

All current research on inhibitors for the treatment of pancreatic cancer developed based on histone methylation modification. "-" means that the content does not exist here. This table is sorted according to the correlation with histone methyltransferases and demethylases. CAF: Cancer-associated fibroblast; KMT: Histone lysine methyltransferases; PDO: Patient-derived organoid; PRC2: Polycomb repressive complex 2; TGF-β: Transforming growth factor β.

Bromodomain and extra-terminal (BET) inhibitors and EZH2 inhibitors are designed to rescue the dysregulated KMT2C/MLL3-KDM6A/UTX-PRC2 regulatory axis and have achieved preliminary success in preclinical models. The regulatory axis regulates the expression of various downstream tumor suppressor genes[169]. Therefore, rebalancing this axis represents a new approach to PDAC therapy.

Defects in KDM6A make sex-specific squamous PC sensitive to bromouracil and BET inhibitors[169]. BET inhibitor JQ1 reverses squamous cell differentiation and inhibits tumor growth *in vivo* by decreasing MYC pathway activity and p63 levels [176]. JQ1 affects cancer-associated fibroblast (CAF) activation by acting on the Hedgehog and TGF-β pathways. JQ1 inhibitor converts α-SMA-positive CAFs to α-SMA-negative CAFs, but does not eliminate CAFs[177].

Small molecules containing 8-hydroxyquinoline structure are competitive inhibitors of KDM4 (also known as JMJD2) family, binding active iron to inhibit the activity of KDM4 and regulate demethylation of H3K9 sites[178]. KDM4C inhibitor SD70 can inhibit the growth of prostate cancer cells[179].

Many types of inhibitors of KDM1A have been reported, but the inhibitors of this enzyme are mainly targeted at acute myeloid leukemia or small cell lung cancer, *etc.* And there are few studies on PC. For example, SP2509 is a noncompetitive inhibitor, and is used in current clinical trials for the treatment of acute myeloid leukemia or small cell lung cancer[180]. Ory-1001 effectively inactivates LSD1 and is highly selective for FAD-dependent ammonia oxidase[181]. The application of histone demethylase inhibitors in the treatment of PC is still limited, so it is necessary to strengthen the exploration of the treatment of PC based on the existing research.

FUTURE DIRECTIONS

Histone writers and erasers do not work independently. In fact, the interactions between writers and erasers include the positive correlativity between EZH2 and KDM2B, and the synergistic effects of EZH2 and KDM6A[182,183]. In bladder cancer, the H3K27 demethylase KDM6A gene often has mutations[131,184]. This makes cancer tissues that have lost KDM6A more vulnerable to EZH2 attack[185]. This accelerates the onset of tumors. The expression of EZH2 and KDM2B in ovarian cancer is

positively correlated[183]. Therefore, knocking down the KDM2B gene is beneficial to inhibit the migration of ovarian cancer cells *in vitro*.

Many problems remain in the research of histone modifications. Research on histone methyltransferases is relatively adequate, but there are few articles about the mechanism of SMYD2, so SMYD2 is not mentioned in our review. Current research on histone arginine residue demethylases has not yet fully achieved results. Therefore, only histone lysine residue demethylases are discussed. However, the effect of KDM7 subfamily demethylases on PC has seldom been proved, so only some guesses about the effect of KDM7A are mentioned. Besides, the study of the interactions between writers and erasers in PC is still in a blank state. The role of the reader domain in PC remains unclear. This review only lists the roles of the PHD domain in the localization of histone modifications and the recruitment of related protein complexes. Reader domain is still a potential research direction in PC.

The study of histone methylation and demethylation has enlightening effects on the diagnosis, treatment, and prognosis of PC. Histone modifications can be used to predict in the prognosis of PC patients[171]. Histone methyltransferase and demethylase inhibitors are used clinically to treat PC. The corresponding inhibitors act on the signal regulatory pathway and change the signal expression of downstream target cells, thus regulating the growth and development of cancer cells. At present, the research of histone demethylase inhibitors is inadequate. Therefore, histone demethylase inhibitors need to be further explored.

The effect of histone modifications on PC is interdependent. The interactions between histone modifications and other epigenetic forms can influence the occurrence and progression of cancers such as cervical cancer and breast cancer. The effect of these interactions enlightens the research on PC. DNA methylation and the expression of miRNAs can be regulated by histone methyltransferases and demethylases, thereby causing alternations of developing process of cancer. Histone methyltransferase EZH2 epigenetically silences tumor-suppressor miRNAs, such as miR-139-5p, miR-125b, miR-101, let-7c and miR-200b, thereby promoting cancer cell metastasis[186]. Histone demethylase KDM5B targets H3K4 demethylation of miR-let-7e and promotes tumor cell proliferation through epigenetically inhibiting the tumor suppressor miR[187]. The combination of EZH2 and promoter region induces the expression of specific target protein H3K27me3, thereby reducing the expression of downstream gene, DNA (cytosine-5)-methyltransferase 3A (DNMT3A)[10]. EZH2-H3K27me3-DNMT3A is the key factor of regulating cervical total stimulus molecule Tim-3/galectin-9, which results in immune escape in the process of malignant transformation[10]. It is reasonable to speculate that the interaction between histone methylation and other epigenetic modifications may also play a role in PC. This opinion draws some inspiration and reference to future research of PC.

CONCLUSION

This review focuses on the mechanism of histone methylation in PC. Histone methylation is mainly regulated by writer, reader and eraser. Writer refers to histone methyltransferase, eraser refers to histone demethylase and reader refers to the modification domain of histone methyltransferase and demethylase. Reader can be an independent polypeptide or a component of methyltransferase and demethylase. On the one hand, histone methyltransferase can promote the proliferation and invasion of PC cells. On the other hand, histone methyltransferase can inhibit the proliferation of cancer cells. Histone demethylase promotes the occurrence of PC and is related to apoptosis. Reader domain plays a role in guiding related methyltransferases and demethylases to identify corresponding sites during the methylation and demethylation process.

REFERENCES

1 **Daoud AZ**, Mulholland EJ, Cole G, McCarthy HO. MicroRNAs in Pancreatic Cancer: biomarkers, prognostic, and therapeutic modulators. *BMC Cancer* 2019; **19**: 1130 [PMID: 31752758 DOI: 10.1186/s12885-019-6284-y]

2 **Duffy MJ**, Sturgeon C, Lamerz R, Haglund C, Holubec VL, Klapdor R, Nicolini A, Topolcan O, Heinemann V. Tumor markers in pancreatic cancer: a European Group on Tumor Markers (EGTM) status report. *Ann Oncol* 2010; **21**: 441-447 [PMID: 19690057 DOI: 10.1093/annonc/mdp332]

3 **Ansari D**, Torén W, Zhou Q, Hu D, Andersson R. Proteomic and genomic profiling of pancreatic

cancer. *Cell Biol Toxicol* 2019; **35**: 333-343 [PMID: 30771135 DOI: 10.1007/s10565-019-09465-9]
4 **Goral V**. Pancreatic Cancer: Pathogenesis and Diagnosis. *Asian Pac J Cancer Prev* 2015; **16**: 5619-5624 [PMID: 26320426 DOI: 10.7314/apjcp.2015.16.14.5619]
5 **Dumont R**, Puleo F, Collignon J, Meurisse N, Chavez M, Seidel L, Gast P, Polus M, Loly C, Delvenne P, Meunier P, Hustinx R, Deroover A, Detry O, Louis E, Martinive P, Van Daele D. A single center experience in resectable pancreatic ductal adenocarcinoma : the limitations of the surgery-first approach. Critical review of the literature and proposals for practice update. *Acta Gastroenterol Belg* 2017; **80**: 451-461 [PMID: 29560639]
6 **Puckett Y**, Garfield K. Pancreatic Cancer 2021 [PMID: 30085538]
7 **Labori KJ**, Katz MH, Tzeng CW, Bjørnbeth BA, Cvancarova M, Edwin B, Kure EH, Eide TJ, Dueland S, Buanes T, Gladhaug IP. Impact of early disease progression and surgical complications on adjuvant chemotherapy completion rates and survival in patients undergoing the surgery first approach for resectable pancreatic ductal adenocarcinoma - A population-based cohort study. *Acta Oncol* 2016; **55**: 265-277 [PMID: 26213211 DOI: 10.3109/0284186X.2015.1068445]
8 **Zeng S**, Pöttler M, Lan B, Grützmann R, Pilarsky C, Yang H. Chemoresistance in Pancreatic Cancer. *Int J Mol Sci* 2019; **20** [PMID: 31514451 DOI: 10.3390/ijms20184504]
9 **Hanahan D**, Weinberg RA. Hallmarks of cancer: the next generation. *Cell* 2011; **144**: 646-674 [PMID: 21376230 DOI: 10.1016/j.cell.2011.02.013]
10 **Zhang L**, Tian S, Pei M, Zhao M, Wang L, Jiang Y, Yang T, Zhao J, Song L, Yang X. Crosstalk between histone modification and DNA methylation orchestrates the epigenetic regulation of the costimulatory factors, Tim3 and galectin9, in cervical cancer. *Oncol Rep* 2019; **42**: 2655-2669 [PMID: 31661141 DOI: 10.3892/or.2019.7388]
11 **Ning B**, Li W, Zhao W, Wang R. Targeting epigenetic regulations in cancer. *Acta Biochim Biophys Sin (Shanghai)* 2016; **48**: 97-109 [PMID: 26508480 DOI: 10.1093/abbs/gmv116]
12 **Greer EL**, Shi Y. Histone methylation: a dynamic mark in health, disease and inheritance. *Nat Rev Genet* 2012; **13**: 343-357 [PMID: 22473383 DOI: 10.1038/nrg3173]
13 **Suganuma T**, Workman JL. Signals and combinatorial functions of histone modifications. *Annu Rev Biochem* 2011; **80**: 473-499 [PMID: 21529160 DOI: 10.1146/annurev-biochem-061809-175347]
14 **Bell O**, Tiwari VK, Thomä NH, Schübeler D. Determinants and dynamics of genome accessibility. *Nat Rev Genet* 2011; **12**: 554-564 [PMID: 21747402 DOI: 10.1038/nrg3017]
15 **de Almeida SF**, Grosso AR, Koch F, Fenouil R, Carvalho S, Andrade J, Levezinho H, Gut M, Eick D, Gut I, Andrau JC, Ferrier P, Carmo-Fonseca M. Splicing enhances recruitment of methyltransferase HYPB/Setd2 and methylation of histone H3 Lys36. *Nat Struct Mol Biol* 2011; **18**: 977-983 [PMID: 21792193 DOI: 10.1038/nsmb.2123]
16 **Hyun K**, Jeon J, Park K, Kim J. Writing, erasing and reading histone lysine methylations. *Exp Mol Med* 2017; **49**: e324 [PMID: 28450737 DOI: 10.1038/emm.2017.11]
17 **Klein BJ**, Piao L, Xi Y, Rincon-Arano H, Rothbart SB, Peng D, Wen H, Larson C, Zhang X, Zheng X, Cortazar MA, Peña PV, Mangan A, Bentley DL, Strahl BD, Groudine M, Li W, Shi X, Kutateladze TG. The histone-H3K4-specific demethylase KDM5B binds to its substrate and product through distinct PHD fingers. *Cell Rep* 2014; **6**: 325-335 [PMID: 24412361 DOI: 10.1016/j.celrep.2013.12.021]
18 **Varier RA**, Timmers HT. Histone lysine methylation and demethylation pathways in cancer. *Biochim Biophys Acta* 2011; **1815**: 75-89 [PMID: 20951770 DOI: 10.1016/j.bbcan.2010.10.002]
19 **Zhang J**, Jing L, Li M, He L, Guo Z. Regulation of histone arginine methylation/demethylation by methylase and demethylase (Review). *Mol Med Rep* 2019; **19**: 3963-3971 [PMID: 30942418 DOI: 10.3892/mmr.2019.10111]
20 **McCabe MT**, Mohammad HP, Barbash O, Kruger RG. Targeting Histone Methylation in Cancer. *Cancer J* 2017; **23**: 292-301 [PMID: 28926430 DOI: 10.1097/PPO.0000000000000283]
21 **Chi P**, Allis CD, Wang GG. Covalent histone modifications--miswritten, misinterpreted and mis-erased in human cancers. *Nat Rev Cancer* 2010; **10**: 457-469 [PMID: 20574448 DOI: 10.1038/nrc2876]
22 **Shi Y**, Lan F, Matson C, Mulligan P, Whetstine JR, Cole PA, Casero RA, Shi Y. Histone demethylation mediated by the nuclear amine oxidase homolog LSD1. *Cell* 2004; **119**: 941-953 [PMID: 15620353 DOI: 10.1016/j.cell.2004.12.012]
23 **Tsukada Y**, Fang J, Erdjument-Bromage H, Warren ME, Borchers CH, Tempst P, Zhang Y. Histone demethylation by a family of JmjC domain-containing proteins. *Nature* 2006; **439**: 811-816 [PMID: 16362057 DOI: 10.1038/nature04433]
24 **Karytinos A**, Forneris F, Profumo A, Ciossani G, Battaglioli E, Binda C, Mattevi A. A novel mammalian flavin-dependent histone demethylase. *J Biol Chem* 2009; **284**: 17775-17782 [PMID: 19407342 DOI: 10.1074/jbc.M109.003087]
25 **Fang R**, Barbera AJ, Xu Y, Rutenberg M, Leonor T, Bi Q, Lan F, Mei P, Yuan GC, Lian C, Peng J, Cheng D, Sui G, Kaiser UB, Shi Y, Shi YG. Human LSD2/KDM1b/AOF1 regulates gene transcription by modulating intragenic H3K4me2 methylation. *Mol Cell* 2010; **39**: 222-233 [PMID: 20670891 DOI: 10.1016/j.molcel.2010.07.008]
26 **Torres IO**, Fujimori DG. Functional coupling between writers, erasers and readers of histone and DNA methylation. *Curr Opin Struct Biol* 2015; **35**: 68-75 [PMID: 26496625 DOI: 10.1016/j.sbi.2015.09.007]
27 **Musselman CA**, Khorasanizadeh S, Kutateladze TG. Towards understanding methyllysine readout. *Biochim Biophys Acta* 2014; **1839**: 686-693 [PMID: 24727128 DOI: 10.1016/j.bbagrm.2014.04.001]

28 **Upadhyay AK**, Horton JR, Zhang X, Cheng X. Coordinated methyl-lysine erasure: structural and functional linkage of a Jumonji demethylase domain and a reader domain. *Curr Opin Struct Biol* 2011; **21**: 750-760 [PMID: 21872465 DOI: 10.1016/j.sbi.2011.08.003]

29 **Verrier L**, Vandromme M, Trouche D. Histone demethylases in chromatin cross-talks. *Biol Cell* 2011; **103**: 381-401 [PMID: 21736555 DOI: 10.1042/BC20110028]

30 **Musselman CA**, Kutateladze TG. Handpicking epigenetic marks with PHD fingers. *Nucleic Acids Res* 2011; **39**: 9061-9071 [PMID: 21813457 DOI: 10.1093/nar/gkr613]

31 **Lalonde ME**, Cheng X, Côté J. Histone target selection within chromatin: an exemplary case of teamwork. *Genes Dev* 2014; **28**: 1029-1041 [PMID: 24831698 DOI: 10.1101/gad.236331.113]

32 **Hard R**, Li N, He W, Ross B, Mo GCH, Peng Q, Stein RSL, Komives E, Wang Y, Zhang J, Wang W. Deciphering and engineering chromodomain-methyllysine peptide recognition. *Sci Adv* 2018; **4**: eaau1447 [PMID: 30417094 DOI: 10.1126/sciadv.aau1447]

33 **Yap KL**, Zhou MM. Structure and mechanisms of lysine methylation recognition by the chromodomain in gene transcription. *Biochemistry* 2011; **50**: 1966-1980 [PMID: 21288002 DOI: 10.1021/bi101885m]

34 **El Agha E**, Kramann R, Schneider RK, Li X, Seeger W, Humphreys BD, Bellusci S. Mesenchymal Stem Cells in Fibrotic Disease. *Cell Stem Cell* 2017; **21**: 166-177 [PMID: 28777943 DOI: 10.1016/j.stem.2017.07.011]

35 **Bergamin E**, Blais A, Couture JF. Keeping them all together: β-propeller domains in histone methyltransferase complexes. *J Mol Biol* 2014; **426**: 3363-3375 [PMID: 24853063 DOI: 10.1016/j.jmb.2014.05.010]

36 **Xu C**, Min J. Structure and function of WD40 domain proteins. *Protein Cell* 2011; **2**: 202-214 [PMID: 21468892 DOI: 10.1007/s13238-011-1018-1]

37 **Adams-Cioaba MA**, Min J. Structure and function of histone methylation binding proteins. *Biochem Cell Biol* 2009; **87**: 93-105 [PMID: 19234526 DOI: 10.1139/O08-129]

38 **Liu R**, Gao J, Yang Y, Qiu R, Zheng Y, Huang W, Zeng Y, Hou Y, Wang S, Leng S, Feng D, Yu W, Sun G, Shi H, Teng X, Wang Y. PHD finger protein 1 (PHF1) is a novel reader for histone H4R3 symmetric dimethylation and coordinates with PRMT5-WDR77/CRL4B complex to promote tumorigenesis. *Nucleic Acids Res* 2018; **46**: 6608-6626 [PMID: 29846670 DOI: 10.1093/nar/gky461]

39 **Ma F**, Zhang CY. Histone modifying enzymes: novel disease biomarkers and assay development. *Expert Rev Mol Diagn* 2016; **16**: 297-306 [PMID: 26750583 DOI: 10.1586/14737159.2016.1135057]

40 **Morera L**, Lübbert M, Jung M. Targeting histone methyltransferases and demethylases in clinical trials for cancer therapy. *Clin Epigenetics* 2016; **8**: 57 [PMID: 27222667 DOI: 10.1186/s13148-016-0223-4]

41 **Poulard C**, Corbo L, Le Romancer M. Protein arginine methylation/demethylation and cancer. *Oncotarget* 2016; **7**: 67532-67550 [PMID: 27556302 DOI: 10.18632/oncotarget.11376]

42 **Rakow S**, Pullamsetti SS, Bauer UM, Bouchard C. Assaying epigenome functions of PRMTs and their substrates. *Methods* 2020; **175**: 53-65 [PMID: 31542509 DOI: 10.1016/j.ymeth.2019.09.014]

43 **Zurita-Lopez CI**, Sandberg T, Kelly R, Clarke SG. Human protein arginine methyltransferase 7 (PRMT7) is a type III enzyme forming ω-NG-monomethylated arginine residues. *J Biol Chem* 2012; **287**: 7859-7870 [PMID: 22241471 DOI: 10.1074/jbc.M111.336271]

44 **Song C**, Chen T, He L, Ma N, Li JA, Rong YF, Fang Y, Liu M, Xie D, Lou W. PRMT1 promotes pancreatic cancer growth and predicts poor prognosis. *Cell Oncol (Dordr)* 2020; **43**: 51-62 [PMID: 31520395 DOI: 10.1007/s13402-019-00435-1]

45 **Ge L**, Wang H, Xu X, Zhou Z, He J, Peng W, Du F, Zhang Y, Gong A, Xu M. PRMT5 promotes epithelial-mesenchymal transition *via* EGFR-β-catenin axis in pancreatic cancer cells. *J Cell Mol Med* 2020; **24**: 1969-1979 [PMID: 31851779 DOI: 10.1111/jcmm.14894]

46 **Choucair A**, Pham TH, Omarjee S, Jacquemetton J, Kassem L, Trédan O, Rambaud J, Marangoni E, Corbo L, Treilleux I, Le Romancer M. The arginine methyltransferase PRMT1 regulates IGF-1 signaling in breast cancer. *Oncogene* 2019; **38**: 4015-4027 [PMID: 30692633 DOI: 10.1038/s41388-019-0694-9]

47 **Li Z**, Wang D, Lu J, Huang B, Wang Y, Dong M, Fan D, Li H, Gao Y, Hou P, Li M, Liu H, Pan ZQ, Zheng J, Bai J. Methylation of EZH2 by PRMT1 regulates its stability and promotes breast cancer metastasis. *Cell Death Differ* 2020; **27**: 3226-3242 [PMID: 32895488 DOI: 10.1038/s41418-020-00615-9]

48 **He L**, Hu Z, Sun Y, Zhang M, Zhu H, Jiang L, Zhang Q, Mu D, Zhang J, Gu L, Yang Y, Pan FY, Jia S, Guo Z. PRMT1 is critical to FEN1 expression and drug resistance in lung cancer cells. *DNA Repair (Amst)* 2020; **95**: 102953 [PMID: 32861926 DOI: 10.1016/j.dnarep.2020.102953]

49 **Li M**, An W, Xu L, Lin Y, Su L, Liu X. The arginine methyltransferase PRMT5 and PRMT1 distinctly regulate the degradation of anti-apoptotic protein $CFLAR_L$ in human lung cancer cells. *J Exp Clin Cancer Res* 2019; **38**: 64 [PMID: 30736843 DOI: 10.1186/s13046-019-1064-8]

50 **Yu L**, Li X, Li H, Chen H, Liu H. Rab11a sustains GSK3β/Wnt/β-catenin signaling to enhance cancer progression in pancreatic cancer. *Tumour Biol* 2016; **37**: 13821-13829 [PMID: 27481517 DOI: 10.1007/s13277-016-5172-1]

51 **Ji M**, Fan D, Yuan L, Zhang Y, Dong W, Peng X. EBP50 inhibits pancreatic cancer cell growth and invasion by targeting the β-catenin/E-cadherin pathway. *Exp Ther Med* 2015; **10**: 1311-1316 [PMID: 26622484 DOI: 10.3892/etm.2015.2684]

52 **Zhou W**, Li Y, Gou S, Xiong J, Wu H, Wang C, Yan H, Liu T. MiR-744 increases tumorigenicity of pancreatic cancer by activating Wnt/β-catenin pathway. *Oncotarget* 2015; **6**: 37557-37569 [PMID: 26485754 DOI: 10.18632/oncotarget.5317]

53 **Lin Z**, Chen Y, Lin Z, Chen C, Dong Y. Overexpressing PRMT1 Inhibits Proliferation and Invasion in Pancreatic Cancer by Inverse Correlation of ZEB1. *IUBMB Life* 2018; **70**: 1032-1039 [PMID: 30194893 DOI: 10.1002/iub.1917]

54 **Wang Y**, Hsu JM, Kang Y, Wei Y, Lee PC, Chang SJ, Hsu YH, Hsu JL, Wang HL, Chang WC, Li CW, Liao HW, Chang SS, Xia W, Ko HW, Chou CK, Fleming JB, Wang H, Hwang RF, Chen Y, Qin J, Hung MC. Oncogenic Functions of Gli1 in Pancreatic Adenocarcinoma Are Supported by Its PRMT1-Mediated Methylation. *Cancer Res* 2016; **76**: 7049-7058 [PMID: 27758883 DOI: 10.1158/0008-5472.Can-16-0715]

55 **Yuan Y**, Nie H. Protein arginine methyltransferase 5: a potential cancer therapeutic target. *Cell Oncol (Dordr)* 2021; **44**: 33-44 [PMID: 33469838 DOI: 10.1007/s13402-020-00577-7]

56 **Qin Y**, Hu Q, Xu J, Ji S, Dai W, Liu W, Xu W, Sun Q, Zhang Z, Ni Q, Zhang B, Yu X, Xu X. PRMT5 enhances tumorigenicity and glycolysis in pancreatic cancer *via* the FBW7/cMyc axis. *Cell Commun Signal* 2019; **17**: 30 [PMID: 30922330 DOI: 10.1186/s12964-019-0344-4]

57 **Kim H**, Ronai ZA. PRMT5 function and targeting in cancer. *Cell Stress* 2020; **4**: 199-215 [PMID: 32743345 DOI: 10.15698/cst2020.08.228]

58 **Davis RJ**, Welcker M, Clurman BE. Tumor suppression by the Fbw7 ubiquitin ligase: mechanisms and opportunities. *Cancer Cell* 2014; **26**: 455-464 [PMID: 25314076 DOI: 10.1016/j.ccell.2014.09.013]

59 **Shimizu K**, Nihira NT, Inuzuka H, Wei W. Physiological functions of FBW7 in cancer and metabolism. *Cell Signal* 2018; **46**: 15-22 [PMID: 29474981 DOI: 10.1016/j.cellsig.2018.02.009]

60 **Black JC**, Van Rechem C, Whetstine JR. Histone lysine methylation dynamics: establishment, regulation, and biological impact. *Mol Cell* 2012; **48**: 491-507 [PMID: 23200123 DOI: 10.1016/j.molcel.2012.11.006]

61 **McGrath J**, Trojer P. Targeting histone lysine methylation in cancer. *Pharmacol Ther* 2015; **150**: 1-22 [PMID: 25578037 DOI: 10.1016/j.pharmthera.2015.01.002]

62 **Zhu CL**, Huang Q. Overexpression of the SMYD3 Promotes Proliferation, Migration, and Invasion of Pancreatic Cancer. *Dig Dis Sci* 2020; **65**: 489-499 [PMID: 31441002 DOI: 10.1007/s10620-019-05797-y]

63 **Patil S**, Steuber B, Kopp W, Kari V, Urbach L, Wang X, Küffer S, Bohnenberger H, Spyropoulou D, Zhang Z, Versemann L, Bösherz MS, Brunner M, Gaedcke J, Ströbel P, Zhang JS, Neesse A, Ellenrieder V, Singh SK, Johnsen SA, Hessmann E. EZH2 Regulates Pancreatic Cancer Subtype Identity and Tumor Progression *via* Transcriptional Repression of *GATA6*. *Cancer Res* 2020; **80**: 4620-4632 [PMID: 32907838 DOI: 10.1158/0008-5472.CAN-20-0672]

64 **Giakountis A**, Moulos P, Sarris ME, Hatzis P, Talianidis I. Smyd3-associated regulatory pathways in cancer. *Semin Cancer Biol* 2017; **42**: 70-80 [PMID: 27554136 DOI: 10.1016/j.semcancer.2016.08.008]

65 **Foreman KW**, Brown M, Park F, Emtage S, Harriss J, Das C, Zhu L, Crew A, Arnold L, Shaaban S, Tucker P. Structural and functional profiling of the human histone methyltransferase SMYD3. *PLoS One* 2011; **6**: e22290 [PMID: 21779408 DOI: 10.1371/journal.pone.0022290]

66 **Hamamoto R**, Furukawa Y, Morita M, Iimura Y, Silva FP, Li M, Yagyu R, Nakamura Y. SMYD3 encodes a histone methyltransferase involved in the proliferation of cancer cells. *Nat Cell Biol* 2004; **6**: 731-740 [PMID: 15235609 DOI: 10.1038/ncb1151]

67 **Hamamoto R**, Silva FP, Tsuge M, Nishidate T, Katagiri T, Nakamura Y, Furukawa Y. Enhanced SMYD3 expression is essential for the growth of breast cancer cells. *Cancer Sci* 2006; **97**: 113-118 [PMID: 16441421 DOI: 10.1111/j.1349-7006.2006.00146.x]

68 **Silva FP**, Hamamoto R, Kunizaki M, Tsuge M, Nakamura Y, Furukawa Y. Enhanced methyltransferase activity of SMYD3 by the cleavage of its N-terminal region in human cancer cells. *Oncogene* 2008; **27**: 2686-2692 [PMID: 17998933 DOI: 10.1038/sj.onc.1210929]

69 **Tsuge M**, Hamamoto R, Silva FP, Ohnishi Y, Chayama K, Kamatani N, Furukawa Y, Nakamura Y. A variable number of tandem repeats polymorphism in an E2F-1 binding element in the 5' flanking region of SMYD3 is a risk factor for human cancers. *Nat Genet* 2005; **37**: 1104-1107 [PMID: 16155568 DOI: 10.1038/ng1638]

70 **Wang H**, Liu Y, Tan W, Zhang Y, Zhao N, Jiang Y, Lin C, Hao B, Zhao D, Qian J, Lu D, Jin L, Wei Q, Lin D, He F. Association of the variable number of tandem repeats polymorphism in the promoter region of the SMYD3 gene with risk of esophageal squamous cell carcinoma in relation to tobacco smoking. *Cancer Sci* 2008; **99**: 787-791 [PMID: 18294291 DOI: 10.1111/j.1349-7006.2008.00729.x]

71 **Paladino D**, Yue P, Furuya H, Acoba J, Rosser CJ, Turkson J. A novel nuclear Src and p300 signaling axis controls migratory and invasive behavior in pancreatic cancer. *Oncotarget* 2016; **7**: 7253-7267 [PMID: 26695438 DOI: 10.18632/oncotarget.6635]

72 **Kim KH**, Roberts CW. Targeting EZH2 in cancer. *Nat Med* 2016; **22**: 128-134 [PMID: 26845405 DOI: 10.1038/nm.4036]

73 **Bao Y**, Oguz G, Lee WC, Lee PL, Ghosh K, Li J, Wang P, Lobie PE, Ehmsen S, Ditzel HJ, Wong A, Tan EY, Lee SC, Yu Q. EZH2-mediated PP2A inactivation confers resistance to HER2-targeted breast cancer therapy. *Nat Commun* 2020; **11**: 5878 [PMID: 33208750 DOI: 10.1038/s41467-020-19704-x]

74 **Biswas A**, Mukherjee G, Kondaiah P, Desai KV. Both EZH2 and JMJD6 regulate cell cycle genes in breast cancer. *BMC Cancer* 2020; **20**: 1159 [PMID: 33246425 DOI: 10.1186/s12885-020-07531-8]

75 **Chen J**, Wang F, Xu H, Xu L, Chen D, Wang J, Huang S, Wen Y, Fang L. Long Non-Coding RNA SNHG1 Regulates the Wnt/β-Catenin and PI3K/AKT/mTOR Signaling Pathways *via* EZH2 to Affect the Proliferation, Apoptosis, and Autophagy of Prostate Cancer Cell. *Front Oncol* 2020; **10**: 552907 [PMID: 33194612 DOI: 10.3389/fonc.2020.552907]

76 **Jin X**, Yang C, Fan P, Xiao J, Zhang W, Zhan S, Liu T, Wang D, Wu H. CDK5/FBW7-dependent ubiquitination and degradation of EZH2 inhibits pancreatic cancer cell migration and invasion. *J Biol Chem* 2017; **292**: 6269-6280 [PMID: 28242758 DOI: 10.1074/jbc.M116.764407]

77 **Zhou X**, Gao W, Hua H, Ji Z. LncRNA-BLACAT1 Facilitates Proliferation, Migration and Aerobic Glycolysis of Pancreatic Cancer Cells by Repressing CDKN1C *via* EZH2-Induced H3K27me3. *Front Oncol* 2020; **10**: 539805 [PMID: 33072570 DOI: 10.3389/fonc.2020.539805]

78 **Ma J**, Zhang J, Weng YC, Wang JC. EZH2-Mediated microRNA-139-5p Regulates Epithelial-Mesenchymal Transition and Lymph Node Metastasis of Pancreatic Cancer. *Mol Cells* 2018; **41**: 868-880 [PMID: 30304920 DOI: 10.14348/molcells.2018.0109]

79 **Ma Z**, Huang H, Wang J, Zhou Y, Pu F, Zhao Q, Peng P, Hui B, Ji H, Wang K. Long non-coding RNA SNHG15 inhibits P15 and KLF2 expression to promote pancreatic cancer proliferation through EZH2-mediated H3K27me3. *Oncotarget* 2017; **8**: 84153-84167 [PMID: 29137412 DOI: 10.18632/oncotarget.20359]

80 **Rotili D**, Mai A. Targeting Histone Demethylases: A New Avenue for the Fight against Cancer. *Genes Cancer* 2011; **2**: 663-679 [PMID: 21941621 DOI: 10.1177/1947601911417976]

81 **Suzuki T**, Terashima M, Tange S, Ishimura A. Roles of histone methyl-modifying enzymes in development and progression of cancer. *Cancer Sci* 2013; **104**: 795-800 [PMID: 23560485 DOI: 10.1111/cas.12169]

82 **Burg JM**, Link JE, Morgan BS, Heller FJ, Hargrove AE, McCafferty DG. KDM1 class flavin-dependent protein lysine demethylases. *Biopolymers* 2015; **104**: 213-246 [PMID: 25787087 DOI: 10.1002/bip.22643]

83 **Scoumanne A**, Chen X. The lysine-specific demethylase 1 is required for cell proliferation in both p53-dependent and -independent manners. *J Biol Chem* 2007; **282**: 15471-15475 [PMID: 17409384 DOI: 10.1074/jbc.M701023200]

84 **Shi Y**, Whetstine JR. Dynamic regulation of histone lysine methylation by demethylases. *Mol Cell* 2007; **25**: 1-14 [PMID: 17218267 DOI: 10.1016/j.molcel.2006.12.010]

85 **Liu Y**, Zhang JB, Qin Y, Wang W, Wei L, Teng Y, Guo L, Zhang B, Lin Z, Liu J, Ren ZG, Ye QH, Xie Y. PROX1 promotes hepatocellular carcinoma metastasis by way of up-regulating hypoxia-inducible factor 1α expression and protein stability. *Hepatology* 2013; **58**: 692-705 [PMID: 23505027 DOI: 10.1002/hep.26398]

86 **Ouyang H**, Qin Y, Liu Y, Xie Y, Liu J. Prox1 directly interacts with LSD1 and recruits the LSD1/NuRD complex to epigenetically co-repress CYP7A1 transcription. *PLoS One* 2013; **8**: e62192 [PMID: 23626788 DOI: 10.1371/journal.pone.0062192]

87 **Qin Y**, Zhu W, Xu W, Zhang B, Shi S, Ji S, Liu J, Long J, Liu C, Liu L, Xu J, Yu X. LSD1 sustains pancreatic cancer growth *via* maintaining HIF1α-dependent glycolytic process. *Cancer Lett* 2014; **347**: 225-232 [PMID: 24561118 DOI: 10.1016/j.canlet.2014.02.013]

88 **Chen F**, Yang H, Dong Z, Fang J, Wang P, Zhu T, Gong W, Fang R, Shi YG, Li Z, Xu Y. Structural insight into substrate recognition by histone demethylase LSD2/KDM1b. *Cell Res* 2013; **23**: 306-309 [PMID: 23357850 DOI: 10.1038/cr.2013.17]

89 **Ciccone DN**, Su H, Hevi S, Gay F, Lei H, Bajko J, Xu G, Li E, Chen T. KDM1B is a histone H3K4 demethylase required to establish maternal genomic imprints. *Nature* 2009; **461**: 415-418 [PMID: 19727073 DOI: 10.1038/nature08315]

90 **van Essen D**, Zhu Y, Saccani S. A feed-forward circuit controlling inducible NF-κB target gene activation by promoter histone demethylation. *Mol Cell* 2010; **39**: 750-760 [PMID: 20832726 DOI: 10.1016/j.molcel.2010.08.010]

91 **Lin SL**, Chang DC, Lin CH, Ying SY, Leu D, Wu DT. Regulation of somatic cell reprogramming through inducible mir-302 expression. *Nucleic Acids Res* 2011; **39**: 1054-1065 [PMID: 20870751 DOI: 10.1093/nar/gkq850]

92 **Katz TA**, Huang Y, Davidson NE, Jankowitz RC. Epigenetic reprogramming in breast cancer: from new targets to new therapies. *Ann Med* 2014; **46**: 397-408 [PMID: 25058177 DOI: 10.3109/07853890.2014.923740]

93 **Wang Y**, Sun L, Luo Y, He S. Knockdown of KDM1B inhibits cell proliferation and induces apoptosis of pancreatic cancer cells. *Pathol Res Pract* 2019; **215**: 1054-1060 [PMID: 30846414 DOI: 10.1016/j.prp.2019.02.014]

94 **Noble P**, Vyas M, Al-Attar A, Durrant S, Scholefield J, Durrant L. High levels of cleaved caspase-3 in colorectal tumour stroma predict good survival. *Br J Cancer* 2013; **108**: 2097-2105 [PMID: 23591201 DOI: 10.1038/bjc.2013.166]

95 **Cloos PA**, Christensen J, Agger K, Maiolica A, Rappsilber J, Antal T, Hansen KH, Helin K. The putative oncogene GASC1 demethylates tri- and dimethylated lysine 9 on histone H3. *Nature* 2006; **442**: 307-311 [PMID: 16732293 DOI: 10.1038/nature04837]

96 **Fodor BD**, Kubicek S, Yonezawa M, O'Sullivan RJ, Sengupta R, Perez-Burgos L, Opravil S, Mechtler K, Schotta G, Jenuwein T. Jmjd2b antagonizes H3K9 trimethylation at pericentric heterochromatin in mammalian cells. *Genes Dev* 2006; **20**: 1557-1562 [PMID: 16738407 DOI:

10.1101/gad.388206]
97 **Klose RJ**, Yamane K, Bae Y, Zhang D, Erdjument-Bromage H, Tempst P, Wong J, Zhang Y. The transcriptional repressor JHDM3A demethylates trimethyl histone H3 Lysine 9 and lysine 36. *Nature* 2006; **442**: 312-316 [PMID: 16732292 DOI: 10.1038/nature04853]
98 **Whetstine JR**, Nottke A, Lan F, Huarte M, Smolikov S, Chen Z, Spooner E, Li E, Zhang G, Colaiacovo M, Shi Y. Reversal of histone lysine trimethylation by the JMJD2 family of histone demethylases. *Cell* 2006; **125**: 467-481 [PMID: 16603238 DOI: 10.1016/j.cell.2006.03.028]
99 **Agger K**, Cloos PA, Christensen J, Pasini D, Rose S, Rappsilber J, Issaeva I, Canaani E, Salcini AE, Helin K. UTX and JMJD3 are histone H3K27 demethylases involved in HOX gene regulation and development. *Nature* 2007; **449**: 731-734 [PMID: 17713478 DOI: 10.1038/nature06145]
100 **Christensen J**, Agger K, Cloos PA, Pasini D, Rose S, Sennels L, Rappsilber J, Hansen KH, Salcini AE, Helin K. RBP2 belongs to a family of demethylases, specific for tri-and dimethylated lysine 4 on histone 3. *Cell* 2007; **128**: 1063-1076 [PMID: 17320161 DOI: 10.1016/j.cell.2007.02.003]
101 **De Santa F**, Totaro MG, Prosperini E, Notarbartolo S, Testa G, Natoli G. The histone H3 Lysine-27 demethylase Jmjd3 Links inflammation to inhibition of polycomb-mediated gene silencing. *Cell* 2007; **130**: 1083-1094 [PMID: 17825402 DOI: 10.1016/j.cell.2007.08.019]
102 **Frescas D**, Guardavaccaro D, Bassermann F, Koyama-Nasu R, Pagano M. JHDM1B/FBXL10 is a nucleolar protein that represses transcription of ribosomal RNA genes. *Nature* 2007; **450**: 309-313 [PMID: 17994099 DOI: 10.1038/nature06255]
103 **Klose RJ**, Yan Q, Tothova Z, Yamane K, Erdjument-Bromage H, Tempst P, Gilliland DG, Zhang Y, Kaelin WG Jr. The retinoblastoma binding protein RBP2 is an H3K4 demethylase. *Cell* 2007; **128**: 889-900 [PMID: 17320163 DOI: 10.1016/j.cell.2007.02.013]
104 **Lan F**, Bayliss PE, Rinn JL, Whetstine JR, Wang JK, Chen S, Iwase S, Alpatov R, Issaeva I, Canaani E, Roberts TM, Chang HY, Shi Y. A histone H3 Lysine 27 demethylase regulates animal posterior development. *Nature* 2007; **449**: 689-694 [PMID: 17851529 DOI: 10.1038/nature06192]
105 **Tahiliani M**, Mei P, Fang R, Leonor T, Rutenberg M, Shimizu F, Li J, Rao A, Shi Y. The histone H3K4 demethylase SMCX links REST target genes to X-linked mental retardation. *Nature* 2007; **447**: 601-605 [PMID: 17468742 DOI: 10.1038/nature05823]
106 **Yamane K**, Tateishi K, Klose RJ, Fang J, Fabrizio LA, Erdjument-Bromage H, Taylor-Papadimitriou J, Tempst P, Zhang Y. PLU-1 is an H3K4 demethylase involved in transcriptional repression and breast cancer cell proliferation. *Mol Cell* 2007; **25**: 801-812 [PMID: 17363312 DOI: 10.1016/j.molcel.2007.03.001]
107 **Liu W**, Tanasa B, Tyurina OV, Zhou TY, Gassmann R, Liu WT, Ohgi KA, Benner C, Garcia-Bassets I, Aggarwal AK, Desai A, Dorrestein PC, Glass CK, Rosenfeld MG. PHF8 mediates histone H4 Lysine 20 demethylation events involved in cell cycle progression. *Nature* 2010; **466**: 508-512 [PMID: 20622854 DOI: 10.1038/nature09272]
108 **Kim TD**, Oh S, Shin S, Janknecht R. Regulation of tumor suppressor p53 and HCT116 cell physiology by histone demethylase JMJD2D/KDM4D. *PLoS One* 2012; **7**: e34618 [PMID: 22514644 DOI: 10.1371/journal.pone.0034618]
109 **Tzatsos A**, Pfau R, Kampranis SC, Tsichlis PN. Ndy1/KDM2B immortalizes mouse embryonic fibroblasts by repressing the Ink4a/Arf locus. *Proc Natl Acad Sci U S A* 2009; **106**: 2641-2646 [PMID: 19202064 DOI: 10.1073/pnas.0813139106]
110 **Tzatsos A**, Paskaleva P, Lymperi S, Contino G, Stoykova S, Chen Z, Wong KK, Bardeesy N. Lysine-specific demethylase 2B (KDM2B)-let-7-enhancer of zester homolog 2 (EZH2) pathway regulates cell cycle progression and senescence in primary cells. *J Biol Chem* 2011; **286**: 33061-33069 [PMID: 21757686 DOI: 10.1074/jbc.M111.257667]
111 **He J**, Kallin EM, Tsukada Y, Zhang Y. The H3K36 demethylase Jhdm1b/Kdm^{2}b regulates cell proliferation and senescence through p15(Ink4b). *Nat Struct Mol Biol* 2008; **15**: 1169-1175 [PMID: 18836456 DOI: 10.1038/nsmb.1499]
112 **Pfau R**, Tzatsos A, Kampranis SC, Serebrennikova OB, Bear SE, Tsichlis PN. Members of a family of JmjC domain-containing oncoproteins immortalize embryonic fibroblasts *via* a JmjC domain-dependent process. *Proc Natl Acad Sci U S A* 2008; **105**: 1907-1912 [PMID: 18250326 DOI: 10.1073/pnas.0711865105]
113 **Kottakis F**, Polytarchou C, Foltopoulou P, Sanidas I, Kampranis SC, Tsichlis PN. FGF-2 regulates cell proliferation, migration, and angiogenesis through an NDY1/KDM2B-miR-101-EZH2 pathway. *Mol Cell* 2011; **43**: 285-298 [PMID: 21777817 DOI: 10.1016/j.molcel.2011.06.020]
114 **Tzatsos A**, Paskaleva P, Ferrari F, Deshpande V, Stoykova S, Contino G, Wong KK, Lan F, Trojer P, Park PJ, Bardeesy N. KDM2B promotes pancreatic cancer *via* Polycomb-dependent and -independent transcriptional programs. *J Clin Invest* 2013; **123**: 727-739 [PMID: 23321669 DOI: 10.1172/JCI64535]
115 **Yamane K**, Toumazou C, Tsukada Y, Erdjument-Bromage H, Tempst P, Wong J, Zhang Y. JHDM2A, a JmjC-containing H3K9 demethylase, facilitates transcription activation by androgen receptor. *Cell* 2006; **125**: 483-495 [PMID: 16603237 DOI: 10.1016/j.cell.2006.03.027]
116 **Okada Y**, Scott G, Ray MK, Mishina Y, Zhang Y. Histone demethylase JHDM2A is critical for Tnp1 and Prm1 transcription and spermatogenesis. *Nature* 2007; **450**: 119-123 [PMID: 17943087 DOI: 10.1038/nature06236]
117 **Bailey JM**, Alsina J, Rasheed ZA, McAllister FM, Fu YY, Plentz R, Zhang H, Pasricha PJ, Bardeesy N, Matsui W, Maitra A, Leach SD. DCLK1 marks a morphologically distinct subpopulation of cells with stem cell properties in preinvasive pancreatic cancer. *Gastroenterology*

2014; **146**: 245-256 [PMID: 24096005 DOI: 10.1053/j.gastro.2013.09.050]

118 **Dandawate P**, Ghosh C, Palaniyandi K, Paul S, Rawal S, Pradhan R, Sayed AAA, Choudhury S, Standing D, Subramaniam D, Padhye SB, Gunewardena S, Thomas SM, Neil MO, Tawfik O, Welch DR, Jensen RA, Maliski S, Weir S, Iwakuma T, Anant S, Dhar A. The Histone Demethylase KDM3A, Increased in Human Pancreatic Tumors, Regulates Expression of DCLK1 and Promotes Tumorigenesis in Mice. *Gastroenterology* 2019; **157**: 1646-1659.e11 [PMID: 31442435 DOI: 10.1053/j.gastro.2019.08.018]

119 **Labbé RM**, Holowatyj A, Yang ZQ. Histone lysine demethylase (KDM) subfamily 4: structures, functions and therapeutic potential. *Am J Transl Res* 2013; **6**: 1-15 [PMID: 24349617]

120 **Ding G**, Xu X, Li D, Chen Y, Wang W, Ping D, Jia S, Cao L. Fisetin inhibits proliferation of pancreatic adenocarcinoma by inducing DNA damage *via* RFXAP/KDM4A-dependent histone H3K36 demethylation. *Cell Death Dis* 2020; **11**: 893 [PMID: 33093461 DOI: 10.1038/s41419-020-03019-2]

121 **Gokturk B**, Artac H, van Eggermond MJ, van den Elsen P, Reisli İ. Type III bare lymphocyte syndrome associated with a novel RFXAP mutation: a case report. *Int J Immunogenet* 2012; **39**: 362-364 [PMID: 22390233 DOI: 10.1111/j.1744-313X.2012.01105.x]

122 **Hanna S**, Etzioni A. MHC class I and II deficiencies. *J Allergy Clin Immunol* 2014; **134**: 269-275 [PMID: 25001848 DOI: 10.1016/j.jaci.2014.06.001]

123 **Li S**, Wu L, Wang Q, Li Y, Wang X. KDM4B promotes epithelial-mesenchymal transition through up-regulation of ZEB1 in pancreatic cancer. *Acta Biochim Biophys Sin (Shanghai)* 2015; **47**: 997-1004 [PMID: 26511091 DOI: 10.1093/abbs/gmv107]

124 **Isohookana J**, Haapasaari KM, Soini Y, Karihtala P. KDM4D Predicts Recurrence in Exocrine Pancreatic Cells of Resection Margins from Patients with Pancreatic Adenocarcinoma. *Anticancer Res* 2018; **38**: 2295-2302 [PMID: 29599352 DOI: 10.21873/anticanres.12474]

125 **Rasmussen PB**, Staller P. The KDM5 family of histone demethylases as targets in oncology drug discovery. *Epigenomics* 2014; **6**: 277-286 [PMID: 25111482 DOI: 10.2217/epi.14.14]

126 **Cui J**, Quan M, Xie D, Gao Y, Guha S, Fallon MB, Chen J, Xie K. A novel KDM5A/MPC-1 signaling pathway promotes pancreatic cancer progression *via* redirecting mitochondrial pyruvate metabolism. *Oncogene* 2020; **39**: 1140-1151 [PMID: 31641207 DOI: 10.1038/s41388-019-1051-8]

127 **Hong S**, Cho YW, Yu LR, Yu H, Veenstra TD, Ge K. Identification of JmjC domain-containing UTX and JMJD3 as histone H3 Lysine 27 demethylases. *Proc Natl Acad Sci U S A* 2007; **104**: 18439-18444 [PMID: 18003914 DOI: 10.1073/pnas.0707292104]

128 **Bailey P**, Chang DK, Nones K, Johns AL, Patch AM, Gingras MC, Miller DK, Christ AN, Bruxner TJ, Quinn MC, Nourse C, Murtaugh LC, Harliwong I, Idrisoglu S, Manning S, Nourbakhsh E, Wani S, Fink L, Holmes O, Chin V, Anderson MJ, Kazakoff S, Leonard C, Newell F, Waddell N, Wood S, Xu Q, Wilson PJ, Cloonan N, Kassahn KS, Taylor D, Quek K, Robertson A, Pantano L, Mincarelli L, Sanchez LN, Evers L, Wu J, Pinese M, Cowley MJ, Jones MD, Colvin EK, Nagrial AM, Humphrey ES, Chantrill LA, Mawson A, Humphris J, Chou A, Pajic M, Scarlett CJ, Pinho AV, Giry-Laterriere M, Rooman I, Samra JS, Kench JG, Lovell JA, Merrett ND, Toon CW, Epari K, Nguyen NQ, Barbour A, Zeps N, Moran-Jones K, Jamieson NB, Graham JS, Duthie F, Oien K, Hair J, Grützmann R, Maitra A, Iacobuzio-Donahue CA, Wolfgang CL, Morgan RA, Lawlor RT, Corbo V, Bassi C, Rusev B, Capelli P, Salvia R, Tortora G, Mukhopadhyay D, Petersen GM; Australian Pancreatic Cancer Genome Initiative, Munzy DM, Fisher WE, Karim SA, Eshleman JR, Hruban RH, Pilarsky C, Morton JP, Sansom OJ, Scarpa A, Musgrove EA, Bailey UM, Hofmann O, Sutherland RL, Wheeler DA, Gill AJ, Gibbs RA, Pearson JV, Waddell N, Biankin AV, Grimmond SM. Genomic analyses identify molecular subtypes of pancreatic cancer. *Nature* 2016; **531**: 47-52 [PMID: 26909576 DOI: 10.1038/nature16965]

129 **Biankin AV**, Waddell N, Kassahn KS, Gingras MC, Muthuswamy LB, Johns AL, Miller DK, Wilson PJ, Patch AM, Wu J, Chang DK, Cowley MJ, Gardiner BB, Song S, Harliwong I, Idrisoglu S, Nourse C, Nourbakhsh E, Manning S, Wani S, Gongora M, Pajic M, Scarlett CJ, Gill AJ, Pinho AV, Rooman I, Anderson M, Holmes O, Leonard C, Taylor D, Wood S, Xu Q, Nones K, Fink JL, Christ A, Bruxner T, Cloonan N, Kolle G, Newell F, Pinese M, Mead RS, Humphris JL, Kaplan W, Jones MD, Colvin EK, Nagrial AM, Humphrey ES, Chou A, Chin VT, Chantrill LA, Mawson A, Samra JS, Kench JG, Lovell JA, Daly RJ, Merrett ND, Toon C, Epari K, Nguyen NQ, Barbour A, Zeps N; Australian Pancreatic Cancer Genome Initiative, Kakkar N, Zhao F, Wu YQ, Wang M, Muzny DM, Fisher WE, Brunicardi FC, Hodges SE, Reid JG, Drummond J, Chang K, Han Y, Lewis LR, Dinh H, Buhay CJ, Beck T, Timms L, Sam M, Begley K, Brown A, Pai D, Panchal A, Buchner N, De Borja R, Denroche RE, Yung CK, Serra S, Onetto N, Mukhopadhyay D, Tsao MS, Shaw PA, Petersen GM, Gallinger S, Hruban RH, Maitra A, Iacobuzio-Donahue CA, Schulick RD, Wolfgang CL, Morgan RA, Lawlor RT, Capelli P, Corbo V, Scardoni M, Tortora G, Tempero MA, Mann KM, Jenkins NA, Perez-Mancera PA, Adams DJ, Largaespada DA, Wessels LF, Rust AG, Stein LD, Tuveson DA, Copeland NG, Musgrove EA, Scarpa A, Eshleman JR, Hudson TJ, Sutherland RL, Wheeler DA, Pearson JV, McPherson JD, Gibbs RA, Grimmond SM. Pancreatic cancer genomes reveal aberrations in axon guidance pathway genes. *Nature* 2012; **491**: 399-405 [PMID: 23103869 DOI: 10.1038/nature11547]

130 **Hoadley KA**, Yau C, Wolf DM, Cherniack AD, Tamborero D, Ng S, Leiserson MDM, Niu B, McLellan MD, Uzunangelov V, Zhang J, Kandoth C, Akbani R, Shen H, Omberg L, Chu A, Margolin AA, Van't Veer LJ, Lopez-Bigas N, Laird PW, Raphael BJ, Ding L, Robertson AG, Byers LA, Mills GB, Weinstein JN, Van Waes C, Chen Z, Collisson EA; Cancer Genome Atlas Research

Network, Benz CC, Perou CM, Stuart JM. Multiplatform analysis of 12 cancer types reveals molecular classification within and across tissues of origin. *Cell* 2014; **158**: 929-944 [PMID: 25109877 DOI: 10.1016/j.cell.2014.06.049]

131 **van Haaften G**, Dalgliesh GL, Davies H, Chen L, Bignell G, Greenman C, Edkins S, Hardy C, O'Meara S, Teague J, Butler A, Hinton J, Latimer C, Andrews J, Barthorpe S, Beare D, Buck G, Campbell PJ, Cole J, Forbes S, Jia M, Jones D, Kok CY, Leroy C, Lin ML, McBride DJ, Maddison M, Maquire S, McLay K, Menzies A, Mironenko T, Mulderrig L, Mudie L, Pleasance E, Shepherd R, Smith R, Stebbings L, Stephens P, Tang G, Tarpey PS, Turner R, Turrell K, Varian J, West S, Widaa S, Wray P, Collins VP, Ichimura K, Law S, Wong J, Yuen ST, Leung SY, Tonon G, DePinho RA, Tai YT, Anderson KC, Kahnoski RJ, Massie A, Khoo SK, Teh BT, Stratton MR, Futreal PA. Somatic mutations of the histone H3K27 demethylase gene UTX in human cancer. *Nat Genet* 2009; **41**: 521-523 [PMID: 19330029 DOI: 10.1038/ng.349]

132 **Waddell N**, Pajic M, Patch AM, Chang DK, Kassahn KS, Bailey P, Johns AL, Miller D, Nones K, Quek K, Quinn MC, Robertson AJ, Fadlullah MZ, Bruxner TJ, Christ AN, Harliwong I, Idrisoglu S, Manning S, Nourse C, Nourbakhsh E, Wani S, Wilson PJ, Markham E, Cloonan N, Anderson MJ, Fink JL, Holmes O, Kazakoff SH, Leonard C, Newell F, Poudel B, Song S, Taylor D, Waddell N, Wood S, Xu Q, Wu J, Pinese M, Cowley MJ, Lee HC, Jones MD, Nagrial AM, Humphris J, Chantrill LA, Chin V, Steinmann AM, Mawson A, Humphrey ES, Colvin EK, Chou A, Scarlett CJ, Pinho AV, Giry-Laterriere M, Rooman I, Samra JS, Kench JG, Pettitt JA, Merrett ND, Toon C, Epari K, Nguyen NQ, Barbour A, Zeps N, Jamieson NB, Graham JS, Niclou SP, Bjerkvig R, Grützmann R, Aust D, Hruban RH, Maitra A, Iacobuzio-Donahue CA, Wolfgang CL, Morgan RA, Lawlor RT, Corbo V, Bassi C, Falconi M, Zamboni G, Tortora G, Tempero MA; Australian Pancreatic Cancer Genome Initiative, Gill AJ, Eshleman JR, Pilarsky C, Scarpa A, Musgrove EA, Pearson JV, Biankin AV, Grimmond SM. Whole genomes redefine the mutational landscape of pancreatic cancer. *Nature* 2015; **518**: 495-501 [PMID: 25719666 DOI: 10.1038/nature14169]

133 **Witkiewicz AK**, McMillan EA, Balaji U, Baek G, Lin WC, Mansour J, Mollaee M, Wagner KU, Koduru P, Yopp A, Choti MA, Yeo CJ, McCue P, White MA, Knudsen ES. Whole-exome sequencing of pancreatic cancer defines genetic diversity and therapeutic targets. *Nat Commun* 2015; **6**: 6744 [PMID: 25855536 DOI: 10.1038/ncomms7744]

134 **Welstead GG**, Creyghton MP, Bilodeau S, Cheng AW, Markoulaki S, Young RA, Jaenisch R. X-linked H3K27me3 demethylase Utx is required for embryonic development in a sex-specific manner. *Proc Natl Acad Sci U S A* 2012; **109**: 13004-13009 [PMID: 22826230 DOI: 10.1073/pnas.1210787109]

135 **Agger K**, Cloos PA, Rudkjaer L, Williams K, Andersen G, Christensen J, Helin K. The H3K27me3 demethylase JMJD3 contributes to the activation of the INK4A-ARF locus in response to oncogene- and stress-induced senescence. *Genes Dev* 2009; **23**: 1171-1176 [PMID: 19451217 DOI: 10.1101/gad.510809]

136 **Barradas M**, Anderton E, Acosta JC, Li S, Banito A, Rodriguez-Niedenführ M, Maertens G, Banck M, Zhou MM, Walsh MJ, Peters G, Gil J. Histone demethylase JMJD3 contributes to epigenetic control of INK4a/ARF by oncogenic RAS. *Genes Dev* 2009; **23**: 1177-1182 [PMID: 19451218 DOI: 10.1101/gad.511109]

137 **Kanda M**, Matthaei H, Wu J, Hong SM, Yu J, Borges M, Hruban RH, Maitra A, Kinzler K, Vogelstein B, Goggins M. Presence of somatic mutations in most early-stage pancreatic intraepithelial neoplasia. *Gastroenterology* 2012; **142**: 730-733.e9 [PMID: 22226782 DOI: 10.1053/j.gastro.2011.12.042]

138 **Yamamoto K**, Tateishi K, Kudo Y, Sato T, Yamamoto S, Miyabayashi K, Matsusaka K, Asaoka Y, Ijichi H, Hirata Y, Otsuka M, Nakai Y, Isayama H, Ikenoue T, Kurokawa M, Fukayama M, Kokudo N, Omata M, Koike K. Loss of histone demethylase KDM6B enhances aggressiveness of pancreatic cancer through downregulation of C/EBPα. *Carcinogenesis* 2014; **35**: 2404-2414 [PMID: 24947179 DOI: 10.1093/carcin/bgu136]

139 **Pan MR**, Hsu MC, Chen LT, Hung WC. G9a orchestrates PCL3 and KDM7A to promote histone H3K27 methylation. *Sci Rep* 2015; **5**: 18709 [PMID: 26688070 DOI: 10.1038/srep18709]

140 **Aasland R**, Gibson TJ, Stewart AF. The PHD finger: implications for chromatin-mediated transcriptional regulation. *Trends Biochem Sci* 1995; **20**: 56-59 [PMID: 7701562 DOI: 10.1016/s0968-0004(00)88957-4]

141 **Sanchez R**, Zhou MM. The PHD finger: a versatile epigenome reader. *Trends Biochem Sci* 2011; **36**: 364-372 [PMID: 21514168 DOI: 10.1016/j.tibs.2011.03.005]

142 **Ali M**, Hom RA, Blakeslee W, Ikenouye L, Kutateladze TG. Diverse functions of PHD fingers of the MLL/KMT2 subfamily. *Biochim Biophys Acta* 2014; **1843**: 366-371 [PMID: 24291127 DOI: 10.1016/j.bbamcr.2013.11.016]

143 **Yokoyama A**, Ficara F, Murphy MJ, Meisel C, Naresh A, Kitabayashi I, Cleary ML. Proteolytically cleaved MLL subunits are susceptible to distinct degradation pathways. *J Cell Sci* 2011; **124**: 2208-2219 [PMID: 21670200 DOI: 10.1242/jcs.080523]

144 **Wang J**, Muntean AG, Wu L, Hess JL. A subset of mixed lineage leukemia proteins has plant homeodomain (PHD)-mediated E3 Ligase activity. *J Biol Chem* 2012; **287**: 43410-43416 [PMID: 23129768 DOI: 10.1074/jbc.M112.423855]

145 **Chang PY**, Hom RA, Musselman CA, Zhu L, Kuo A, Gozani O, Kutateladze TG, Cleary ML. Binding of the MLL PHD3 finger to histone H3K4me3 is required for MLL-dependent gene transcription. *J Mol Biol* 2010; **400**: 137-144 [PMID: 20452361 DOI: 10.1016/j.jmb.2010.05.005]

146 **Mathioudaki A**, Ljungström V, Melin M, Arendt ML, Nordin J, Karlsson Å, Murén E, Saksena P, Meadows JRS, Marinescu VD, Sjöblom T, Lindblad-Toh K. Targeted sequencing reveals the somatic mutation landscape in a Swedish breast cancer cohort. *Sci Rep* 2020; **10**: 19304 [PMID: 33168853 DOI: 10.1038/s41598-020-74580-1]

147 **Dhar SS**, Lee SH, Kan PY, Voigt P, Ma L, Shi X, Reinberg D, Lee MG. Trans-tail regulation of MLL4-catalyzed H3K4 methylation by H4R3 symmetric dimethylation is mediated by a tandem PHD of MLL4. *Genes Dev* 2012; **26**: 2749-2762 [PMID: 23249737 DOI: 10.1101/gad.203356.112]

148 **Ali M**, Rincón-Arano H, Zhao W, Rothbart SB, Tong Q, Parkhurst SM, Strahl BD, Deng LW, Groudine M, Kutateladze TG. Molecular basis for chromatin binding and regulation of MLL5. *Proc Natl Acad Sci U S A* 2013; **110**: 11296-11301 [PMID: 23798402 DOI: 10.1073/pnas.1310156110]

149 **Lemak A**, Yee A, Wu H, Yap D, Zeng H, Dombrovski L, Houliston S, Aparicio S, Arrowsmith CH. Solution NMR structure and histone binding of the PHD domain of human MLL5. *PLoS One* 2013; **8**: e77020 [PMID: 24130829 DOI: 10.1371/journal.pone.0077020]

150 **Klose RJ**, Kallin EM, Zhang Y. JmjC-domain-containing proteins and histone demethylation. *Nat Rev Genet* 2006; **7**: 715-727 [PMID: 16983801 DOI: 10.1038/nrg1945]

151 **Torres IO**, Kuchenbecker KM, Nnadi CI, Fletterick RJ, Kelly MJ, Fujimori DG. Histone demethylase KDM5A is regulated by its reader domain through a positive-feedback mechanism. *Nat Commun* 2015; **6**: 6204 [PMID: 25686748 DOI: 10.1038/ncomms7204]

152 **Tsai WW**, Wang Z, Yiu TT, Akdemir KC, Xia W, Winter S, Tsai CY, Shi X, Schwarzer D, Plunkett W, Aronow B, Gozani O, Fischle W, Hung MC, Patel DJ, Barton MC. TRIM24 Links a non-canonical histone signature to breast cancer. *Nature* 2010; **468**: 927-932 [PMID: 21164480 DOI: 10.1038/nature09542]

153 **Hillringhaus L**, Yue WW, Rose NR, Ng SS, Gileadi C, Loenarz C, Bello SH, Bray JE, Schofield CJ, Oppermann U. Structural and evolutionary basis for the dual substrate selectivity of human KDM4 histone demethylase family. *J Biol Chem* 2011; **286**: 41616-41625 [PMID: 21914792 DOI: 10.1074/jbc.M111.283689]

154 **Trojer P**, Zhang J, Yonezawa M, Schmidt A, Zheng H, Jenuwein T, Reinberg D. Dynamic Histone H1 Isotype 4 Methylation and Demethylation by Histone Lysine Methyltransferase G9a/KMT1C and the Jumonji Domain-containing JMJD2/KDM4 Proteins. *J Biol Chem* 2009; **284**: 8395-8405 [PMID: 19144645 DOI: 10.1074/jbc.M807818200]

155 **Berry WL**, Janknecht R. KDM4/JMJD2 histone demethylases: epigenetic regulators in cancer cells. *Cancer Res* 2013; **73**: 2936-2942 [PMID: 23644528 DOI: 10.1158/0008-5472.CAN-12-4300]

156 **Højfeldt JW**, Agger K, Helin K. Histone lysine demethylases as targets for anticancer therapy. *Nat Rev Drug Discov* 2013; **12**: 917-930 [PMID: 24232376 DOI: 10.1038/nrd4154]

157 **Iwase S**, Lan F, Bayliss P, de la Torre-Ubieta L, Huarte M, Qi HH, Whetstine JR, Bonni A, Roberts TM, Shi Y. The X-linked mental retardation gene SMCX/JARID1C defines a family of histone H3 Lysine 4 demethylases. *Cell* 2007; **128**: 1077-1088 [PMID: 17320160 DOI: 10.1016/j.cell.2007.02.017]

158 **Wang GG**, Song J, Wang Z, Dormann HL, Casadio F, Li H, Luo JL, Patel DJ, Allis CD. Haematopoietic malignancies caused by dysregulation of a chromatin-binding PHD finger. *Nature* 2009; **459**: 847-851 [PMID: 19430464 DOI: 10.1038/nature08036]

159 **Zhang Y**, Yang H, Guo X, Rong N, Song Y, Xu Y, Lan W, Zhang X, Liu M, Cao C. The PHD1 finger of KDM5B recognizes unmodified H3K4 during the demethylation of histone H3K4me2/3 by KDM5B. *Protein Cell* 2014; **5**: 837-850 [PMID: 24952722 DOI: 10.1007/s13238-014-0078-4]

160 **Shi X**, Hong T, Walter KL, Ewalt M, Michishita E, Hung T, Carney D, Peña P, Lan F, Kaadige MR, Lacoste N, Cayrou C, Davrazou F, Saha A, Cairns BR, Ayer DE, Kutateladze TG, Shi Y, Côté J, Chua KF, Gozani O. ING2 PHD domain links histone H3 Lysine 4 methylation to active gene repression. *Nature* 2006; **442**: 96-99 [PMID: 16728974 DOI: 10.1038/nature04835]

161 **Johansson C**, Velupillai S, Tumber A, Szykowska A, Hookway ES, Nowak RP, Strain-Damerell C, Gileadi C, Philpott M, Burgess-Brown N, Wu N, Kopec J, Nuzzi A, Steuber H, Egner U, Badock V, Munro S, LaThangue NB, Westaway S, Brown J, Athanasou N, Prinjha R, Brennan PE, Oppermann U. Structural analysis of human KDM5B guides histone demethylase inhibitor development. *Nat Chem Biol* 2016; **12**: 539-545 [PMID: 27214403 DOI: 10.1038/nchembio.2087]

162 **Peng Y**, Alexov E. Cofactors-loaded quaternary structure of lysine-specific demethylase 5C (KDM5C) protein: Computational model. *Proteins* 2016; **84**: 1797-1809 [PMID: 27696497 DOI: 10.1002/prot.25162]

163 **Zhu Z**, Wang Y, Li X, Xu L, Wang X, Sun T, Dong X, Chen L, Mao H, Yu Y, Li J, Chen PA, Chen CD. PHF8 is a histone H3K9me2 demethylase regulating rRNA synthesis. *Cell Res* 2010; **20**: 794-801 [PMID: 20531378 DOI: 10.1038/cr.2010.75]

164 **Horton JR**, Upadhyay AK, Qi HH, Zhang X, Shi Y, Cheng X. Enzymatic and structural insights for substrate specificity of a family of jumonji histone lysine demethylases. *Nat Struct Mol Biol* 2010; **17**: 38-43 [PMID: 20023638 DOI: 10.1038/nsmb.1753]

165 **Zhang H**, Song Y, Yang C, Wu X. UHRF1 mediates cell migration and invasion of gastric cancer. *Biosci Rep* 2018; **38** [PMID: 30352833 DOI: 10.1042/bsr20181065]

166 **Guo X**, Xu Y, Wang P, Li Z, Yang H. Crystallization and preliminary crystallographic analysis of a PHD domain of human JARID1B. *Acta Crystallogr Sect F Struct Biol Cryst Commun* 2011; **67**: 907-910 [PMID: 21821892 DOI: 10.1107/S1744309111021981]

167 **Thompson B**, Townsley F, Rosin-Arbesfeld R, Musisi H, Bienz M. A new nuclear component of the Wnt signalling pathway. *Nat Cell Biol* 2002; **4**: 367-373 [PMID: 11988739 DOI: 10.1038/ncb786]

168 **Wang J**, Zhong M, Liu B, Sha L, Lun Y, Zhang W, Li X, Wang X, Cao J, Ning A, Huang M. Expression and functional analysis of novel molecule - Latcripin-13 domain from Lentinula edodes C91-3 produced in prokaryotic expression system. *Gene* 2015; **555**: 469-475 [PMID: 25447899 DOI: 10.1016/j.gene.2014.11.014]

169 **Qian Y**, Gong Y, Fan Z, Luo G, Huang Q, Deng S, Cheng H, Jin K, Ni Q, Yu X, Liu C. Molecular alterations and targeted therapy in pancreatic ductal adenocarcinoma. *J Hematol Oncol* 2020; **13**: 130 [PMID: 33008426 DOI: 10.1186/s13045-020-00958-3]

170 **Manuyakorn A**, Paulus R, Farrell J, Dawson NA, Tze S, Cheung-Lau G, Hines OJ, Reber H, Seligson DB, Horvath S, Kurdistani SK, Guha C, Dawson DW. Cellular histone modification patterns predict prognosis and treatment response in resectable pancreatic adenocarcinoma: results from RTOG 9704. *J Clin Oncol* 2010; **28**: 1358-1365 [PMID: 20142597 DOI: 10.1200/JCO.2009.24.5639]

171 **Hinton J**, Callan R, Bodine C, Glasgow W, Brower S, Jiang SW, Li J. Potential epigenetic biomarkers for the diagnosis and prognosis of pancreatic ductal adenocarcinomas. *Expert Rev Mol Diagn* 2013; **13**: 431-443 [PMID: 23782251 DOI: 10.1586/erm.13.38]

172 **Mazur PK**, Reynoird N, Khatri P, Jansen PW, Wilkinson AW, Liu S, Barbash O, Van Aller GS, Huddleston M, Dhanak D, Tummino PJ, Kruger RG, Garcia BA, Butte AJ, Vermeulen M, Sage J, Gozani O. SMYD3 Links lysine methylation of MAP3K2 to Ras-driven cancer. *Nature* 2014; **510**: 283-287 [PMID: 24847881 DOI: 10.1038/nature13320]

173 **Peserico A**, Germani A, Sanese P, Barbosa AJ, Di Virgilio V, Fittipaldi R, Fabini E, Bertucci C, Varchi G, Moyer MP, Caretti G, Del Rio A, Simone C. A SMYD3 Small-Molecule Inhibitor Impairing Cancer Cell Growth. *J Cell Physiol* 2015; **230**: 2447-2460 [PMID: 25728514 DOI: 10.1002/jcp.24975]

174 **Driehuis E**, van Hoeck A, Moore K, Kolders S, Francies HE, Gulersonmez MC, Stigter ECA, Burgering B, Geurts V, Gracanin A, Bounova G, Morsink FH, Vries R, Boj S, van Es J, Offerhaus GJA, Kranenburg O, Garnett MJ, Wessels L, Cuppen E, Brosens LAA, Clevers H. Pancreatic cancer organoids recapitulate disease and allow personalized drug screening. *Proc Natl Acad Sci U S A* 2019 [PMID: 31818951 DOI: 10.1073/pnas.1911273116]

175 **Avan A**, Crea F, Paolicchi E, Funel N, Galvani E, Marquez VE, Honeywell RJ, Danesi R, Peters GJ, Giovannetti E. Molecular mechanisms involved in the synergistic interaction of the EZH2 inhibitor 3-deazaneplanocin A with gemcitabine in pancreatic cancer cells. *Mol Cancer Ther* 2012; **11**: 1735-1746 [PMID: 22622284 DOI: 10.1158/1535-7163.MCT-12-0037]

176 **Andricovich J**, Perkail S, Kai Y, Casasanta N, Peng W, Tzatsos A. Loss of KDM6A Activates Super-Enhancers to Induce Gender-Specific Squamous-like Pancreatic Cancer and Confers Sensitivity to BET Inhibitors. *Cancer Cell* 2018; **33**: 512-526.e8 [PMID: 29533787 DOI: 10.1016/j.ccell.2018.02.003]

177 **Yamamoto K**, Tateishi K, Kudo Y, Hoshikawa M, Tanaka M, Nakatsuka T, Fujiwara H, Miyabayashi K, Takahashi R, Tanaka Y, Ijichi H, Nakai Y, Isayama H, Morishita Y, Aoki T, Sakamoto Y, Hasegawa K, Kokudo N, Fukayama M, Koike K. Stromal remodeling by the BET bromodomain inhibitor JQ1 suppresses the progression of human pancreatic cancer. *Oncotarget* 2016; **7**: 61469-61484 [PMID: 27528027 DOI: 10.18632/oncotarget.11129]

178 **King ON**, Li XS, Sakurai M, Kawamura A, Rose NR, Ng SS, Quinn AM, Rai G, Mott BT, Beswick P, Klose RJ, Oppermann U, Jadhav A, Heightman TD, Maloney DJ, Schofield CJ, Simeonov A. Quantitative high-throughput screening identifies 8-hydroxyquinolines as cell-active histone demethylase inhibitors. *PLoS One* 2010; **5**: e15535 [PMID: 21124847 DOI: 10.1371/journal.pone.0015535]

179 **Jin C**, Yang L, Xie M, Lin C, Merkurjev D, Yang JC, Tanasa B, Oh S, Zhang J, Ohgi KA, Zhou H, Li W, Evans CP, Ding S, Rosenfeld MG. Chem-seq permits identification of genomic targets of drugs against androgen receptor regulation selected by functional phenotypic screens. *Proc Natl Acad Sci U S A* 2014; **111**: 9235-9240 [PMID: 24928520 DOI: 10.1073/pnas.1404303111]

180 **Sonnemann J**, Zimmermann M, Marx C, Ebert F, Becker S, Lauterjung ML, Beck JF. LSD1 (KDM1A)-independent effects of the LSD1 inhibitor SP2509 in cancer cells. *Br J Haematol* 2018; **183**: 494-497 [PMID: 29205263 DOI: 10.1111/bjh.14983]

181 **Fang Y**, Liao G, Yu B. LSD1/KDM1A inhibitors in clinical trials: advances and prospects. *J Hematol Oncol* 2019; **12**: 129 [PMID: 31801559 DOI: 10.1186/s13045-019-0811-9]

182 **Yamagishi M**, Uchimaru K. Targeting EZH2 in cancer therapy. *Curr Opin Oncol* 2017; **29**: 375-381 [PMID: 28665819 DOI: 10.1097/CCO.0000000000000390]

183 **Kuang Y**, Lu F, Guo J, Xu H, Wang Q, Xu C, Zeng L, Yi S. Histone demethylase KDM2B upregulates histone methyltransferase EZH2 expression and contributes to the progression of ovarian cancer *in vitro* and in vivo. *Onco Targets Ther* 2017; **10**: 3131-3144 [PMID: 28706445 DOI: 10.2147/OTT.S134784]

184 **Lawrence MS**, Stojanov P, Mermel CH, Robinson JT, Garraway LA, Golub TR, Meyerson M, Gabriel SB, Lander ES, Getz G. Discovery and saturation analysis of cancer genes across 21 tumour types. *Nature* 2014; **505**: 495-501 [PMID: 24390350 DOI: 10.1038/nature12912]

185 **Ler LD**, Ghosh S, Chai X, Thike AA, Heng HL, Siew EY, Dey S, Koh LK, Lim JQ, Lim WK, Myint SS, Loh JL, Ong P, Sam XX, Huang D, Lim T, Tan PH, Nagarajan S, Cheng CW, Ho H, Ng LG, Yuen J, Lin PH, Chuang CK, Chang YH, Weng WH, Rozen SG, Tan P, Creasy CL, Pang ST, McCabe MT, Poon SL, Teh BT. Loss of tumor suppressor KDM6A amplifies PRC2-regulated transcriptional repression in bladder cancer and can be targeted through inhibition of EZH2. *Sci*

Transl Med 2017; **9** [PMID: 28228601 DOI: 10.1126/scitranslmed.aai8312]

186 **Au SL**, Wong CC, Lee JM, Fan DN, Tsang FH, Ng IO, Wong CM. Enhancer of zeste homolog 2 epigenetically silences multiple tumor suppressor microRNAs to promote liver cancer metastasis. *Hepatology* 2012; **56**: 622-631 [PMID: 22370893 DOI: 10.1002/hep.25679]

187 **Mitra D**, Das PM, Huynh FC, Jones FE. Jumonji/ARID1 B (JARID1B) protein promotes breast tumor cell cycle progression through epigenetic repression of microRNA let-7e. *J Biol Chem* 2011; **286**: 40531-40535 [PMID: 21969366 DOI: 10.1074/jbc.M111.304865]

188 **Kwak YT**, Guo J, Prajapati S, Park KJ, Surabhi RM, Miller B, Gehrig P, Gaynor RB. Methylation of SPT5 regulates its interaction with RNA polymerase II and transcriptional elongation properties. *Mol Cell* 2003; **11**: 1055-1066 [PMID: 12718890 DOI: 10.1016/s1097-2765(03)00101-1]

189 **Jansson M**, Durant ST, Cho EC, Sheahan S, Edelmann M, Kessler B, La Thangue NB. Arginine methylation regulates the p53 response. *Nat Cell Biol* 2008; **10**: 1431-1439 [PMID: 19011621 DOI: 10.1038/ncb1802]

190 **Han T**, Jiao F, Hu H, Yuan C, Wang L, Jin ZL, Song WF, Wang LW. EZH2 promotes cell migration and invasion but not alters cell proliferation by suppressing E-cadherin, partly through association with MALAT-1 in pancreatic cancer. *Oncotarget* 2016; **7**: 11194-11207 [PMID: 26848980 DOI: 10.18632/oncotarget.7156]

191 **Kooistra SM**, Helin K. Molecular mechanisms and potential functions of histone demethylases. *Nat Rev Mol Cell Biol* 2012; **13**: 297-311 [PMID: 22473470 DOI: 10.1038/nrm3327]

192 **Pfister SX**, Ahrabi S, Zalmas LP, Sarkar S, Aymard F, Bachrati CZ, Helleday T, Legube G, La Thangue NB, Porter AC, Humphrey TC. SETD2-dependent histone H3K36 trimethylation is required for homologous recombination repair and genome stability. *Cell Rep* 2014; **7**: 2006-2018 [PMID: 24931610 DOI: 10.1016/j.celrep.2014.05.026]

193 **Lee GS**, Subramanian N, Kim AI, Aksentijevich I, Goldbach-Mansky R, Sacks DB, Germain RN, Kastner DL, Chae JJ. The calcium-sensing receptor regulates the NLRP3 inflammasome through Ca2+ and cAMP. *Nature* 2012; **492**: 123-127 [PMID: 23143333 DOI: 10.1038/nature11588]

194 **Khoury-Haddad H**, Nadar-Ponniah PT, Awwad S, Ayoub N. The emerging role of lysine demethylases in DNA damage response: dissecting the recruitment mode of KDM4D/JMJD2D to DNA damage sites. *Cell Cycle* 2015; **14**: 950-958 [PMID: 25714495 DOI: 10.1080/15384101.2015.1014147]

195 **Horton JR**, Liu X, Gale M, Wu L, Shanks JR, Zhang X, Webber PJ, Bell JSK, Kales SC, Mott BT, Rai G, Jansen DJ, Henderson MJ, Urban DJ, Hall MD, Simeonov A, Maloney DJ, Johns MA, Fu H, Jadhav A, Vertino PM, Yan Q, Cheng X. Structural Basis for KDM5A Histone Lysine Demethylase Inhibition by Diverse Compounds. *Cell Chem Biol* 2016; **23**: 769-781 [PMID: 27427228 DOI: 10.1016/j.chembiol.2016.06.006]

196 **Gong F**, Clouaire T, Aguirrebengoa M, Legube G, Miller KM. Histone demethylase KDM5A regulates the ZMYND8-NuRD chromatin remodeler to promote DNA repair. *J Cell Biol* 2017; **216**: 1959-1974 [PMID: 28572115 DOI: 10.1083/jcb.201611135]

197 **Liu H**, Liu L, Holowatyj A, Jiang Y, Yang ZQ. Integrated genomic and functional analyses of histone demethylases identify oncogenic KDM2A isoform in breast cancer. *Mol Carcinog* 2016; **55**: 977-990 [PMID: 26207617 DOI: 10.1002/mc.22341]

198 **Longbotham JE**, Chio CM, Dharmarajan V, Trnka MJ, Torres IO, Goswami D, Ruiz K, Burlingame AL, Griffin PR, Fujimori DG. Histone H3 binding to the PHD1 domain of histone demethylase KDM5A enables active site remodeling. *Nat Commun* 2019; **10**: 94 [PMID: 30626866 DOI: 10.1038/s41467-018-07829-z]

199 **Lan F**, Collins RE, De Cegli R, Alpatov R, Horton JR, Shi X, Gozani O, Cheng X, Shi Y. Recognition of unmethylated histone H3 Lysine 4 Links BHC80 to LSD1-mediated gene repression. *Nature* 2007; **448**: 718-722 [PMID: 17687328 DOI: 10.1038/nature06034]

200 **Fair K**, Anderson M, Bulanova E, Mi H, Tropschug M, Diaz MO. Protein interactions of the MLL PHD fingers modulate MLL target gene regulation in human cells. *Mol Cell Biol* 2001; **21**: 3589-3597 [PMID: 11313484 DOI: 10.1128/mcb.21.10.3589-3597.2001]

201 **Li SS**, Jiang WL, Xiao WQ, Li K, Zhang YF, Guo XY, Dai YQ, Zhao QY, Jiang MJ, Lu ZJ, Wan R. KMT2D deficiency enhances the anti-cancer activity of L48H37 in pancreatic ductal adenocarcinoma. *World J Gastrointest Oncol* 2019; **11**: 599-621 [PMID: 31435462 DOI: 10.4251/wjgo.v11.i8.599]

202 **Zhang X**, Novera W, Zhang Y, Deng LW. MLL5 (KMT2E): structure, function, and clinical relevance. *Cell Mol Life Sci* 2017; **74**: 2333-2344 [PMID: 28188343 DOI: 10.1007/s00018-017-2470-8]

World Journal of Gastroenterology

Submit a Manuscript: https://www.f6publishing.com

World J Gastroenterol 2021 September 28; 27(36): 6025-6038

DOI: 10.3748/wjg.v27.i36.6025

ISSN 1007-9327 (print) ISSN 2219-2840 (online)

REVIEW

Hepatitis B virus infection and hepatocellular carcinoma in sub-Saharan Africa: Implications for elimination of viral hepatitis by 2030?

Edina Amponsah-Dacosta

ORCID number: Edina Amponsah-Dacosta 0000-0002-3913-0457.

Author contributions: Amponsah-Dacosta E defined the topic, performed the literature search, screened, and reviewed the literature, and wrote the manuscript.

Supported by The Harry Crossley Postdoctoral Research Fellowship 2021.

Conflict-of-interest statement: The author has no conflict of interest to disclose.

Manuscript source: Invited manuscript

Edina Amponsah-Dacosta, Vaccines for Africa Initiative, School of Public Health and Family Medicine, University of Cape Town, Cape Town 7925, Western Cape, South Africa

Corresponding author: Edina Amponsah-Dacosta, PhD, Postdoctoral Fellow, Vaccines for Africa Initiative, School of Public Health and Family Medicine, University of Cape Town, Anzio Road, Observatory, Cape Town 7925, Western Cape, South Africa. edina.amponsah-dacosta@uct.ac.za

Abstract

Elimination of viral hepatitis in sub-Saharan Africa by 2030 is an ambitious feat. However, as stated by the World Health Organization, there are unprecedented opportunities to act and make significant contributions to the elimination target. With 60 million people chronically infected with hepatitis B virus (HBV) of whom 38800 are at risk of developing highly fatal hepatocellular carcinoma (HCC) every year, sub-Saharan Africa faces one of the greatest battles towards elimination of viral hepatitis. There is a need to examine progress in controlling the disproportionate burden of HBV-associated HCC in sub-Saharan Africa within the context of this elimination target. By scaling-up coverage of hepatitis B birth dose and early childhood vaccination, we can significantly reduce new cases of HCC by as much as 50% within the next three to five decades. Given the substantial reservoir of chronic HBV carriers however, projections show that HCC incidence and mortality rates in sub-Saharan Africa will double by 2040. This warrants urgent public health attention. The trends in the burden of HCC over the next two decades, will be determined to a large extent by progress in achieving early diagnosis and appropriate linkage to care for high-risk chronic HBV infected persons.

Key Words: Hepatitis B virus; Viral hepatitis, Hepatocellular Carcinoma; Elimination; Human Immunodeficiency Virus; Sub-Saharan Africa

Core Tip: Chronic hepatitis B virus (HBV) infection is the primary risk factor for

Specialty type: Gastroenterology and hepatology

Country/Territory of origin: South Africa

Peer-review report's scientific quality classification
Grade A (Excellent): 0
Grade B (Very good): B
Grade C (Good): 0
Grade D (Fair): 0
Grade E (Poor): 0

Received: February 28, 2021
Peer-review started: February 28, 2021
First decision: May 1, 2021
Revised: May 10, 2021
Accepted: August 13, 2021
Article in press: August 13, 2021
Published online: September 28, 2021

P-Reviewer: Peng S
S-Editor: Wang JL
L-Editor: Webster JR
P-Editor: Li JH

hepatocellular carcinoma (HCC) in sub-Saharan Africa. In 2020, HBV-associated HCC accounted for approximately 36700 deaths. By 2040, it is projected that approximately 72200 people will die each year from this disease without an intensive public health response. The high mortality-to-incidence ratio associated with HCC in sub-Saharan Africa suggests significant inequities in access to appropriate health care. This review examines the evidence on the extent of the disease burden in sub-Saharan Africa and advocates for prioritizing HCC control as part of ongoing viral hepatitis elimination strategies within this region.

Citation: Amponsah-Dacosta E. Hepatitis B virus infection and hepatocellular carcinoma in sub-Saharan Africa: Implications for elimination of viral hepatitis by 2030? *World J Gastroenterol* 2021; 27(36): 6025-6038
URL: https://www.wjgnet.com/1007-9327/full/v27/i36/6025.htm
DOI: https://dx.doi.org/10.3748/wjg.v27.i36.6025

INTRODUCTION

Despite the availability of a safe and effective prophylactic vaccine since 1982, chronic hepatitis B which is a serious liver disease caused by hepatitis B virus (HBV), remains a major global public health threat. Estimates from the World Health Organization's (WHO) current Global Hepatitis Report suggest that in 2015, 3.5% (257 million persons) of the world's population were living with chronic hepatitis B, with the Western Pacific and sub-Saharan African regions bearing the brunt (68%) of the disease burden (WHO, 2017). In addition to this, 887000 deaths due to HBV-associated hepatic sequelae such as acute hepatitis, liver cirrhosis and liver cancer or hepatocellular carcinoma (HCC), were recorded worldwide[1].

With an estimated 830180 associated deaths recorded in 2020, liver cancer remains a leading cause of cancer-related death worldwide, third only to lung (1.8 million deaths) and colorectal (935153 deaths) cancers[2]. Globally, incidence rates of liver cancer have remained high, with 905677 newly diagnosed cases in 2020 [compared to 748000 (5.9% of all cancers) new cases in 2008, for example[3]], representing 4.7% of all cancer cases recorded in that year alone[2]. The most common type of malignant transformation in the liver is HCC (75%-85%), followed by intrahepatic cholangiocarcinoma (10%-15%), with other rare types accounting for the remainder of all primary liver cancers. The geographic distribution of the incidence of HCC tends to mirror that of its major risk factors, chronic hepatitis B and hepatitis C virus (HCV) infection, which account for approximately 56% and 20% of all HCC cases, respectively[2,4-6]. This implies that the highest incidence rates [age-standardized incidence rate (ASIR) > 20 cases per 100000 persons per year] of HCC are recorded in hepatitis B endemic countries including those in sub-Saharan Africa, while non-endemic regions like Europe and North America report relatively lower incidence rates (ASIR < 10 cases per 100000 persons per year)[2,7-9]. A further cause for concern in most resource limited countries within regions like sub-Saharan Africa where HCC screening and diagnostic services, and medical interventions are often inadequate, is the poor survival and extremely high mortality rates associated with HCC. Approximately 93% of patients die within a year of the onset of symptoms[7,9-11]. Evidently, elimination of viral hepatitis caused by HBV and HCV presents the best opportunity to reduce the incidence of HCC, especially in regions like sub-Saharan Africa, where the disease burden and need for intervention are oftentimes the greatest.

Recognizing the devastating impact of viral hepatitis on global health, the WHO in May 2016 adopted a Global Health Sector Strategy on Viral Hepatitis aimed at achieving a 90% reduction in new cases and a 65% reduction in mortality due to HBV and HCV infection, towards an ambitious target of eliminating viral hepatitis by 2030 [12]. To eliminate chronic hepatitis B, the health service targets to be attained by 2030 include; 90% coverage of routine childhood hepatitis B vaccination, a reduction in mother-to-child transmission (MTCT) of HBV such as through > 90% coverage of hepatitis B birth dose vaccination, 100% of all blood donations screened for HBV, 90% of all HBV infections diagnosed, and 80% of eligible persons with chronic hepatitis B linked to appropriate treatment and care[12]. While largely in the planning phase of executing this global strategy, a recent WHO report suggests that overall, member

states are making progress in developing national viral hepatitis management guidelines and strategic plans towards attaining the elimination targets, although availability of dedicated funding to support implementation appears to be an important challenge in some countries[13].

To contribute to the knowledgebase on the scope of the burden of chronic hepatitis B in sub-Saharan Africa, the status and public health response to HBV-associated HCC in sub-Saharan Africa are reviewed. Opportunities and challenges towards achieving the 2030 viral hepatitis elimination target – at least where chronic hepatitis B and HCC are concerned – are also identified, with the intent of arguing for continued financial and technical investments to support ongoing health sector strategies and interventions within sub-Saharan Africa.

GLOBAL BURDEN OF CHRONIC HEPATITIS B

The seroprevalence of chronic hepatitis B which is based on the detection of the hepatitis B surface antigen (HBsAg) within the general population, is highly variable worldwide. This variability is demonstrated by substantial regional and inter-country disparities in the burden of the disease. Available estimates[14] suggest that HBsAg prevalence rates in the Americas, for example, range from < 2% in countries like the United States of America, Mexico, and Guatemala, to 13.55% (95%CI: 9.00-19.89) in Haiti. In the South East Asian region, HBsAg prevalence rates range from 0.82% (95%CI: 0.80–0.84) in Nepal to as high as 6.42% (95%CI: 6.37–6.47) in Thailand. Overall, countries within the Eastern Mediterranean and European regions mostly have lower-intermediate endemicity levels (HBsAg prevalence ranging from 2% to 4.99%) while the Western Pacific can be classified as a high-intermediate endemic region with most countries recording HBsAg prevalence rates > 5%. Within the African region, the lowest HBsAg prevalence rates are reported in countries like Seychelles [0.48% (95%CI: 0.12-1.90)], Eritrea [2.49% (95%CI: 2.32-2.67)], and Algeria [2.89% (95%CI: 2.50-3.33)], while Mauritania [16.16% (95%CI: 14.92-17.49)], Liberia [17.55% (95%CI: 15.70-19.55)], Swaziland [19% (95%CI: 17.65-20.43)], and South Sudan [22.38% (95%CI: 20.10-24.83)] have recorded some of the highest prevalence estimates[14].

EPIDEMIOLOGICAL SHIFT IN THE BURDEN OF CHRONIC HEPATITIS B IN SUB-SAHARAN AFRICA

Historically, sub-Saharan Africa has been classified as hyper-endemic for chronic hepatitis B based on the detection of HBsAg among ≥ 8% of the general population. Table 1 shows the variable prevalence of HBsAg among populations in some sub-Saharan African countries prior to introduction of universal hepatitis B vaccination and how this has changed over time post-vaccine introduction[15-47]. At the peak of the hepatitis B epidemic in sub-Saharan Africa, the disease burden was characterized by a preponderance of horizontal transmission of HBV among young children (between 1-4 years of age), 30%-50% of whom would go on to develop chronic hepatitis B, and later progress to potentially fatal sequelae (mainly liver cirrhosis and HCC) within 30-50 years after infection[15,29,48]. This contrasts with HBV infection acquired during adulthood which carries a considerably lower risk (< 5%) of progression to chronic disease as observed in non-endemic regions of the world.

Currently, the prevalence of HBsAg in sub-Saharan Africa is reported to be 6.1%, equating to 60 million people living with chronic hepatitis B, of which approximately 4.8 million are children < 5 years of age[1]. The decline in the prevalence of HBsAg within the population can be largely attributed to the success of universal childhood hepatitis B vaccination programmes implemented in sub-Saharan Africa since the early 1990s[49]. In most sub-Saharan African countries, the first dose of the hepatitis B vaccine is administered at 6 weeks of age, with the remainder of the regimen completed within the 1st year of life in an effort to interrupt transmission and prevent incident HBV infection in early childhood. Coverage of the third dose of the hepatitis B vaccine in the region is currently estimated at 73%[50]. Countries like The Gambia and South Africa with longstanding hepatitis B vaccination programmes have achieved marked declines in incident infections over time, especially among children < 5 years of age (Table 1).

Despite this success, we are still decades away from realizing the full benefits of universal childhood hepatitis B vaccination programmes in sub-Saharan Africa, given

Table 1 Prevalence of hepatitis B surface antigen among pre- *vs* post-hepatitis B vaccine introduction populations in some sub-Saharan African countries

Country	Year of hepatitis B vaccine introduction[1]	Prevalence of HBsAg (%)		
		Pre-vaccine introduction	Post-vaccine introduction	
			< 15-yr-olds	≥ 15-yr-olds
Burundi	2004	11.0[15]	2.6[16]	1.0-4.6[17]
Democratic Republic of Congo	2007	> 20.7[18]	2.2[19]	3.7[19]
Ethiopia	2007	11.0[20]	4.4[21]	7.4[22]
Gambia	1990	20.0[23]	0.4[24]	10.0[25]
Kenya	2002	11.4[26]	0.9[16]	3.4[27]
Mali	2003	> 8.7[28]	4.9[16]	8.5[16]
Mozambique	2001	14.6[29]	3.7[16]	4.5[30]
Namibia	2009	14.0[31]	2.7[32]	1.8[33]
Nigeria	2004	13.3[34]	11.5[35]	8.2[36]
Rwanda	2002	Approximately 5.0[37]	1.7[16]	2.2[38]
Senegal	2004	11.8[39]	1.6[40]	> 11.0[41]
South Africa	1995	9.6[15]	0.4[42]	4.0[43]
Uganda	2002	10.3[44]	0.6[45]	4.1[45]
Zimbabwe	2000	15.4[46]	4.4[16]	3.3[47]

[1]The year the hepatitis B vaccine was introduced into national Expanded Programme on Immunization. HBsAg: Hepatitis B surface antigen.

the protracted natural history of chronic hepatitis B, and the long interval between early childhood infection and development of chronic sequelae[51,52]. As such, high prevalence rates of HBsAg persist among a reservoir of adult populations, including women of childbearing age, most of whom were born before the introduction of the hepatitis B vaccine or were not fully vaccinated in infancy (Table 1). This continues to feed the epidemic in sub-Saharan Africa, contributing to the 87890 HBV-associated deaths (approximately 10% of the global total) recorded each year[1]. What further compounds the situation in sub-Saharan Africa is the disproportionate burden of human immunodeficiency virus (HIV) co-infection (69% of all HBV-HIV co-infected persons reside in sub-Saharan Africa) which is associated with a more severe prognosis than that observed in HBV mono-infected individuals[53-55]. Emerging evidence also suggests that perinatal transmission or MTCT of HBV, which was previously presumed to be insignificant in the epidemiology of chronic hepatitis B in sub-Saharan Africa, actually contributes to 367250 incident HBV infections (twice the number of paediatric HIV infections) among neonates annually[56]. In fact, the risk of HBV MTCT increases by up to 2.5-fold among the substantial population of HBV-HIV co-infected pregnant women in sub-Saharan Africa, compared to their HBV mono-infected counterparts[57-60]. This is concerning, given that perinatally acquired HBV infections carry a 90% risk of progression to chronic hepatitis B. This implies that hepatitis B vaccination from 6 weeks of age may be inadequate in preventing incident HBV infections among neonates, especially where the burden of maternal HBV-HIV co-infection is high and prevention of HBV MTCT (PMTCT) strategies are sub-optimal, as is the case in most sub-Saharan African countries. This is a stark contrast to HIV MTCT in sub-Saharan Africa which is on course for elimination due to rapid expansion of antenatal screening and access to timely HIV antiretroviral therapy[61]. The marked decline in HIV MTCT has led to a growing population of HIV-exposed uninfected children in sub-Saharan Africa. Of the 14.8 million HIV-exposed uninfected children in the world, 90% live in sub-Saharan Africa[62]. Although inconclusive, there is some evidence to suggest that HIV-exposed uninfected children may have a modified immune response to hepatitis B vaccination and may also be at increased risk for HBV infection, presenting an additional complexity to elimination strategies in sub-Saharan Africa[58,63-66].

EPIDEMIOLOGICAL TRENDS IN HBV-ASSOCIATED HCC IN SUB-SAHARAN AFRICA

Of the 60 million people currently living with chronic hepatitis B in sub-Saharan Africa, 38800 are at risk of developing HCC every year, characterized by an aggressive clinical course[2,67,68]. In addition, approximately 93% (36700) of persons with HCC will die within a year of their diagnosis without appropriate and timely medical intervention[2,11,67]. Most of these HCC cases (and deaths) will occur among a predominantly male population (sex ratio of 2:1) with age at diagnosis ranging between 38-67 years (compared to 50-70 years in resource rich countries), who are in their prime reproductive and working years, draining productive capacity, and placing a further burden on already strained economic, societal, and health, systems in sub-Saharan Africa[9,11,69-71]. While cases of paediatric HCC are diagnosed more frequently in some sub-Saharan African countries than those in Europe and North America for example, they remain uncommon when compared to the HCC incidence among adult populations[72-75]. Within the next two decades, HCC incidence and mortality rates in sub-Saharan Africa are predicted to double (Figure 1[67,76,77]) unless addressed through reforms in regional and national health policy and practice, including intensifying prevention, diagnostic and treatment strategies, in a whole system approach.

A comparison of the 2020 estimates of age-standardized liver cancer (mainly HCC) incidence and mortality (ASMR) rates in sub-Saharan Africa *vs* other regions of the world is shown in Figure 2[2,67,78]. With ASIRs of 8.1 and 4.2, and ASMRs of 7.8 and 4.0 per 100000 persons per year among men and women, respectively, HCC is a common cause of cancer-related morbidity and mortality in sub-Saharan Africa. There are substantial regional variations in HCC incidence and mortality rates across sub-Saharan Africa. Among males for example, the highest HCC ASIRs (> 12.9 per 100000 persons per year) and ASMRs (> 12.6 per 100000 persons per year) are recorded in West African countries, while East African countries generally appear to experience a lower burden (ASIRs < 5.1 and ASMRs < 4.9 per 100000 persons per year) of the disease (Figures 3 and 4)[2,67,78]. It should be noted however, that the true burden of HCC in sub-Saharan Africa is grossly underestimated by as much as 40%, given that cases are often underreported due to challenges in effectively diagnosing the disease, while the quality and coverage of data in population-based cancer registries are suboptimal[9,11,79].

The overall HCC mortality-to-incidence ratio (MIR = 0.95) in sub-Saharan Africa is comparable to that in the Western Pacific and South-East Asian regions (MIR = 0.95) but higher than that in Northern America (MIR = 0.82)[80]. This high MIR reflects disparities in outcomes of HCC in sub-Saharan Africa compared to resource-rich regions, owing to limited availability and accessibility of diagnostic and treatment services[81,82]. These disparities go beyond the clinical context and are rooted in socio-economic inequities. A recent South African study[82] investigating trends in liver cancer-associated mortality found key socio-economic and sex disparities. The average MIR for black South African men and women was 4.0 and 3.3 respectively, compared to 2.2 and 1.8 among their white counterparts. This underscores the inequities in HCC prognosis experienced by socio-economically disadvantaged populations[82]. Evidently, addressing the disproportionate burden of HCC in sub-Saharan Africa will require careful consideration of socio-economic and demographic inequities prevalent within its population.

PREDOMINANCE OF HBV-ASSOCIATED HEPATOCARCINOGENESIS IN SUB-SAHARAN AFRICA

The association of chronic hepatitis B with the development of most cases of HCC [attributable fraction, AF = 50% (95%CI: 39-60)] occurring among sub-Saharan African populations is well established in the literature[5,6,83,84]. The remainder of HCC cases are typically associated with HCV infection [AF = 21% (95%CI: 13-32)] and exposure to the dietary carcinogen, aflatoxin B1, although metabolic syndrome is emerging as an important risk factor in sub-Saharan Africa[6,85-88]. In comparison, the major risk factors for HCC development in low incidence regions of the world (North America, and Western, Central, and Eastern Europe) include host and environmental factors such as genetic predisposition to primary liver cancer, chronic alcohol intake, obesity, hemochromatosis, and exposure to nitrosamines, followed by HCV infection[71,89-

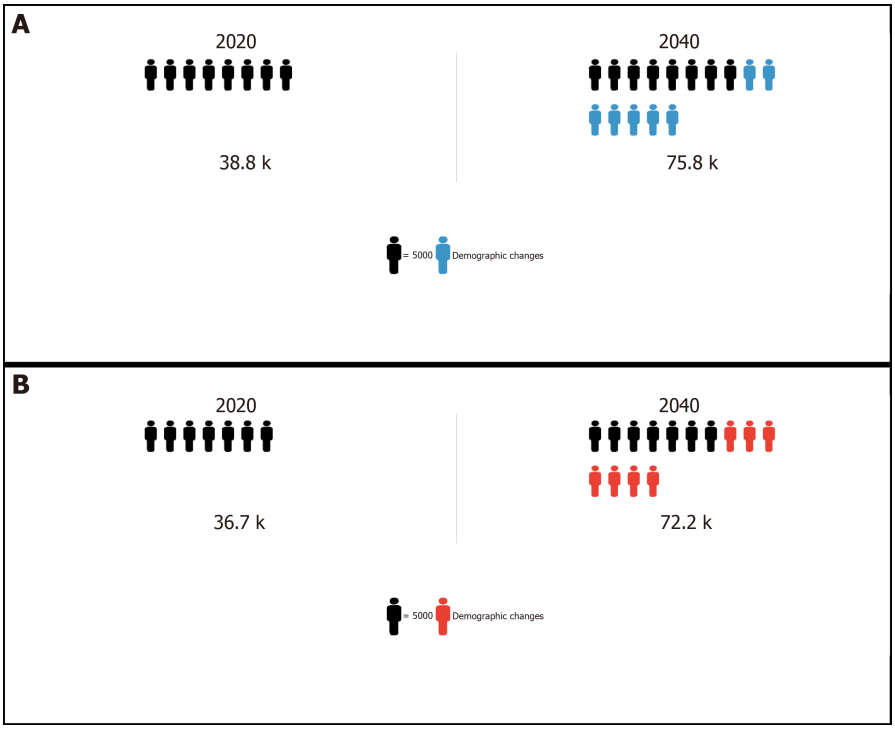

Figure 1 Projected increase in estimated number of cases and deaths due to cancers of the liver and intrahepatic bile ducts within sub-Saharan Africa from 2020 to 2040[67,76,77]. GLOBOCAN 2020 (https://gco.iarc.fr/). A: Estimated number of cases from 2020 to 2040, both sexes, age (0-85+); B: Estimated number of deaths from 2020 to 2040, both sexes, age (0-85+).

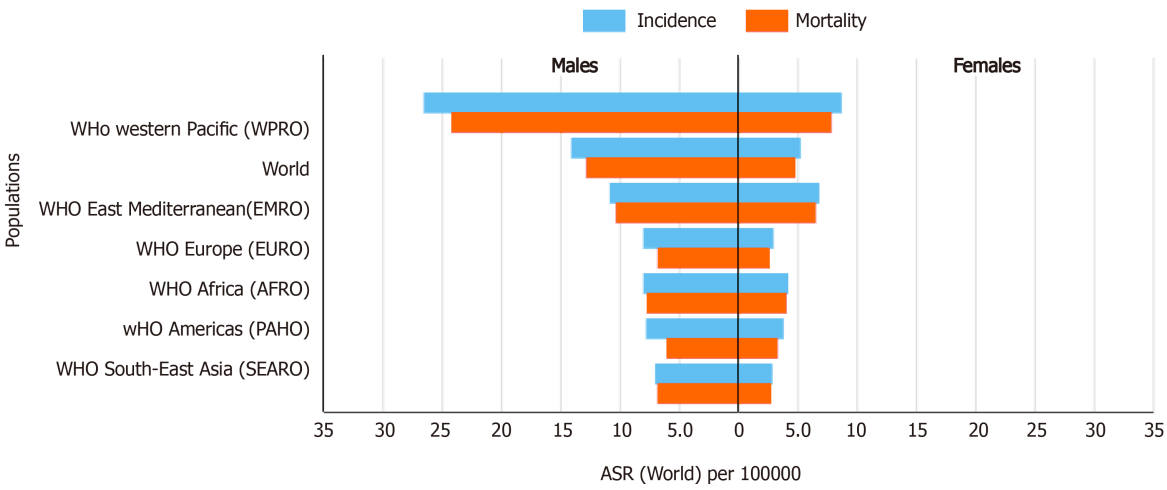

Figure 2 Estimated age-standardized liver cancer incidence and mortality rates per 100000 persons per year shown worldwide in 2020[2,67,78]. GLOBOCAN 2020 (https://gco.iarc.fr/). WHO: World Health Organization; ASR: Liver cancer age standardized incidence rate.

91]. It is worth noting however, that the potential for interaction among these different risk factors, leading to synergistic or additive effects in the development of HCC in both endemic and non-endemic regions of the world cannot be undervalued.

The mechanism underlying HBV-associated hepatocarcinogenesis is multifactorial, involving various direct and indirect viral mechanisms required to stimulate the host oncogenic pathway and achieve hepatocyte transformation[92,93]. These mechanisms, which may act synergistically, include integration of the viral DNA into host genome, persistent and enhanced HBV replication, as well as infection with specific HBV genotypes and HBV genetic variants. Important HBV-specific risk factors involved in the development of HCC have been identified in previous studies conducted in sub-Saharan Africa. In a recent case control study, Atsama Amougou *et al*[94] demonstrated the role of circulating quasi-genotypes and viral genetic variations in HBV-

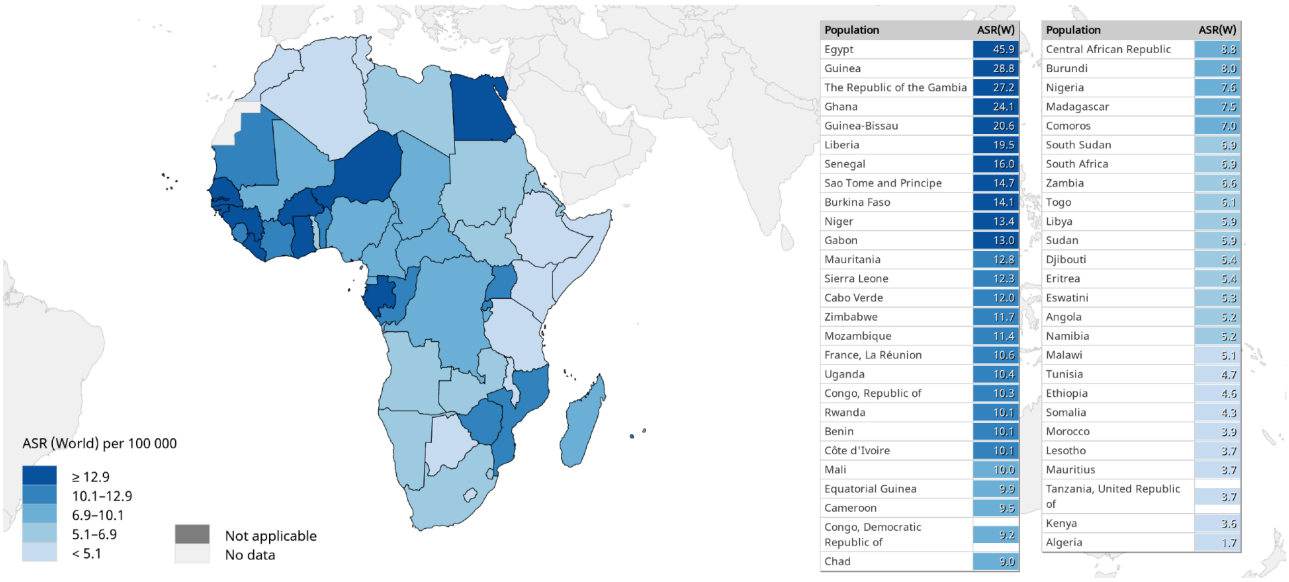

Population	ASR(W)
Egypt	45.9
Guinea	28.8
The Republic of the Gambia	27.2
Ghana	24.1
Guinea-Bissau	20.6
Liberia	19.5
Senegal	16.0
Sao Tome and Principe	14.7
Burkina Faso	14.1
Niger	13.4
Gabon	13.0
Mauritania	12.8
Sierra Leone	12.3
Cabo Verde	12.0
Zimbabwe	11.7
Mozambique	11.4
France, La Réunion	10.6
Uganda	10.4
Congo, Republic of	10.3
Rwanda	10.1
Benin	10.1
Côte d'Ivoire	10.1
Mali	10.0
Equatorial Guinea	9.9
Cameroon	9.5
Congo, Democratic Republic of	9.2
Chad	9.0

Population	ASR(W)
Central African Republic	8.8
Burundi	8.0
Nigeria	7.6
Madagascar	7.5
Comoros	7.0
South Sudan	6.9
South Africa	6.9
Zambia	6.6
Togo	6.1
Libya	5.9
Sudan	5.9
Djibouti	5.4
Eritrea	5.4
Eswatini	5.3
Angola	5.2
Namibia	5.2
Malawi	5.1
Tunisia	4.7
Ethiopia	4.6
Somalia	4.3
Morocco	3.9
Lesotho	3.7
Mauritius	3.7
Tanzania, United Republic of	3.7
Kenya	3.6
Algeria	1.7

Figure 3 Estimated age-standardized liver cancer incidence rates per 100000 persons per year in males in Africa (2020)[2,67,78]. GLOBOCAN 2020 (https://gco.iarc.fr/). The designations employed and the presentation of the material in this publication do not imply the expression of any opinion whatsoever on the part of the World Health Organization/International Agency for Research on Cancer concerning the legal status of any country, territory, city, or area or of its authorities, or concerning the delimitation of its frontiers or boundaries. Dotted or dashed lines on maps represent approximate borderlines for which there may not yet be full agreement.

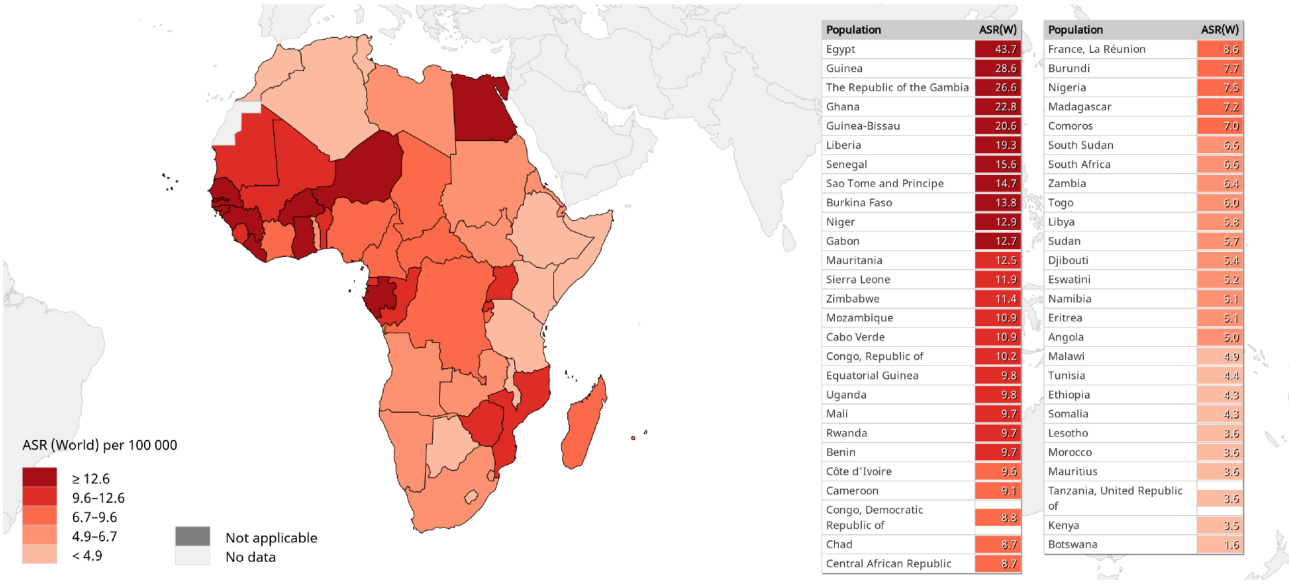

Population	ASR(W)
Egypt	43.7
Guinea	28.6
The Republic of the Gambia	26.6
Ghana	22.8
Guinea-Bissau	20.6
Liberia	19.3
Senegal	15.6
Sao Tome and Principe	14.7
Burkina Faso	13.8
Niger	12.9
Gabon	12.7
Mauritania	12.5
Sierra Leone	11.9
Zimbabwe	11.4
Mozambique	10.9
Cabo Verde	10.9
Congo, Republic of	10.2
Equatorial Guinea	9.8
Uganda	9.8
Mali	9.7
Rwanda	9.7
Benin	9.7
Côte d'Ivoire	9.6
Cameroon	9.1
Congo, Democratic Republic of	8.8
Chad	8.7
Central African Republic	8.7

Population	ASR(W)
France, La Réunion	8.6
Burundi	7.7
Nigeria	7.5
Madagascar	7.2
Comoros	7.0
South Sudan	6.6
South Africa	6.6
Zambia	6.4
Togo	6.0
Libya	5.8
Sudan	5.7
Djibouti	5.4
Eswatini	5.2
Namibia	5.1
Eritrea	5.1
Angola	5.0
Malawi	4.9
Tunisia	4.4
Ethiopia	4.3
Somalia	4.3
Lesotho	3.6
Morocco	3.6
Mauritius	3.6
Tanzania, United Republic of	3.6
Kenya	3.5
Botswana	1.6

Figure 4 Estimated age-standardized liver cancer mortality rates per 100000 persons per year in males in Africa (2020)[2,67,78]. GLOBOCAN 2020 (https://gco.iarc.fr/). The designations employed and the presentation of the material in this publication do not imply the expression of any opinion whatsoever on the part of the World Health Organization/International Agency for Research on Cancer concerning the legal status of any country, territory, city, or area or of its authorities, or concerning the delimitation of its frontiers or boundaries. Dotted or dashed lines on maps represent approximate borderlines for which there may not yet be full agreement.

associated hepatocarcinogenesis among Cameroonian HCC patients. A previous study [95] conducted in South Africa found an increasing risk of HCC with increasing HBV viremia, showing an increasing trend in odds ratio (OR) from ≥ 2000 IU/mL (OR = 8.55, 95%CI: 3.00 ± 24.54) to ≥ 200000 IU/mL (OR 16.93, 95%CI: 8.65 ± 33.13). While this finding is consistent with that from another study conducted in The Gambia, there is evidence to suggest that low-level viremia may also be a significant risk factor for HCC[96]. The South African study further demonstrated a 4-fold increase in the risk of developing HCC among participants with occult HBV infection (HBsAg negative but HBV DNA positive infections) compared to controls[95]. Interestingly, a previous longitudinal study conducted in The Gambia which followed chronic carriers of HBV

over a median duration of 28.4 years (interquartile rage = 17.7-32.7) found that maternal HBsAg positivity – as a proxy of MTCT of HBV – was statistically significantly (P < 0.001) associated with a higher incidence of HCC [crude incidence rates of 89.2 (95%CI: 22.3–356.8) *vs* 0 (unadjusted) per 100 000 persons per year, among those born to HBsAg positive *vs* HBsAg negative mothers][70]. Based on these findings, the authors recommend further investigation into the feasibility of scaling-up implementation of hepatitis B birth dose vaccination and other PMTCT strategies within sub-Saharan Africa in order to interrupt incident HBV infections among neonates[70]. Of the 111 countries which report having introduced a hepatitis B birth dose as part of national routine immunization programmes, only 11 (Algeria, Botswana, Cabo Verde, Côte d'Ivoire, The Gambia, Mauritania, Namibia, Nigeria, Sao Tome and Principe, Senegal, and Zambia) are in Africa[50]. While the global coverage of the birth dose is reported to be suboptimal (43%), that in the sub-Saharan African region is even more dismal at an estimated 6%[50]. When considered together with the reported low coverage of maternal screening for HBV infection and linkage to antiviral prophylaxis, current PMTCT strategies are inadequate to significantly reduce perinatal transmission and avert neonatal HBV infections within the region[97,98].

CHALLENGES AFFECTING MANAGEMENT OF HBV-ASSOCIATED HCC IN SUB-SAHARAN AFRICA

Management of chronic hepatitis B involves suppressing HBV viremia and minimizing the risk of progression to liver cirrhosis, chronic liver failure and HCC, using oral nucleotide/nucleoside analogues like tenofovir disoproxil fumarate (TDF) and entecavir. Treatment with nucleotide/nucleoside analogues is indicated in chronic carriers with elevated HBV viremia, elevated liver enzymes, and evidence of liver fibrosis and cirrhosis. Appropriate linkage to care requires the identification of chronically infected individuals who are eligible for treatment through HBV screening programmes[99]. It is estimated that < 1% of chronic HBV infected individuals in sub-Saharan Africa are currently being diagnosed[100]. In addition, there are major gaps in determining treatment eligibility. Significant limitations have been identified when applying internationally recommended treatment eligibility criteria in the sub-Saharan African context. Only 10%–15% of persons with liver cirrhosis are detected for linkage to appropriate treatment[99-102].

Low uptake of HBV screening and treatment services in sub-Saharan Africa has been attributed to the lack of publicly funded, national HBV screening and treatment programmes. This leaves the responsibility for seeking an HBV test to the patient, which is highly detrimental when considered in the context of limited public awareness of the virus, and the asymptomatic nature of the infection until onset of late-stage sequelae[103]. As currently available nucleotide/nucleoside analogues cannot eradicate intrahepatic HBV DNA, treatment is typically lifelong, and this amounts to a significant cost[100,102]. A recent WHO report indicates that by 2019, < 8 of the 47 member states within the WHO African region (WHO AFRO) had established subsidized HBV treatment programmes[16]. This suggests that a substantial proportion of chronic HBV carriers continue to incur undue financial burden as a consequence of paying out-of-pocket for the treatment they need, while others may be unable to afford it altogether. In Ghana, the annual cost of TDF is estimated at $670 which, when considered against an average annual income of $1778, is a major constraint to accessing lifesaving treatment[104]. It should not come as a surprise then that most patients in sub-Saharan Africa present to health care facilities with established liver cirrhosis or symptomatic advanced-stage HCC, at which point the prognosis is grim and therapeutic options are limited to palliative care.

TOWARDS ELIMINATION OF CHRONIC HEPATITIS B AND CONTROL OF HCC IN SUB-SAHARAN AFRICA

Future trends in the burden of HCC in sub-Saharan Africa will be determined by our progress in preventing new HBV infections, screening and treating existing chronic hepatitis B cases, as well as detecting and appropriately managing HCC. As part of a scorecard to monitor progress towards elimination of viral hepatitis within WHO AFRO in 2019, six core indicators were listed; (1) development of national hepatitis policies in the form of a national strategic plan for viral hepatitis; (2) implementation

of hepatitis B birth dose vaccination; (3) achieving > 90% national coverage of the third dose of the hepatitis B vaccine; (4) being on track for the HBV and HCV 2020 testing target; (5) implementation of a national hepatitis treatment programme; and (6) commemoration of World Hepatitis Day in 2018. Overall, most sub-Saharan African countries were found lagging in almost all indicators[16].

Within the next decade, there is a need to scale-up primary prevention of incident HBV infections in sub-Saharan Africa. Despite adopting resolutions to improve hepatitis B birth dose and routine childhood vaccination in WHO AFRO by 2020, implementation and coverage of the birth dose remains unacceptably low, while coverage of routine childhood vaccination remains well below the global average of 84%[49,105,106]. Recognizing the significant threat of HBV MTCT to public health in sub-Saharan Africa, there have been renewed calls to expand access to the hepatitis B birth dose and leverage HIV PMTCT infrastructure in screening pregnant women and providing timely prophylaxis[56,98,107]. The future research agenda in sub-Saharan Africa should include investigating the need for tailored hepatitis B vaccination strategies for unique populations like HIV-exposed uninfected children.

As national governments grapple with the feasibility of implementing subsidized hepatitis surveillance and treatment programmes, the success of the HIV test and treat model in sub-Saharan Africa has been recognized as an opportunity to expand screening and antiviral treatment for chronic hepatitis B in the interim. To ensure a comprehensive package of care, there is a need to prioritize integration of cost-effective point-of-care screening tests with good diagnostic accuracy, guided by appropriate treatment eligibility criteria[49,108].

Within the past decade, there have been significant advances in the development of new diagnostic and therapeutic approaches for HCC, with prospects for further innovation in the field[109,110]. These advances present unique opportunities to improve surveillance and management of HCC. Biannual surveillance among high-risk chronic carriers of HBV using both liver ultrasonography and serum α-fetoprotein concentrations, is commonly used for early detection of progression to HCC. Curative treatment approaches for early-stage HCC include surgical resection, tumour ablation, or liver transplantation. For advanced-stage HCC, combination treatment using atezolizumab and bevacizumab over sorafenib alone, have shown promising long-term outcomes in phase III clinical trials[110]. Other immunotherapeutic agents for the treatment of late-stage HCC have also been recently explored[109]. While all these advancements present much needed opportunities to improve the quality of life of patients with HCC, the cost and feasibility of implementation within the sub-Saharan African public health context are always important considerations.

CONCLUSION

Ultimately, sub-Saharan Africa faces one of the toughest battles against chronic hepatitis B and HCC. Despite this, there are opportunities to achieve significant reductions in incident HBV infections and alter future trends in the burden of HCC. This calls for strong political will, regional coordination, and effective partnerships with donor agencies and non-governmental organizations in order to mobilize financial investments and technical support. Finally, the role of advocacy and awareness campaigns like World Hepatitis Day in enabling public ownership and demand for accessible, equitable, and quality health services cannot be undervalued.

REFERENCES

1 **World Health Organization**. Global hepatitis report, 2017. Geneva: World Health Organization, 2017

2 **Sung H**, Ferlay J, Siegel RL, Laversanne M, Soerjomataram I, Jemal A, Bray F. Global Cancer Statistics 2020: GLOBOCAN Estimates of Incidence and Mortality Worldwide for 36 Cancers in 185 Countries. *CA Cancer J Clin* 2021; **71**: 209-249 [PMID: 33538338 DOI: 10.3322/caac.21660]

3 **Ferlay J**, Shin HR, Bray F, Forman D, Mathers C, Parkin DM. Estimates of worldwide burden of cancer in 2008: GLOBOCAN 2008. *Int J Cancer* 2010; **127**: 2893-2917 [PMID: 21351269 DOI: 10.1002/ijc.25516]

4 **Herbst DA**, Reddy KR. Risk factors for hepatocellular carcinoma. *Clin Liver Dis (Hoboken)* 2012; **1**: 180-182 [PMID: 31186882 DOI: 10.1002/cld.111]

5 **de Martel C**, Maucort-Boulch D, Plummer M, Franceschi S. World-wide relative contribution of hepatitis B and C viruses in hepatocellular carcinoma. *Hepatology* 2015; **62**: 1190-1200 [PMID:

26146815 DOI: 10.1002/hep.27969]
6 **Maucort-Boulch D**, de Martel C, Franceschi S, Plummer M. Fraction and incidence of liver cancer attributable to hepatitis B and C viruses worldwide. *Int J Cancer* 2018; **142**: 2471-2477 [PMID: 29388206 DOI: 10.1002/ijc.31280]
7 **Ozakyol A**. Global Epidemiology of Hepatocellular Carcinoma (HCC Epidemiology). *J Gastrointest Cancer* 2017; **48**: 238-240 [PMID: 28626852 DOI: 10.1007/s12029-017-9959-0]
8 **Tang A**, Hallouch O, Chernyak V, Kamaya A, Sirlin CB. Epidemiology of hepatocellular carcinoma: target population for surveillance and diagnosis. *Abdom Radiol (NY)* 2018; **43**: 13-25 [PMID: 28647765 DOI: 10.1007/s00261-017-1209-1]
9 **Zakharia K**, Luther CA, Alsabbak H, Roberts LR. Hepatocellular carcinoma: Epidemiology, pathogenesis and surveillance - implications for sub-Saharan Africa. *S Afr Med J* 2018; **108**: 35-40 [PMID: 30182911 DOI: 10.7196/SAMJ.2018.v108i8b.13499]
10 **Kew MC**. Hepatocellular carcinoma in developing countries: Prevention, diagnosis and treatment. *World J Hepatol* 2012; **4**: 99-104 [PMID: 22489262 DOI: 10.4254/wjh.v4.i3.99]
11 **Kew MC**. Epidemiology of hepatocellular carcinoma in sub-Saharan Africa. *Ann Hepatol* 2013; **12**: 173-182 [PMID: 23396727]
12 **World Health Organization**. Global health sector strategy on viral hepatitis 2016–2021: towards ending viral hepatitis. Geneva: World Health Organization, 2016
13 **Smith S**, Harmanci H, Hutin Y, Hess S, Bulterys M, Peck R, Rewari B, Mozalevskis A, Shibeshi M, Mumba M, Le LV, Ishikawa N, Nolna D, Sereno L, Gore C, Goldberg DJ, Hutchinson S. Global progress on the elimination of viral hepatitis as a major public health threat: An analysis of WHO Member State responses 2017. *JHEP Rep* 2019; **1**: 81-89 [PMID: 32039355 DOI: 10.1016/j.jhepr.2019.04.002]
14 **Schweitzer A**, Horn J, Mikolajczyk RT, Krause G, Ott JJ. Estimations of worldwide prevalence of chronic hepatitis B virus infection: a systematic review of data published between 1965 and 2013. *Lancet* 2015; **386**: 1546-1555 [PMID: 26231459 DOI: 10.1016/S0140-6736(15)61412-X]
15 **Kiire CF**. The epidemiology and prophylaxis of hepatitis B in sub-Saharan Africa: a view from tropical and subtropical Africa. *Gut* 1996; **38** Suppl 2: S5-12 [PMID: 8786055 DOI: 10.1136/gut.38.suppl_2.s5]
16 **World Health Organization Regional Office for Africa**. Hepatitis scorecard for the WHO Africa Region implementing the hepatitis elimination strategy. 2019. Available from: https://www.afro.who.int/publications/hepatitis-scorecard-who-africa-region-implementing-hepatitis-elimination-strategy
17 **Kwizera R**, Moibéni A, Shenawy F, Youssif M. The prevalence of hepatitis B and C among blood donors at the National Blood Transfusion Center (CNTS) in Burundi. *Pan Afr Med J* 2018; **31**: 119 [PMID: 31037179 DOI: 10.11604/pamj.2018.31.119.14571]
18 **Werner GT**, Frösner GG, Fresenius K. Prevalence of serological hepatitis A and B markers in a rural area of northern Zaire. *Am J Trop Med Hyg* 1985; **34**: 620-624 [PMID: 2988353 DOI: 10.4269/ajtmh.1985.34.620]
19 **Thompson P**, Parr JB, Holzmayer V, Carrel M, Tshefu A, Mwandagalirwa K, Muwonga J, Welo PO, Fwamba F, Kuhns M, Jhaveri R, Meshnick SR, Cloherty G. Seroepidemiology of Hepatitis B in the Democratic Republic of the Congo. *Am J Trop Med Hyg* 2019; **101**: 226-229 [PMID: 31074406 DOI: 10.4269/ajtmh.18-0883]
20 **Tsega E**, Mengesha B, Nordenfelt E, Hansson BG, Lindberg J. Prevalence of hepatitis B virus markers among Ethiopian blood donors: is HBsAg screening necessary? *Trop Geogr Med* 1987; **39**: 336-340 [PMID: 3451408]
21 **Argaw B**, Mihret A, Aseffa A, Tarekegne A, Hussen S, Wachamo D, Shimelis T, Howe R. Sero-prevalence of hepatitis B virus markers and associated factors among children in Hawassa City, southern Ethiopia. *BMC Infect Dis* 2020; **20**: 528 [PMID: 32698884 DOI: 10.1186/s12879-020-05229-7]
22 **Belyhun Y**, Maier M, Mulu A, Diro E, Liebert UG. Hepatitis viruses in Ethiopia: a systematic review and meta-analysis. *BMC Infect Dis* 2016; **16**: 761 [PMID: 27993129 DOI: 10.1186/s12879-016-2090-1]
23 **Fortuin M**, Chotard J, Jack AD, Maine NP, Mendy M, Hall AJ, Inskip HM, George MO, Whittle HC. Efficacy of hepatitis B vaccine in the Gambian expanded programme on immunisation. *Lancet* 1993; **341**: 1129-1131 [PMID: 8097813 DOI: 10.1016/0140-6736(93)93137-p]
24 **Peto TJ**, Mendy ME, Lowe Y, Webb EL, Whittle HC, Hall AJ. Efficacy and effectiveness of infant vaccination against chronic hepatitis B in the Gambia Hepatitis Intervention Study (1986-90) and in the nationwide immunisation program. *BMC Infect Dis* 2014; **14**: 7 [PMID: 24397793 DOI: 10.1186/1471-2334-14-7]
25 **Bittaye M**, Idoko P, Ekele BA, Obed SA, Nyan O. Hepatitis B virus sero-prevalence amongst pregnant women in the Gambia. *BMC Infect Dis* 2019; **19**: 259 [PMID: 30876397 DOI: 10.1186/s12879-019-3883-9]
26 **Hyams KC**, Okoth FA, Tukei PM, Mugambi M, Johnson B, Morrill JC, Gray GC, Woody JN. Epidemiology of hepatitis B in eastern Kenya. *J Med Virol* 1989; **28**: 106-109 [PMID: 2786919 DOI: 10.1002/jmv.1890280210]
27 **Awili HO**, Gitao GC, Muchemi GM. Seroprevalence and Risk Factors for Hepatitis B Virus Infection in Adolescent Blood Donors within Selected Counties of Western Kenya. *Biomed Res Int* 2020; **2020**: 8578172 [PMID: 32685533 DOI: 10.1155/2020/8578172]

28 **Maupas P**, Chiron JP, Goudeau A, Coursaget P, Perrin J, Barin F, Yvonnet B, Dubois F, Duflo B, Duflo-Moreau B, Sidibe S, Diallo AN. [Epidemiology and pathologic results of chronic carriers state of hepatitis B in Mali]. *Bull Soc Pathol Exot Filiales* 1981; **74**: 722-732 [PMID: 7343138]

29 **Kiire CF**. Hepatitis B infection in sub-Saharan Africa. The African Regional Study Group. *Vaccine* 1990; **8** Suppl: S107-12; discussion S134 [PMID: 2139278 DOI: 10.1016/0264-410x(90)90229-f]

30 **Mabunda N**, Zicai AF, Ismael N, Vubil A, Mello F, Blackard JT, Lago B, Duarte V, Moraes M, Lewis L, Jani I. Molecular and serological characterization of occult hepatitis B among blood donors in Maputo, Mozambique. *Mem Inst Oswaldo Cruz* 2020; **115**: e200006 [PMID: 32997000 DOI: 10.1590/0074-02760200006]

31 **Botha JF**, Ritchie MJ, Dusheiko GM, Mouton HW, Kew MC. Hepatitis B virus carrier state in black children in Ovamboland: role of perinatal and horizontal infection. *Lancet* 1984; **1**: 1210-1212 [PMID: 6144925 DOI: 10.1016/s0140-6736(84)91694-5]

32 **Mhata P**, Rennie TW, Small LF, Nyarang'o PM, Chagla Z, Hunter CJ. Distribution of hepatitis B virus infection in Namibia. *S Afr Med J* 2017; **107**: 882-886 [PMID: 29022533 DOI: 10.7196/SAMJ.2017.v107i10.12171]

33 **Mavenyengwa RT**, Mukesi M, Chipare I, Shoombe E. Prevalence of human immunodeficiency virus, syphilis, hepatitis B and C in blood donations in Namibia. *BMC Public Health* 2014; **14**: 424 [PMID: 24884633 DOI: 10.1186/1471-2458-14-424]

34 **Nasidi A**, Harry TO, Vyazov SO, Munube GM, Azzan BB, Ananiev VA. Prevalence of hepatitis B infection markers in representative areas of Nigeria. *Int J Epidemiol* 1986; **15**: 274-276 [PMID: 3721692 DOI: 10.1093/ije/15.2.274]

35 **Ezeilo MC**, Engwa GA, Iroha RI, Odimegwu DC. Seroprevalence and Associated Risk Factors of Hepatitis B Virus Infection Among Children in Enugu Metropolis. *Virology (Auckl)* 2018; **9**: 1178122X18792859 [PMID: 30150873 DOI: 10.1177/1178122X18792859]

36 **Federal Ministry of Health**, Nigeria. Nigeria HIV/AIDS Indicator and Impact Survey (NAIIS) 2018: Technical Report. Abuja, Nigeria; 2019. Available from: https://www.naiis.ng/resource/NAIIS-Report-2018.pdf

37 **Twagirumugabe T**, Swaibu G, Walker TD, Lindh M, Gahutu JB, Bergström T, Norder H. Hepatitis B virus strains from Rwandan blood donors are genetically similar and form one clade within subgenotype A1. *BMC Infect Dis* 2017; **17**: 32 [PMID: 28056881 DOI: 10.1186/s12879-016-2149-z]

38 **Makuza JD**, Nisingizwe MP, Rwema JOT, Dushimiyimana D, Habimana DS, Umuraza S, Serumondo J, Ngwije A, Semakula M, Gupta N, Nsanzimana S, Janjua NZ. Role of unsafe medical practices and sexual behaviours in the hepatitis B and C syndemic and HIV co-infection in Rwanda: a cross-sectional study. *BMJ Open* 2020; **10**: e036711 [PMID: 32660951 DOI: 10.1136/bmjopen-2019-036711]

39 **Barin F**, Perrin J, Chotard J, Denis F, N'Doye R, Diop Mar I, Chiron JP, Coursaget P, Goudeau A, Maupas P. Cross-sectional and longitudinal epidemiology of hepatitis B in Senegal. *Prog Med Virol* 1981; **27**: 148-162 [PMID: 6972051]

40 **Lô G**, Sow-Sall A, Diop-Ndiaye H, Babacar N, Diouf NN, Daffé SM, Ndao B, Thiam M, Mbow M, Soumboundou MB, Lemoine M, Sylla-Niang M, Ndiaye O, Boye CS, Mboup S, Touré-Kane NC. Hepatitis B virus (HBV) infection amongst children in Senegal: current prevalence and seroprotection level. *Pan Afr Med J* 2019; **32**: 140 [PMID: 31303913 DOI: 10.11604/pamj.2019.32.140.14485]

41 **Coste M**, De Sèze M, Diallo A, Carrieri MP, Marcellin F, Boyer S; ANRS 12356 AmBASS Study Group. Burden and impacts of chronic hepatitis B infection in rural Senegal: study protocol of a cross-sectional survey in the area of Niakhar (AmBASS ANRS 12356). *BMJ Open* 2019; **9**: e030211 [PMID: 31320358 DOI: 10.1136/bmjopen-2019-030211]

42 **Prabdial-Sing N**, Makhathini L, Smit SB, Manamela MJ, Motaze NV, Cohen C, Suchard MS. Hepatitis B sero-prevalence in children under 15 years of age in South Africa using residual samples from community-based febrile rash surveillance. *PLoS One* 2019; **14**: e0217415 [PMID: 31150445 DOI: 10.1371/journal.pone.0217415]

43 **Samsunder N**, Ngcapu S, Lewis L, Baxter C, Cawood C, Khanyile D, Kharsany ABM. Seroprevalence of hepatitis B virus: Findings from a population-based household survey in KwaZulu-Natal, South Africa. *Int J Infect Dis* 2019; **85**: 150-157 [PMID: 31202910 DOI: 10.1016/j.ijid.2019.06.005]

44 **Bwogi J**, Braka F, Makumbi I, Mishra V, Bakamutumaho B, Nanyunja M, Opio A, Downing R, Biryahwaho B, Lewis RF. Hepatitis B infection is highly endemic in Uganda: findings from a national serosurvey. *Afr Health Sci* 2009; **9**: 98-108 [PMID: 19652743]

45 **Ministry of Health**, Uganda. Uganda Population-based HIV Impact Assessment (UPHIA) 2016–2017: Final Report: Kampala, Ministry of Health; 2019. Available from: https://phia.icap.columbia.edu/wp-content/uploads/2019/07/UPHIA_Final_Report_Revise_07.11.2019_Final_for-web.pdf

46 **Tswana S**, Chetsanga C, Nyström L, Moyo S, Nzara M, Chieza L. A sero-epidemiological cross-sectional study of hepatitis B virus in Zimbabwe. *S Afr Med J* 1996; **86**: 72-75 [PMID: 8685787]

47 **Mavenyengwa RT**, Moyo SR, Nordbø SA. Streptococcus agalactiae colonization and correlation with HIV-1 and HBV seroprevalence in pregnant women from Zimbabwe. *Eur J Obstet Gynecol Reprod Biol* 2010; **150**: 34-38 [PMID: 20189288 DOI: 10.1016/j.ejogrb.2010.02.021]

48 **Kew MC**. Epidemiology of chronic hepatitis B virus infection, hepatocellular carcinoma, and hepatitis B virus-induced hepatocellular carcinoma. *Pathol Biol (Paris)* 2010; **58**: 273-277 [PMID:

20378277 DOI: 10.1016/j.patbio.2010.01.005]
49 **Spearman CW**, Afihene M, Ally R, Apica B, Awuku Y, Cunha L, Dusheiko G, Gogela N, Kassianides C, Kew M, Lam P, Lesi O, Lohouès-Kouacou MJ, Mbaye PS, Musabeyezu E, Musau B, Ojo O, Rwegasha J, Scholz B, Shewaye AB, Tzeuton C, Sonderup MW; Gastroenterology and Hepatology Association of sub-Saharan Africa (GHASSA). Hepatitis B in sub-Saharan Africa: strategies to achieve the 2030 elimination targets. *Lancet Gastroenterol Hepatol* 2017; **2**: 900-909 [PMID: 29132759 DOI: 10.1016/S2468-1253(17)30295-9]
50 **World Health Organization**. World Health Organization/UNICEF joint reporting process. Geneva: World Health Organization/UNICEF, 2020
51 **Hadziyannis SJ**. Natural history of chronic hepatitis B in Euro-Mediterranean and African countries. *J Hepatol* 2011; **55**: 183-191 [PMID: 21238520 DOI: 10.1016/j.jhep.2010.12.030]
52 **Croagh CM**, Lubel JS. Natural history of chronic hepatitis B: phases in a complex relationship. *World J Gastroenterol* 2014; **20**: 10395-10404 [PMID: 25132755 DOI: 10.3748/wjg.v20.i30.10395]
53 **Kew MC**. Hepatitis B virus / human immunodeficiency virus co-infection and its hepatocarcinogenic potential in sub-saharan black africans. *Hepat Mon* 2012; **12**: e7876 [PMID: 23166538 DOI: 10.5812/hepatmon.7876]
54 **Matthews PC**, Geretti AM, Goulder PJ, Klenerman P. Epidemiology and impact of HIV coinfection with hepatitis B and hepatitis C viruses in Sub-Saharan Africa. *J Clin Virol* 2014; **61**: 20-33 [PMID: 24973812 DOI: 10.1016/j.jcv.2014.05.018]
55 **Platt L**, French CE, McGowan CR, Sabin K, Gower E, Trickey A, McDonald B, Ong J, Stone J, Easterbrook P, Vickerman P. Prevalence and burden of HBV co-infection among people living with HIV: A global systematic review and meta-analysis. *J Viral Hepat* 2020; **27**: 294-315 [PMID: 31603999 DOI: 10.1111/jvh.13217]
56 **Keane E**, Funk AL, Shimakawa Y. Systematic review with meta-analysis: the risk of mother-to-child transmission of hepatitis B virus infection in sub-Saharan Africa. *Aliment Pharmacol Ther* 2016; **44**: 1005-1017 [PMID: 27630001 DOI: 10.1111/apt.13795]
57 **Andersson MI**, Maponga TG, Ijaz S, Barnes J, Theron GB, Meredith SA, Preiser W, Tedder RS. The epidemiology of hepatitis B virus infection in HIV-infected and HIV-uninfected pregnant women in the Western Cape, South Africa. *Vaccine* 2013; **31**: 5579-5584 [PMID: 23973500 DOI: 10.1016/j.vaccine.2013.08.028]
58 **Chasela CS**, Kourtis AP, Wall P, Drobeniuc J, King CC, Thai H, Teshale EH, Hosseinipour M, Ellington S, Codd MB, Jamieson DJ, Knight R, Fitzpatrick P, Kamili S, Hoffman I, Kayira D, Mumba N, Kamwendo DD, Martinson F, Powderly W, Teo CG, van der Horst C; BAN Study Team. Hepatitis B virus infection among HIV-infected pregnant women in Malawi and transmission to infants. *J Hepatol* 2014; **60**: 508-514 [PMID: 24211737 DOI: 10.1016/j.jhep.2013.10.029]
59 **Thumbiran NV**, Moodley D, Parboosing R, Moodley P. Hepatitis B and HIV co-infection in pregnant women: indication for routine antenatal hepatitis B virus screening in a high HIV prevalence setting. *S Afr Med J* 2014; **104**: 307-309 [PMID: 25118561 DOI: 10.7196/samj.7299]
60 **Kafeero HM**, Ndagire D, Ocama P, Walusansa A, Sendagire H. Sero-prevalence of human immunodeficiency virus-hepatitis B virus (HIV-HBV) co-infection among pregnant women attending antenatal care (ANC) in sub-Saharan Africa (SSA) and the associated risk factors: a systematic review and meta-analysis. *Virol J* 2020; **17**: 170 [PMID: 33160386 DOI: 10.1186/s12985-020-01443-6]
61 **UNAIDS**. UNAIDS data 2020. 2nd edition, February 2021. Available from: https://www.unaids.org/sites/default/files/media_asset/2020_aids-data-book_en.pdf
62 **Slogrove AL**, Powis KM, Johnson LF, Stover J, Mahy M. Estimates of the global population of children who are HIV-exposed and uninfected, 2000-18: a modelling study. *Lancet Glob Health* 2020; **8**: e67-e75 [PMID: 31791800 DOI: 10.1016/S2214-109X(19)30448-6]
63 **Jones CE**, Naidoo S, De Beer C, Esser M, Kampmann B, Hesseling AC. Maternal HIV infection and antibody responses against vaccine-preventable diseases in uninfected infants. *JAMA* 2011; **305**: 576-584 [PMID: 21304083 DOI: 10.1001/jama.2011.100]
64 **Njom Nlend AE**, Nguwoh PS, Ngounouh CT, Tchidjou HK, Pieme CA, Otélé JM, Penlap V, Colizzi V, Moyou RS, Fokam J. HIV-Infected or -Exposed Children Exhibit Lower Immunogenicity to Hepatitis B Vaccine in Yaoundé, Cameroon: An Appeal for Revised Policies in Tropical Settings? *PLoS One* 2016; **11**: e0161714 [PMID: 27656883 DOI: 10.1371/journal.pone.0161714]
65 **Baruti K**, Lentz K, Anderson M, Ajibola G, Phinius BB, Choga WT, Mbangiwa T, Powis KM, Sebunya T, Blackard JT, Lockman S, Moyo S, Shapiro R, Gaseitsiwe S. Hepatitis B virus prevalence and vaccine antibody titers in children HIV exposed but uninfected in Botswana. *PLoS One* 2020; **15**: e0237252 [PMID: 32764801 DOI: 10.1371/journal.pone.0237252]
66 **Tamandjou Tchuem C**, Cotton MF, Nel E, Tedder R, Preiser W, Violari A, Bobat R, Hovind L, Aaron L, Montepiedra G, Mitchell C, Andersson MI. Viral hepatitis B and C in HIV-exposed South African infants. *BMC Pediatr* 2020; **20**: 563 [PMID: 33357228 DOI: 10.1186/s12887-020-02479-x]
67 **Ferlay J**, Colombet M, Soerjomataram I, Mathers C, Parkin DM, Piñeros M, Znaor A, Bray F. Estimating the global cancer incidence and mortality in 2018: GLOBOCAN sources and methods. *Int J Cancer* 2019; **144**: 1941-1953 [PMID: 30350310 DOI: 10.1002/ijc.31937]
68 **Okeke E**, Davwar PM, Roberts L, Sartorius K, Spearman W, Malu A, Duguru M. Epidemiology of Liver Cancer in Africa: Current and Future Trends. *Semin Liver Dis* 2020; **40**: 111-123 [PMID: 31726474 DOI: 10.1055/s-0039-3399566]
69 **Howell J**, Ladepa NG, Lemoinea M, Thursza MR. , Taylor-Robinsona SD. Hepatitis B in sub-

Saharan Africa. *South Sudan Med J* 2014; **7**: 59-61
70 **Shimakawa Y**, Lemoine M, Njai HF, Bottomley C, Ndow G, Goldin RD, Jatta A, Jeng-Barry A, Wegmuller R, Moore SE, Baldeh I, Taal M, D'Alessandro U, Whittle H, Njie R, Thursz M, Mendy M. Natural history of chronic HBV infection in West Africa: a longitudinal population-based study from The Gambia. *Gut* 2016; **65**: 2007-2016 [PMID: 26185161 DOI: 10.1136/gutjnl-2015-309892]
71 **Yang JD**, Mohamed EA, Aziz AO, Shousha HI, Hashem MB, Nabeel MM, Abdelmaksoud AH, Elbaz TM, Afihene MY, Duduyemi BM, Ayawin JP, Gyedu A, Lohouès-Kouacou MJ, Ndam AW, Moustafa EF, Hassany SM, Moussa AM, Ugiagbe RA, Omuemu CE, Anthony R, Palmer D, Nyanga AF, Malu AO, Obekpa S, Abdo AE, Siddig AI, Mudawi HM, Okonkwo U, Kooffreh-Ada M, Awuku YA, Nartey YA, Abbew ET, Awuku NA, Otegbayo JA, Akande KO, Desalegn HM, Omonisi AE, Ajayi AO, Okeke EN, Duguru MJ, Davwar PM, Okorie MC, Mustapha S, Debes JD, Ocama P, Lesi OA, Odeghe E, Bello R, Onyekwere C, Ekere F, Igetei R, Mah'moud MA, Addissie B, Ali HM, Gores GJ, Topazian MD, Roberts LR; Africa Network for Gastrointestinal and Liver Diseases. Characteristics, management, and outcomes of patients with hepatocellular carcinoma in Africa: a multicountry observational study from the Africa Liver Cancer Consortium. *Lancet Gastroenterol Hepatol* 2017; **2**: 103-111 [PMID: 28403980 DOI: 10.1016/S2468-1253(16)30161-3]
72 **Moore SW**, Millar AJ, Hadley GP, Ionescu G, Kruger M, Poole J, Stones D, Wainwright L, Chitnis M, Wessels G. Hepatocellular carcinoma and liver tumors in South African children: a case for increased prevalence. *Cancer* 2004; **101**: 642-649 [PMID: 15274079 DOI: 10.1002/cncr.20398]
73 **Seleye-Fubara D**, Jebbin NJ. Hepatocellular carcinoma in Port Harcourt, Nigeria: clinicopathologic study of 75 cases. *Ann Afr Med* 2007; **6**: 54-57 [PMID: 18240703 DOI: 10.4103/1596-3519.55716]
74 **Carreira H**, Lorenzoni C, Carrilho C, Ferro J, Sultane T, Garcia C, Amod F, Augusto O, Silva-Matos C, La Vecchia C, Lunet N. Spectrum of pediatric cancers in Mozambique: an analysis of hospital and population-based data. *Pediatr Hematol Oncol* 2014; **31**: 498-508 [PMID: 24852201 DOI: 10.3109/08880018.2014.909547]
75 **Stefan C**, Bray F, Ferlay J, Liu B, Maxwell Parkin D. Cancer of childhood in sub-Saharan Africa. *Ecancermedicalscience* 2017; **11**: 755 [PMID: 28900468 DOI: 10.3332/ecancer.2017.755]
76 **Bray F**, Møller B. Predicting the future burden of cancer. *Nat Rev Cancer* 2006; **6**: 63-74 [PMID: 16372017 DOI: 10.1038/nrc1781]
77 **Ferlay J**, Laversanne M, Ervik M, Lam F, Colombet M, Mery L, Piñeros M, Znaor A, Soerjomataram I, Bray F. Global Cancer Observatory: Cancer Tomorrow. Lyon: International Agency for Research on Cancer, 2020
78 **Ferlay J**, Ervik M, Lam F, Colombet M, Mery L, Piñeros M, Znaor A, Soerjomataram I, Bray F. Global Cancer Observatory: Cancer Today. Lyon, France: International Agency for Research on Cancer, 2020
79 **Sartorius K**, Sartorius B, Aldous C, Govender PS, Madiba TE. Global and country underestimation of hepatocellular carcinoma (HCC) in 2012 and its implications. *Cancer Epidemiol* 2015; **39**: 284-290 [PMID: 25922178 DOI: 10.1016/j.canep.2015.04.006]
80 **Wang CC**, Tsai MC, Peng CM, Lee HL, Chen HY, Yang TW, Sung WW, Lin CC. Favorable liver cancer mortality-to-incidence ratios of countries with high health expenditure. *Eur J Gastroenterol Hepatol* 2017; **29**: 1397-1401 [PMID: 29023320 DOI: 10.1097/MEG.0000000000000969]
81 **Spearman CW**, Sonderup MW. Health disparities in liver disease in sub-Saharan Africa. *Liver Int* 2015; **35**: 2063-2071 [PMID: 26053588 DOI: 10.1111/liv.12884]
82 **Mak D**, Sengayi M, Chen WC, Babb de Villiers C, Singh E, Kramvis A. Liver cancer mortality trends in South Africa: 1999-2015. *BMC Cancer* 2018; **18**: 798 [PMID: 30086727 DOI: 10.1186/s12885-018-4695-9]
83 **Kirk GD**, Lesi OA, Mendy M, Akano AO, Sam O, Goedert JJ, Hainaut P, Hall AJ, Whittle H, Montesano R. The Gambia Liver Cancer Study: Infection with hepatitis B and C and the risk of hepatocellular carcinoma in West Africa. *Hepatology* 2004; **39**: 211-219 [PMID: 14752840 DOI: 10.1002/hep.20027]
84 **Otedo A**, Simbiri KO, Were V, Ongati O, Estambale BA. Risk factors for liver Cancer in HIV endemic areas of Western Kenya. *Infect Agent Cancer* 2018; **13**: 41 [PMID: 30607173 DOI: 10.1186/s13027-018-0214-5]
85 **Kirk GD**, Lesi OA, Mendy M, Szymañska K, Whittle H, Goedert JJ, Hainaut P, Montesano R. 249(ser) TP53 mutation in plasma DNA, hepatitis B viral infection, and risk of hepatocellular carcinoma. *Oncogene* 2005; **24**: 5858-5867 [PMID: 16007211 DOI: 10.1038/sj.onc.1208732]
86 **Kew MC**. Aflatoxins as a cause of hepatocellular carcinoma. *J Gastrointestin Liver Dis* 2013; **22**: 305-310 [PMID: 24078988]
87 **Kew MC**. Hepatitis C virus-induced hepatocellular carcinoma in sub-Saharan Africa. *J Afr Cancer* 2013; **5**: 169-174 [DOI: 10.1007/s12558-013-0275-8]
88 **Amponsah-Dacosta E**, Tamandjou Tchuem C, Anderson M. Chronic hepatitis B-associated liver disease in the context of human immunodeficiency virus co-infection and underlying metabolic syndrome. *World J Virol* 2020; **9**: 54-66 [PMID: 33362998 DOI: 10.5501/wjv.v9.i5.54]
89 **Yu MC**, Yuan JM. Environmental factors and risk for hepatocellular carcinoma. *Gastroenterology* 2004; **127**: S72-S78 [PMID: 15508106 DOI: 10.1016/j.gastro.2004.09.018]
90 **Baecker A**, Liu X, La Vecchia C, Zhang ZF. Worldwide incidence of hepatocellular carcinoma cases attributable to major risk factors. *Eur J Cancer Prev* 2018; **27**: 205-212 [PMID: 29489473 DOI: 10.1097/CEJ.0000000000000428]
91 **Petruzziello A**. Epidemiology of Hepatitis B Virus (HBV) and Hepatitis C Virus (HCV) Related

Hepatocellular Carcinoma. *Open Virol J* 2018; **12**: 26-32 [PMID: 29541276 DOI: 10.2174/1874357901812010026]

92 **Levrero M**, Zucman-Rossi J. Mechanisms of HBV-induced hepatocellular carcinoma. *J Hepatol* 2016; **64**: S84-S101 [PMID: 27084040 DOI: 10.1016/j.jhep.2016.02.021]

93 **Torresi J**, Tran BM, Christiansen D, Earnest-Silveira L, Schwab RHM, Vincan E. HBV-related hepatocarcinogenesis: the role of signalling pathways and innovative ex vivo research models. *BMC Cancer* 2019; **19**: 707 [PMID: 31319796 DOI: 10.1186/s12885-019-5916-6]

94 **Atsama Amougou M**, Marchio A, Bivigou-Mboumba B, Noah Noah D, Banai R, Atangana PJA, Fewou Moundipa P, Pineau P, Njouom R. Enrichment in selected genotypes, basal core and precore mutations of hepatitis B virus in patients with hepatocellular carcinoma in Cameroon. *J Viral Hepat* 2019; **26**: 1086-1093 [PMID: 31106515 DOI: 10.1111/jvh.13131]

95 **Mak D**, Babb de Villiers C, Chasela C, Urban MI, Kramvis A. Analysis of risk factors associated with hepatocellular carcinoma in black South Africans: 2000-2012. *PLoS One* 2018; **13**: e0196057 [PMID: 29718992 DOI: 10.1371/journal.pone.0196057]

96 **Mendy ME**, Welzel T, Lesi OA, Hainaut P, Hall AJ, Kuniholm MH, McConkey S, Goedert JJ, Kaye S, Rowland-Jones S, Whittle H, Kirk GD. Hepatitis B viral load and risk for liver cirrhosis and hepatocellular carcinoma in The Gambia, West Africa. *J Viral Hepat* 2010; **17**: 115-122 [PMID: 19874478 DOI: 10.1111/j.1365-2893.2009.01168.x]

97 **Polaris Observatory Collaborators**. Global prevalence, treatment, and prevention of hepatitis B virus infection in 2016: a modelling study. *Lancet Gastroenterol Hepatol* 2018; **3**: 383-403 [PMID: 29599078 DOI: 10.1016/S2468-1253(18)30056-6]

98 **Wilson P**, Parr JB, Jhaveri R, Meshnick SR. Call to Action: Prevention of Mother-to-Child Transmission of Hepatitis B in Africa. *J Infect Dis* 2018; **217**: 1180-1183 [PMID: 29351639 DOI: 10.1093/infdis/jiy028]

99 **Sonderup MW**, Dusheiko G, Desalegn H, Lemoine M, Tzeuton C, Taylor-Robinson SD, Spearman CW. Hepatitis B in sub-Saharan Africa-How many patients need therapy? *J Viral Hepat* 2020; **27**: 560-567 [PMID: 31800145 DOI: 10.1111/jvh.13247]

100 **Béguelin C**, Fall F, Seydi M, Wandeler G. The current situation and challenges of screening for and treating hepatitis B in sub-Saharan Africa. *Expert Rev Gastroenterol Hepatol* 2018; **12**: 537-546 [PMID: 29737218 DOI: 10.1080/17474124.2018.1474097]

101 **Desalegn H**, Aberra H, Berhe N, Gundersen SG, Johannessen A. Are non-invasive fibrosis markers for chronic hepatitis B reliable in sub-Saharan Africa? *Liver Int* 2017; **37**: 1461-1467 [PMID: 28222249 DOI: 10.1111/liv.13393]

102 **Lemoine M**, Thursz MR. Battlefield against hepatitis B infection and HCC in Africa. *J Hepatol* 2017; **66**: 645-654 [PMID: 27771453 DOI: 10.1016/j.jhep.2016.10.013]

103 **Boye S**, Shimakawa Y, Vray M, Giles-Vernick T. Limited Awareness of Hepatitis B but Widespread Recognition of Its Sequelae in Rural Senegal: A Qualitative Study. *Am J Trop Med Hyg* 2020; **102**: 637-643 [PMID: 31971148 DOI: 10.4269/ajtmh.19-0477]

104 **Adjei CA**, Stutterheim SE, Naab F, Ruiter RAC. Barriers to chronic Hepatitis B treatment and care in Ghana: A qualitative study with people with Hepatitis B and healthcare providers. *PLoS One* 2019; **14**: e0225830 [PMID: 31794577 DOI: 10.1371/journal.pone.0225830]

105 **World Health Organization Regional Office for Africa**. Sixty-fourth session of the WHO Regional Committee for Africa. 2014. Available from: https://www.afro.who.int/about-us/governance/sessions/sixty-fourth-session-who-regional-committee-africa

106 **World Health Organization Regional Office for Africa**. Regional strategic plan for immunization 2014 – 2020. 2015. Available from: https://www.afro.who.int/sites/default/files/2017-06/oms-ivb-rvap-afro-en-20150408_final_sent140317.pdf

107 **Andersson MI**, Rajbhandari R, Kew MC, Vento S, Preiser W, Hoepelman AI, Theron G, Cotton M, Cohn J, Glebe D, Lesi O, Thursz M, Peters M, Chung R, Wiysonge C. Mother-to-child transmission of hepatitis B virus in sub-Saharan Africa: time to act. *Lancet Glob Health* 2015; **3**: e358-e359 [PMID: 26087980 DOI: 10.1016/S2214-109X(15)00056-X]

108 **Stockdale AJ**, Geretti AM. Chronic hepatitis B infection in sub-Saharan Africa: a grave challenge and a great hope. *Trans R Soc Trop Med Hyg* 2015; **109**: 421-422 [PMID: 26065660 DOI: 10.1093/trstmh/trv044]

109 **Jia L**, Gao Y, He Y, Hooper JD, Yang P. HBV induced hepatocellular carcinoma and related potential immunotherapy. *Pharmacol Res* 2020; **159**: 104992 [PMID: 32505833 DOI: 10.1016/j.phrs.2020.104992]

110 **Yang JD**, Heimbach JK. New advances in the diagnosis and management of hepatocellular carcinoma. *BMJ* 2020; **371**: m3544 [PMID: 33106289 DOI: 10.1136/bmj.m3544]

World Journal of Gastroenterology

Submit a Manuscript: https://www.f6publishing.com

World J Gastroenterol 2021 September 28; 27(36): 6039-6052

DOI: 10.3748/wjg.v27.i36.6039

ISSN 1007-9327 (print) ISSN 2219-2840 (online)

MINIREVIEWS

Liver disease in the era of COVID-19: Is the worst yet to come?

Ivana Mikolasevic, Dorotea Bozic, Tajana Pavić, Alen Ruzic, Goran Hauser, Marija Radic, Delfa Radic-Kristo, Melanija Razov-Radas, Zeljko Puljiz, Sandra Milic

ORCID number: Ivana Mikolasevic 0000-0001-9676-0642; Dorotea Bozic 0000-0001-9234-4203; Tajana Pavić 0000-0002-0370-5001; Alen Ruzic 0000-0001-5031-2975; Goran Hauser 0000-0002-4758-1717; Marija Radic 0000-0002-7746-2065; Delfa Radic-Kristo 0000-0002-2827-7808; Melanija Razov-Radas 0000-0003-4530-4350; Zeljko Puljiz 0000-0002-3465-4227; Sandra Milic 0000-0002-6635-5360.

Author contributions: Mikolasevic I researched the database, wrote the manuscript and is the guarantor of this work; Bozic D, Pavić T, Ruzic A, Hauser G, Milic S, Radic M, Radic-Kristo D, Razov-Radas M and Puljiz Z contributed to the discussion and reviewed/edited the manuscript.

Conflict-of-interest statement: Authors declare no conflict of interest for this article.

Ivana Mikolasevic, Goran Hauser, Sandra Milic, Department of Gastroenterology, Clinical Hospital Center Rijeka, Rijeka 51000, Croatia

Ivana Mikolasevic, Department of Gastroenterology, University Hospital Merkur, Zagreb 10000, Croatia

Ivana Mikolasevic, Alen Ruzic, Goran Hauser, Sandra Milic, Faculty of Medicine, University of Rijeka, Rijeka 51000, Croatia

Dorotea Bozic, Zeljko Puljiz, Department for Gastroenterology and Hepatology, University Hospital Center Split, Split 21000, Croatia

Tajana Pavić, Department of Gastroenterology and Hepatology, Faculty of Medicine, Sestre Milosrdnice University Hospital Center, Zagreb 10000, Croatia

Alen Ruzic, Clinic for Cardiology, University Hospital Center Rijeka, Rijeka 51000, Croatia

Goran Hauser, Faculty of Health Studies, University of Rijeka, Rijeka 51000, Croatia

Marija Radic, Delfa Radic-Kristo, Faculty of Medicine, Zagreb 10000, Croatia

Delfa Radic-Kristo, Department of Hematology, University Hospital Merkur, Zagreb 10000, Croatia

Melanija Razov-Radas, Division of Gastroenterology, General Hospital Zadar, Zadar 23000, Croatia

Zeljko Puljiz, University of Split, School of Medicine, Split 21000, Croatia

Corresponding author: Ivana Mikolasevic, PhD, Professor, Department of Gastroenterology, Clinical Hospital Center Rijeka, Kresimirova 42, Rijeka 51000, Croatia. ivana.mikolasevic@gmail.com

Abstract

The global social, economic and political crises related to coronavirus disease 2019 (COVID-19) presumably had more indirect than direct negative impacts on health systems. Drastic lifestyle changes, social isolation and distancing, and individual and global financial crises resulted in robust populations forfeiting healthy habits and seeking comfort in alcoholic beverages, drugs and unhealthy diets. The inevitable consequences are increases in the incidence of nonalcoholic fatty liver disease, viral hepatitis, acute alcoholic hepatitis, liver cirrhosis decompensation

Manuscript source: Invited manuscript

Specialty type: Gastroenterology and hepatology

Country/Territory of origin: Croatia

Peer-review report's scientific quality classification

Grade A (Excellent): 0
Grade B (Very good): 0
Grade C (Good): C, C, C, C
Grade D (Fair): 0
Grade E (Poor): 0

Received: February 28, 2021
Peer-review started: February 28, 2021
First decision: July 3, 2021
Revised: July 18, 2021
Accepted: September 1, 2021
Article in press: September 1, 2021
Published online: September 28, 2021

P-Reviewer: Ferraioli G, Gupta MK, Skok K
S-Editor: Gao CC
L-Editor: A
P-Editor: Yuan YY

and ultimately liver-related mortality. The inaccessibility of regular clinical and sonographic monitoring systems has caused difficulties in the treatment of patients with chronic liver disease (CLD) and has prevented prompt hepatocellular carcinoma detection and treatment. A dramatic reduction in the number of liver donors and the transformation of numerous transplantation centers into COVID-19 units drastically decreased the rate of orthotopic liver transplantation. The indirect, unavoidable effects of the COVID-19 pandemic in the following years have yet to be determined. Substantial efforts in the management of patients with liver disease in order to overcome the inevitable COVID-19-related morbidity and mortality that will follow have yet to be initiated. Several questions regarding the impact of the COVID-19 pandemic on liver disease remain. The most important question for general CLD patients is: How will the modification of clinical practice during this pandemic affect the outcomes of CLD patients? This article reviews the influence of COVID-19 on patients with liver disease during the pandemic, with particular emphasis on the disease course associated with pandemic resolution.

Key Words: COVID-19; Pandemic; Chronic liver disease; Management; Impact; Liver-related mortality

Core Tip: The global social, economic and political crises related to coronavirus disease 2019 (COVID-19) presumably cause more indirect than direct negative impacts on the health system. Drastic lifestyle changes, social isolation and distancing, and individual and global financial crises resulted in a robust population forfeiting healthy habits and seeking comfort in alcoholic beverages, drugs and unhealthy diets. The inevitable consequence is the increasing incidence of liver disease, liver cirrhosis decompensation and ultimately liver-related mortality. The indirect unavoidable effects of the COVID-19 pandemic in the following years have yet to be determined.

Citation: Mikolasevic I, Bozic D, Pavić T, Ruzic A, Hauser G, Radic M, Radic-Kristo D, Razov-Radas M, Puljiz Z, Milic S. Liver disease in the era of COVID-19: Is the worst yet to come? *World J Gastroenterol* 2021; 27(36): 6039-6052
URL: https://www.wjgnet.com/1007-9327/full/v27/i36/6039.htm
DOI: https://dx.doi.org/10.3748/wjg.v27.i36.6039

INTRODUCTION

The coronavirus disease 2019 (COVID-19) pandemic has spread rapidly worldwide and poses a serious threat to healthcare systems globally. It is common to encounter patients with both COVID-19 and abnormal liver function. Because COVID-19 is a newly discovered disease, additional data are needed to improve our understanding of its impact on the liver and of the appropriate management of such patients[1-15]. Information on how COVID-19 infection affects the liver and the relevance of pre-existing liver disease in acquiring the infection or developing severe disease is increasing, although we still do not know the exact mechanism. Additionally, considerations with regard to liver transplant patients, those with hepatocellular carcinoma (HCC) and those under immunosuppressive therapy are being analyzed as information is being generated. Various treatments for COVID-19 are currently under study but some of these may be potentially hepatotoxic[4-6,15].

The first and most evident consequence of the COVID-19 pandemic is its impact on the routine care of patients with chronic liver disease (CLD). The COVID-19 pandemic shifted our perception of ambulatory patient care from face-to-face examinations to virtual patient management[15-18]. Expert recommendations guiding clinicians in the treatment of patients with CLD and of transplanted patients during the pandemic are available in the form of guidelines published by the European Association for the Study of the Liver (EASL) and the American Association for the Study of Liver

Diseases (AASLD)[16-18].

Although patients with CLD are not at higher risk of acquiring the infection, whether COVID-19 and the underlying liver disease will follow an unfavorable course remains to be answered[19]. Nonetheless, questions regarding the treatment of patients with CLD following resolution of the COVID-19 pandemic remain unknown. One must consider that a considerable number of patients with CLD did not attend regular appointments, prevented by fear of acquiring the infection. Preventive, surgical and transplant programs have become secondary focuses. In light of the present circumstances, it is evident that the burdens of the pandemic-related consequences have yet to be elucidated, not only regarding global economics but also global health[19].

This article reviews the effects of COVID-19 in patients with liver disease during the pandemic, with particular emphasis on the disease course associated with pandemic resolution (Figure 1). We performed a PubMed search using the keywords "chronic liver disease" and "COVID-19". When using this algorithm there were 396 results. In this review, 74 articles with particular emphasis on COVID-19 and liver disease were analyzed.

PRE-EXISTING CLD AND COVID-19

The reported prevalence of patients with CLD in cohorts of patients with COVID-19 does not exceed 1%, suggesting that the risk of infection acquisition is similar to that in the general population[18,20]. However, the risk of a severe course of disease might be increased due to the etiology of the underlying liver disease along with the degree of liver fibrosis[18].

Liver test abnormalities

According to reports from regular and intensive care units, elevated liver enzymes, lactate dehydrogenase, creatinine kinase and myoglobin, as well as prolonged prothrombin time, are found in more than one-third of patients during COVID-19 progression[21]. A retrospective Chinese study revealed a dynamic pattern of liver molecules regardless of the severity of infection: Aspartate aminotransferase (AST) increased, followed by an increase in alanine aminotransferase (ALT) concurrent with mild oscillations in bilirubin levels. AST levels were significantly associated with mortality risk in this group of patients[22]. Another comprehensive Chinese review also reported elevated AST and ALT levels in 6%-22% and 21%-28% of patients, respectively[23]. Compared to other Chinese regions in which 16% of patients had AST elevation, studies from Wuhan reported a higher percentage, ranging from 24% to 37%. Studies have revealed a high prevalence of liver test abnormalities in men and elderly individuals[23,24]. A large American study including 5700 patients reported that 58.4% of patients had elevated AST levels (> 40 U/L) and 39% had elevated ALT levels (> 60 U/L)[25]. Two percent of patients developed acute hepatic injury and the majority of this subgroup (95%) did not survive[25]. A severe cholestatic pattern has not been reported as correlating with COVID-19 but studies have reported hyperbilirubinemia in 11%-18% of cases[21].

Several pathological mechanisms are considered to be involved in liver injury, including direct viral infection of liver cells, drug hepatotoxicity, cytokine storm and pneumonia-associated hypoxia[15,26,27]. According to several studies, the expression of ACE2 receptors on liver cells facilitates SARS CoV-2 entrance; expression is increased in bile duct cells, whose destruction appears to be primarily responsible for COVID-19-related liver injury[15,26]. Studies clarifying the exact mechanisms of liver injury are warranted[15,27-30].

It must be considered that elevated aminotransferases might be of cardiac or muscular origin and that abnormalities in liver tests are frequently transient. On the other hand, studies have reported an increased risk of severe disease in patients who present with liver injury on admission[15,28]. The severity of liver dysfunction seems to be closely associated with the severity of COVID-19[15]. As predicted by multiple studies, the usual culprits of pathological biochemical liver abnormalities are underlying CLD, sepsis-related cholestasis and drug hepatotoxicity[6]. We must not ignore the fact that the frequency and severity of liver injury in asymptomatic individuals and patients under out-of-hospital treatment remains unknown[6]. Therefore, further investigations are needed to strengthen conclusions.

Finally, the most crucial question for clinicians treating COVID-19 patients is in whom and how often to perform liver function tests. The optimal interval has not yet

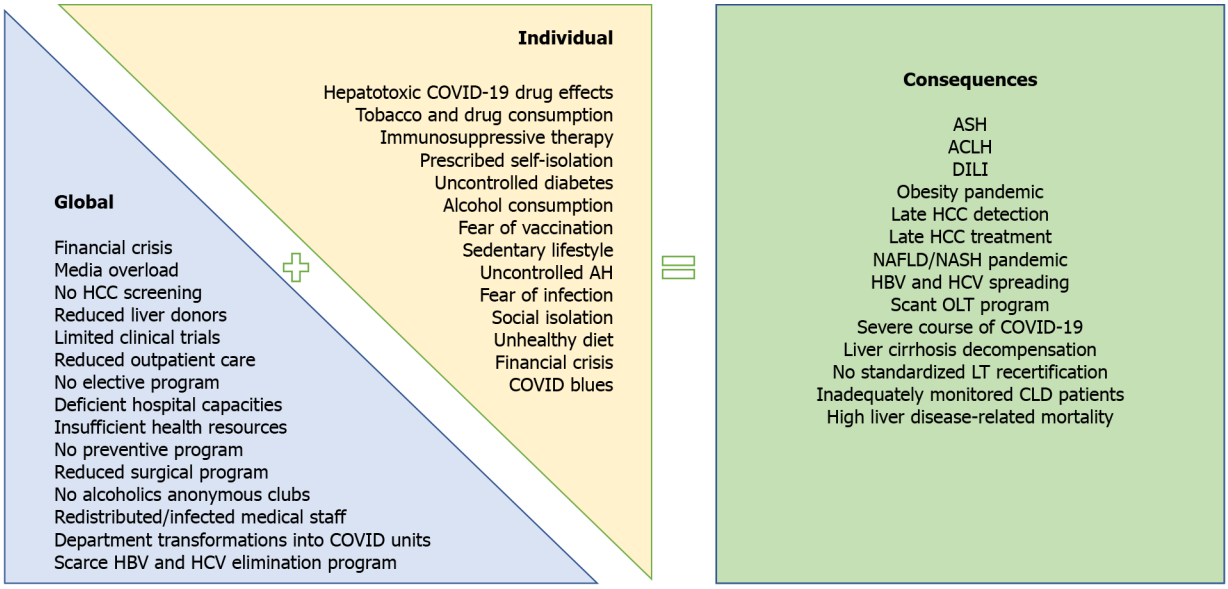

Figure 1 Global and individual effects of the coronavirus disease 2019 pandemic on liver-related morbidity and mortality. ACLF: Acute-on-chronic liver failure; AH: Arterial hypertension; ASH: Alcoholic steatohepatitis; CLD: Chronic liver disease; COVID-19: Coronavirus disease 2019; DILI: Drug-induced liver injury; HBV: Hepatitis B virus; HCC: Hepatocellular carcinoma; HCV: Hepatitis C virus; NAFLD: Non-alcoholic fatty liver disease; NASH: Non-alcoholic steatohepatitis; OLT: Orthotopic liver transplantation.

been defined, but physicians should certainly be attentive when treating severely ill patients and individuals taking novel antiviral drugs such as remdesivir or tocilizumab[6].

Nonalcoholic fatty liver disease and COVID-19

Nonalcoholic fatty liver disease (NAFLD), also known as metabolic dysfunction-associated fatty liver disease, is a common manifestation of metabolic syndrome and is remarkably prevalent in Western industrialized countries[21]. It is usually comorbid with obesity, which represents a significant risk factor for severe COVID-19 pneumonia[3,18,31]. The assumed mechanism relies on the immunological properties of adipose tissue, which also plays a role as a viral reservoir[3,18,25]. Additional risk factors accompanying NAFLD, such as arterial hypertension, obesity and diabetes, are also commonly observed in patients with a severe COVID-19 course[3,18,25].

As predicted in several studies, patients with NAFLD seem to have a longer period of viral replication and dispersion[32] and experience progression to the severe form of disease, with worsening dyspnea, hypoxia and typical radiological findings [32], even in younger patients without other comorbidities[33,34]. Among patients with NAFLD, the underlying liver fibrosis seems to correlate with severe COVID-19 presentation, regardless of other metabolic comorbidities[11,21,35]. Targher *et al*[35] also found an interrelation between advanced liver fibrosis (defined as increased Fibrosis 4 and NAFLD fibrosis scores) and severe COVID-19 presentation in a subgroup of 94 (30.3%) patients with NAFLD. However, Lopez-Mendez *et al*[36] did not confirm these findings. According to their study, although the prevalence of NAFLD and significant liver fibrosis was high in COVID-19 patients, it was not associated with worse clinical outcomes.

The exact mechanism of NAFLD-associated liver fibrosis leading to an undesired COVID-19 course has not yet been defined but presumably is potentiated by the hepatic release of multiple proinflammatory cytokines, exacerbating the severe acute respiratory syndrome coronavirus 2 (SARS-CoV-2)-induced cytokine storm[35]. On the other hand, virus-related cytokines might increase the risk of liver inflammation. This interplay of cytokine-related events forms a vicious cycle, making the NAFLD population at very high risk of COVID-19 complications[11,21].

Additional large-scale analyses are needed to determine whether NAFLD is an independent risk factor for severe COVID-19 or whether confounding factors are responsible for the previously published results. Studies based on other available noninvasive methods, including transient elastography and acoustic radiation force impulse-based techniques, are also warranted.

It is also important to note the increased predisposition for drug-induced liver injury in patients with liver steatosis[6]. Antiretrovirals such as lopinavir/ritonavir, antibiotics, antifungal agents and other drugs required to treat acute respiratory distress syndrome and systemic inflammation may induce drug-induced liver injury [37]. The possible mechanism of increased susceptibility in this group of patients is associated with oxidative stress, diminished activity of xenobiotic-metabolizing enzymes, mitochondrial malfunction and changes in lipid homeostasis[37-39]. Caution must be taken with steatogenic drugs such as amiodarone, sodium valproate, tamoxifen, methotrexate and frequently used glucocorticoids because they may induce steatohepatitis in predisposed individuals[40].

Finally, the effect of the COVID-19 pandemic on the social aspects of an individual's daily routine is the last but not least important undesirable sequela. A sedentary lifestyle, social isolation and increased consumption of processed foods are all metabolic antagonists that are especially unfavorable in patients with NAFLD[18]. The COVID-19 "blues" associated with lockdowns, loss of income and deterioration of socioeconomic status might lead to unhealthy lifestyles and consequently the promotion of obesity and associated metabolic diseases[41]. Therefore, COVID-19 will presumably be an indirect cause of expansion of the NAFLD epidemic[42]. In light of the global psychosociological COVID-19 burden, the Mayo Clinic advocates increased caution against NAFLD-promoting behaviors[42,43].

Increases in body mass index uncontrollable arterial hypertension and underregulated diabetes will certainly contribute to the worsening of NAFLD. It is therefore mandatory to treat associated metabolic comorbidities in these patients[18]. In addition, the deleterious effects of delayed detection of HCC in hepatic steatosis patients are the consequences of missed routine ultrasound examinations.

In conclusion, the EASL suggests considering early admission for all patients with NAFLD and COVID-19[18]. Encouraged by the AASLD guidelines, we recommend regular monitoring of liver function in all hospitalized COVID-19 patients[17,21]. Governments and policy makers should implement certain interventions in response to the increase in NAFLD that will insidiously follow after the COVID-19 pandemic [41]. Finally, when contemplating the introduction of lockdown in the future, the potential consequences on metabolic health should be considered[41].

Autoimmune liver disease and COVID-19

Evidence of the influence of immunosuppressive regimens on the acquisition of COVID-19 is still scarce. However, observational studies have suggested an association between glucocorticoid therapy and a severe COVID-19 course[18,44]. When treating autoimmune hepatitis (AIH) flares, the EASL suggests the administration of budesonide rather than systemic corticosteroid therapy in patients without liver cirrhosis[18]. In the clinical setting of a chronic immunosuppressive regimen it is recommended to continue treatment, except in cases of severe COVID-19, superinfections or lymphopenia that frequently follow SARS-CoV-2 infection[16]. According to the largest study of patients with AIH and COVID-19 infection there were no significant differences in the incidence of major adverse COVID-19 outcomes between patients with AIH and those with other CLD[10]. However, in this study, independent risk factors for adverse events (*i.e.*, death) in these patients were age and baseline liver disease severity. In this study, the use of immunosuppression was not associated with death in AIH patients[10]. Additional studies are needed to determine whether AIH per se or adjacent immunosuppressive treatment affect COVID-19 outcomes[18].

Alcoholic liver disease and COVID-19

Patients with alcohol use disorder (AUD) and alcohol-associated liver disease (ALD) are exemplars of the wide range of potentially negative impacts of COVID-19[45]. Primarily, social isolation and the unavailability of professional help may lead to psychological decompensation and an increased risk of relapse[45]. Depressed immune systems and other underlying comorbidities, including renal failure, obesity, chronic viral hepatitis, sarcopenia, alcoholic cardiomyopathy, tobacco use disorder and many others, make these patients easy targets for viral infection. Finally, according to published data, these patients are more prone to developing interstitial pneumonia and acute respiratory distress syndrome secondary to SARS-CoV-2 infection than their counterparts[18]. Case series of ALD individuals reported a rapid disease course, including bilobar pneumonia and acute respiratory distress syndrome requiring mechanical ventilation, with unfavorable outcomes including cardiopulmonary insufficiency and multiorgan failure[46,47]. Patients admitted for acute alcoholic steatohepatitis (ASH) are usually assessed using Maddrey's discriminant function (DF) score, with DF > 32 predicting a higher mortality rate[46]. The usual

treatment of ASH in patients with DF > 32 using the classical prednisone regimen is an additional risk factor for a severe course of COVID-19 and is therefore not recommended for patients who are self-isolating or considered at high risk of acquiring SARS-CoV-2 infection[45]. Liver impairment is frequently observed in patients with COVID-19[46]. It is also well known that ASH increases the risk of hepatorenal syndrome development, especially after contrast agent application. Cytokine damage, inadequate organ perfusion, nephrotoxic drug effects and nosocomial infections all potentiate the acute kidney injury, usually resulting in the need for continuous renal replacement therapy[47].

In order to obviate the described critical disease course with severe consequences and high mortality rate, we should focus on two main aspects in the care of ALD patients. The primary focus is the prevention, of infection by following strict epidemiologic recommendations, as well as the prevention of AUD relapse by implementing vigorous social and psychiatric care by telephone. The unavailability of support groups such as Alcoholics Anonymous should be bridged using individual or smaller group treatment[47]. The secondary focus is the prevention of a deleterious disease course using vigilant intrahospital clinical care and timely recognition of hepatobiliary, renal and respiratory complications[18].

Viral hepatitis and COVID-19

Whether chronic viral hepatitis specifically affects the COVID-19 course remains unknown. In a retrospective Italian multicenter study that included 50 patients with liver cirrhosis and SARS-CoV-2 infection, 28% had hepatitis C virus (HCV)-related cirrhosis and 10% had hepatitis B virus (HBV)-related cirrhosis. The patients were either HCV-RNA negative after anti-HCV treatment or on long-term anti-HBV treatment. The severity of liver disease was an independent predictor of mortality[29]. The same conclusion was derived from an international registry that included 152 patients with CLD and COVID-19, among which 22.5% of the CLD was due to chronic HBV or HCV infection[30].

In the last year, the COVID-19 outbreak has redirected attention from other morbidities, including viral hepatitis: as a consequence of this pandemic, most viral hepatitis elimination programs have diminished or stopped altogether[14,19,48,49]. The World Health Organization's goal of eliminating HBV and HCV and thus significantly reducing the associated mortality until 2030 has therefore been put on hold. Elimination programs are already scarce, as well as involvement by liver disease societies, epidemiologists, infection specialists and general practitioners, despite the WHO Global Hepatitis Report 2017 stating that the viral hepatitis global mortality is 1.5 million per year[19,48,49]. Preventing mother-to-child transmission and promoting blood safety are presumably the only intact weapons in the battle against HBV and HCV[19,48]. Although we will realize the full impact of reducing or delaying programs targeting hepatitis elimination in the near future, there are some mathematical models that can predict the possible impact on the global burden of viral hepatitis and hepatitis-associated morbidity and mortality that will result as a consequence of program delay[49]. A recent study used certain mathematical models to analyze the impact of delayed programs on viral hepatitis elimination[49]. The authors reported that a 1-year delay in viral hepatitis diagnosis and treatment will result in an additional 44800 HCC cases as well as 72300 deaths from HCV globally in the next 10 years[49].

If we cannot make progress in achieving the aforementioned elimination goals due to the COVID-19 crisis, then education campaigns, extensive screening, diagnostic tests, vaccination programs and treatment should at least be maintained at the former level[19,48,49].

Liver cirrhosis and COVID-19

Patients with liver cirrhosis, particularly decompensated cirrhosis, are by far the most vulnerable liver disease patients. Immune dysfunction makes them prone to any kind of infection, including SARS-CoV-2, with potentially deleterious effects on the disease course. Data suggest that the course of COVID-19 is directly connected to the degree of liver disease defined by the Child-Pugh (CP) and Model for End Stage Liver Disease scores[18].

An international registry including 103 patients with liver cirrhosis reported a 40% mortality rate, strongly correlated with the grade of liver failure: 23.9% mortality in patients with CP class A, 43.3% mortality in patients with CP class B and 63.0% mortality in patients with CP class C cirrhosis[50]. Similarly, an Italian study involving 50 patients with liver cirrhosis suffering from COVID-19 found a 30-d mortality rate of 34%, among which 71% of patients died due to COVID-related respiratory failure[51].

The largest published study to date was based on two international registries and included 745 patients with CLD (among which 52% had liver cirrhosis) and acute COVID-19 infection. When compared to the data of non-CLD patients with SARS-CoV-2 infection in a UK hospital network, a statistically significant difference in mortality ($P < 0.001$) was reported: 32% in patients with liver cirrhosis compared to 8% in those without[52]. The main cause of death was respiratory failure, with acute decompensation of liver cirrhosis occurring in 46% of patients. The authors concluded that the CP score and ALD were independent risk factors for death due to COVID-19 [52].

A prospective American multicenter study by Singh and Khan[53] compared patients with both liver cirrhosis and COVID-19 to patients with only COVID-19 and found a significant difference in the outcome (30% *vs* 13%, $P = 0.03$). However, the fact that there was no significant difference in the outcomes of patients with liver cirrhosis regarding COVID-19 infection is intriguing. It seems important to emphasize that the proportion of SARS-CoV-2-positive cirrhosis patients in this study was approximately three times lower than that in the other two subgroups.

In summary, in patients suffering from COVID-19, mortality is significantly greater in those with liver cirrhosis than in those without and is directly related to the stage of liver failure[18]. However, it remains unclear whether COVID-19-related mortality is higher than that related to other causes of decompensation that are often also infective in origin[18].

Liver cirrhosis causes 2 million deaths globally per year. Prevention of liver decompensation and prompt diagnosis and treatment of cirrhosis-related complications are of the utmost importance[54,55]. Management with endoscopic variceal screening, primary and secondary prophylaxis, implementation of telecommunication and electronic communication in drug titration, especially regarding beta-blockers and diuretic therapies, is warranted. HCC screening and diagnostic persuasion, including radiologic methods and liver biopsy, as well as therapeutic treatments ranging from radiofrequency ablation to liver transplantation (LT), should be preserved despite scarce resources, physician burnout and lack of hospital capacity[54,55].

Tapper and Asrani[55] proposed a three-wave theory to explain the effects of the COVID-19 pandemic on liver cirrhosis from the current period to future years. The first wave describes the period of physical distancing and is defined by high-acuity care and delayed elective procedures[55]. For example, patients with esophageal varices are admitted only for bleeding episodes, and elective endoscopic band ligation (EBL) is not performed due to fear of viral spread and limited healthcare resources. The direct consequence of the first phase is the second wave, appearing after the resolution of physical distancing and characterized by a high frequency of cirrhosis decompensation[55]. Continuing with the given example, a substantial number of patients with indefinitely delayed or skipped EBL procedures will begin to experience variceal bleeding episodes, leading to cirrhosis decompensation or even acute-on-chronic liver failure. Accessible, inexpensive, processed foods rich in salt, as well as alcoholic beverages, both highly consumed during pandemics, will result in the exacerbation of volume overload and also potentiate sarcopenia, which is a well-known risk factor for cirrhosis-associated morbidity and mortality[55]. The third wave will presumably comprise long-term complications. Delayed diagnosis of hepatobiliary malignancies, progression of HCC reaching the Milan criteria and the consequent elimination of patients from transplant lists, insidious deterioration of renal function, no standardized recertification of patients awaiting LT and many more complications are to be encountered. As Tapper and Asrani[55] stated, the curable will be transformed into the incurable.

HCC and COVID-19

Although there are no specific data on the outcomes of patients with HCC and COVID-19 infection, it is assumed that HCC patients will have poor outcomes, similar to those in other oncology patients[15]. However, we know that most HCC patients have pre-existing CLD and in comparison to other patients with cancers we can assume that such patients are more susceptible to the effects of COVID-19: that is, hepatic injury caused by COVID-19 can complicate existing CLD in most patients with HCC. The COVID-19 pandemic has greatly limited the medical care of HCC patients, with effects ranging from early diagnosis to treatment. As ultrasound screening examinations have mostly been delayed indefinitely, without precise upcoming appointment dates and resulting in prolonged periods without control, the risk of discovering HCC at a later stage increased in approximately 25% of patients with the biologically aggressive type of disease[55,56].

Elective hospital admissions were also delayed in the peak of the COVID-19 pandemic due to low hospital capacity and the fear of viral spread. Outpatient ambulatory care was unavailable for a certain time. Subsequently, a substantial number of patients were afraid to visit medical facilities. Therefore, diagnostic procedures such as contrast-enhanced ultrasound, multislice computed tomography, magnetic resonance imaging and liver biopsies have been delayed. Additionally, treatment options have been insufficiently maintained. Surgical resection and LT are the most affected due to a shortage of anesthetists and other medical personnel[6]. Procedures such as transarterial (chemo)embolization (TACE/TAE) and radiofrequency ablation are therefore the most important tools in treating patients with HCC. Data on the impact of COVID-19 on HCC patient care are underrepresented[56,57]. A colleague from an Italian center managed HCC patients with the goal of minimizing the impact of COVID-19 and reported their experience from February 24 to March 20, 2020, regarding the treatment of HCC patients in comparison to the same period during 2019[57]. The authors found that 11% of patients had delayed treatment of HCC for 2 mo or longer. The delayed treatment modalities comprised transarterial procedures in eight HCC patients, thermal ablation in three HCC patients and systemic therapy in two patients. Thermal ablation in the three patients was performed as an alternative procedure to surgical treatment. The results of this study represent the best efforts of clinicians to manage HCC during the COVID-19 pandemic[57].

In the case of early-stage HCC, the capacity of most hospitals for surgical treatment (resection) is limited due to the limited number of anesthesiologists as well as shortages in intensive care unit beds. Clinicians can select some patients who have been prioritized for resection and have a relatively low disease burden. Treatment modalities such as radiofrequency and microwave ablation, upfront transarterial treatment and systemic therapy may be considered as alternative methods according to the guidelines for each treatment modality[56,58]. Additionally, during the pandemic, the number of LTs were reduced or reached zero for some time due to reduced anesthetic capacity as well as a shortage of donors[56,58]. In the case of intermediate-stage HCC, a more selective approach can be used with respect to TACE in hospitals that are greatly affected by the COVID-19 pandemic. Additionally, if a specific center cannot perform TACE, systemic therapy or adequate surveillance, then imaging could be an alternative approach[56,58]. Finally, in the case of advanced-stage HCC, HCC patients who receive oral multitargeted tyrosine kinase inhibitors could be followed by clinicians for prolonged intervals or monitored by telephone or another telemedicine interface, depending on the patient's tolerance and clinical status during the COVID-19 pandemic[56,58]. The impact on the long-term outcomes of HCC due to these modifications in treatment options, as well as the delays in treatment, will soon be realized[57].

The decision to treat HCC during the pandemic should consider the availability of medical staff, risk of infection and the risk-benefit ratio for an individual patient. The management of HCC in patients is complex because it relies heavily on multidisciplinary approaches involving gastroenterologists, radiologists, hepatobiliary surgeons and oncologists, who are significantly burdened during this pandemic[15,56]. Extra coordination among different specialties is necessary to maintain clinical services for patients with HCC. It is recommended that the care and treatment of HCC patients is maintained according to the guidelines by using alternative methods of communication whenever possible in order to minimize the COVID-19 exposure risk to medical staff[15]. Widely available SARS-CoV-2 polymerase chain reaction testing is recommended before elective hospital admission, although there can never be a definite guarantee for medical personnel because a patient may be in the incubation phase of infection or the patient may contract the infection in the hospital. If the patient is acutely infected, it is reasonable to defer HCC treatment for a few weeks until after recovery from COVID-19[6].

LT AND COVID-19

LT programs have been weakened globally, even in regions where the COVID-19 prevalence has been low[59-61]. During this period of readjustment no specific guidelines were offered; however, multiple organizations released recommendations for medical personnel involved in solid organ transplantation[59-66].

Primarily, obtaining an organ from a SARS-CoV-2-infected patient is contraindicated. Moreover, screening of deceased donors, as well as recipients, is highly recommended[59-66]. In the case of unidentified infection, the donor could spread the

virus to multiple recipients, which would presumably have an unfavorable or even lethal course under severe immunosuppression[6,62].

As the risk of contracting the virus is high, even under hospital conditions, it would be appropriate to limit the number of face-to-face contacts for patients at risk of severe COVID-19. They should be advised against travel and should strictly practice physical distancing[6]. Due to cirrhosis-associated immune dysfunction, the aforementioned recommendations apply to all patients awaiting transplantation.

A further challenge is related to the staff involved in LT, who cannot be easily replaced. Quarantined, infected or redistributed personnel can prevent program realization for a certain period of time, which can have deleterious effects on potential LT recipients[59]. Therefore, splitting the team involved in LT and postoperative care into smaller subteams, as well as screening and segregating staff working with immediate post-LT patients, is recommended[59]. Compared to some other solid organ transplantations, LT is performed to preserve life. In contrast, although renal transplantation reduces dialysis morbidity and future medical costs, it is not directly lifesaving and can therefore be postponed[62]. Lifesaving transplantations, such as liver, heart and lung, have far more urgent indications and postponement may have deleterious consequences. Accordingly, it is of utmost importance that LT centers worldwide aim to restore their transplantation services.

Finally, according to preliminary data, age and comorbidity are key to determining the outcome from SARS-CoV-2 infection in LT patients[6,9].

Whether to receive vaccination is currently an unavoidable global question potentiated by substantial social media involvement. Three vaccines were approved by February 2021. Two of these, the BNT162b2 (Pfizer-BioNTech) and mRNA-1273 (Moderna) vaccines, are based on mRNAs that encode variants of the SARS-CoV-2-spiked glycoprotein[63]. Both must be administered twice, 21-28 d apart. The third approved vaccine is AZD1222, also known as the Oxford-AstraZeneca vaccine. This is an adenovirus vector that contains the full-length, codon-optimized gene that encodes the SARS-CoV-2 spike protein and should also be administered in two doses, with the second dose administered 4-12 wk after the first dose[63]. The EASL position paper recommends vaccination against SARS-CoV-2 in patients with CLD, hepatobiliary cancer and LT[63].

Post-transplant patients and COVID-19

Patients taking immunosuppressive drugs after transplantation are at increased risk of infection or viral reactivation. The exact influence of the SARS-CoV-2 virus in post-LT patients is unclear[15].

Regarding the disease course in post-transplant patients, it seems that immunosuppression might have favorable effects by disabling cytokine release syndrome, characterized by increased serum levels of interleukin (IL)-6, IL-8 and tumor necrosis factor [15,64]. A Spanish study analyzed 111 LT patients diagnosed with COVID-19[65]. During a median follow-up of approximately 3 wk, 86.5% of patients were admitted to hospital, among which 19.8% required respiratory support[65]. Surprisingly, their mortality rate (18%) was lower than in the complementary general population. Mycophenolate mofetil (MMF) administered at a dose of > 1000 mg/d was an independent predictor of severe COVID-19[65]. In contrast, treatment with calcineurin inhibitors and the mammalian target of rapamycin (mTOR) inhibitor everolimus were not associated with a severe COVID-19 course. Complete withdrawal of immunosuppression showed no benefit[65]. Therefore, MMF withdrawal or transient conversion to calcineurin inhibitors or everolimus could be beneficial for hospitalized patients until the COVID-19 resolves[65].

Vaccination in post-LT patients is recommended at approximately 3-6 mo after transplantation when immunosuppression can be reduced. This is because the immune system is too suppressed to mount the proper vaccination response in the early post-transplant period. Accordingly, vaccination of household members and of healthcare professionals caring for immunocompromised patients is advocated[63].

LIVER DISEASE AND COVID-19 IN CHILDREN

A recent review by Di Giorgio *et al*[67] nicely summarizes the current data from 105 studies on the association among pre-existing CLD and COVID-19 infection in children. According to the data, the most common liver manifestation was an elevation of transaminases[67]. The authors found that children with CLD, including those on immunosuppressive therapy (autoimmune liver disease and LT), actually do not have

a higher risk for a severe disease course of COVID-19. Additionally, they have little or no liver dysfunction[67]. As mentioned earlier, we still do not know the exact pathogenetic mechanism of liver damage in either adults or children, therefore we still do not fully understand the clinical outcomes of patients with CLD infected with COVID-19. Furthermore, there are no clear data on infectivity rates in children with CLD or regarding the presence of asymptomatic carriage of the virus in children[67]. Finally, there are no data regarding the long-term outcome of COVID-19 infection in this group of immunocompromised children[67]. Thus, further data are needed.

CURRENT STUDIES AND FUTURE DIRECTIONS

The COVID-19 pandemic has caused serious damage to the global health system and prevented the anticipation, recruitment or completion of numerous clinical trials. However, according to ClinicaTrials.gov, there are currently more than 1500 studies related to 'liver disease' in the recruitment phase[68]. In line with active clinical research and databases including patients with NAFLD and CLD, it is evident that this remains a trending topic, despite the COVID-19 pandemonium. The utilization of noninvasive methods in the assessment of liver and spleen stiffness and indirect prediction of portal hypertension remains the desired goal in the field of CLD. At the same time, clinicians worldwide are determined to find a proper therapy for NAFLD. The effects of glucagon-like peptide agonist (GLP-1) semaglutide, peroxisome proliferator-activated receptor (PPAR) agonist lanifibranor, thiazolidinediones, sodium-glucose cotransporter 2 inhibitors, prebiotics and probiotics are currently being tested in clinical trials[69-73]. Furthermore, the impact of fecal microbiota transplantation on obese patients with NAFLD is being researched on participants in India[74]. A selective thyroid hormone receptor-β agonist, resmetirom (MGL-3196), is in its third trial phase and the mitochondrial-derived peptide (MOTS-c) analog CB4211 is in its 1a/1b phase of evaluation among the NAFLD population[75,76]. Considering the global proportion of obese patients suffering from NAFLD, whose number under the COVID-19-created environment will undoubtedly grow, extension of the mentioned research and anticipation of future studies is encouraged.

CONCLUSION

The global social, economic and political crises related to the COVID-19 pandemic presumably had more indirect than direct negative impacts on health systems. Drastic lifestyle changes, social isolation and distancing, and individual and global financial crises resulted in a robust population forfeiting healthy habits and seeking comfort in alcoholic beverages, drugs and unhealthy diets[19,41]. The inevitable consequences are the rising incidence of NAFLD, viral hepatitis, acute alcoholic hepatitis, liver cirrhosis decompensation and ultimately liver-related mortality[19].

The inaccessibility of regular clinical and sonographic examinations has resulted in difficulties in the treatment of patients with CLD or prompt HCC detection and treatment. A dramatic reduction in the number of liver donors and the transformation of numerous transplantation centers into COVID-19 units have greatly reduced the rate of orthotopic LT.

The indirect unavoidable effects of the COVID-19 pandemic in the following years have yet to be determined[19]. Although the health system has been tremendously challenged, resulting in overwhelming damage that is continuously being revealed, focus should remain on the current and upcoming periods involving patients with uncontrolled chronic diseases[16,19]. Swift resumption of care practices, especially for patients with HCC or individuals requiring LT, must be initiated while simultaneously maintaining social distancing and balancing inadequate hospital resources[16,19].

Substantial efforts should be initiated for the management of patients with liver disease in order to prevent and control the inevitable COVID-19-related morbidity and mortality that will follow.

Several questions regarding the impact of the COVID-19 pandemic on liver disease remain. One of the most important questions is: What will be the effect of long-term anticoagulants on liver disease? The main question for general CLD patients is: How will the modification of clinical practice during this pandemic affect outcomes in CLD patients.

REFERENCES

1 **Téllez L**, Martín Mateos RM. COVID-19 and liver disease: An update. *Gastroenterol Hepatol* 2020; **43**: 472-480 [PMID: 32727662 DOI: 10.1016/j.gastrohep.2020.06.006]

2 **Lax SF**, Skok K, Zechner P, Kessler HH, Kaufmann N, Koelblinger C, Vander K, Bargfrieder U, Trauner M. Pulmonary Arterial Thrombosis in COVID-19 With Fatal Outcome : Results From a Prospective, Single-Center, Clinicopathologic Case Series. *Ann Intern Med* 2020; **173**: 350-361 [PMID: 32422076 DOI: 10.7326/M20-2566]

3 **Williamson EJ**, Walker AJ, Bhaskaran K, Bacon S, Bates C, Morton CE, Curtis HJ, Mehrkar A, Evans D, Inglesby P, Cockburn J, McDonald HI, MacKenna B, Tomlinson L, Douglas IJ, Rentsch CT, Mathur R, Wong AYS, Grieve R, Harrison D, Forbes H, Schultze A, Croker R, Parry J, Hester F, Harper S, Perera R, Evans SJW, Smeeth L, Goldacre B. Factors associated with COVID-19-related death using OpenSAFELY. *Nature* 2020; **584**: 430-436 [PMID: 32640463 DOI: 10.1038/s41586-020-2521-4]

4 **Nardo AD**, Schneeweiss-Gleixner M, Bakail M, Dixon ED, Lax SF, Trauner M. Pathophysiological mechanisms of liver injury in COVID-19. *Liver Int* 2021; **41**: 20-32 [PMID: 33190346 DOI: 10.1111/liv.14730]

5 **Sonzogni A**, Previtali G, Seghezzi M, Grazia Alessio M, Gianatti A, Licini L, Morotti D, Zerbi P, Carsana L, Rossi R, Lauri E, Pellegrinelli A, Nebuloni M. Liver histopathology in severe COVID 19 respiratory failure is suggestive of vascular alterations. *Liver Int* 2020; **40**: 2110-2116 [PMID: 32654359 DOI: 10.1111/liv.14601]

6 **Wong GL**, Wong VW, Thompson A, Jia J, Hou J, Lesmana CRA, Susilo A, Tanaka Y, Chan WK, Gane E, Ong-Go AK, Lim SG, Ahn SH, Yu ML, Piratvisuth T, Chan HL; Asia-Pacific Working Group for Liver Derangement during the COVID-19 Pandemic. Management of patients with liver derangement during the COVID-19 pandemic: an Asia-Pacific position statement. *Lancet Gastroenterol Hepatol* 2020; **5**: 776-787 [PMID: 32585136 DOI: 10.1016/S2468-1253(20)30190-4]

7 **Cevik M**, Bamford CGG, Ho A. COVID-19 pandemic-a focused review for clinicians. *Clin Microbiol Infect* 2020; **26**: 842-847 [PMID: 32344166 DOI: 10.1016/j.cmi.2020.04.023]

8 **Cha MH**, Regueiro M, Sandhu DS. Gastrointestinal and hepatic manifestations of COVID-19: A comprehensive review. *World J Gastroenterol* 2020; **26**: 2323-2332 [PMID: 32476796 DOI: 10.3748/wjg.v26.i19.2323]

9 **Webb GJ**, Moon AM, Barnes E, Barritt AS 4th, Marjot T. Age and comorbidity are central to the risk of death from COVID-19 in liver transplant recipients. *J Hepatol* 2021; **75**: 226-228 [PMID: 33556419 DOI: 10.1016/j.jhep.2021.01.036]

10 **Marjot T**, Buescher G, Sebode M, Barnes E, Barritt AS 4th, Armstrong MJ, Baldelli L, Kennedy J, Mercer C, Ozga AK, Casar C, Schramm C; contributing Members and Collaborators of ERN RARE-LIVER/COVID-Hep/SECURE-Cirrhosis, Moon AM, Webb GJ, Lohse AW. SARS-CoV-2 infection in patients with autoimmune hepatitis. *J Hepatol* 2021; **74**: 1335-1343 [PMID: 33508378 DOI: 10.1016/j.jhep.2021.01.021]

11 **Portincasa P**, Krawczyk M, Smyk W, Lammert F, Di Ciaula A. COVID-19 and non-alcoholic fatty liver disease: Two intersecting pandemics. *Eur J Clin Invest* 2020; **50**: e13338 [PMID: 32589264 DOI: 10.1111/eci.13338]

12 **Pedersen SF**, Ho YC. SARS-CoV-2: a storm is raging. *J Clin Invest* 2020; **130**: 2202-2205 [PMID: 32217834 DOI: 10.1172/JCI137647]

13 **Mehta P**, McAuley DF, Brown M, Sanchez E, Tattersall RS, Manson JJ; HLH Across Speciality Collaboration, UK. COVID-19: consider cytokine storm syndromes and immunosuppression. *Lancet* 2020; **395**: 1033-1034 [PMID: 32192578 DOI: 10.1016/S0140-6736(20)30628-0]

14 **Samarasekera U**. COVID-19 hits viral hepatitis care for vulnerable populations. *Lancet Gastroenterol Hepatol* 2021; **6**: 166 [PMID: 33581759 DOI: 10.1016/S2468-1253(21)00029-7]

15 **Ridruejo E**, Soza A. The liver in times of COVID-19: What hepatologists should know. *Ann Hepatol* 2020; **19**: 353-358 [PMID: 32425991 DOI: 10.1016/j.aohep.2020.05.001]

16 **Bollipo S**, Kapuria D, Rabiee A, Ben-Yakov G, Lui RN, Lee HW, Kumar G, Siau K, Turnes J, Dhanasekaran R. One world, one pandemic, many guidelines: management of liver diseases during COVID-19. *Gut* 2020; **69**: 1369-1372 [PMID: 32499304 DOI: 10.1136/gutjnl-2020-321553]

17 **Fix OK**, Hameed B, Fontana RJ, Kwok RM, McGuire BM, Mulligan DC, Pratt DS, Russo MW, Schilsky ML, Verna EC, Loomba R, Cohen DE, Bezerra JA, Reddy KR, Chung RT. Clinical Best Practice Advice for Hepatology and Liver Transplant Providers During the COVID-19 Pandemic: AASLD Expert Panel Consensus Statement. *Hepatology* 2020; **72**: 287-304 [PMID: 32298473 DOI: 10.1002/hep.31281]

18 **Boettler T**, Newsome PN, Mondelli MU, Maticic M, Cordero E, Cornberg M, Berg T. Care of patients with liver disease during the COVID-19 pandemic: EASL-ESCMID position paper. *JHEP Rep* 2020; **2**: 100113 [PMID: 32289115 DOI: 10.1016/j.jhepr.2020.100113]

19 **Pawlotsky JM**. COVID-19 and the liver-related deaths to come. *Nat Rev Gastroenterol Hepatol* 2020; **17**: 523-525 [PMID: 32528138 DOI: 10.1038/s41575-020-0328-2]

20 **CDC COVID-19 Response Team**. Preliminary Estimates of the Prevalence of Selected Underlying Health Conditions Among Patients with Coronavirus Disease 2019 - United States, February 12-March 28, 2020. *MMWR Morb Mortal Wkly Rep* 2020; **69**: 382-386 [PMID: 32240123 DOI: 10.15585/mmwr.mm6913e2]

21 **Portincasa P**, Krawczyk M, Machill A, Lammert F, Di Ciaula A. Hepatic consequences of COVID-

19 infection. Lapping or biting? *Eur J Intern Med* 2020; **77**: 18-24 [PMID: 32507608 DOI: 10.1016/j.ejim.2020.05.035]

22 **Lei F**, Liu YM, Zhou F, Qin JJ, Zhang P, Zhu L, Zhang XJ, Cai J, Lin L, Ouyang S, Wang X, Yang C, Cheng X, Liu W, Li H, Xie J, Wu B, Luo H, Xiao F, Chen J, Tao L, Cheng G, She ZG, Zhou J, Wang H, Lin J, Luo P, Fu S, Ye P, Xiao B, Mao W, Liu L, Yan Y, Chen G, Huang X, Zhang BH, Yuan Y. Longitudinal Association Between Markers of Liver Injury and Mortality in COVID-19 in China. *Hepatology* 2020; **72**: 389-398 [PMID: 32359177 DOI: 10.1002/hep.31301]

23 **Feng G**, Zheng KI, Yan QQ, Rios RS, Targher G, Byrne CD, Poucke SV, Liu WY, Zheng MH. COVID-19 and Liver Dysfunction: Current Insights and Emergent Therapeutic Strategies. *J Clin Transl Hepatol* 2020; **8**: 18-24 [PMID: 32274342 DOI: 10.14218/JCTH.2020.00018]

24 **Fan Z**, Chen L, Li J, Cheng X, Yang J, Tian C, Zhang Y, Huang S, Liu Z, Cheng J. Clinical Features of COVID-19-Related Liver Functional Abnormality. *Clin Gastroenterol Hepatol* 2020; **18**: 1561-1566 [PMID: 32283325 DOI: 10.1016/j.cgh.2020.04.002]

25 **Richardson S**, Hirsch JS, Narasimhan M, Crawford JM, McGinn T, Davidson KW; the Northwell COVID-19 Research Consortium, Barnaby DP, Becker LB, Chelico JD, Cohen SL, Cookingham J, Coppa K, Diefenbach MA, Dominello AJ, Duer-Hefele J, Falzon L, Gitlin J, Hajizadeh N, Harvin TG, Hirschwerk DA, Kim EJ, Kozel ZM, Marrast LM, Mogavero JN, Osorio GA, Qiu M, Zanos TP. Presenting Characteristics, Comorbidities, and Outcomes Among 5700 Patients Hospitalized With COVID-19 in the New York City Area. *JAMA* 2020; **323**: 2052-2059 [PMID: 32320003 DOI: 10.1001/jama.2020.6775]

26 **Xu L**, Liu J, Lu M, Yang D, Zheng X. Liver injury during highly pathogenic human coronavirus infections. *Liver Int* 2020; **40**: 998-1004 [PMID: 32170806 DOI: 10.1111/liv.14435]

27 **Zhang C**, Shi L, Wang FS. Liver injury in COVID-19: management and challenges. *Lancet Gastroenterol Hepatol* 2020; **5**: 428-430 [PMID: 32145190 DOI: 10.1016/S2468-1253(20)30057-1]

28 **Cai Q**, Huang D, Yu H, Zhu Z, Xia Z, Su Y, Li Z, Zhou G, Gou J, Qu J, Sun Y, Liu Y, He Q, Chen J, Liu L, Xu L. COVID-19: Abnormal liver function tests. *J Hepatol* 2020; **73**: 566-574 [PMID: 32298767 DOI: 10.1016/j.jhep.2020.04.006]

29 **Iavarone M**, D'Ambrosio R, Soria A, Triolo M, Pugliese N, Del Poggio P, Perricone G, Massironi S, Spinetti A, Buscarini E, Viganò M, Carriero C, Fagiuoli S, Aghemo A, Belli LS, Lucà M, Pedaci M, Rimondi A, Rumi MG, Invernizzi P, Bonfanti P, Lampertico P. High rates of 30-day mortality in patients with cirrhosis and COVID-19. *J Hepatol* 2020; **73**: 1063-1071 [PMID: 32526252 DOI: 10.1016/j.jhep.2020.06.001]

30 **Sun J**, Aghemo A, Forner A, Valenti L. COVID-19 and liver disease. *Liver Int* 2020; **40**: 1278-1281 [PMID: 32251539 DOI: 10.1111/liv.14470]

31 **Docherty AB**, Harrison EM, Green CA, Hardwick HE, Pius R, Norman L, Holden KA, Read JM, Dondelinger F, Carson G, Merson L, Lee J, Plotkin D, Sigfrid L, Halpin S, Jackson C, Gamble C, Horby PW, Nguyen-Van-Tam JS, Ho A, Russell CD, Dunning J, Openshaw PJ, Baillie JK, Semple MG; ISARIC4C investigators. Features of 20 133 UK patients in hospital with covid-19 using the ISARIC WHO Clinical Characterisation Protocol: prospective observational cohort study. *BMJ* 2020; **369**: m1985 [PMID: 32444460 DOI: 10.1136/bmj.m1985]

32 **Ji D**, Qin E, Xu J, Zhang D, Cheng G, Wang Y, Lau G. Non-alcoholic fatty liver diseases in patients with COVID-19: A retrospective study. *J Hepatol* 2020; **73**: 451-453 [PMID: 32278005 DOI: 10.1016/j.jhep.2020.03.044]

33 **Zhou YJ**, Zheng KI, Wang XB, Yan HD, Sun QF, Pan KH, Wang TY, Ma HL, Chen YP, George J, Zheng MH. Younger patients with MAFLD are at increased risk of severe COVID-19 illness: A multicenter preliminary analysis. *J Hepatol* 2020; **73**: 719-721 [PMID: 32348790 DOI: 10.1016/j.jhep.2020.04.027]

34 **Gao F**, Zheng KI, Wang XB, Yan HD, Sun QF, Pan KH, Wang TY, Chen YP, George J, Zheng MH. Metabolic associated fatty liver disease increases coronavirus disease 2019 disease severity in nondiabetic patients. *J Gastroenterol Hepatol* 2021; **36**: 204-207 [PMID: 32436622 DOI: 10.1111/jgh.15112]

35 **Targher G**, Mantovani A, Byrne CD, Wang XB, Yan HD, Sun QF, Pan KH, Zheng KI, Chen YP, Eslam M, George J, Zheng MH. Risk of severe illness from COVID-19 in patients with metabolic dysfunction-associated fatty liver disease and increased fibrosis scores. *Gut* 2020; **69**: 1545-1547 [PMID: 32414813 DOI: 10.1136/gutjnl-2020-321611]

36 **Lopez-Mendez I**, Aquino-Matus J, Gall SM, Prieto-Nava JD, Juarez-Hernandez E, Uribe M, Castro-Narro G. Association of liver steatosis and fibrosis with clinical outcomes in patients with SARS-CoV-2 infection (COVID-19). *Ann Hepatol* 2021; **20**: 100271 [PMID: 33099028 DOI: 10.1016/j.aohep.2020.09.015]

37 **Ferron PJ**, Gicquel T, Mégarbane B, Clément B, Fromenty B. Treatments in Covid-19 patients with pre-existing metabolic dysfunction-associated fatty liver disease: A potential threat for drug-induced liver injury? *Biochimie* 2020; **179**: 266-274 [PMID: 32891697 DOI: 10.1016/j.biochi.2020.08.018]

38 **Huang C**, Wang Y, Li X, Ren L, Zhao J, Hu Y, Zhang L, Fan G, Xu J, Gu X, Cheng Z, Yu T, Xia J, Wei Y, Wu W, Xie X, Yin W, Li H, Liu M, Xiao Y, Gao H, Guo L, Xie J, Wang G, Jiang R, Gao Z, Jin Q, Wang J, Cao B. Clinical features of patients infected with 2019 novel coronavirus in Wuhan, China. *Lancet* 2020; **395**: 497-506 [PMID: 31986264 DOI: 10.1016/S0140-6736(20)30183-5]

39 **Gao B**, Tsukamoto H. Inflammation in Alcoholic and Nonalcoholic Fatty Liver Disease: Friend or Foe? *Gastroenterology* 2016; **150**: 1704-1709 [PMID: 26826669 DOI: 10.1053/j.gastro.2016.01.025]

40 **Boeckmans J**, Rodrigues RM, Demuyser T, Piérard D, Vanhaecke T, Rogiers V. COVID-19 and

drug-induced liver injury: a problem of plenty or a petty point? *Arch Toxicol* 2020; **94**: 1367-1369 [PMID: 32266419 DOI: 10.1007/s00204-020-02734-1]

41 **Clemmensen C**, Petersen MB, Sørensen TIA. Will the COVID-19 pandemic worsen the obesity epidemic? *Nat Rev Endocrinol* 2020; **16**: 469-470 [PMID: 32641837 DOI: 10.1038/s41574-020-0387-z]

42 **Stanfield D**, Lucey MR. The Heightened Risk of Fatty Liver Disorders in the Time of COVID-19. *Mayo Clin Proc* 2020; **95**: 2580-2581 [PMID: 33276827 DOI: 10.1016/j.mayocp.2020.10.020]

43 **Peeraphatdit TB**, Ahn JC, Choi DH, Allen AM, Simonetto DA, Kamath PS, Shah VH. A Cohort Study Examining the Interaction of Alcohol Consumption and Obesity in Hepatic Steatosis and Mortality. *Mayo Clin Proc* 2020; **95**: 2612-2620 [PMID: 33276835 DOI: 10.1016/j.mayocp.2020.04.046]

44 **Merli M**, Perricone G, Lauterio A, Prosperi M, Travi G, Roselli E, Petrò L, De Carlis L, Belli L, Puoti M. Coronaviruses and Immunosuppressed Patients: The Facts During the Third Epidemic. *Liver Transpl* 2020; **26**: 1543-1544 [PMID: 32475054 DOI: 10.1002/lt.25806]

45 **Da BL**, Im GY, Schiano TD. Coronavirus Disease 2019 Hangover: A Rising Tide of Alcohol Use Disorder and Alcohol-Associated Liver Disease. *Hepatology* 2020; **72**: 1102-1108 [PMID: 32369624 DOI: 10.1002/hep.31307]

46 **Wiśniewska H**, Skowron M, Bander D, Hornung M, Jurczyk K, Karpińska E, Laurans Ł, Socha Ł, Czajkowski Z, Wawrzynowicz-Syczewska M. Nosocomial COVID-19 Infection and Severe COVID-19 Pneumonia in Patients Hospitalized for Alcoholic Liver Disease: A Case Report. *Am J Case Rep* 2020; **21**: e927452 [PMID: 32973125 DOI: 10.12659/AJCR.927452]

47 **Kapuria D**, Upadhyay S, Shekhar R, Torrazza-Perez E. Alcoholic Liver Disease and COVID-19 Pneumonia: A Case Series. *J Clin Transl Hepatol* 2020; **8**: 463-466 [PMID: 33447531 DOI: 10.14218/JCTH.2020.00053]

48 **Karimi-Sari H**, Rezaee-Zavareh MS. COVID-19 and viral hepatitis elimination programs: Are we stepping backward? *Liver Int* 2020; **40**: 2042 [PMID: 32319207 DOI: 10.1111/liv.14486]

49 **Blach S**, Kondili LA, Aghemo A, Cai Z, Dugan E, Estes C, Gamkrelidze I, Ma S, Pawlotsky JM, Razavi-Shearer D, Razavi H, Waked I, Zeuzem S, Craxi A. Impact of COVID-19 on global HCV elimination efforts. *J Hepatol* 2021; **74**: 31-36 [PMID: 32777322 DOI: 10.1016/j.jhep.2020.07.042]

50 **Moon AM**, Webb GJ, Aloman C, Armstrong MJ, Cargill T, Dhanasekaran R, Genescà J, Gill US, James TW, Jones PD, Marshall A, Mells G, Perumalswami PV, Qi X, Su F, Ufere NN, Barnes E, Barritt AS, Marjot T. High mortality rates for SARS-CoV-2 infection in patients with pre-existing chronic liver disease and cirrhosis: Preliminary results from an international registry. *J Hepatol* 2020; **73**: 705-708 [PMID: 32446714 DOI: 10.1016/j.jhep.2020.05.013]

51 **Hunt RH**, East JE, Lanas A, Malfertheiner P, Satsangi J, Scarpignato C, Webb GJ. COVID-19 and Gastrointestinal Disease: Implications for the Gastroenterologist. *Dig Dis* 2021; **39**: 119-139 [PMID: 33040064 DOI: 10.1159/000512152]

52 **Marjot T**, Moon AM, Cook JA, Abd-Elsalam S, Aloman C, Armstrong MJ, Pose E, Brenner EJ, Cargill T, Catana MA, Dhanasekaran R, Eshraghian A, García-Juárez I, Gill US, Jones PD, Kennedy J, Marshall A, Matthews C, Mells G, Mercer C, Perumalswami PV, Avitabile E, Qi X, Su F, Ufere NN, Wong YJ, Zheng MH, Barnes E, Barritt AS 4th, Webb GJ. Outcomes following SARS-CoV-2 infection in patients with chronic liver disease: An international registry study. *J Hepatol* 2021; **74**: 567-577 [PMID: 33035628 DOI: 10.1016/j.jhep.2020.09.024]

53 **Singh S**, Khan A. Clinical Characteristics and Outcomes of Coronavirus Disease 2019 Among Patients With Preexisting Liver Disease in the United States: A Multicenter Research Network Study. *Gastroenterology* 2020; **159**: 768-771.e3 [PMID: 32376408 DOI: 10.1053/j.gastro.2020.04.064]

54 **Asrani SK**, Devarbhavi H, Eaton J, Kamath PS. Burden of liver diseases in the world. *J Hepatol* 2019; **70**: 151-171 [PMID: 30266282 DOI: 10.1016/j.jhep.2018.09.014]

55 **Tapper EB**, Asrani SK. The COVID-19 pandemic will have a long-lasting impact on the quality of cirrhosis care. *J Hepatol* 2020; **73**: 441-445 [PMID: 32298769 DOI: 10.1016/j.jhep.2020.04.005]

56 **Chan SL**, Kudo M. Impacts of COVID-19 on Liver Cancers: During and after the Pandemic. *Liver Cancer* 2020; **9**: 491-502 [PMID: 33078127 DOI: 10.1159/000510765]

57 **Iavarone M**, Sangiovanni A, Carrafiello G, Rossi G, Lampertico P. Management of hepatocellular carcinoma in the time of COVID-19. *Ann Oncol* 2020; **31**: 1084-1085 [PMID: 32330540 DOI: 10.1016/j.annonc.2020.04.007]

58 **European Association for the Study of the Liver**. EASL Clinical Practice Guidelines: Management of hepatocellular carcinoma. *J Hepatol* 2018; **69**: 182-236 [PMID: 29628281 DOI: 10.1016/j.jhep.2018.03.019]

59 **Niriella MA**, Siriwardana RC, Perera MTPR, Narasimhan G, Chan SC, Dassanayake AS. Challenges for Liver Transplantation During Recovery From the COVID-19 Pandemic: Insights and Recommendations. *Transplant Proc* 2020; **52**: 2601-2606 [PMID: 32586665 DOI: 10.1016/j.transproceed.2020.05.032]

60 **Di Maira T**, Berenguer M. COVID-19 and liver transplantation. *Nat Rev Gastroenterol Hepatol* 2020; **17**: 526-528 [PMID: 32651555 DOI: 10.1038/s41575-020-0347-z]

61 **Ritschl PV**, Nevermann N, Wiering L, Wu HH, Moroder P, Brandl A, Hillebrandt K, Tacke F, Friedersdorff F, Schlomm T, Schöning W, Öllinger R, Schmelzle M, Pratschke J. Solid organ transplantation programs facing lack of empiric evidence in the COVID-19 pandemic: A By-proxy Society Recommendation Consensus approach. *Am J Transplant* 2020; **20**: 1826-1836 [PMID: 32323460 DOI: 10.1111/ajt.15933]

62 **Kumar D**, Manuel O, Natori Y, Egawa H, Grossi P, Han SH, Fernández-Ruiz M, Humar A. COVID-19: A global transplant perspective on successfully navigating a pandemic. *Am J Transplant* 2020; **20**: 1773-1779 [PMID: 32202064 DOI: 10.1111/ajt.15876]

63 **Cornberg M**, Buti M, Eberhardt CS, Grossi PA, Shouval D. EASL position paper on the use of COVID-19 vaccines in patients with chronic liver diseases, hepatobiliary cancer and liver transplant recipients. *J Hepatol* 2021; **74**: 944-951 [PMID: 33563499 DOI: 10.1016/j.jhep.2021.01.032]

64 **D'Antiga L**. Coronaviruses and Immunosuppressed Patients: The Facts During the Third Epidemic. *Liver Transpl* 2020; **26**: 832-834 [PMID: 32196933 DOI: 10.1002/lt.25756]

65 **Colmenero J**, Rodríguez-Perálvarez M, Salcedo M, Arias-Milla A, Muñoz-Serrano A, Graus J, Nuño J, Gastaca M, Bustamante-Schneider J, Cachero A, Lladó L, Caballero A, Fernández-Yunquera A, Loinaz C, Fernández I, Fondevila C, Navasa M, Iñarrairaegui M, Castells L, Pascual S, Ramírez P, Vinaixa C, González-Dieguez ML, González-Grande R, Hierro L, Nogueras F, Otero A, Álamo JM, Blanco-Fernández G, Fábrega E, García-Pajares F, Montero JL, Tomé S, De la Rosa G, Pons JA. Epidemiological pattern, incidence, and outcomes of COVID-19 in liver transplant patients. *J Hepatol* 2021; **74**: 148-155 [PMID: 32750442 DOI: 10.1016/j.jhep.2020.07.040]

66 **Qin J**, Wang H, Qin X, Zhang P, Zhu L, Cai J, Yuan Y, Li H. Perioperative Presentation of COVID-19 Disease in a Liver Transplant Recipient. *Hepatology* 2020; **72**: 1491-1493 [PMID: 32220017 DOI: 10.1002/hep.31257]

67 **Di Giorgio A**, Hartleif S, Warner S, Kelly D. COVID-19 in Children With Liver Disease. *Front Pediatr* 2021; **9**: 616381 [PMID: 33777864 DOI: 10.3389/fped.2021.616381]

68 **U.S. National Library of Medicine**. Identifier NCT00287391. [cited 27 Feb 2021]. In: ClinicalTrials.gov [Internet]. 2000 Feb 29 - . [about 15 screens]. Available from: URL: https://clinicaltrials.gov/ct2/results?cond=liver+disease&Search=Apply&recrs=a&age_v=&gndr=&type=&rslt=

69 **Erlandson K**, Lake JE. Study of Semaglutide for Non-Alcoholic Fatty Liver Disease (NAFLD), a Metabolic Syndrome With Insulin Resistance, Increased Hepatic Lipids, and Increased Cardiovascular Disease Risk (The SLIM LIVER Study). [accessed 2021 Feb 27]. In: ClinicalTrials.gov [Internet]. Birmingham (AL): U.S. National Library of Medicine. Available from: https://clinicaltrials.gov/ct2/show/NCT04216589?recrs=a&cond=liver+disease&draw=3&rank=58 ClinicalTrials.gov Identifier: NCT04216589

70 **Rotman Y**. Non-Alcoholic Fatty Liver Disease, the Hepatic Response to Oral Glucose, and the Effect of Semaglutide (NAFLD HEROES). [accessed 2021 Feb 27]. In: ClinicalTrials.gov [Internet]. Bethesda (MD): U.S. National Library of Medicine. Available from: https://clinicaltrials.gov/ct2/show/NCT03884075?recrs=a&cond=liver+disease&draw=3&rank=44 ClinicalTrials.gov Identifier: NCT03884075

71 **Cha BS**. Comparison of The Effects of Thiazolidinediones(TZD), Sodium- Glucose Cotransporter 2 Inhibitors(SGLT2i) Alone and TZD / SGLT2i Combination Therapy on Non-alcoholic Fatty Liver Disease in Type 2 Diabetic Patients With Fatty Liver. [accessed 2021 Feb 27]. In: ClinicalTrials.gov [Internet]. Seoul: U.S. National Library of Medicine. Available from: https://clinicaltrials.gov/ct2/show/NCT03646292?recrs=a&cond=liver+disease&draw=3&rank=47 ClinicalTrials.gov Identifier: NCT03646292

72 **Ahuja K**, Sheflin-Findling S. Role of Probiotics in Treatment of Pediatric NAFLD Patients by Assessing With Fibroscan. [accessed 2021 Feb 27]. In: ClinicalTrials.gov [Internet]. New Hyde Park (NY): U.S. National Library of Medicine. Available from: https://clinicaltrials.gov/ct2/show/NCT04671186?recrs=a&cond=liver+disease&draw=3&rank=60 ClinicalTrials.gov Identifier: NCT04671186

73 **Cusi K**. Lanifibranor in Patients With Type 2 Diabetes & Nonalcoholic Fatty Liver Disease. [accessed 2021 Feb 27]. In: ClinicalTrials.gov [Internet]. Gainesville (FL): U.S. National Library of Medicine. Available from: https://clinicaltrials.gov/ct2/show/NCT03459079?recrs=a&cond=liver+disease&draw=3&rank=53 ClinicalTrials.gov Identifier: NCT03459079

74 **Kar PS**. Effects of Fecal Microbiota Transplantation on Weight in Obese Patients With Non-alcoholic Fatty Liver Disease. [accessed 2021 Feb 27]. In: ClinicalTrials.gov [Internet]. New Delhi: U.S. National Library of Medicine. Available from: https://clinicaltrials.gov/ct2/show/NCT04594954?recrs=a&cond=liver+disease&draw=3&rank=26 ClinicalTrials.gov Identifier: NCT04594954

75 **Taub R**. A Phase 3 Study to Evaluate the Safety and Biomarkers of Resmetirom (MGL-3196) in Non Alcoholic Fatty Liver Disease (NAFLD) Patients (MAESTRO-NAFLD1). [accessed 2021 Feb 27]. In: ClinicalTrials.gov [Internet]. Birmingham (AL): U.S. National Library of Medicine. Available from: https://clinicaltrials.gov/ct2/show/NCT04197479?recrs=a&cond=liver+disease&draw=3&rank=24 ClinicalTrials.gov Identifier: NCT04197479

76 **CohBar, Inc**. A Phase 1a/1b Study of CB4211 in Healthy Non-obese Subjects and Subjects With Nonalcoholic Fatty Liver Disease. [accessed 2021 Feb 27]. In: ClinicalTrials.gov [Internet]. Chula Vista (CA): U.S. National Library of Medicine. Available from: https://clinicaltrials.gov/ct2/show/NCT03998514?recrs=a&cond=liver+disease&draw=3 ClinicalTrials.gov Identifier: NCT03998514

World Journal of Gastroenterology

Submit a Manuscript: https://www.f6publishing.com

World J Gastroenterol 2021 September 28; 27(36): 6053-6063

DOI: 10.3748/wjg.v27.i36.6053

ISSN 1007-9327 (print) ISSN 2219-2840 (online)

MINIREVIEWS

Treatment of hepatitis B virus infection in children and adolescents

Mariangela Stinco, Chiara Rubino, Sandra Trapani, Giuseppe Indolfi

ORCID number: Mariangela Stinco 0000-0003-3970-5000; Chiara Rubino 0000-0001-7480-3613; Sandra Trapani 0000-0003-1105-1500; Giuseppe Indolfi 0000-0003-3830-9823.

Author contributions: Stinco M and Indolfi G wrote the paper; Rubino C and Trapani S reviewed it critically for significant intellectual content.

Conflict-of-interest statement: The authors declare that they have no competing interests.

Manuscript source: Invited manuscript

Specialty type: Gastroenterology and hepatology

Country/Territory of origin: Italy

Peer-review report's scientific

Mariangela Stinco, Chiara Rubino, Sandra Trapani, Department of Health Sciences, Pediatric Section, Meyer Children's University Hospital, Florence 50139, Italy

Giuseppe Indolfi, Department Neurofarba, University of Florence and Meyer Children's University Hospital, Florence 50139, Italy

Corresponding author: Giuseppe Indolfi, MD, Professor, Department Neurofarba, University of Florence and Meyer Children's University Hospital, 6 Gaetano Pieraccini, Florence 50139, Italy. giuseppe.indolfi@meyer.it

Abstract

Hepatitis B virus (HBV) infection is one of the main causes of morbidity and mortality worldwide. Most children acquire the infection perinatally or during early childhood and develop a chronic hepatitis characterized by a high viral replication and a low-inflammation phase of infection, with normal or only slightly raised aminotransferases. Although a conservative approach in children is usually recommended, different therapies exist and different therapeutic approaches are possible. The main goals of antiviral treatment for children with chronic HBV infection are to suppress viral replication and to warn the disease progression to cirrhosis and hepatocellular carcinoma, although these complications are rare in children. Both United States Food and Drug Administration (US-FDA) and European Medicines Agency (EMA) have approved interferon alfa-2b for children aged 1 year and older, pegylated interferon alfa-2a and lamivudine for children aged 3 years and older, entecavir for use in children aged 2 years and older, and adefovir for use in those 12 years of age and older. Tenofovir disoproxil fumarate is approved by EMA for children aged 2 years and older and by US-FDA for treatment in children aged 12 years and older. Finally, EMA has approved the use of tenofovir alafenamide for treatment of children aged 12 years and older or for children weighing more than 35 kg independent of age. This narrative review will provide the framework for summarizing indications to antiviral therapy in the management of chronic HBV infection in children and adolescents.

Key Words: Hepatitis B; Children; Adolescents; Antiviral therapy; Tenofovir disoproxil fumarate; Entecavir; Interferon

quality classification
Grade A (Excellent): 0
Grade B (Very good): B
Grade C (Good): C
Grade D (Fair): 0
Grade E (Poor): 0

Received: April 17, 2021
Peer-review started: April 17, 2021
First decision: June 3, 2021
Revised: June 30, 2021
Accepted: August 13, 2021
Article in press: August 13, 2021
Published online: September 28, 2021

P-Reviewer: Kayesh MEH, Kishida Y
S-Editor: Gong ZM
L-Editor: Filipodia
P-Editor: Li JH

Core Tip: Hepatitis B virus (HBV) is a major cause of acute and chronic liver disease. During childhood, asymptomatic chronic hepatitis B is the most common outcome of the infection, and a conservative approach is usually recommended. In selected patients there is a strict indication for treatment. Different drugs have been approved by United States Food and Drug Administration and European Medicines Agency for treatment of children and adolescents with chronic HBV infection. The main goal of the treatment is to reduce the risk of progression to cirrhosis and hepatocellular carcinoma through the suppression of HBV replication.

Citation: Stinco M, Rubino C, Trapani S, Indolfi G. Treatment of hepatitis B virus infection in children and adolescents. *World J Gastroenterol* 2021; 27(36): 6053-6063
URL: https://www.wjgnet.com/1007-9327/full/v27/i36/6053.htm
DOI: https://dx.doi.org/10.3748/wjg.v27.i36.6053

INTRODUCTION

Hepatitis B virus (HBV) infection is one of the major causes of acute and chronic liver disease and associated morbidity and mortality worldwide. In 2015, 257 million people were estimated as being chronically infected by the World Health Organization (WHO), with a global prevalence of 3%-5%, and 887,000 people died due to chronic HBV infection (CHB)[1].

Hepatitis B is a vaccine-preventable disease but, despite the availability of effective vaccine and vaccination programs, it remains a global health problem[2]. It has been estimated that annually there are almost 2 million new infections in children younger than 5 years of age. Most of the infected children acquire the infection around the time of birth through vertical transmission or during early childhood through horizontal transmission[3-5].

NATURAL HISTORY OF HBV INFECTION IN CHILDREN

The natural history and the long-term outcome of HBV infection acquired in childhood vary depending upon the age at infection. CHB is the most common outcome (90%) of the infection acquired vertically in neonates and infants. The risk of CHB is reduced to 30% when infection occurs during the first 5 years of life and < 5% for older immunocompetent children and adults[5].

HBV infection is usually asymptomatic during childhood, but sometimes acute infection could present with severe symptoms and fulminant hepatitis both in adult and children[6]. The development of complications of CHB, such as cirrhosis, hepatocellular carcinoma, and extrahepatic manifestations, is manly observed in adulthood but can also present in infancy and early childhood[7-10].

In 2017 the European Association for the Study of the Liver (EASL) proposed a new nomenclature for CHB that is no more based on the concept of immune-tolerant, immune-active, immune-control, and immune-escape, which have been previously used to describe the different phases of infection[7]. The new nomenclature emphasizes the distinction between infection and active hepatitis (defined basing on the presence of normal or raised alanine aminotransferase levels, respectively) and is based on Hepatitis B e Antigen (HBeAg) status, HBV viremia, and liver histology (Table 1)[11].

Another biomarker to monitoring HBV infection is the covalently closed circular DNA (ccc-DNA), a new biomarker related to viral replication and persistence of infection. A "complete cure" of HBV infection requires also the clearance of ccc-DNA, as well as HBsAg loss and undetectable serum HBV DNA (otherwise it is defined "functional cure")[12].

TREATMENT FOR CHRONIC HBV INFECTION

The common and main goals of antiviral treatment for adults, adolescents, and

Table 1 Patients' categories and phases in natural history of chronic hepatitis B virus infection defined by European Association for the Study of the Liver guidelines 2017[11]

	HBeAg positive	HBeAg negative	HBsAg negative
HBV infection (normal ALT)	High HBsAg	Low HBsAg	HBcAb-positive with/without positive HBsAb
	HBV DNA > 10^7 IU/mL	HBV DNA < 2000 IU/mL	HBV DNA usually undetectable
	None/minimal liver disease	No liver disease	No liver disease
	Old terminology: Immune-tolerant	Old terminology: Inactive carrier/immune control	Old terminology: Occult HBV infection
Hepatitis B (abnormal ALT)	High or intermediate HBsAg	Intermediate HBsAg	
	HBV DNA 10^4-10^7 IU/mL	HBV DNA > 2000 IU/mL	
	Moderate to severe liver disease	Moderate to severe liver disease	
	Old terminology: immune-active	Old terminology: immune escape	

HBV: Hepatitis B virus; ALT: Alanine aminotransferase levels; HBeAg: Hepatitis B e antigen; HBsAg: Hepatitis B s antigen; DNA: Deoxyribonucleic acid; HBcAb: Hepatitis B c antibodies.

children with chronic HBV infection are the effective and sustained suppression of HBV replication and consequently to decrease the risk of disease progression to cirrhosis and hepatocellular carcinoma[13-15]. Guidelines for treatment of children and adolescents have been issued by the European Society for Pediatric Gastroenterology Hepatology and Nutrition (ESPGHAN), EASL, American Association for the Study of Liver Diseases (AASLD), and Asian Pacific Association for the Study of the Liver (APASL)[11,16-18].

The aim of this narrative review is to summarize the available evidence on the use of drugs for treatment of CHB in children and adolescents, to summarize the main recommendations for treatment, and to highlight research gaps.

Interferon alfa-2b

Interferon alfa-2b has both antiviral and immunomodulatory actions. Binding to the specific transmembrane receptor, it activates intracellular signaling and gene transcription, resulting in the reduction of viral DNA level and viral injury. Furthermore, it directly stimulates the cell-mediated immune response against HBV-infected hepatocytes, thus reducing the number of cells containing ccc-DNA[19].

Interferon alfa-2b for subcutaneous injection is approved by European Medicines Agency (EMA) and United States Food and Drug Administration (US-FDA) for treatment of children and adolescents (1-17 years of age) with CHB. Treatment duration is 16 to 24 wk. The recommended dose is 6 million IU/m^2 three times a week (Table 2).

A large open-label, multinational randomized controlled trial evaluated the safety and efficacy of interferon alfa-2b[20]. Interferon alfa-2b was started at a dose of 3 million IU/m^2 of body surface area three times a week for 1 week. The dose was increased to 6 million IU/m^2 of body surface area at the second week, and this was continued for a minimum of 16 wk and a maximum of 24 wk based on results of virological testing for evidence of response (treatment was stopped at 16 or 20 wk if HBeAg was undetectable on two serum determinations taken 1 month apart). One hundred and forty-nine children were enrolled, 144 were evaluable of whom 70 received the treatment and 77 were untreated controls. Patients in the treatment arm had a better response (loss of HBV DNA and HBeAg at 24 wk of follow-up) compared to the untreated controls (26% *vs* 11%, P = 0.02). Loss of HBsAg occurred in 7 treated children (10%) but in only 1 untreated child (1.2%) (P = 0.03). Patients with lower baseline HBV DNA (< 50 pg/mL) were more likely to respond to interferon alfa-2b therapy than patients with a baseline HBV DNA greater than 200 pg/mL (41% *vs* 7%, respectively). All children in the treatment group reported at least one adverse event, the most common being influenza-like symptoms (100%), irritability, sleep disturbance and depression (40%), nausea or vomiting (40%), diarrhea or gastrointestinal distress (46%), alopecia (17%), and neutropenia (19%). The dose of interferon alfa-2b was reduced in 17 children (23%), most commonly because of neutropenia, thrombocytopenia, and fever. Three children discontinued treatment because of an adverse event. Subsequent studies confirmed the same efficacy and safety results[21-23].

Table 2 Antiviral drugs approved for children and adolescents with chronic hepatitis B virus infection[14]

	Ages approved for drug administration	Drug dosage	Drug formulations
Interferon alfa-2b	≥ 1 yr	6 million UI/m^2 three times a week	Subcutaneous injection
Peginterferon alfa-2a	≥ 3 yr	180 μg/1.73 m^2 once a week	Subcutaneous injection
Lamivudine	≥ 3 yr	3 mg/kg daily (maximum 100 mg)	Oral solution (5 mg/mL) or tablets (100 mg)
Entecavir	≥ 2 yr	10-30 kg: 0.015 mg/kg daily (maximum 0.5 mg)	Oral solution (0.05 mg/mL) or tablets (0.5 mg and 1 mg)
		> 30 kg: 0.5 mg daily	
Adefovir	≥ 12 yr	10 mg daily	Tablets (10 mg)
Tenofovir disoproxil fumarate	≥ 2 yr[1]	8 mg/kg daily (maximum 300 mg)	Oral powder (40 mg per 1 g) or tablets (150 mg, 200 mg, 250 mg and 300 mg)
	≥ 12 yr[1]	300 mg daily	
Tenofovir alafenamide	≥ 12 yr[2]	25 mg daily	Tablet (25 mg)

[1]Approved for ≥ 2 yr by the European Medicines Agency and ≥ 12 yr by the United States Food and Drug Administration.
[2]Approved independent of age for weight > 35 kg.

Peginterferon alfa

Peginterferon alfa comprises an inert, branched, 40 kD polyethylene glycol molecule attached to interferon alfa. Through the direct stimulation of immune system, it is effective in the achievement of serological response and reduction of ccc-DNA level [19].

Peginterferon alfa-2a

Peginterferon alfa-2a for subcutaneous injection is approved by EMA and US-FDA for treatment of children and adolescents (3-17 years of age) with CHB. Treatment duration is 16 to 24 wk. The recommended dose is 180 μg/1.73 m^2 once a week (Table 2).

The efficacy and safety of peginterferon alfa-2a treatment in children with CHB was assessed in the PEG-B-ACTIVE study, a phase III randomized, controlled, open-label, multicenter study[24]. Peginterferon alfa-2a was prescribed at a dose of 180 μg/1.73 m^2 once a week and was continued for a minimum of 48 wk. One hundred and sixty-one HBeAg-positive children with raised aminotransferase levels without advanced fibrosis or cirrhosis were enrolled. One hundred and fifty-one were evaluable, of whom 101 received the treatment and 50 were untreated controls. Twenty-four weeks after the end of treatment, patients who received peginterferon alfa-2a had a better response compared to untreated controls with higher HBeAg seroconversion rates (25.7% *vs* 6%, P = 0.0043), higher rates of hepatitis B surface antigen (HBsAg) clearance (8.9% *vs* 0%, P = 0.03), HBV DNA < 2000 IU/mL (28.7% *vs* 2%, P < 0.001) or undetectable (16.8% *vs* 2.0%, P = 0.0069), and alanine aminotransferase (ALT) normalization (51.5% *vs* 12%, P < 0.001). Loss of HBsAg occurred in 9 treated children (8.9%) and in none of those who were untreated. The most common adverse events included fever (49%), headache (30%), abdominal pain (19%), and neuropsychiatric disorder (12%). Laboratory abnormalities reported during treatment were ALT flares (53%) and neutropenia (10%) and were managed without dose modification. Short-term effects on growth appeared minimal. The study highlighted the efficacy and positive benefit/risk profile of peginterferon alfa-2a for the treatment in children and adolescents with CHB, consistent with the extensive data available in adults.

Peginterferon alfa-2b

Peginterferon alfa-2b is not approved by the US-FDA or EMA for treatment of children or adolescents with CHB but is approved for treatment of chronic hepatitis C for children 3 years of age or older (Table 2)[25-30].

Lamivudine

Lamivudine is a synthetic nucleoside analogue (analogue of cytidine) that inhibits viral replication in human cells by interfering with the DNA polymerase enzyme of HBV, and it acts as a chain terminator of DNA synthesis. If the nucleoside analogue is

incorporated in the DNA chain, it prevents the formation of the 5' to 3' phosphodiester linkage essential for DNA chain elongation, consequently terminating viral DNA growth[31].

Lamivudine is approved by EMA and US-FDA for treatment of children and adolescents (3-17 years of age) with CHB. The recommended dose is 3 mg/kg daily, oral (maximum 100 mg; Table 2).

The efficacy and safety of lamivudine treatment in children with CHB was originally assessed in one randomized, double-blind, placebo-controlled study[32]. Children and adolescents aged between 2 and 17 years received either oral lamivudine (n = 191) or placebo (n = 97) once daily for 52 wk. This study demonstrated that treatment with lamivudine was safe, efficacious, and superior to placebo, consistent with the results observed in adults with CHB. Virologic response defined by the loss of serum HBeAg and by the reduction of serum HBV DNA to undetectable levels occurred by week 52 in 23% of the children in the treatment group, as compared with 13% of children in the placebo group (P = 0.04). The rate of virologic response increased with higher baseline ALT values and scores on the histologic activity index. Loss of HBsAg occurred in 3 treated children (2%) and in none of those who were untreated. The treatment was highly safe and the nature, incidence, and severity of adverse clinical events and abnormal laboratory values in patients receiving lamivudine were similar to those receiving placebo. The emergence of YMDD-variant HBV was detected in 19% of patients who received lamivudine for 52 wk. YMDD-variant HBV may reverse the response in some patients and has been considered a limitation of lamivudine therapy.

The efficacy of lamivudine was explored in other studies. According to a recent systematic review with meta-analysis, lamivudine, when compared to placebo, was associated with significantly higher likelihood of ALT normalization, HBeAg clearance or loss, and HBV DNA suppression but not HBeAg seroconversion or HBsAg clearance after 48 wk of treatment[33-35].

Although lamivudine is a safe drug, it has low barrier to resistance.

Entecavir

Entecavir is a nucleoside analogue (analogue of deoxyguanosine). In the intracellular environment, it is rapidly phosphorylated to the active intracellular 50-triphosphate form; this active metabolite competes with the natural substrate (*i.e.*, deoxyguanosine triphosphate) of HBV polymerase and inhibits HBV replication[36].

Entecavir is approved by US-FDA and EMA for treatment of children and adolescents aged 2 years and older with CHB. The recommended treatment dose is 0.015 mg/kg daily (maximum 0.5 mg; weight > 30 kg: 0.5 mg daily; Table 2).

The efficacy and safety of entecavir were studied in a randomized, double-blind, multicenter study including children and adolescents (2 to < 18 years) with CHB[37]. Blinded treatment was administered for a minimum of 48 wk. One hundred and seventeen patients received entecavir treatment, and 56 received placebo. Patients who achieved HBeAg seroconversion continued blinded treatment while those who did not (n = 50) were switched to open-label entecavir up to week 96 of treatment. Response rates for the combined endpoint of HBeAg seroconversion and HBV DNA < 50 IU/mL at treatment week 48 occurred in 24.2% in the entecavir group, as compared with 3.3% in the placebo group (P = 0.0008). After 48 wk of treatment, patients who received entecavir had a better response compared to untreated controls with higher rates of virological suppression (49.2% *vs* 3.3%, P < 0.0001), ALT normalization (67.5% *vs* 23.3%, P < 0.0001), and HBeAg seroconversion (24.2% *vs* 10, P = 0.02). At week 96, loss of HBsAg occurred in 7 treated children (5.8%) and in none of those who were untreated. The rate of virologic response increased with low baseline HBV DNA (< 8 Log_{10} IU/mL) and high baseline ALT (> 2 × upper limit of normal). The cumulative probability of emergent entecavir resistance through years 1 and 2 of entecavir was 0.6% and 2.6%, respectively. The treatment was well tolerated with no observed differences in adverse events or changes in growth compared with placebo. A subsequent study confirmed the same efficacy and safety results[38].

Adefovir

Adefovir is an acyclic nucleotide analogue (analogue of deoxyadenosine-5´-monophosphate). It is converted by adenylate kinase to adefovir diphosphate, an active derivate that selectively inhibits the HBV polymerase. Adefovir diphosphate competes with deoxyadenosine-5´-triphosphate during HBV DNA synthesis, and, when incorporated into the HBV DNA chain, it discontinues further elongation of DNA chain, stopping HBV replication[39].

Adefovir is approved by US-FDA and EMA for treatment adolescents aged 12 years and older with CHB. The recommended treatment dose is 10 mg daily (Table 2).

The efficacy and safety of adefovir were studied in a randomized, double-blind, multicenter study including children and adolescents (2 to < 18 years) with CHB[40]. Treatment was administered for 48 wk. One hundred and eighteen patients have received adefovir treatment and 58 received placebo. Response rates for the combined endpoint of HBV DNA < 1000 copies/mL and normal ALT at treatment week 48 occurred in 19.1% in the adefovir group, as compared with 1.7% in the placebo group ($P < 0.001$). This result was primarily due to response in the 12 to 17 years age group as in the younger children, although there were apparent differences in response to those treated with adefovir compared to those who received placebo, they did not reach statistical significance. After 48 wk of treatment, patients who received tenofovir had a better response compared to untreated controls with higher rates of ALT normalization (56% *vs* 21%, $P < 0.0001$) and HBeAg seroconversion (15.9% *vs* 5.3%). More patients treated with adefovir met the combined endpoint of HBeAg seroconversion and HBV DNA < 1000 copies/mL plus normal ALT (10.6% *vs* 0/57, $P = 0.009$). Only 1 patient in the adefovir group achieved HBsAg seroconversion. The rate of virologic response increased with low baseline HBV DNA (< 8.8 Log_{10} IU/mL) and high baseline ALT (> 2.3 X upper limit of normal). No subject developed the rtA181V or rtN236T mutation associated with adefovir resistance by treatment week 48. The treatment was well tolerated with no observed differences in adverse events compared with placebo.

A subsequent study confirmed the same efficacy and safety results[41].

Tenofovir disoproxil fumarate

Tenofovir disoproxil fumarate (DF) is an inhibitor of DNA polymerase. *In vivo* it is converted by diester hydrolysis to tenofovir, an acyclic nucleotide analogue (analogue of deoxyadenosine-5´-monophosphate), and after two phosphorylation steps to its active metabolite, tenofovir diphosphate. In this form, tenofovir binds to active site of enzyme, avoiding the attaching of the natural substrate deoxyadenosine-5´-triphosphate, and inhibits the HBV DNA polymerase activity[42].

Tenofovir DF is approved by EMA for children aged 2 years and older and by US-FDA for treatment of children aged 12 years and older with CHB. The recommended treatment dose is 8 mg/kg daily (maximum 300 mg) for younger children and 300 mg daily for those older than 12 years (Table 2).

The efficacy and safety profile of tenofovir DF were studied in a randomized, double-blind, multicenter study including adolescents (12 to < 18 years) with CHB [43]. Blinded treatment was administered for 72 wk. One hundred six patients were enrolled, and 101 completed 72 wk of treatment. Fifty-two patients have received tenofovir DF treatment and 54 received placebo. Virologic response (HBV DNA < 400 copies/mL) at treatment week 72 was observed in 89% of patients who received tenofovir DF and none of those who received placebo ($P < 0.001$). The treatment was well tolerated with no observed differences in adverse events compared with placebo. No resistance to tenofovir DF developed through week 72.

Tenofovir alafenamide

Tenofovir alafenamide is a pro-drug of tenofovir diphosphate, thus it presents the same action mechanism of tenofovir DF causing causes viral DNA chain termination and preventing viral DNA transcription[42].

Tenofovir alafenamide is approved by EMA for treatment of children aged 12 years and older and, independent of age, for children weighing more than 35 kg. The recommended treatment dose is 25 mg daily. Tenofovir alafenamide was approved on the basis of studies in children with human immunodeficiency virus infection[44,45].

Telbivudine

Telbivudine is not approved by the FDA or EMA for pediatric use.

Pros and cons of anti-HBV treatment

Overall interferon based treatments are associated with higher HBeAg and HBsAg seroconversion rates and could be used for treatment of finite duration. Concerns are present with regard to tolerance and safety, and recently the availability of the drug on the market has been questioned. Furthermore, interferon and peginterferon treatments have the disadvantage of subcutaneous administration that is relevant for treatment of children.

Nucleot(s)ide analogues have been classified as having low (lamivudine, adefovir, telbivudine) and high (tenofovir, entecavir) genetic barrier to resistance and are generally used for oral treatment of indefinite duration, with an overall good safety profile[14,15].

New prospective antiviral treatment strategies

Recently, there is a growing interest in some new therapeutic strategies, targeting viral life cycle or improving antiviral immune response, that could eliminate all replicative intermediates, including ccc-DNA. The drugs targeting different steps of HBV life cycle include entry inhibitors; polymerase inhibitors; core protein (nucleocapsid) inhibitors; HBsAg release inhibitors; RNA silencers. On the other hand, the new therapies to improve anti-HBV immunity response include therapeutic vaccines, generating "new" T cells; toll-like receptor 7 and toll-like receptor 8 agonists, stimulating antiviral effector cells; retinoic acid-inducible gene I agonist; anti-HBV antibodies; checkpoint inhibitors; programmed cell death protein 1 (PD1) and PD1 ligand inhibitors, rescuing the T-cell exhaustion that can be observed in chronic HBV infection. Results of preclinical and early clinical studies are promising; thus, soon, these treatment options could be available and could potentially transform the future indications for hepatitis B treatment[46-49].

INDICATION FOR TREATMENT

The decision to start treatment in a child with CHB is based on the combined assessment of stage of liver disease, HBV DNA and ALT concentrations, and HBeAg status. Presence of other features, such as a family history of hepatocellular carcinoma, human immunodeficiency virus coinfection or other concomitant liver disease, is an additional factor to support treatment initiation. Regardless of age, all guidelines recommend treatment for children with cirrhosis, histological evidence of necroinflammation and fibrosis (active hepatitis), and fulminant or severe acute hepatitis B infection and for those undergoing immunosuppression or chemotherapy with evidence of past or ongoing HBV infection[11,13,16-18].

There are some differences between recommendations provided by the available guidelines for the treatment of CHB in children not satisfying the above treatment criteria that are highlighted in Table 3[14].

Interferon, entecavir, and tenofovir DF are recommended for treatment of chronic HBV infection in children by ESPGHAN, AASLD, and APASL. Entecavir is recommended for children aged 2–12 years in WHO guidelines while interferon is not included because its use in resource limited settings is often not feasible as a result of its high cost, requirement for injection, and high rate of adverse effects that require careful monitoring. The advantages of interferon and peginterferon as compared with nucleoside and nucleotide analogues are the absence of viral resistance and the predictable finite duration of treatment. However, the use of interferon and peginterferon requires subcutaneous injections and is associated with a high risk of adverse events. Tenofovir (tenofovir DF or tenofovir alafenamide) or entecavir have high genetic barrier and are recommended as preferred initial therapies for adults by EASL, AASLD, and WHO.

CONCLUSION

Treatment guidelines provided by the different major scientific international societies (ESPGHAN, AASLD, APASL, EASL) clearly agree on treating all patients with advanced liver disease (cirrhosis) and histological features of active hepatitis and patients with fulminant or severe acute hepatitis B infection, preventing uncontrolled HBV replication and serious complications such as cirrhosis and hepatocellular carcinoma in young adult life. The guidelines also recommended antiviral therapy for children and adolescents with HBV infection (immune-tolerant patients) undergoing immunosuppressive therapy, such as those patients who will be receiving chemotherapy or stem cell or solid organ transplantation.

All others HBV infected children who not satisfy the above treatment criteria are not typically candidates for treatment. For these patients a tight clinical, biochemical and no invasive imaging (abdominal ultrasound) follow-up will be important to monitoring the natural course of HBV infection, to identify patients undergoing

Table 3 Differences among recommendations and indications for treatment of chronic hepatitis B virus infection in adults, adolescents, and children from five professional societies or international organizations

Organization	
ESPGHAN[16]	HBeAg-positive adolescents and children with persistent alanine aminotransferase elevation for at least 6 mo
	HBeAg-negative adolescents and children with persistent alanine aminotransferase elevation for at least 6 mo for at least 12 mo
	HBV DNA > 2000 IU/mL and either
	Moderate necroinflammation or fibrosis
	Mild inflammation or fibrosis with a family history of hepatocellular carcinoma
AASLD[17]	HBeAg-positive adolescents and children with both elevated alanine aminotransferase and measurable HBV DNA concentrations
	Therapy should be deferred when HBV DNA is < 10000 IU/mL, until spontaneous HBeAg seroconversion is excluded
APASL[18]	Non-cirrhotic HBeAg-positive adolescents and children when HBV DNA level is higher than 20000 IU/mL and alanine aminotransferase is more than twice the upper limit of normal for more than 12 mo
	Non-cirrhotic HBeAg-positive adolescents and children either HBV DNA > 20000 IU/mL and ALT more than two times ULN for more than 12 mo, or a family history of hepatocellular carcinoma or cirrhosis and moderate-to-severe inflammation or pronounced fibrosis
	Non-cirrhotic, HBeAg-positive chronic HBV infection, HBV DNA < 20000 IU/mL and moderate to severe inflammation or pronounced fibrosis
	Non-cirrhotic, HBeAg-negative chronic HBV infection, HBV DNA > 2000 IU/mL, and ALT more than two times ULNNon-cirrhotic, HBeAg-negative chronic HBV infection and moderate to severe inflammation or pronounced fibrosis, regardless of HBV DNA concentration
EASL[11]	A conservative approach is warranted

ESPGHAN: European Society for Paediatric Gastroenterology Hepatology and Nutrition; HBeAg: Hepatitis B e antigen; HBV: Hepatitis B virus; DNA: Deoxyribonucleic acid; AASLD: American Association for the Study of Liver Diseases; APASL: Asian Pacific Association for the Study of the Liver; ALT: Alanine aminotransferase levels; ULN: Upper limit of normal; EASL: European Association for the Study of the Liver.

spontaneous HBeAg seroconversion, and above all to recognize rapidly those children with chronic HBV infection who may benefit from treatment (*e.g.*, patients with persistently abnormal ALT levels).

The establishment of pediatric treatment registries and of new international associations would be the most important strategy to inform best practices for the management, care, and treatment of children with HBV infection and to promote collaborative research.

REFERENCES

1 **World Health Organization**. Global hepatitis report 2017. [cited 17 April 2021]. Available from: https://www.who.int/publications/i/item/global-hepatitis-report-2017

2 B vaccines: WHO position paper – July 2017. *Wkly Epidemiol Rec* 2017; **92**: 369-392 [PMID: 28685564]

3 **Schweitzer A**, Horn J, Mikolajczyk RT, Krause G, Ott JJ. Estimations of worldwide prevalence of chronic hepatitis B virus infection: a systematic review of data published between 1965 and 2013. *Lancet* 2015; **386**: 1546-1555 [PMID: 26231459 DOI: 10.1016/S0140-6736(15)61412-X]

4 **Polaris Observatory Collaborators**. Global prevalence, treatment, and prevention of hepatitis B virus infection in 2016: a modelling study. *Lancet Gastroenterol Hepatol* 2018; **3**: 383-403 [PMID: 29599078 DOI: 10.1016/S2468-1253(18)30056-6]

5 **McMahon BJ**, Alward WL, Hall DB, Heyward WL, Bender TR, Francis DP, Maynard JE. Acute hepatitis B virus infection: relation of age to the clinical expression of disease and subsequent development of the carrier state. *J Infect Dis* 1985; **151**: 599-603 [PMID: 3973412 DOI: 10.1093/infdis/151.4.599]

6 **Tseng YR**, Wu JF, Kong MS, Hu FC, Yang YJ, Yeung CY, Huang FC, Huang IF, Ni YH, Hsu HY, Chang MH, Chen HL. Infantile hepatitis B in immunized children: risk for fulminant hepatitis and long-term outcomes. *PLoS One* 2014; **9**: e111825 [PMID: 25380075 DOI: 10.1371/journal.pone.0111825]

7 **McMahon BJ**. The natural history of chronic hepatitis B virus infection. *Hepatology* 2009; **49**: S45-S55 [PMID: 19399792 DOI: 10.1002/hep.22898]

8 **Nguyen VT**, Law MG, Dore GJ. Hepatitis B-related hepatocellular carcinoma: epidemiological characteristics and disease burden. *J Viral Hepat* 2009; **16**: 453-463 [PMID: 19302335 DOI: 10.1111/j.1365-2893.2009.01117.x]

9 **Sun YH**, Lei XY, Sai YP, Chen JH, Sun YC, Gao X. Relationship between genotypes and clinical manifestation, pathology, and cccDNA in Chinese children with hepatitis B virus-associated glomerulonephritis. *World J Pediatr* 2016; **12**: 347-352 [PMID: 27059747 DOI: 10.1007/s12519-016-0015-0]

10 **Arnone OC**, Serranti D, Bartolini E, Mastrangelo G, Stinco M, Trapani S, Ricci S, Resti M, Indolfi G. Chronic hepatitis B in children, report of a single-centre longitudinal study on 152 children. *J Viral Hepat* 2020; **27**: 1344-1351 [PMID: 32853482 DOI: 10.1111/jvh.13382]

11 **European Association for the Study of the Liver**. EASL 2017 Clinical Practice Guidelines on the management of hepatitis B virus infection. *J Hepatol* 2017; **67**: 370-398 [PMID: 28427875 DOI: 10.1016/j.jhep.2017.03.021]

12 **Allweiss L**, Dandri M. The Role of cccDNA in HBV Maintenance. *Viruses* 2017; **9** [PMID: 28635668 DOI: 10.3390/v9060156]

13 **World Health Organization**. Guidelines for the prevention, care and treatment of persons with chronic hepatitis B infection. 2015 [cited 17 April 2021]. Available from: https://www.who.int/publications/i/item/9789241549059

14 **Indolfi G**, Easterbrook P, Dusheiko G, Siberry G, Chang MH, Thorne C, Bulterys M, Chan PL, El-Sayed MH, Giaquinto C, Jonas MM, Meyers T, Walsh N, Wirth S, Penazzato M. Hepatitis B virus infection in children and adolescents. *Lancet Gastroenterol Hepatol* 2019; **4**: 466-476 [PMID: 30982722 DOI: 10.1016/S2468-1253(19)30042-1]

15 **Jonas MM**, Lok AS, McMahon BJ, Brown RS Jr, Wong JB, Ahmed AT, Farah W, Mouchli MA, Singh S, Prokop LJ, Murad MH, Mohammed K. Antiviral therapy in management of chronic hepatitis B viral infection in children: A systematic review and meta-analysis. *Hepatology* 2016; **63**: 307-318 [PMID: 26566163 DOI: 10.1002/hep.28278]

16 **Sokal EM**, Paganelli M, Wirth S, Socha P, Vajro P, Lacaille F, Kelly D, Mieli-Vergani G; European Society of Pediatric Gastroenterology, Hepatology and Nutrition. Management of chronic hepatitis B in childhood: ESPGHAN clinical practice guidelines: consensus of an expert panel on behalf of the European Society of Pediatric Gastroenterology, Hepatology and Nutrition. *J Hepatol* 2013; **59**: 814-829 [PMID: 23707367 DOI: 10.1016/j.jhep.2013.05.016]

17 **Terrault NA**, Lok ASF, McMahon BJ, Chang KM, Hwang JP, Jonas MM, Brown RS Jr, Bzowej NH, Wong JB. Update on prevention, diagnosis, and treatment of chronic hepatitis B: AASLD 2018 hepatitis B guidance. *Hepatology* 2018; **67**: 1560-1599 [PMID: 29405329 DOI: 10.1002/hep.29800]

18 **Sarin SK**, Kumar M, Lau GK, Abbas Z, Chan HL, Chen CJ, Chen DS, Chen HL, Chen PJ, Chien RN, Dokmeci AK, Gane E, Hou JL, Jafri W, Jia J, Kim JH, Lai CL, Lee HC, Lim SG, Liu CJ, Locarnini S, Al Mahtab M, Mohamed R, Omata M, Park J, Piratvisuth T, Sharma BC, Sollano J, Wang FS, Wei L, Yuen MF, Zheng SS, Kao JH. Asian-Pacific clinical practice guidelines on the management of hepatitis B: a 2015 update. *Hepatol Int* 2016; **10**: 1-98 [PMID: 26563120 DOI: 10.1007/s12072-015-9675-4]

19 **Yeh ML**, Huang JF, Dai CY, Yu ML, Chuang WL. Pharmacokinetics and pharmacodynamics of pegylated interferon for the treatment of hepatitis B. *Expert Opin Drug Metab Toxicol* 2019; **15**: 779-785 [PMID: 31593639 DOI: 10.1080/17425255.2019.1678584]

20 **Sokal EM**, Conjeevaram HS, Roberts EA, Alvarez F, Bern EM, Goyens P, Rosenthal P, Lachaux A, Shelton M, Sarles J, Hoofnagle J. Interferon alfa therapy for chronic hepatitis B in children: a multinational randomized controlled trial. *Gastroenterology* 1998; **114**: 988-995 [PMID: 9558288 DOI: 10.1016/s0016-5085(98)70318-x]

21 **Hu Y**, Ye YZ, Ye LJ, Wang XH, Yu H. Efficacy and safety of interferon alpha-2b versus pegylated interferon alpha-2a monotherapy in children with chronic hepatitis B: a real-life cohort study from Shanghai, China. *World J Pediatr* 2019; **15**: 595-600 [PMID: 31487005 DOI: 10.1007/s12519-019-00303-w]

22 **van Zonneveld M**, Flink HJ, Verhey E, Senturk H, Zeuzem S, Akarca US, Cakaloglu Y, Simon C, So TM, Gerken G, de Man RA, Hansen BE, Schalm SW, Janssen HL; HBV 99-01 Study Group. The safety of pegylated interferon alpha-2b in the treatment of chronic hepatitis B: predictive factors for dose reduction and treatment discontinuation. *Aliment Pharmacol Ther* 2005; **21**: 1163-1171 [PMID: 15854180 DOI: 10.1111/j.1365-2036.2005.02453.x]

23 **Zhao H**, Si CW, Wei L, Wan MB, Ying YK, Hou JL, Niu JQ. [A multicenter, randomized, open-label study of the safety and effectiveness of pegylated interferon alpha 2b and interferon alpha 2b in treating HBeAg positive chronic hepatitis B patients]. *Zhonghua Gan Zang Bing Za Zhi* 2006; **14**: 323-326 [PMID: 16732903]

24 **Wirth S**, Zhang H, Hardikar W, Schwarz KB, Sokal E, Yang W, Fan H, Morozov V, Mao Q, Deng H, Huang Y, Yang L, Frey N, Nasmyth-Miller C, Pavlovic V, Wat C. Efficacy and Safety of Peginterferon Alfa-2a (40KD) in Children With Chronic Hepatitis B: The PEG-B-ACTIVE Study. *Hepatology* 2018; **68**: 1681-1694 [PMID: 29689122 DOI: 10.1002/hep.30050]

25 **Wirth S**, Ribes-Koninckx C, Calzado MA, Bortolotti F, Zancan L, Jara P, Shelton M, Kerkar N, Galoppo M, Pedreira A, Rodriguez-Baez N, Ciocca M, Lachaux A, Lacaille F, Lang T, Kullmer U, Huber WD, Gonzalez T, Pollack H, Alonso E, Broue P, Ramakrishna J, Neigut D, Valle-Segarra AD, Hunter B, Goodman Z, Xu CR, Zheng H, Noviello S, Sniukiene V, Brass C, Albrecht JK. High sustained virologic response rates in children with chronic hepatitis C receiving peginterferon alfa-2b

plus ribavirin. *J Hepatol* 2010; **52**: 501-507 [PMID: 20189674 DOI: 10.1016/j.jhep.2010.01.016]

26 **Indolfi G**, Bailey H, Serranti D, Giaquinto C, Thorne C; PENTAHep Study Group. Treatment and monitoring of children with chronic hepatitis C in the Pre-DAA era: A European survey of 38 paediatric specialists. *J Viral Hepat* 2019; **26**: 961-968 [PMID: 30980773 DOI: 10.1111/jvh.13111]

27 **Indolfi G**, Easterbrook P, Dusheiko G, El-Sayed MH, Jonas MM, Thorne C, Bulterys M, Siberry G, Walsh N, Chang MH, Meyers T, Giaquinto C, Wirth S, Chan PL, Penazzato M. Hepatitis C virus infection in children and adolescents. *Lancet Gastroenterol Hepatol* 2019; **4**: 477-487 [PMID: 30982721 DOI: 10.1016/S2468-1253(19)30046-9]

28 **Indolfi G**, Nebbia G, Cananzi M, Maccabruni A, Zaramella M, D'Antiga L, Grisotto L, Azzari C, Resti M; Italian Study Group for Treatment of Chronic Hepatitis C in Children. Kinetic of Virologic Response to Pegylated Interferon and Ribavirin in Children With Chronic Hepatitis C Predicts the Effect of Treatment. *Pediatr Infect Dis J* 2016; **35**: 1300-1303 [PMID: 27636721 DOI: 10.1097/INF.0000000000001325]

29 **Bortolotti F**, Indolfi G, Zancan L, Giacchino R, Verucchi G, Cammà C, Barbera C, Resti M, Marazzi MG, Guido M. Management of chronic hepatitis C in childhood: the impact of therapy in the clinical practice during the first 2 decades. *Dig Liver Dis* 2011; **43**: 325-329 [PMID: 21111693 DOI: 10.1016/j.dld.2010.10.008]

30 **Serranti D**, Indolfi G, Nebbia G, Cananzi M, D'Antiga L, Ricci S, Stagi S, Azzari C, Resti M; Italian Study Group for Treatment of Chronic Hepatitis C in Children. Transient Hypothyroidism and Autoimmune Thyroiditis in Children With Chronic Hepatitis C Treated With Pegylated-interferon-α -2b and Ribavirin. *Pediatr Infect Dis J* 2018; **37**: 287-291 [PMID: 28953189 DOI: 10.1097/INF.0000000000001791]

31 **Porche D**. Treatment review: lamivudine. *JANAC* 1996; **7**: 51-53

32 **Jonas MM**, Mizerski J, Badia IB, Areias JA, Schwarz KB, Little NR, Greensmith MJ, Gardner SD, Bell MS, Sokal EM; International Pediatric Lamivudine Investigator Group. Clinical trial of lamivudine in children with chronic hepatitis B. *N Engl J Med* 2002; **346**: 1706-1713 [PMID: 12037150 DOI: 10.1056/NEJMoa012452]

33 **Figlerowicz M**, Kowala-Piaskowska A, Filipowicz M, Bujnowska A, Mozer-Lisewska I, Słuzewski W. Efficacy of lamivudine in the treatment of children with chronic hepatitis B. *Hepatol Res* 2005; **31**: 217-222 [PMID: 15799860 DOI: 10.1016/j.hepres.2005.02.003]

34 **Luo A**, Jiang X, Ren H. Lamivudine therapy for chronic hepatitis B in children: a meta-analysis. *Virol J* 2019; **16**: 88 [PMID: 31272463 DOI: 10.1186/s12985-019-1193-x]

35 **Jonas MM**, Little NR, Gardner SD; International Pediatric Lamivudine Investigator Group. Long-term lamivudine treatment of children with chronic hepatitis B: durability of therapeutic responses and safety. *J Viral Hepat* 2008; **15**: 20-27 [PMID: 18088241 DOI: 10.1111/j.1365-2893.2007.00891.x]

36 **Robinson DM**, Scott LJ, Plosker GL. Entecavir: a review of its use in chronic hepatitis B. *Drugs* 2006; **66**: 1605-22; discussion 1623 [PMID: 16956310 DOI: 10.2165/00003495-200666120-00009]

37 **Jonas MM**, Chang MH, Sokal E, Schwarz KB, Kelly D, Kim KM, Ling SC, Rosenthal P, Oraseanu D, Reynolds L, Thiry A, Ackerman P. Randomized, controlled trial of entecavir versus placebo in children with hepatitis B envelope antigen-positive chronic hepatitis B. *Hepatology* 2016; **63**: 377-387 [PMID: 26223345 DOI: 10.1002/hep.28015]

38 **Lee KJ**, Choe BH, Choe JY, Kim JY, Jeong IS, Kim JW, Yang HR, Chang JY, Kim KM, Moon JS, Ko JS. A Multicenter Study of the Antiviral Efficacy of Entecavir Monotherapy Compared to Lamivudine Monotherapy in Children with Nucleos(t)ide-naïve Chronic Hepatitis B. *J Korean Med Sci* 2018; **33**: e63 [PMID: 29441755 DOI: 10.3346/jkms.2018.33.e63]

39 **Hadziyannis SJ**, Papatheodoridis GV. Adefovir dipivoxil in the treatment of chronic hepatitis B virus infection. *Expert Rev Anti Infect Ther* 2004; **2**: 475-483 [PMID: 15482214 DOI: 10.1586/14787210.2.4.475]

40 **Jonas MM**, Kelly D, Pollack H, Mizerski J, Sorbel J, Frederick D, Mondou E, Rousseau F, Sokal E. Safety, efficacy, and pharmacokinetics of adefovir dipivoxil in children and adolescents (age 2 to <18 years) with chronic hepatitis B. *Hepatology* 2008; **47**: 1863-1871 [PMID: 18433023 DOI: 10.1002/hep.22250]

41 **Jonas MM**, Kelly D, Pollack H, Mizerski J, Sorbel J, Frederick D, Mondou E, Rousseau F, Sokal E. Efficacy and safety of long-term adefovir dipivoxil therapy in children with chronic hepatitis B infection. *Pediatr Infect Dis J* 2012; **31**: 578-582 [PMID: 22466329 DOI: 10.1097/INF.0b013e318255ffe7]

42 **Grim SA**, Romanelli F. Tenofovir disoproxil fumarate. *Ann Pharmacother* 2003; **37**: 849-859 [PMID: 12773076 DOI: 10.1345/aph.1C388]

43 **Murray KF**, Szenborn L, Wysocki J, Rossi S, Corsa AC, Dinh P, McHutchison J, Pang PS, Luminos LM, Pawlowska M, Mizerski J. Randomized, placebo-controlled trial of tenofovir disoproxil fumarate in adolescents with chronic hepatitis B. *Hepatology* 2012; **56**: 2018-2026 [PMID: 22544804 DOI: 10.1002/hep.25818]

44 **Gaur AH**, Kizito H, Prasitsueubsai W, Rakhmanina N, Rassool M, Chakraborty R, Batra J, Kosalaraksa P, Luesomboon W, Porter D, Shao Y, Myers M, Ting L, SenGupta D, Quirk E, Rhee MS. Safety, efficacy, and pharmacokinetics of a single-tablet regimen containing elvitegravir, cobicistat, emtricitabine, and tenofovir alafenamide in treatment-naive, HIV-infected adolescents: a single-arm, open-label trial. *Lancet HIV* 2016; **3**: e561-e568 [PMID: 27765666 DOI: 10.1016/S2352-3018(16)30121-7]

45 **Lockman S**, Brummel SS, Ziemba L, Stranix-Chibanda L, McCarthy K, Coletti A, Jean-Philippe P, Johnston B, Krotje C, Fairlie L, Hoffman RM, Sax PE, Moyo S, Chakhtoura N, Stringer JS, Masheto G, Korutaro V, Cassim H, Mmbaga BT, João E, Hanley S, Purdue L, Holmes LB, Momper JD, Shapiro RL, Thoofer NK, Rooney JF, Frenkel LM, Amico KR, Chinula L, Currier J; IMPAACT 2010/VESTED Study Team and Investigators. Efficacy and safety of dolutegravir with emtricitabine and tenofovir alafenamide fumarate or tenofovir disoproxil fumarate, and efavirenz, emtricitabine, and tenofovir disoproxil fumarate HIV antiretroviral therapy regimens started in pregnancy (IMPAACT 2010/VESTED): a multicentre, open-label, randomised, controlled, phase 3 trial. *Lancet* 2021; **397**: 1276-1292 [PMID: 33812487 DOI: 10.1016/S0140-6736(21)00314-7]

46 **Gane EJ**. Future anti-HBV strategies. *Liver Int* 2017; **37** Suppl 1: 40-44 [PMID: 28052637 DOI: 10.1111/liv.13304]

47 **Testoni B**, Durantel D, Zoulim F. Novel targets for hepatitis B virus therapy. *Liver Int* 2017; **37** Suppl 1: 33-39 [PMID: 28052622 DOI: 10.1111/liv.13307]

48 **Lin CL**, Yang HC, Kao JH. Hepatitis B virus: new therapeutic perspectives. *Liver Int* 2016; **36** Suppl 1: 85-92 [PMID: 26725903 DOI: 10.1111/liv.13003]

49 **Soriano V**, Barreiro P, Benitez L, Peña JM, de Mendoza C. New antivirals for the treatment of chronic hepatitis B. *Expert Opin Investig Drugs* 2017; **26**: 843-851 [PMID: 28521532 DOI: 10.1080/13543784.2017.1333105]

World Journal of Gastroenterology

Submit a Manuscript: https://www.f6publishing.com

World J Gastroenterol 2021 September 28; 27(36): 6064-6078

DOI: 10.3748/wjg.v27.i36.6064

ISSN 1007-9327 (print) ISSN 2219-2840 (online)

ORIGINAL ARTICLE

Basic Study

CircRNA_0084927 promotes colorectal cancer progression by regulating miRNA-20b-3p/glutathione S-transferase mu 5 axis

Feng Liu, Xiao-Li Xiao, Yu-Jing Liu, Ruo-Hui Xu, Wen-Jun Zhou, Han-Chen Xu, Ai-Guang Zhao, Yang-Xian Xu, Yan-Qi Dang, Guang Ji

ORCID number: Feng Liu 0000-0001-9370-7512; Xiao-Li Xiao 0000-0002-4053-0802; Yu-Jing Liu 0000-0002-9879-4413; Ruo-Hui Xu 0000-0003-1621-2326; Wen-Jun Zhou 0000-0003-4167-0337; Han-Chen Xu 0000-0003-2335-5421; Ai-Guang Zhao 0000-0002-8185-6171; Yang-Xian Xu 0000-0001-8738-3291; Yan-Qi Dang 0000-0001-8651-6937; Guang Ji 0000-0003-0842-3676.

Author contributions: Liu F and Xiao XL contributed equally to this work. Ji G and Dang YQ should be regarded as co-corresponding authors; Ji G and Dang YQ conceived, designed, and supervised the study; Dang YQ, Xu YX, and Xu HC collected the samples; Liu F, Xiao XL, Liu YJ, and Xu RH performed the experiments; Dang YQ, Liu F, and Zhou WJ analyzed the data; Dang YQ and Liu F wrote the paper; Zhou WJ, Zhao AG, and Ji G revised the manuscript; all authors reviewed and approved the final manuscript.

Supported by the National Natural Science Foundation of China, No. 81804018 and No. 81874206; and the Key Project of the Shanghai 3-Year Plan, No. ZY[2018-2020]CCCX-2002-01.

Institutional review board

Feng Liu, Xiao-Li Xiao, Yu-Jing Liu, Ruo-Hui Xu, Wen-Jun Zhou, Han-Chen Xu, Yan-Qi Dang, Guang Ji, Institute of Digestive Diseases, Longhua Hospital, China-Canada Center of Research for Digestive Diseases (ccCRDD), Shanghai University of Traditional Chinese Medicine, Shanghai 200032, China

Feng Liu, Ai-Guang Zhao, Department of Oncology, Longhua Hospital, Shanghai University of Traditional Chinese Medicine, Shanghai 200032, China

Yang-Xian Xu, Department of General Surgery, Longhua Hospital, Shanghai University of Traditional Chinese Medicine, Shanghai 200032, China

Corresponding author: Guang Ji, MD, PhD, Professor, Institute of Digestive Diseases, Longhua Hospital, China-Canada Center of Research for Digestive Diseases (ccCRDD), Shanghai University of Traditional Chinese Medicine, No. 725 South Wanping Road, Shanghai 200032, China. jiliver@vip.sina.com

Abstract

BACKGROUND

Colorectal cancer (CRC) is the third most common cancer and the second most common cause of cancer-related death worldwide. The 5-year survival rate of patients with early-stage CRC could reach 90%, but it is very low in patients with advanced-stage CRC. Recent studies have shown that circular RNAs play important roles in regulating the migration and invasion of CRC cells.

AIM

To elucidate the role of circRNA_0084927 (circ_0084927) in the migration and invasion of CRC cells and its underlying mechanism.

METHODS

Clinical tissue samples and cells were collected, and the expression of circ_0084927 was detected by quantitative polymerase chain reaction (qPCR). The diagnostic performance of circ_0084927 was assessed by receiver operating characteristic curve analysis. The role of circ_0084927 in CRC cell proliferation, migration, and invasion was determined using cell counting kit-8 assay, wound healing assay, and transwell assay, respectively. The regulatory relationship among circ_0084927, miRNA-20b-3p (miR-20b-3p), and glutathione S-transferase mu 5 (GSTM5) was identified using databases, luciferase reporter assay, qPCR,

and Western blot analysis. AKT-mTOR signaling was also verified after circ_0084927 knockdown or miR-20b-3p mimic treatment.

RESULTS

The expression of circ_0084927 was significantly increased in CRC tissues and cells, and it was higher in advanced-stage CRC compared with early-stage CRC. The area under the curve (AUC) of circ_0084927 was 0.806 [95% confidence interval (CI): 0.683-0.896]. In addition, the AUC was 0.874 (95%CI: 0.738-0.956) in patients with advanced-stage CRC and 0.713 (95%CI: 0.555-0.840) in those with early-stage CRC. Knockdown of circ_0084927 inhibited the migration and invasion of HCT116 cells. Moreover, circ_0084927 was found to act as a sponge of miR-20b-3p. MiR-20b-3p activation reduced the circ_0084927 level, whereas miR-20b-3p inhibition increased the circ_0084927 level. But the effect was not found after circ_0084927 mutation. In addition, miR-20b-3p expression in CRC patients was also reduced and negatively correlated with circ_0084927 expression. The function of circ_0084927 in HCT116 cells with circ_0084927 knockdown was rescued by miR-20b-3p. Moreover, GSTM5 expression was significantly decreased after overexpressing miR-20b-3p or inhibiting circ_0084927, but its expression was rescued when circ_0084927 and miR-20b-3p were both inhibited. Finally, AKT-mTOR signaling was markedly regulated by circ_0084927 and miR-20b-3p.

CONCLUSION

The expression of circ_0084927 is significantly increased in CRC and higher in advanced-stage CRC than in early-stage CRC. Moreover, circ_0084927 potentially regulates CRC cell migration and invasion *via* the miR-20b-3p/GSTM5/AKT/mTOR pathway.

Key Words: Colorectal cancer; CircRNA_0084927; MiRNA-20b-3p; Glutathione S-transferase mu 5; Migration; Invasion

Core Tip: The 5-year survival rate of patients with early-stage colorectal cancer (CRC) could reach 90%, but it is very low in patients with advanced-stage CRC. Recent studies have shown that circular RNAs play important roles in regulating the migration and invasion of CRC cells. To elucidate the role of circRNA_0084927 (circ_0084927) in the migration and invasion of CRC cells and the underlying mechanism, this study was performed. The expression of circ_0084927 was significantly increased in CRC tissues and cells, and it was markedly higher in advanced-stage CRC compared with early-stage CRC. Knockdown of circ_0084927 inhibited the migration and invasion of HCT116 cells. Moreover, circ_0084927 potentially regulates CRC migration and invasion *via* the miRNA-20b-3p/glutathione S-transferase mu 5 pathway.

Citation: Liu F, Xiao XL, Liu YJ, Xu RH, Zhou WJ, Xu HC, Zhao AG, Xu YX, Dang YQ, Ji G. CircRNA_0084927 promotes colorectal cancer progression by regulating miRNA-20b-3p/glutathione S-transferase mu 5 axis. *World J Gastroenterol* 2021; 27(36): 6064-6078
URL: https://www.wjgnet.com/1007-9327/full/v27/i36/6064.htm
DOI: https://dx.doi.org/10.3748/wjg.v27.i36.6064

INTRODUCTION

Colorectal cancer (CRC) is the third most common cancer and the second most common cause of cancer-related death worldwide, and the numbers of new cases and deaths in 2018 were 1.8 million and 881000, respectively[1]. With the development of diagnostic and therapeutic technologies, the 5-year survival rate for CRC patients has reached 65%[2] and can reach 90% in early-stage CRC patients. However, the 5-year survival rate of patients with advanced-stage CRC is very low due to tumor metastasis and other complications. Although colonoscopy is the gold standard of CRC screening, approximately 60% of CRC patients are diagnosed at an advanced stage

statement: The study was reviewed and approved by the Medical Ethics Committee of Longhua Hospital Affiliated to Shanghai University of Traditional Chinese Medicine (No. 2019LCSY020).

Conflict-of-interest statement: The authors have no conflicts of interest to declare.

Data sharing statement: The original data of this study will be available upon request from corresponding author.

Manuscript source: Unsolicited manuscript

Specialty type: Oncology

Country/Territory of origin: China

Peer-review report's scientific quality classification
Grade A (Excellent): 0
Grade B (Very good): B
Grade C (Good): 0
Grade D (Fair): 0
Grade E (Poor): 0

Received: March 3, 2021
Peer-review started: March 3, 2021
First decision: June 3, 2021
Revised: June 4, 2021
Accepted: August 9, 2021
Article in press: August 9, 2021
Published online: September 28, 2021

P-Reviewer: Lomperta K
S-Editor: Wu YXJ
L-Editor: Wang TQ

P-Editor: Liu JH

given the rate of missed lesions and incomplete colonoscopy coverage[3-5]. Therefore, it is urgent to elucidate the pathogenesis and molecular mechanism of CRC with metastasis.

Circular RNAs (circRNAs), as important regulatory noncoding RNAs, have become a new research hotspot following microRNAs (miRNAs) and long noncoding RNAs. Researchers have demonstrated that circRNAs play important roles in tumors, including CRC[6-9], and their functions are completed in a variety of ways, such as acting as sponges of miRNAs[6,7], acting as transcriptional regulators[10,11], and translating proteins by combining with RNA binding proteins[12-15]. However, to date, the functions of circRNAs in CRC remain largely unknown, especially in CRC with metastasis. Further study to elucidate the function of circRNAs in CRC with metastasis is needed.

In this study, we first verified the differential expression of circRNA_0084927 (circ_0084927) according to previous circRNA sequencing data[16] and further found that circ_0084927 was associated with the pathological stage of CRC. Then, we demonstrated that knockdown of circ_0084927 markedly inhibited HCT116 cell migration and invasion. Regarding the regulatory mechanism of circ_0084927, it acts as a sponge of miRNA-20b-3p (miR-20b-3p), regulating glutathione S-transferase mu 5 (GSTM5) and the AKT-mTOR pathway. Therefore, our findings elucidated the role of circ_0084927 and provided a new treatment strategy for CRC with metastasis.

MATERIALS AND METHODS

Clinical tissue specimens

Thirty pairs of CRC tissues and adjacent normal tissues (normal) were obtained during surgery at the Longhua Hospital Affiliated to Shanghai University of Traditional Chinese Medicine (Shanghai, China). The diagnosis of CRC was confirmed based on pathological evidence. Tissues were snap-frozen in liquid nitrogen and stored at -80 °C before detection. The study was approved by the Ethics Committee of Longhua Hospital (No. 2019LCSY020), and informed consent was obtained from all participants.

Cell culture and transfection

Normal colon cells (FHC) and CRC cells (HCT116, HT29, SW480, and SW620) (Shanghai Cell Bank, shanghai, China) were cultured in Dulbecco's modified Eagle's medium supplemented with 10% fetal bovine serum and penicillin/streptomycin (100 U/mL) (Gibco, Carlsbad, United States) in an incubator with 5% CO_2 at 37 °C. In addition, human embryonic kidney 293T (HEK-293T) cells obtained from American Type Culture Collection (ATCC) (Manassas, United States) were cultured in Roswell Park Memorial Institute 1640 medium with 10% fetal bovine serum and penicillin/streptomycin (100 U/mL). Short hairpin circ_0084927 plasmid (sh-circ_0084927; GeneChem, China) and miR-20b-3p mimic/inhibitor or negative control (NC, Genomeditech, China; 200 nM) were transfected using FuGene HD transfection reagent (Promega, United States) according to previous studies[17,18].

Cell counting kit-8 assay

After transfection, HCT116 cells were seeded into 96-well plates at a concentration of 1 × 10^4 cells and cultured for 0 h, 24 h, 48 h, and 72 h. Then, 10 μL of cell counting kit-8 reagent was added to each well. After incubation at 37 °C for 1 h, the absorbance value was detected at 450 nm.

Wound healing assay

After transfection, HCT116 cells were seeded in a 6-well dish with a culture insert (Ibidi, Germany) at a concentration of 3 × 10^4 cells. After 24 h, the culture insert was removed, and the cells were washed twice with polybutylene succinate. Two milliliters of serum-free medium were added to each dish for 48 h. Images were captured, and the wound area was measured using Image J software (National Institutes of Health, United States).

Cell migration invasion assay

Six-well plates with 8-μm chambers (Corning, United States) were used to assess cellular migration (without Matrigel) or invasion (with Matrigel). Briefly, transfected HCT116 cells were seeded in 6-well plates at a concentration of 1 × 10^5 cells. Two

hundred microliters of serum-free medium was added to the upper chamber, and six hundred microliters of medium with 30% fetal bovine serum was added to the lower chamber for 48 h. Then, the cells were fixed with 4% paraformaldehyde for 30 min and stained with 0.1% crystal violet solution for 15 min. Four fields were randomly selected to calculate the number of migrating or invading cells and to evaluate the ability of cell migration or invasion.

Quantitative polymerase chain reaction

Total RNA was extracted using TRIzol reagent (Ambion, United States). For circRNA and mRNA analysis, cDNA was synthesized using an EVM-MLV reverse transcription kit (Aikeri Biotech, Hunan, China). For miRNA analysis, cDNA was synthesized using a miRNA cDNA synthesis kit (Sangon Biotech, Shanghai, China). The amplification reaction was performed using the SYBR-Green quantitative polymerase chain reaction (qPCR) kit (Thermo Fisher Scientific, MA, United States) or the miRNA fluorescence quantitative PCR kit (Sangon Biotech). Gene expression was normalized using β-actin or U6. The primers are listed in Table 1.

Western blot analysis

Cells were collected and lysed. Protein concentration was determined using a protein assay kit (Beyotime, China). The protein was separated and transferred to a polyvinylidene fluoride membrane followed by incubation with 5% milk at room temperature for 1 h. The membrane was incubated at 4 °C overnight with the following antibodies: GSTM5 (GTX108776, Genetex, United States), PI3 kinase p85 (PI3K, 4292S, CST, United States), phospho-PI3K (BS-3332R, Bioss, China), Akt (4685S, CST), phospho-Akt (4060S, CST), mTOR (2983S, CST), phospho-mTOR (5536S, CST), and β-actin (4970s, CST). Then, the secondary antibody was added and incubated at room temperature for 2 h, and protein expression was observed using a chemiluminescence gel imaging system (Tanon 5200, China).

Double luciferase reporter assay

HEK-293T cells were seeded in 24-well plates and transfected using FuGene HD transfection reagent (Promega, United States) according to previous studies[17,18]. Briefly, HEK-293T cells were transfected using circ_0084927 wild type (circ_0084927-WT; Genomeditech, China) or circ_0084927 mutant (circ_0084927-Mut; Genomeditech) plasmid with or without miR-20b-3p mimic/inhibitor. After transfection for 22 h, luciferase activity was detected using the dual-luciferase reporter system (Promega).

Statistical analysis

Statistical analyses were conducted using SPSS 24.0 software. Data were assessed using Student's *t*-test or one-way ANOVA. Pearson correlation was used to analyze the correlation between circRNA and miRNA. Receiver operating characteristic (ROC) curve analysis was performed to evaluate the diagnostic value using MedCalc software. $P < 0.05$ was considered statistically significant. Dr. Ming Yang from the Good Clinical Practice Office, Longhua Hospital, Shanghai University of Traditional Chinese Medicine reviewed the statistical methods of this study before submission.

RESULTS

Circ_0084927 is markedly increased in CRC and associated with the pathological stage of CRC

Our previous study has proved that circRNAs play important roles in the transition of adenoma into CRC[16], but the function of circRNAs in advanced-stage CRC remains largely undetermined. According to previous circRNA sequencing data[16], five differentially expressed circRNAs were chosen and verified. The results showed that circ_0084927 expression was significantly increased in the CRC group compared with the normal group and was higher in advanced-stage CRC compared with early-stage CRC (Figure 1A and B). The other four circRNAs were not significantly different (Supplementary Figure 1). In addition, circ_0084927 expression in CRC cells (HCT116, HT29, and SW620) was also increased (Figure 1C). ROC curve analysis was used to evaluate the diagnostic performance of circ_0084927 in CRC. The area under the curve (AUC) of circ_0084927 was 0.806 (95%CI: 0.683 to 0.896) ($P < 0.001$). In addition, the AUC was 0.874 (95%CI: 0.738-0.956) in patients with advanced-stage CRC and 0.713 (95%CI: 0.555-0.840) in those with early-stage CRC, indicating that circ_0084927 had

Table 1 Sequence of primers used in the study

Gene name	Forward (5'→3')	Reverse (5'→3')
β-actin	GGCTGTATTCCCCTCCATCG	CCAGTTGGTAACAATGCCATGT
circRNA_0084927	AGCACTACAGAGGCACAAACATC	GTGCCCTGACTACGGTGTTATC
circRNA_0138996	CTGATCCCAATGGATTGCATC	GTCCTCCCGTTCCTCTTCG
circRNA_0110477	CGAATCAAAGCAGCCTATCAAG	TGCCACATAGAATTTGGGTGTC
circRNA_0133544	CATGAGGTTAGGCAGTTGTATCG	TGTTTTTAGCCTTTTCTCCATCTC
circRNA_0002867	AACCAGAGCACATTAGCCAAAG	CAAACTCGGCGTGTTCTTCTC
GSTM5	GAAGATGGGAGGGAGGAG	CCTTGGGGAAGAGAAGAGA
U6	AGAGAAGATTAGCATGGCCCCTG	ATCCAGTGCAGGGTCCGAGG
miRNA-20b-3p	ACTGTAGTATGGGCACTTCCAG	ATCCAGTGCAGGGTCCGAGG

GSTM5: Glutathione S-transferase mu 5; U6: U6 small nuclear RNA 1.

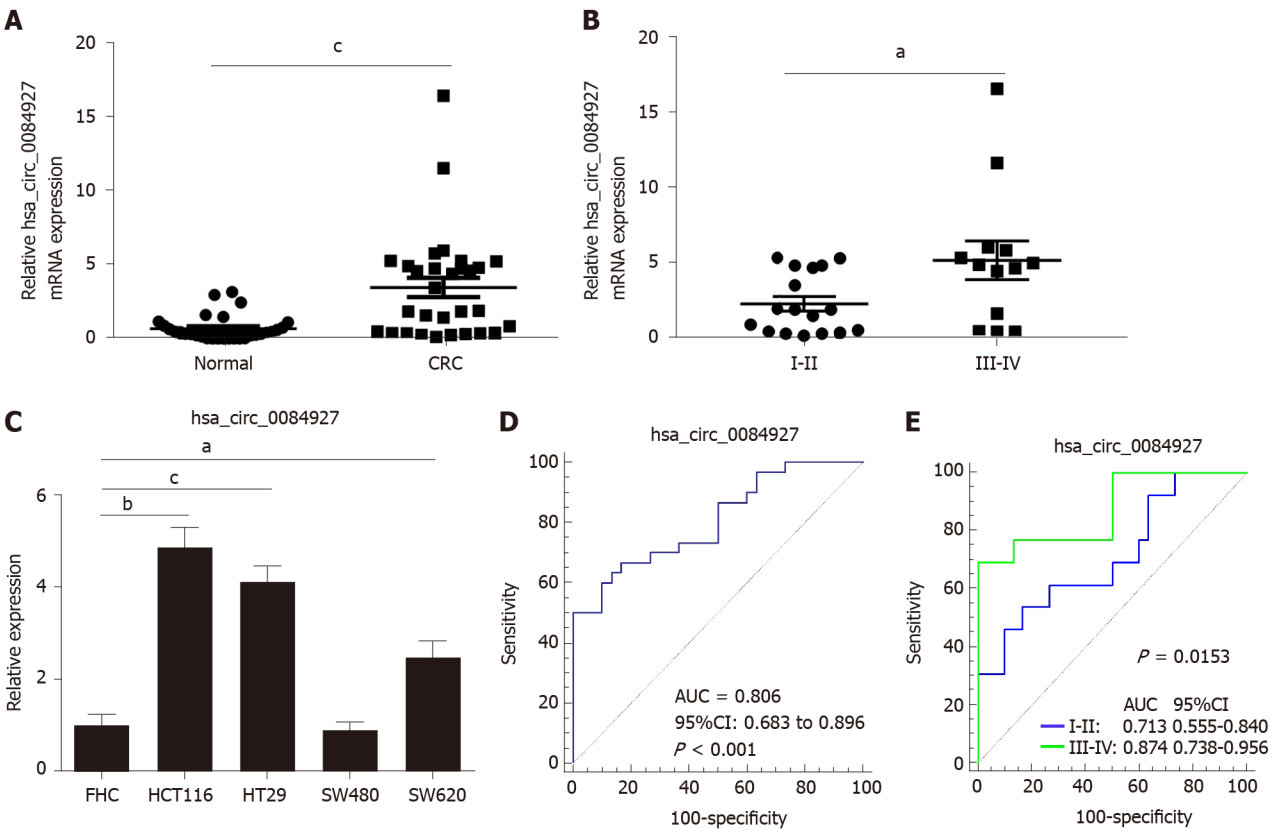

Figure 1 CircRNA_0084927 expression is markedly increased in colorectal cancer. A: Expression of circRNA_0084927 (circ_0084927) in colorectal cancer (CRC); B: Expression of circ_0084927 in advanced-stage and early-stage CRC; C: Expression of circ_0084927 in CRC cells; D: Receiver operating characteristic (ROC) curve analysis of circ_0084927; E: ROC analysis of circ_0084927 in advanced-stage and early-stage CRC. Data are presented as the mean ± SEM. $^aP < 0.05$; $^bP < 0.01$; $^cP < 0.001$. Circ_0084927: CircRNA_0084927; Normal: Adjacent normal tissues; CRC: Colorectal cancer; ROC: Receiver operating characteristic; AUC: Area under the curve.

higher diagnostic performance in advanced-stage CRC ($P = 0.0153$) (Figure 1D and E).

Knockdown of circ_0084927 inhibits HCT116 cell migration and invasion

To explore the function of circ_0084927 in CRC, circ_0084927 expression was inhibited in HCT116 cells using shRNA plasma (Figure 2A), and circ_0084927 knockdown markedly inhibited HCT116 cell proliferation at 48 h and 72 h (Figure 2B). In addition, circ_0084927 knockdown also significantly inhibited HCT116 cell migration and invasion (Figure 2C-G). These results demonstrated that circ_0084927 is an oncogene

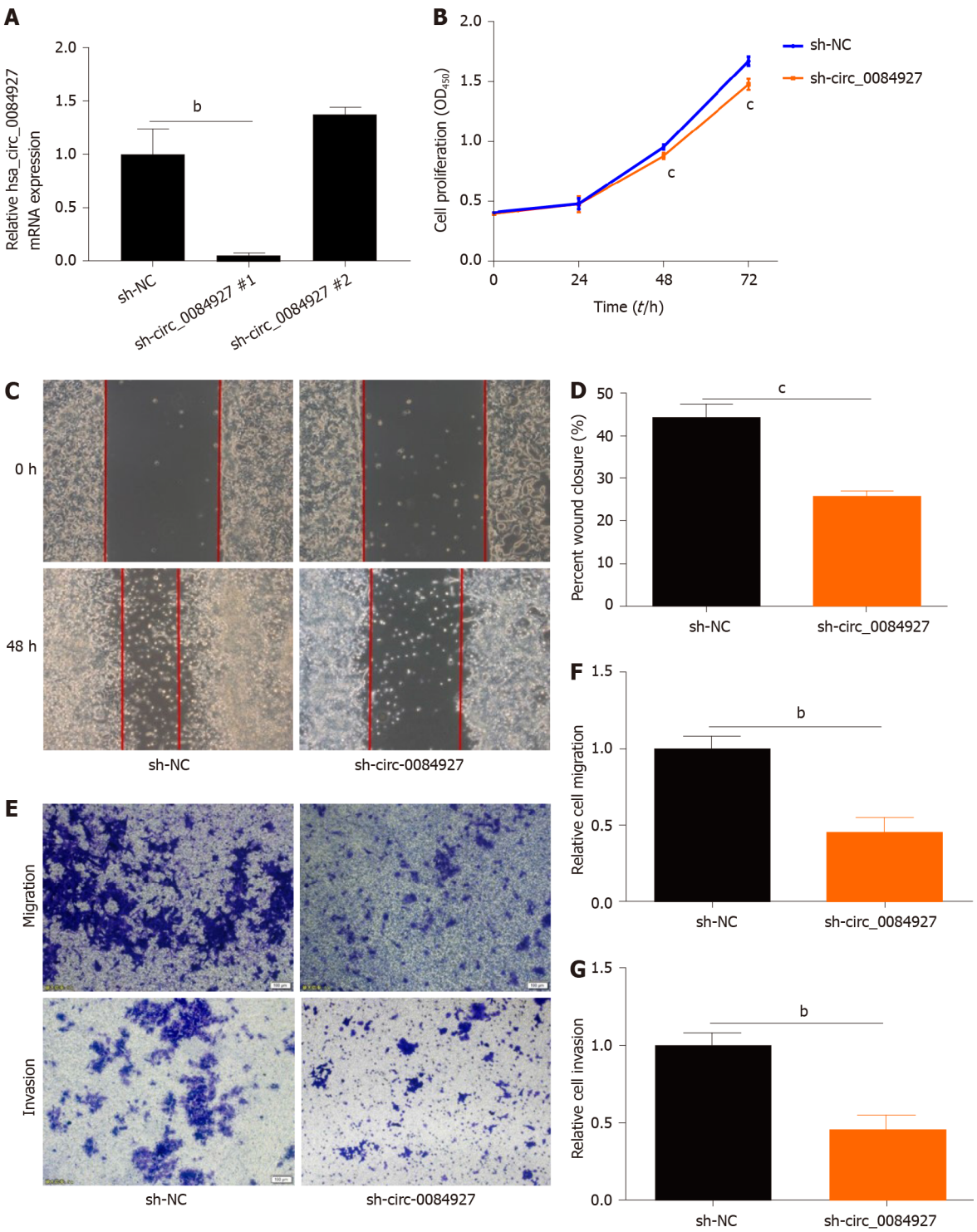

Figure 2 Knockdown of circRNA_0084927 inhibits the migration and invasion of HCT116 cells. A: Knockdown of circRNA_0084927 (circ_0084927); B: Vability of HCT116 cells after circ_0084927 knockdown; C-G: Migration and invasion of HCT116 cells tested by wound healing assay (C and D) and transwell assay (E-G). Data are presented as the mean ± SEM. $^{b}P < 0.01$; $^{c}P < 0.001$. Circ_0084927: CircRNA_0084927; Sh-circ_0084927: Short hairpin circ_0084927 plasmid; Sh-NC: Short hairpin negative control plasmid.

that promotes CRC function.

Circ_0084927 acts as a sponge of miR-20b-3p in CRC

The biological function of circRNAs mainly involves acting as a sponge of miRNAs [19]. In this study, circ_0084927 may act as a sponge of miR-20b-3p as demonstrated by bioinformatics analysis (Figure 3A). The miR-20b-3p mimic markedly reduced the luciferase activity of circ_0084927, whereas the miR-20b-3p inhibitor markedly increased the luciferase activity of circ_0084927, but had no effect on circ_0084927-Mut (Figure 3B and C). qPCR results also indicated that knockdown of circ_0084927

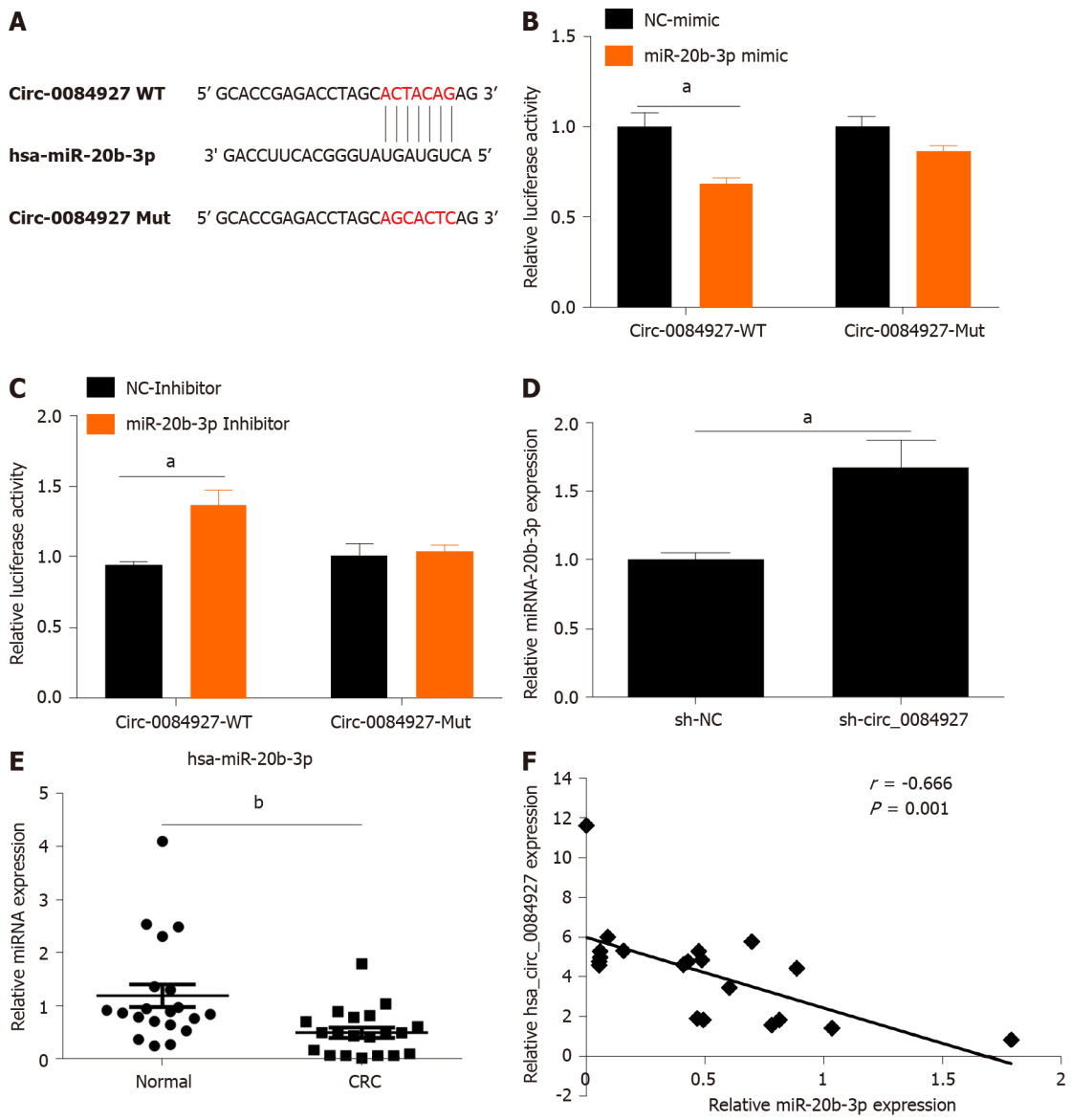

Figure 3 CircRNA_0084927 acts as a sponge of miRNA-20b-3p in colorectal cancer. A: CircRNA_0084927 (Circ_0084927) potentially acts as a sponge of miRNA-20b-3p (miR-20b-3p) in database; B: miR-20b-3p mimic could markedly reduce the luciferase activity of circ_0084927; C: miR-20b-3p inhibitor could markedly increase the luciferase activity of circ_0084927; D: circ_0084927 knockdown markedly increased the level of miR-20b-3p; E: Expression of miR-20b-3p in colorectal cancer (CRC); F: Correlation of circ_0084927 and miR-20b-3p. Data are presented as the mean ± SEM. $^{a}P < 0.05$; $^{b}P < 0.01$. Circ_0084927: CircRNA_0084927; MiR-20b-3p: MiRNA-20b-3p; NC: Negative control; CRC: Colorectal cancer; Normal: Adjacent normal tissues; Circ_0084927-WT: CircRNA_0084927 wild type; Circ_0084927-Mut: CircRNA_0084927 mutant; Sh-circ_0084927: Short hairpin circ_0084927 plasmid; Sh-NC: Short hairpin negative control plasmid.

promoted the expression of miR-20b-3p (Figure 3D). We also tested the expression of miR-20b-3p in CRC tissue samples, and its expression was significantly reduced (Figure 3E). Spearman correlation coefficient analysis revealed that circ_0084927 was negatively correlated with miR-20b-3p (Figure 3F). All of the data suggested that circ_0084927 acts as a sponge of miR-20b-3p.

The function of circ_0084927 in HCT116 cells with circ_0084927 knockdown is rescued by miR-20b-3p

To assess whether the function of circ_0084927 in HCT116 cells is mediated by miR-20b-3p, HCT116 cells with circ_0084927 knockdown was transfected with or without miR-20b-3p inhibitor (Figure 4A). The CCK-8 assay showed that circ_0084927 knockdown inhibited the proliferation of HCT116 cells, while the effect was rescued by the miR-20b-3p inhibitor (Figure 4B). Wound healing and transwell assays showed that circ_0084927 knockdown inhibited the migration and invasion of HCT116 cells, whereas miR-20b-3p inhibition rescued this effect (Figure 4C-G).

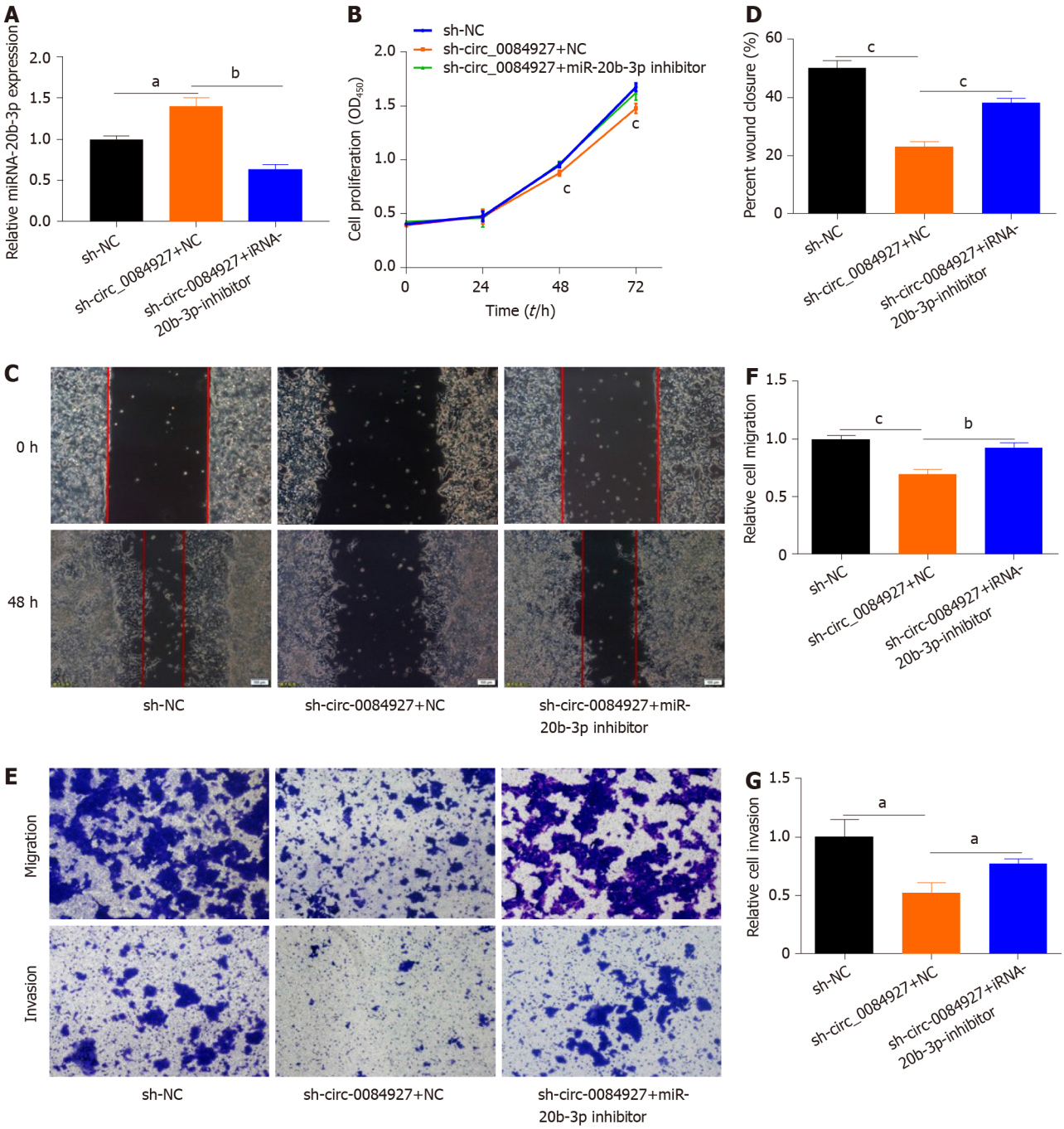

Figure 4 The function of circRNA_0084927 in HCT116 cells with circRNA_0084927 knockdown is rescued by miRNA-20b-3p. A: Expression of miRNA-20b-3p (miR-20b-3p); B: Viability of HCT116 cells detected after transfecting circRNA_0084927 (circ_0084927) or miR-20b-3p inhibitor; C-G: Migration and invasion of HCT116 cells tested by wound healing assay (C and D) and transwell assay (E-G) after transfecting sh-circ_0084927 plasmid or miR-20b-3p inhibitor. Data are presented as the mean ± SEM. $^{a}P < 0.05$; $^{b}P < 0.01$; $^{c}P < 0.001$. Sh-circ_0084927: Short hairpin circ_0084927 plasmid; Sh-NC: Short hairpin negative control plasmid; miR-20b-3p: miRNA-20b-3p.

GSTM5 is a target of miR-20b-3p

According to bioinformatics analysis, we found that GSTM5 is a target of miR-20b-3p. We then assessed GSTM5 expression after overexpressing miR-20b-3p. The results showed that *GSTM5* mRNA expression was significantly reduced after overexpressing miR-20b-3p (Figure 5A). GSTM5 protein level was consistent with its mRNA level (Figure 5B). Moreover, GSTM5 mRNA and protein expression was also markedly reduced after silencing circ_0084927 (Figure 5C and D). After transfecting the miR-20b-3p inhibitor into HCT116 cells with circ_0084927 knockdown, GSTM5 mRNA and protein expression was rescued (Figure 5E and F). The survival curve results using The Cancer Genome Atlas (TCGA) data also showed that patients with high GSTM5 levels had a poor survival, indicating that GSTM5 was negatively correlated with CRC

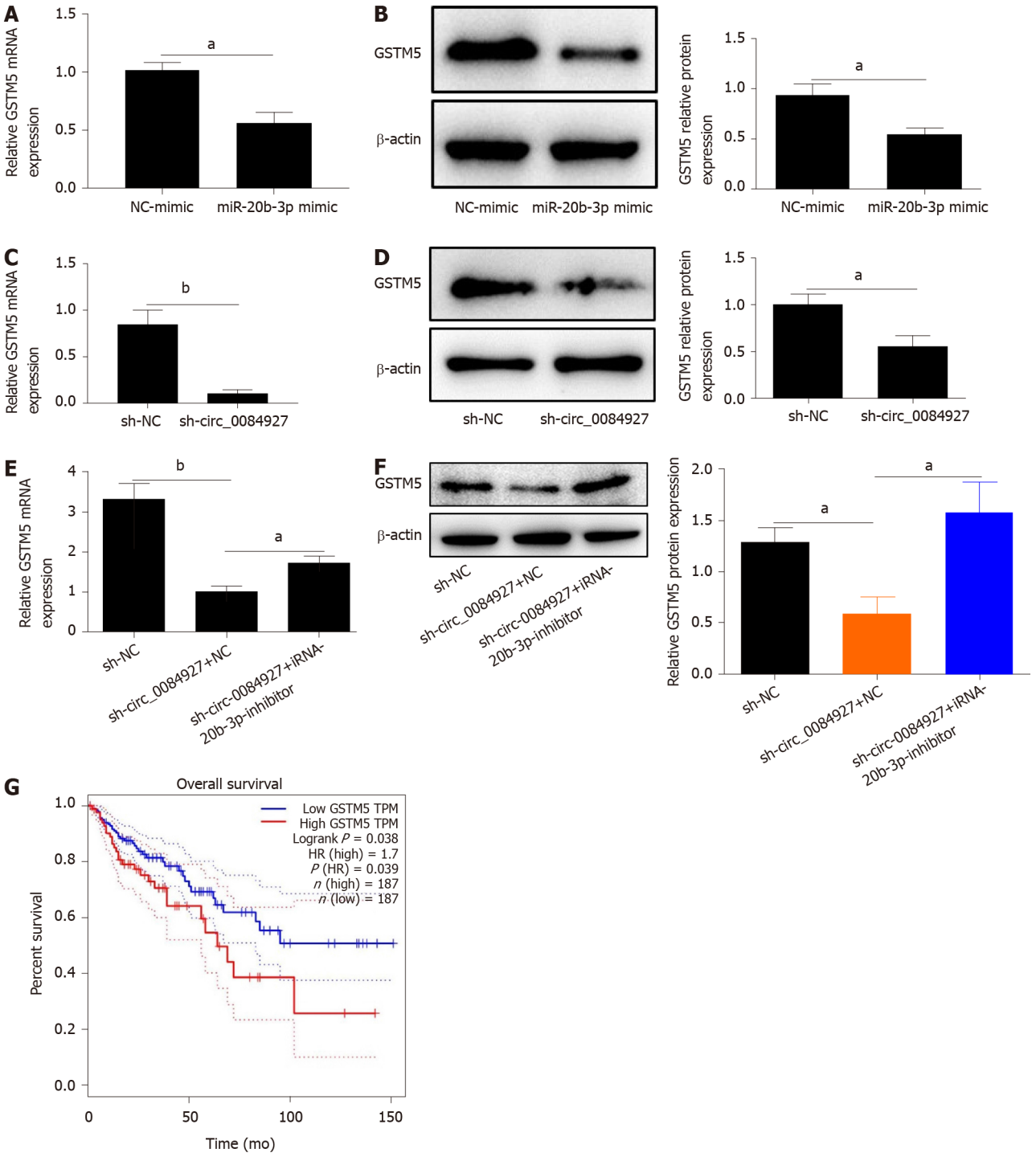

Figure 5 Glutathione S-transferase mu 5 is a target of miRNA-20b-3p. A and B: Expression of glutathione S-transferase mu 5 (GSTM5) after transfecting miRNA-20b-3p (miR-20b-3p) mimic; C and D: Expression of GSTM5 after transfecting circRNA_0084927 (circ_0084927); E and F: Expression of GSTM5 after transfecting sh-circ_0084927 plasmid and miR-20b-3p inhibitor; G: Overall survival by GSTM5 expression. Data are presented as the mean ± SEM. $^{a}P < 0.05$, $^{b}P < 0.01$. NC mimic: Negative control mimic; GSTM5: Glutathione S-transferase mu 5; miR-20b-3p: miRNA-20b-3p; Sh-circ_0084927: Short hairpin circ_0084927 plasmid; Sh-NC: Short hairpin negative control plasmid.

patient survival (Figure 5G).

The AKT-mTOR pathway is inactivated by circ_0084927 knockdown and rescued by miR-20b-3p

Further experiments found that circ_0084927 knockdown or miR-20b-3p overexpression both reduced the phosphorylation levels of AKT and mTOR (Figure 6A and B). In addition, AKT and mTOR phosphorylation levels were rescued after inhibiting miR-20b-3p in HCT116 cells with circ_0084927 knockdown (Figure 6C). These results showed that circ_0084927 regulated CRC migration and invasion *via* the miR-20b-

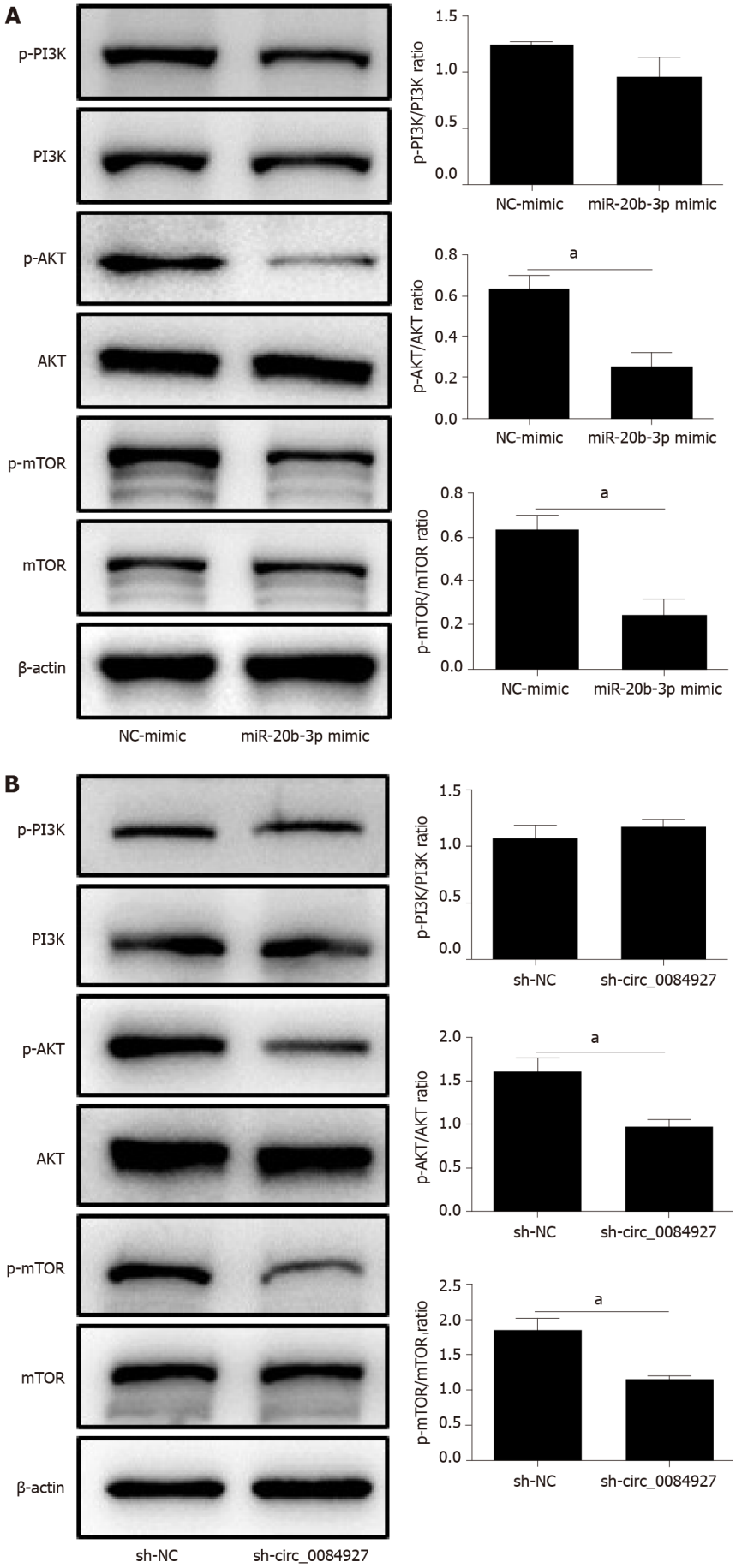
A
p-PI3K
PI3K
p-AKT
AKT
p-mTOR
mTOR
β-actin
NC-mimic
miR-20b-3p mimic
p-PI3K/PI3K ratio
p-AKT/AKT ratio
p-mTOR/mTOR ratio
a
B
sh-NC
sh-circ_0084927

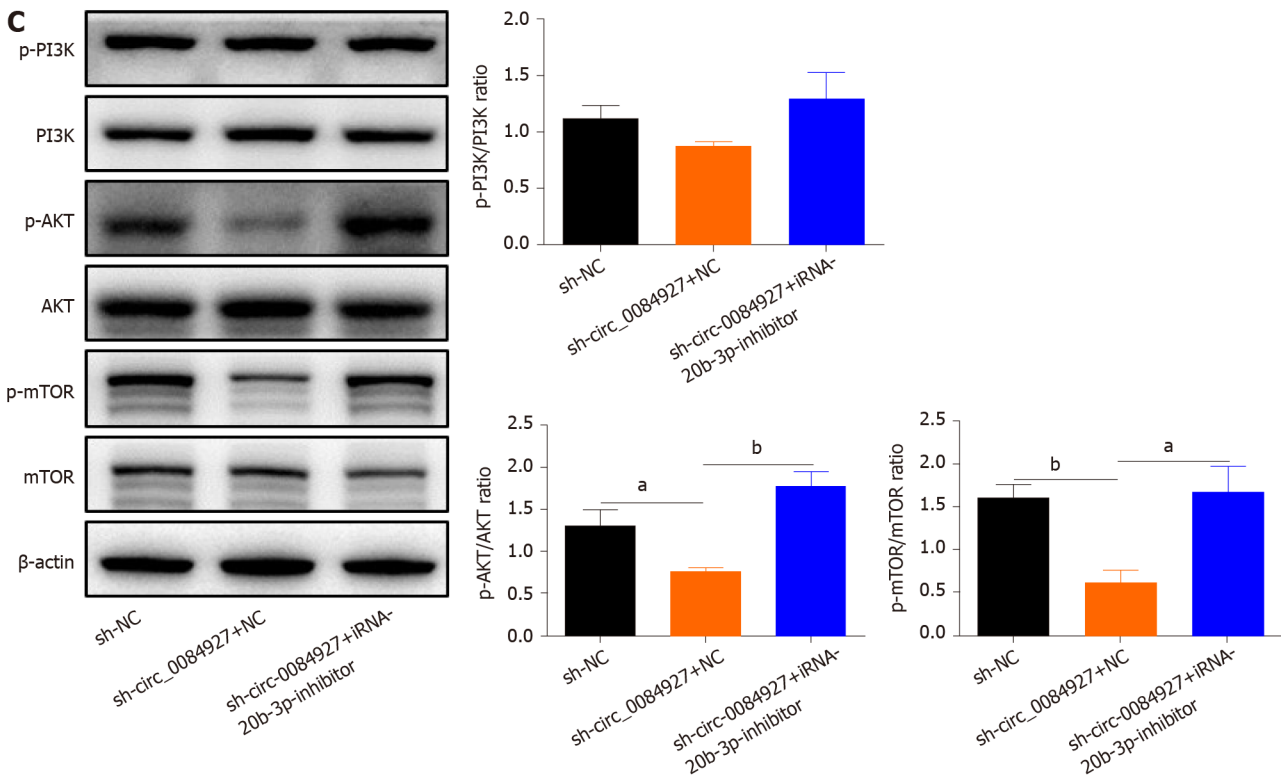

Figure 6 AKT-mTOR pathway is inactivated by circRNA_0084927 knockdown and rescued by miRNA-20b-3p. A: Expression of AKT-mTOR pathway molecules after transfecting miRNA-20b-3p (miR-20b-3p) mimic; B: Expression of AKT-mTOR pathway molecules after transfecting circRNA_0084927 (circ_0084927); C: Expression of AKT-mTOR pathway molecules after transfecting sh-circ_0084927 plasmid and miR-20b-3p inhibitor. Data are presented as the mean ± SEM. $^{a}P < 0.05$; $^{b}P < 0.01$. Sh-circ_0084927: Short hairpin circ_0084927 plasmid; Sh-NC: Short hairpin negative control plasmid; NC mimic: Negative control mimic.

3p/GSTM5/AKT-mTOR pathway.

DISCUSSION

As a malignant tumor, the incidence of CRC has recently increased. Although the 5-year survival rate of CRC patients is 65%[2], it is very low in patients with advanced-stage CRC. Therefore, it is urgent to develop techniques for the early diagnosis of CRC, which would improve patient survival. Moreover, new treatment strategies for advanced-stage CRC are also very important. Studies have indicated that circRNAs are very stable and not easily degraded due to loop properties[20] and have demonstrated the specificity of their expression in particular tissues and tumor developmental stages[20-23]. Therefore, circRNAs, such as serum exosomal hsa-circ-0004771 and circ-PNN[24,25], could act as biomarkers for the diagnosis of CRC. In addition, circRNAs could promote the progression of CRC and act as therapeutic targets[6,8,26,27]. Circ_0084927 originates from epithelial splicing regulatory protein 1 (ESRP1), which is upregulated in CRC (Supplementary Figure 2) and associated with the pathogenesis of CRC[28]. Studies have demonstrated that circ_0084927 facilitates cervical cancer advancement[29-31], but its function in CRC is unclear. In this study, we found that circ_0084927 expression was significantly increased in CRC tissues and cells, and was higher in advanced-stage CRC than in early-stage CRC. Further studies indicated that knockdown of circ_0084927 inhibited the migration and invasion of CRC cells, showing that circ_0084927 played an important role in CRC progression.

CircRNAs perform biological functions by acting as sponges of miRNAs[6,7]. In cervical cancer, miRNAs related to circ_0084927 mainly include miR-142-3p, miR-634, and miR-1179[29-31]. Our study found that circ_0084927 acts as a sponge of miR-20b-3p in CRC. In addition, miR-20b-3p activation reduced circ_0084927 level, whereas miR-20b-3p inhibition increased circ_0084927 level. The expression of circ_0084927 was not altered after the binding site with miR-20b-3p was mutated. In addition, miR-20b-3p expression in CRC patients was also reduced and was negatively correlated with circ_0084927. Studies have shown that miR-20b-3p is related to temozolomide

resistance in glioblastoma[32] and diabetic retinopathy progression[33], but the function of miR-20b-3p in CRC has not been reported. In this study, we demonstrated that miR-20b-3p rescued the effect of circ_0084927 on CRC cells, indicating the role of miR-20b-3p in CRC.

Further studies found that GSTM5 is a target of miR-20b-3p. GSTM5 expression was significantly reduced after overexpressing miR-20b-3p or silencing circ_0084927. However, GSTM5 expression was rescued after silencing circ_0084927 and inhibiting miR-20b-3p. Studies have demonstrated that glutathione S-transferases are pro-carcinogenic in CRC[34]. AS a glutathione S-transferase, GSTM5 is also involved in various tumors, including breast cancer[35,36], prostate cancer[36], ovarian carcinoma [37], and CRC[38,39]. Although previous studies have demonstrated that glutathione metabolism is involved in the progression of tumors[40-42] and GSTM5 could be a prognostic and predictive marker in CRC[38,39], the regulatory mechanism is unknown. In this study, we demonstrated that circ_0084927 regulated the migration and invasion of CRC by the miR-20b-3p/GSTM5 axis and finally regulated the AKT-mTOR pathway, which plays an important role in CRC[43-45]. Therefore, our results revealed that circ_0084927 regulated the progression of CRC *via* the miR-20b-3p/GSTM5/AKT-mTOR pathway.

CONCLUSION

In summary, we have demonstrated that circ_0084927 expression is significantly increased in CRC and is higher in advanced-stage CRC than in early-stage CRC. Mechanistically, circ_0084927 regulates the migration and invasion of CRC cells *via* the miR-20b-3p/GSTM5/AKT-mTOR pathway. This is the first study to demonstrate the role of circ_0084927 in CRC, and these findings provide a new perspective for targeted therapy of CRC with metastasis.

ARTICLE HIGHLIGHTS

Research background

Colorectal cancer (CRC) is the third most common cancer and the second most common cause of cancer-related death worldwide. Recent studies have shown that circular RNAs play important roles in regulating the progression of CRC. However, the biological role and underlying mechanism of circRNA_0084927 (circ_0084927) in CRC remain unclear.

Research motivation

Due to tumor metastasis and other complications, the 5-year survival rate of patients with advanced-stage CRC is very low. We hope to provide a new treatment strategy for CRC with metastasis.

Research objectives

The present study aimed to investigate the role and mechanism of circ_0084927 in regulating the progression of CRC.

Research methods

Clinical tissue samples and cells were collected, and the expression of circ_0084927 was detected by quantitative polymerase chain reaction (qPCR) The diagnostic performance of circ_0084927 was assessed by receiver operating characteristic curve analysis. The role of circ_0084927 in proliferation, migration, and invasion was determined using cell counting kit-8 assay, wound healing assay, and transwell assay, respectively. The regulatory relationship among circ_0084927, miRNA-20b-3p (miR-20b-3p), and glutathione S-transferase mu 5 (GSTM5) was identified using databases, luciferase reporter assays, qPCR, and Western blot analysis. AKT-mTOR signaling was also verified after circ_0084927 knockdown or miR-20b-3p mimic treatment.

Research results

The expression of circ_0084927 was significantly increased in CRC tissues and cells, and was increased in advanced-stage CRC compared with in early-stage CRC. The area under the curve (AUC) of circ_0084927 was 0.806 (95%CI: 0.683 to 0.896). In

addition, the AUC was 0.874 (95%CI: 0.738-0.956) in patients with advanced-stage CRC and 0.713 (95%CI: 0.555-0.840) in those with early-stage CRC. Knockdown of circ_0084927 inhibited the migration and invasion of HCT116 cells. Moreover, circ_0084927 was found to act as a sponge of miR-20b-3p. MiR-20b-3p activation reduced the circ_0084927 level, whereas miR-20b-3p inhibition increased the circ_0084927 level. But the effect was not found after circ_0084927 mutation. In addition, miR-20b-3p expression in CRC patients was also reduced and negatively correlated with circ_0084927 expression. The function of circ_0084927 in HCT116 cells with circ_0084927 knockdown was rescued by miR-20b-3p. Moreover, GSTM5 expression was significantly decreased after overexpressing miR-20b-3p or inhibiting circ_0084927, but its expression was rescued when circ_0084927 and miR-20b-3p were both inhibited. Finally, AKT-mTOR signaling was markedly regulated by circ_0084927 and miR-20b-3p.

Research conclusions

The expression of circ_0084927 is significantly increased in CRC and higher in advanced-stage CRC than in early-stage CRC. Moreover, circ_0084927 potentially regulates CRC migration and invasion *via* the miR-20b-3p/GSTM5/AKT/mTOR pathway.

Research perspectives

Circ_0084927 could promote CRC progression and provide a new treatment strategy for CRC with metastasis.

REFERENCES

1 **Bray F**, Ferlay J, Soerjomataram I, Siegel RL, Torre LA, Jemal A. Global cancer statistics 2018: GLOBOCAN estimates of incidence and mortality worldwide for 36 cancers in 185 countries. *CA Cancer J Clin* 2018; **68**: 394-424 [PMID: 30207593 DOI: 10.3322/caac.21492]

2 **Burgers K**, Moore C, Bednash L. Care of the Colorectal Cancer Survivor. *Am Fam Physician* 2018; **97**: 331-336 [PMID: 29671505]

3 **Zauber AG**, Winawer SJ, O'Brien MJ, Lansdorp-Vogelaar I, van Ballegooijen M, Hankey BF, Shi W, Bond JH, Schapiro M, Panish JF, Stewart ET, Waye JD. Colonoscopic polypectomy and long-term prevention of colorectal-cancer deaths. *N Engl J Med* 2012; **366**: 687-696 [PMID: 22356322 DOI: 10.1056/NEJMoa1100370]

4 **Zhao S**, Wang S, Pan P, Xia T, Chang X, Yang X, Guo L, Meng Q, Yang F, Qian W, Xu Z, Wang Y, Wang Z, Gu L, Wang R, Jia F, Yao J, Li Z, Bai Y. Magnitude, Risk Factors, and Factors Associated With Adenoma Miss Rate of Tandem Colonoscopy: A Systematic Review and Meta-analysis. *Gastroenterology* 2019; **156**: 1661-1674.e11 [PMID: 30738046 DOI: 10.1053/j.gastro.2019.01.260]

5 **Miller KD**, Nogueira L, Mariotto AB, Rowland JH, Yabroff KR, Alfano CM, Jemal A, Kramer JL, Siegel RL. Cancer treatment and survivorship statistics, 2019. *CA Cancer J Clin* 2019; **69**: 363-385 [PMID: 31184787 DOI: 10.3322/caac.21565]

6 **Jian X**, He H, Zhu J, Zhang Q, Zheng Z, Liang X, Chen L, Yang M, Peng K, Zhang Z, Liu T, Ye Y, Jiao H, Wang S, Zhou W, Ding Y, Li T. Hsa_circ_001680 affects the proliferation and migration of CRC and mediates its chemoresistance by regulating BMI1 through miR-340. *Mol Cancer* 2020; **19**: 20 [PMID: 32005118 DOI: 10.1186/s12943-020-1134-8]

7 **Shang A**, Gu C, Wang W, Wang X, Sun J, Zeng B, Chen C, Chang W, Ping Y, Ji P, Wu J, Quan W, Yao Y, Zhou Y, Sun Z, Li D. Exosomal circPACRGL promotes progression of colorectal cancer *via* the miR-142-3p/miR-506-3p- TGF-β1 axis. *Mol Cancer* 2020; **19**: 117 [PMID: 32713345 DOI: 10.1186/s12943-020-01235-0]

8 **Li XN**, Wang ZJ, Ye CX, Zhao BC, Li ZL, Yang Y. RNA sequencing reveals the expression profiles of circRNA and indicates that circDDX17 acts as a tumor suppressor in colorectal cancer. *J Exp Clin Cancer Res* 2018; **37**: 325 [PMID: 30591054 DOI: 10.1186/s13046-018-1006-x]

9 **Yang H**, Li X, Meng Q, Sun H, Wu S, Hu W, Liu G, Yang Y, Chen R. CircPTK2 (hsa_circ_0005273) as a novel therapeutic target for metastatic colorectal cancer. *Mol Cancer* 2020; **19**: 13 [PMID: 31973707 DOI: 10.1186/s12943-020-1139-3]

10 **Ashwal-Fluss R**, Meyer M, Pamudurti NR, Ivanov A, Bartok O, Hanan M, Evantal N, Memczak S, Rajewsky N, Kadener S. circRNA biogenesis competes with pre-mRNA splicing. *Mol Cell* 2014; **56**: 55-66 [PMID: 25242144 DOI: 10.1016/j.molcel.2014.08.019]

11 **Li Z**, Huang C, Bao C, Chen L, Lin M, Wang X, Zhong G, Yu B, Hu W, Dai L, Zhu P, Chang Z, Wu Q, Zhao Y, Jia Y, Xu P, Liu H, Shan G. Exon-intron circular RNAs regulate transcription in the nucleus. *Nat Struct Mol Biol* 2015; **22**: 256-264 [PMID: 25664725 DOI: 10.1038/nsmb.2959]

12 **Shang Q**, Yang Z, Jia R, Ge S. The novel roles of circRNAs in human cancer. *Mol Cancer* 2019; **18**: 6 [PMID: 30626395 DOI: 10.1186/s12943-018-0934-6]

13 **Yang Y**, Gao X, Zhang M, Yan S, Sun C, Xiao F, Huang N, Yang X, Zhao K, Zhou H, Huang S, Xie

B, Zhang N. Novel Role of FBXW7 Circular RNA in Repressing Glioma Tumorigenesis. *J Natl Cancer Inst* 2018; **110** [PMID: 28903484 DOI: 10.1093/jnci/djx166]

14 **Zhang M**, Huang N, Yang X, Luo J, Yan S, Xiao F, Chen W, Gao X, Zhao K, Zhou H, Li Z, Ming L, Xie B, Zhang N. A novel protein encoded by the circular form of the SHPRH gene suppresses glioma tumorigenesis. *Oncogene* 2018; **37**: 1805-1814 [PMID: 29343848 DOI: 10.1038/s41388-017-0019-9]

15 **Wesselhoeft RA**, Kowalski PS, Anderson DG. Engineering circular RNA for potent and stable translation in eukaryotic cells. *Nat Commun* 2018; **9**: 2629 [PMID: 29980667 DOI: 10.1038/s41467-018-05096-6]

16 **Zhu M**, Dang Y, Yang Z, Liu Y, Zhang L, Xu Y, Zhou W, Ji G. Comprehensive RNA Sequencing in Adenoma-Cancer Transition Identified Predictive Biomarkers and Therapeutic Targets of Human CRC. *Mol Ther Nucleic Acids* 2020; **20**: 25-33 [PMID: 32145677 DOI: 10.1016/j.omtn.2020.01.031]

17 **Dang Y**, Hu D, Xu J, Li C, Tang Y, Yang Z, Liu Y, Zhou W, Zhang L, Xu H, Xu Y, Ji G. Comprehensive analysis of 5-hydroxymethylcytosine in zw10 kinetochore protein as a promising biomarker for screening and diagnosis of early colorectal cancer. *Clin Transl Med* 2020; **10**: e125 [PMID: 32628818 DOI: 10.1002/ctm2.125]

18 **Dang Y**, Xu J, Zhu M, Zhou W, Zhang L, Ji G. Gan-Jiang-Ling-Zhu decoction alleviates hepatic steatosis in rats by the miR-138-5p/CPT1B axis. *Biomed Pharmacother* 2020; **127**: 110127 [PMID: 32325349 DOI: 10.1016/j.biopha.2020.110127]

19 **Hansen TB**, Jensen TI, Clausen BH, Bramsen JB, Finsen B, Damgaard CK, Kjems J. Natural RNA circles function as efficient microRNA sponges. *Nature* 2013; **495**: 384-388 [PMID: 23446346 DOI: 10.1038/nature11993]

20 **Memczak S**, Jens M, Elefsinioti A, Torti F, Krueger J, Rybak A, Maier L, Mackowiak SD, Gregersen LH, Munschauer M, Loewer A, Ziebold U, Landthaler M, Kocks C, le Noble F, Rajewsky N. Circular RNAs are a large class of animal RNAs with regulatory potency. *Nature* 2013; **495**: 333-338 [PMID: 23446348 DOI: 10.1038/nature11928]

21 **Li X**, Yang L, Chen LL. The Biogenesis, Functions, and Challenges of Circular RNAs. *Mol Cell* 2018; **71**: 428-442 [PMID: 30057200 DOI: 10.1016/j.molcel.2018.06.034]

22 **Chen LL**. The biogenesis and emerging roles of circular RNAs. *Nat Rev Mol Cell Biol* 2016; **17**: 205-211 [PMID: 26908011 DOI: 10.1038/nrm.2015.32]

23 **Cui X**, Wang J, Guo Z, Li M, Liu S, Liu H, Li W, Yin X, Tao J, Xu W. Emerging function and potential diagnostic value of circular RNAs in cancer. *Mol Cancer* 2018; **17**: 123 [PMID: 30111313 DOI: 10.1186/s12943-018-0877-y]

24 **Pan B**, Qin J, Liu X, He B, Wang X, Pan Y, Sun H, Xu T, Xu M, Chen X, Xu X, Zeng K, Sun L, Wang S. Identification of Serum Exosomal hsa-circ-0004771 as a Novel Diagnostic Biomarker of Colorectal Cancer. *Front Genet* 2019; **10**: 1096 [PMID: 31737058 DOI: 10.3389/fgene.2019.01096]

25 **Xie Y**, Li J, Li P, Li N, Zhang Y, Binang H, Zhao Y, Duan W, Chen Y, Wang Y, Du L, Wang C. RNA-Seq Profiling of Serum Exosomal Circular RNAs Reveals Circ-PNN as a Potential Biomarker for Human Colorectal Cancer. *Front Oncol* 2020; **10**: 982 [PMID: 32626660 DOI: 10.3389/fonc.2020.00982]

26 **Zeng K**, Chen X, Xu M, Liu X, Hu X, Xu T, Sun H, Pan Y, He B, Wang S. CircHIPK3 promotes colorectal cancer growth and metastasis by sponging miR-7. *Cell Death Dis* 2018; **9**: 417 [PMID: 29549306 DOI: 10.1038/s41419-018-0454-8]

27 **Chen LY**, Wang L, Ren YX, Pang Z, Liu Y, Sun XD, Tu J, Zhi Z, Qin Y, Sun LN, Li JM. The circular RNA circ-ERBIN promotes growth and metastasis of colorectal cancer by miR-125a-5p and miR-138-5p/4EBP-1 mediated cap-independent HIF-1α translation. *Mol Cancer* 2020; **19**: 164 [PMID: 33225938 DOI: 10.1186/s12943-020-01272-9]

28 **Mager LF**, Koelzer VH, Stuber R, Thoo L, Keller I, Koeck I, Langenegger M, Simillion C, Pfister SP, Faderl M, Genitsch V, Tcymbarevich I, Juillerat P, Li X, Xia Y, Karamitopoulou E, Lyck R, Zlobec I, Hapfelmeier S, Bruggmann R, McCoy KD, Macpherson AJ, Müller C, Beutler B, Krebs P. The ESRP1-GPR137 axis contributes to intestinal pathogenesis. *Elife* 2017; **6** [PMID: 28975893 DOI: 10.7554/eLife.28366]

29 **Chen L**, Zhang X, Wang S, Lin X, Xu L. Circ_0084927 Facilitates Cervical Cancer Development *via* Sponging miR-142-3p and Upregulating ARL2. *Cancer Manag Res* 2020; **12**: 9271-9283 [PMID: 33061617 DOI: 10.2147/CMAR.S263596]

30 **Qu X**, Zhu L, Song L, Liu S. circ_0084927 promotes cervical carcinogenesis by sponging miR-1179 that suppresses CDK2, a cell cycle-related gene. *Cancer Cell Int* 2020; **20**: 333 [PMID: 32699532 DOI: 10.1186/s12935-020-01417-2]

31 **Shi P**, Zhang X, Lou C, Xue Y, Guo R, Chen S. Hsa_circ_0084927 Regulates Cervical Cancer Advancement *via* Regulation of the miR-634/TPD52 Axis. *Cancer Manag Res* 2020; **12**: 9435-9448 [PMID: 33061631 DOI: 10.2147/CMAR.S272478]

32 **Wu P**, Cai J, Chen Q, Han B, Meng X, Li Y, Li Z, Wang R, Lin L, Duan C, Kang C, Jiang C. Lnc-TALC promotes O^6-methylguanine-DNA methyltransferase expression *via* regulating the c-Met pathway by competitively binding with miR-20b-3p. *Nat Commun* 2019; **10**: 2045 [PMID: 31053733 DOI: 10.1038/s41467-019-10025-2]

33 **Wang S**, Du S, Lv Y, Wang W, Zhang F. Elevated microRNA-20b-3p and reduced thioredoxin-interacting protein ameliorate diabetic retinopathy progression by suppressing the NLRP3 inflammasomes. *IUBMB Life* 2020; **72**: 1433-1448 [PMID: 32150340 DOI: 10.1002/iub.2267]

34 **Gorukmez O**, Yakut T, Gorukmez O, Sag SO, Topak A, Sahinturk S, Kanat O. Glutathione S-transferase T1, M1 and P1 Genetic Polymorphisms and Susceptibility to Colorectal Cancer in Turkey.

Asian Pac J Cancer Prev 2016; **17**: 3855-3859 [PMID: 27644629]

35 **Yu KD**, Fan L, Di GH, Yuan WT, Zheng Y, Huang W, Chen AX, Yang C, Wu J, Shen ZZ, Shao ZM. Genetic variants in GSTM3 gene within GSTM4-GSTM2-GSTM1-GSTM5-GSTM3 cluster influence breast cancer susceptibility depending on GSTM1. *Breast Cancer Res Treat* 2010; **121**: 485-496 [PMID: 19856098 DOI: 10.1007/s10549-009-0585-9]

36 **Sun C**, Gu Y, Chen G, Du Y. Bioinformatics Analysis of Stromal Molecular Signatures Associated with Breast and Prostate Cancer. *J Comput Biol* 2019; **26**: 1130-1139 [PMID: 31180245 DOI: 10.1089/cmb.2019.0045]

37 **Wang Y**, Lei L, Chi YG, Liu LB, Yang BP. A comprehensive understanding of ovarian carcinoma survival prognosis by novel biomarkers. *Eur Rev Med Pharmacol Sci* 2019; **23**: 8257-8264 [PMID: 31646556 DOI: 10.26355/eurrev_201910_19136]

38 **Sun YL**, Zhang Y, Guo YC, Yang ZH, Xu YC. A Prognostic Model Based on Six Metabolism-Related Genes in Colorectal Cancer. *Biomed Res Int* 2020; **2020**: 5974350 [PMID: 32953885 DOI: 10.1155/2020/5974350]

39 **Kap EJ**, Seibold P, Scherer D, Habermann N, Balavarca Y, Jansen L, Zucknick M, Becker N, Hoffmeister M, Ulrich A, Benner A, Ulrich CM, Burwinkel B, Brenner H, Chang-Claude J. SNPs in transporter and metabolizing genes as predictive markers for oxaliplatin treatment in colorectal cancer patients. *Int J Cancer* 2016; **138**: 2993-3001 [PMID: 26835885 DOI: 10.1002/ijc.30026]

40 **Yu D**, Liu Y, Zhou Y, Ruiz-Rodado V, Larion M, Xu G, Yang C. Triptolide suppresses IDH1-mutated malignancy *via* Nrf2-driven glutathione metabolism. *Proc Natl Acad Sci USA* 2020; **117**: 9964-9972 [PMID: 32312817 DOI: 10.1073/pnas.1913633117]

41 **Xiao Y**, Meierhofer D. Glutathione Metabolism in Renal Cell Carcinoma Progression and Implications for Therapies. *Int J Mol Sci* 2019; **20** [PMID: 31357507 DOI: 10.3390/ijms20153672]

42 **Miess H**, Dankworth B, Gouw AM, Rosenfeldt M, Schmitz W, Jiang M, Saunders B, Howell M, Downward J, Felsher DW, Peck B, Schulze A. The glutathione redox system is essential to prevent ferroptosis caused by impaired lipid metabolism in clear cell renal cell carcinoma. *Oncogene* 2018; **37**: 5435-5450 [PMID: 29872221 DOI: 10.1038/s41388-018-0315-z]

43 **Duan S**, Huang W, Liu X, Chen N, Xu Q, Hu Y, Song W, Zhou J. IMPDH2 promotes colorectal cancer progression through activation of the PI3K/AKT/mTOR and PI3K/AKT/FOXO1 signaling pathways. *J Exp Clin Cancer Res* 2018; **37**: 304 [PMID: 30518405 DOI: 10.1186/s13046-018-0980-3]

44 **Weng ML**, Chen WK, Chen XY, Lu H, Sun ZR, Yu Q, Sun PF, Xu YJ, Zhu MM, Jiang N, Zhang J, Zhang JP, Song YL, Ma D, Zhang XP, Miao CH. Fasting inhibits aerobic glycolysis and proliferation in colorectal cancer *via* the Fdft1-mediated AKT/mTOR/HIF1α pathway suppression. *Nat Commun* 2020; **11**: 1869 [PMID: 32313017 DOI: 10.1038/s41467-020-15795-8]

45 **Tan X**, Zhang Z, Yao H, Shen L. Tim-4 promotes the growth of colorectal cancer by activating angiogenesis and recruiting tumor-associated macrophages *via* the PI3K/AKT/mTOR signaling pathway. *Cancer Lett* 2018; **436**: 119-128 [PMID: 30118845 DOI: 10.1016/j.canlet.2018.08.012]

World Journal of Gastroenterology

Submit a Manuscript: https://www.f6publishing.com

World J Gastroenterol 2021 September 28; 27(36): 6079-6092

DOI: 10.3748/wjg.v27.i36.6079

ISSN 1007-9327 (print) ISSN 2219-2840 (online)

ORIGINAL ARTICLE

Basic Study

Exosomal microRNA-588 from M2 polarized macrophages contributes to cisplatin resistance of gastric cancer cells

Hai-Yan Cui, Jian-Sheng Rong, Ju Chen, Jie Guo, Jia-Qin Zhu, Mei Ruan, Rong-Rong Zuo, Shuang-Shuang Zhang, Jun-Mei Qi, Bao-Hua Zhang

ORCID number: Hai-Yan Cui 0000-0001-7701-2999; Jian-Sheng Rong 0000-0002-4408-3325; Ju Chen 0000-0002-8036-7835; Jie Guo 0000-0002-5245-2856; Jia-Qin Zhu 0000-0002-3829-2956; Mei Ruan 0000-0001-6700-0687; Rong-Rong Zuo 0000-0001-6975-6015; Shuang-Shuang Zhang 0000-0002-3322-433X; Jun-Mei Qi 0000-0001-9552-8200; Bao-Hua Zhang 0000-0003-2789-6348.

Author contributions: Cui HY, Rong JS, and Chen J designed the study; Guo J, Zhu JQ, and Ruan M performed the experiments; Zuo RR and Zhang SS collected and analysed the data; Qi JM and Zhang BH wrote the manuscript.

Institutional review board statement: This study was reviewed and approved by the Zibo Central Hospital.

Institutional animal care and use committee statement: All animal experiments in this study were approved by the Zibo Central Hospital.

Conflict-of-interest statement: The authors declare no conflict of interest for this manuscript.

Data sharing statement: No additional data are available.

ARRIVE guidelines statement: The

Hai-Yan Cui, Rong-Rong Zuo, Shuang-Shuang Zhang, Jun-Mei Qi, Department of Pathology, The Fourth People's Hospital of Zibo City, Zibo 255000, Shandong Province, China

Jian-Sheng Rong, Bao-Hua Zhang, Department of Pathology, Zibo Central Hospital, Zibo 255036, Shandong Province, China

Ju Chen, Department of Ultrasound Medicine, Zibo Central Hospital, Zibo 255036, Shandong Province, China

Jie Guo, Department of Health, The Fourth People's Hospital of Zibo City, Zibo 255000, Shandong Province, China

Jia-Qin Zhu, Department of Gastroenterology, The Fourth People's Hospital of Zibo City, Zibo 255000, Shandong Province, China

Mei Ruan, Department of Oncology, The Fourth People's Hospital of Zibo City, Zibo 255000, Shandong Province, China

Corresponding author: Bao-Hua Zhang, MSc, Chief Physician, Department of Pathology, Zibo Central Hospital, No. 54 Gongqingtuan West Road, Zhangdian District, Zibo 255036, Shandong Province, China. zhangbaohua314@163.com

Abstract

BACKGROUND

Gastric cancer is a prevalent malignant cancer with a high incidence and significantly affects the health of modern people globally. Cisplatin (DDP) is one of the most common and effective chemotherapies for patients with gastric cancer, but DDP resistance remains a severe clinical challenge.

AIM

To explore the function of M2 polarized macrophages-derived exosomal microRNA (miR)-588 in the modulation of DDP resistance of gastric cancer cells.

METHODS

M2 polarized macrophages were isolated and identified by specific markers using flow cytometry analysis. The exosomes from M2 macrophages were identified by transmission electron microscopy and related markers. The uptake of the PKH67-

labelled M2 macrophages-derived exosomes was detected in SGC7901 cells. The function and mechanism of exosomal miR-588 from M2 macrophages in the modulation of DDP resistance of gastric cancer cells was analyzed by CCK-8 assay, apoptosis analysis, colony formation assay, Western blot analysis, qPCR analysis, and luciferase reporter assay in SGC7901 and SGC7901/DDP cells, and by tumorigenicity analysis in nude mice.

RESULTS

M2 polarized macrophages were isolated from mouse bone marrow stimulated with interleukin (IL)-13 and IL-4. Co-cultivation of gastric cancer cells with M2 polarized macrophages promoted DDP resistance. M2 polarized macrophages-derived exosomes could transfer in gastric cancer cells to enhance DDP resistance. Exosomal miR-588 from M2 macrophages contributed to DDP resistance of gastric cancer cells. miR-588 promoted DDP-resistant gastric cancer cell growth *in vivo*. miR-588 was able to target cylindromatosis (CYLD) in gastric cancer cells. The depletion of CYLD reversed miR-588 inhibition-regulated cell proliferation and apoptosis of gastric cancer cells exposed to DDP.

CONCLUSION

In conclusion, we uncovered that exosomal miR-588 from M2 macrophages contributes to DDP resistance of gastric cancer cells by partly targeting CYLD. miR-588 may be applied as a potential therapeutic target for the treatment of gastric cancer.

Key Words: Gastric cancer; Cisplatin resistance; M2 polarized macrophages; Exosome; miR-588; Cylindromatosis

Core Tip: In this study, we uncovered that exosomal miR-588 from M2 macrophages contributes to cisplatin resistance of gastric cancer cells by partly targeting cylindromatosis. miR-588 may be applied as a potential therapeutic target for the treatment of gastric cancer.

Citation: Cui HY, Rong JS, Chen J, Guo J, Zhu JQ, Ruan M, Zuo RR, Zhang SS, Qi JM, Zhang BH. Exosomal microRNA-588 from M2 polarized macrophages contributes to cisplatin resistance of gastric cancer cells. *World J Gastroenterol* 2021; 27(36): 6079-6092
URL: https://www.wjgnet.com/1007-9327/full/v27/i36/6079.htm
DOI: https://dx.doi.org/10.3748/wjg.v27.i36.6079

INTRODUCTION

Gastric cancer belongs to the most common malignant tumors and is the third cause of cancer-related death throughout the world[1]. Patients diagnosed with gastric cancer are usually at an advanced or late stage, which makes chemotherapy a prevalent strategy over the past decades[2]. Among the clinical chemotherapy agents, cisplatin (DDP) is capable of disrupting DNA repairment, which further causes DNA damage and apoptosis of cancer cells[3]. However, the developed therapeutic resistance makes the chemotherapy far less satisfactory in clinical application, which makes it urgent to decipher the mechanisms underlying this chemoresistance[4].

Tumor-associated macrophage (TAMs) are macrophages that participate in the tumor microenvironment function, and play a critical role in tumor development, including growth, metastasis, angiogenesis, and therapeutic resistance[5]. Recent studies have proposed that TAMs were capable of communicating with neighboring or distant cells *via* secreting exosomes[6,7]. Exosomes are membrane-derived transporting vesicles secreted by almost all types of cells, usually defined with a diameter ranging from 40 nm to 100 nm[8]. It is widely recognized that exosomes act as a communicator between cells through transporting various cargos such as mRNA, lipid, proteins, as well as microRNAs (miRNAs), and hence are related to various

authors have read the ARRIVE guidelines, and the manuscript was prepared and revised according to the ARRIVE guidelines.

Manuscript source: Unsolicited manuscript

Specialty type: Gastroenterology and hepatology

Country/Territory of origin: China

Peer-review report's scientific quality classification
Grade A (Excellent): 0
Grade B (Very good): B
Grade C (Good): C, C
Grade D (Fair): 0
Grade E (Poor): 0

Received: April 23, 2021
Peer-review started: April 23, 2021
First decision: May 27, 2021
Revised: June 7, 2021
Accepted: August 11, 2021
Article in press: August 11, 2021
Published online: September 28, 2021

P-Reviewer: Tanabe S, Yashiro M
S-Editor: Wu YXJ
L-Editor: Wang TQ
P-Editor: Li JH

functions of targeted cells[9,10]. miRNAs are endogenous short noncoding RNAs that play pivotal roles in the regulation of cancer development by directly targeting mRNA [11]. Besides, miRNAs are recently proposed to be involved in drug resistance of cancer cells[12-14]. Among which, miR-588 is upregulated in human prostate cancer with prognostic significance and notably facilitates the proliferation of prostate cancer cells[15]. Importantly, it has been reported that miR-588 serves as a promising prognostic marker for gastric cancer[16]. However, the role of miR-588 in DDP resistance of gastric cancer cells is still unknown. Accordingly, we were interested in the correlation of TAM-derived exosomes with miR-588 and its role in the modulation of DDP resistance of gastric cancer cells.

Cylindromatosis (CYLD) is a representative deubiquitinating enzyme that could counteract the E3 ubiquitin ligases-mediated protein ubiquitination[17]. It plays an important role in multiple cellular processes during tumorigenesis, such as cell apoptosis, cell cycle, cell migration, and DNA damage[17]. Mechanistically, CYLD is profoundly related to multiple critical signaling transduction pathways, especially the NF-κB signaling pathway, and acts as a tumor suppressor[18]. It has been extensively demonstrated that CYLD could negatively regulate the activation of NF-kB through deubiquitinating its upstream K63, which further inhibits the activation of NF-kB-related pro-survival signaling and promotes caspase-8-induced cell apoptosis[19]. It is noteworthy that recent studies also proposed that loss of CYLD could trigger DDP resistance in several cancers, including gastric cancer and oral squamous cell carcinoma[20,21].

In this study, we adopted a M2-polarized macrophage model to mimic TAM function, and testified that TAM-derived exosomes conferred DDP resistance in gastric cancer. We showed that the exosomes secreted by TAM contained miR-588, which directly interacts with the 3′ untranslated region of *CYLD* to suppress its expression and its tumor-suppressing function. This process subsequently hindered cell apoptosis and promoted the proliferation as well as DDP resistance of gastric cancer cells. Our study illustrated the connection between TAM and DDP resistance of gastric cancer cells, providing a potential target for gastric cancer therapy.

MATERIALS AND METHODS

Cell culture and treatment

Gastric cancer cell line SGC7901, purchased from ATCC, was maintained in DMEM containing 10% fetal bovine serum (FBS) and 1% penicillin and streptomycin (Sigma, United States) at 37 °C with 5% CO2. DDP-resistant SGC7901/DDP cells were developed from the parental SGC7901 cells that were subjected to persistent gradient exposure to DDP for about 12 mo, through increasing DDP concentration from 0.05 μg/mL until the cells acquired resistance to 1 μg/mL[22]. Mouse bone marrow cells (MBMCs) were purchased from Chinese Academy of Sciences Cell Bank of Type Culture Collection, and cultured in a normal DMEM:F12 medium containing 10% FBS and macrophage colony-stimulating factor (Sigma). To achieve polarization to M2, MBMCs were stimulated with interleukin (IL)-4 and IL-13 (30 ng/mL, Sigma) for 2 d. A transwell chamber assay was adopted to perform co-culture experiments, in which polarized macrophages were placed in the upper tanswell chamber and gastric cancer cells were cultured in the bottom well.

Flow cytometry

The M2 polarization was determined by staining for critical biomarkers and detection by flow cytometry. Briefly, cells were collected and incubated with fluorescence probe-conjugated antibodies against CD86, CD68, CD11b, CD80, CD206, CD163, and F4/80 at 4 °C for 30 min. Next, the cells were washed with PBS and analyzed by flow cytometry (BD Biosciences, United States). The antibodies used in this experiment were purchased from Abcam (United States).

For cell apoptosis, cells were processed with an apoptosis detection kit (Solarbio, China). Briefly, cells were collected and suspended in binding buffer, followed by staining with PI and Annexin V at room temperature for 20 min in dark. Next, the stained cells were collected and resuspended in binding buffer for analysis by flow cytometry.

Exosome isolation and analysis

Macrophages were cultured in medium containing 10% exosome-free FBS for 48 h. The medium was collected for extraction of exosomes with an exoEasy Maxi Kit (QIAGEN,

Germany) following the manufacturer's instruction.

To determine exosome internalization, the exosomes were labeled with PKH67 (Sigma) according to the manufacturer's protocol. Subsequently, the labeled exosomes were used to incubate with cells in each experiment, and observed using a confocal microscope (Carl Zeiss, Germany).

Transmission electron microscopy

The images of exosomes were captured by transmission electron microscopy (TEM). In brief, the samples were dropped on cleaned cooper grids coated with carbon, and washed with Milli-Q water to remove extra samples, followed by 1-min staining with uranyl acetate and air dry. Then, the samples were observed and pictured with a transmission electron microscope (Carl Zeiss).

Cell transfection

SGC7901 cells were placed in 6-well plate at a density of 3×10^5 cells per well. After incubation for 12 h, miR-588 mimic (RiboBio, China), miR-588 inhibitor (RiboBio, China), or negative control (RiboBio, China) was mixed with lipofectamine 200 (Invitrogen, United States) in Opti-MEM medium (Sigma, United States) for 20 min and added into cell culture medium. Eight hours after transfection, the medium was replaced with fresh DMEM containing 10% FBS to incubate for another 24 h. Then, the cells were used for further experiments.

Cell viability and colony formation assay

Cell viability was determined with a CCK-8 kit (Beyotime, China). MFC cells and SGC7901 cells were seeded in 96-well plates at a density of 3×10^3 cells/well and processed accordingly. Twenty-four hours after incubation, the CCK-8 reagent was added into each well. The absorbance values were detected at 450 nm at 24 h, 48 h, and 72 h, respectively.

For colony formation experiment, SGC7901 cells transfected with miR-588 inhibitor or negative control were placed in a 6-well plate (1000 cells per well), and incubated in complete medium for 2 wk to form visible colonies. Subsequently, the colonies were washed, stained with crystal violet, and captured with a microscope (Carl Zeiss).

RNA extraction and quantitative real-time PCR

Total RNA was extracted with TRIzol reagent (Takara, Japan) and reversely transcribed to cDNA with an EasyScript Reverse Transcriptase kit (TransGen, China). The quantification of cDNA was performed by using a TransStart Green qPCR SuperMix kit (TransGen), and PCR was performed on a Real-Time PCR System (BD bioscience). For detection of miR-588, the extracted RNA was processed with a poly(A) tailing kit (Invitrogen) before reverse transcription. For normalization of mRNA and miRNA, *GAPDH* and *U6* were used as the internal controls, respectively. The quantification of cDNA was analyzed by the $2^{-\Delta\Delta Ct}$ method. The sequences of primers are as follows: *GAPDH* sense, 5'- ACAACTTTGGTATCGTGGAAGG-3' and antisense, 5'-GCCATCACGCCACAGTTTC-3'; *U6* sense, 5'-AGTAAGCCCTTGCTGTCAGTG-3' and antisense, 5'-CCTGGGTCTGATAATGCTGGG-3'; *Arg1* sense, 5'-GTGGAAACT-TGCATGGACAAC-3' and antisense, 5'-AATCCTGGCACATCGGGAATC-3'; *IL-10* sense, 5'-GTACCACAGCAATGGCTACC-3 and antisense, 5'-TGTTGGTGACG-GTCCAGTTG-3'; *TGF-β* sense, 5'-CTAATGGTGGAAACCCACAACG-3' and antisense, 5'-TATCGCCAGGAATTGTTGCTG-3'; miR-588, 5'-CCGCTATTGCACAT-TACTAAGTTGCA-3

Western blot analysis

SGC7901 cells were placed in a 6-well plate at a density of 3×10^5 cells per well and transfected with miR-588 inhibitor. Total protein was extracted by using ice-cold RIPA buffer, separated by SDS-PAGE, and transferred to a nitrocellulose membrane. The membrane was then blocked by 5% non-fat milk at room temperature for 1 h, and incubated with specific primary antibodies against CD63 (1:1000, Abcam), CD9 (1:1000, Abcam), CD81 (1:1000, Abcam), HSP70 (1:500, Abcam), GAPDH (1:1000, Proteintech), Bax (1:1000, CST), pro-caspase-3 (1:2000, CST), cleaved caspase-3 (1:1000, CST), pro-caspase-9 (1:1000, CST), cleaved caspase-9 (1:1000, CST), CYLD (1:1000, Proteintech), and β-actin (1:2000, Proteintech) at 4 °C overnight. Next day, the blots were washed and incubated with secondary antibodies at room temperature for 2 h. The blots were visualized by using an ECL reagent and a gel imaging system (BD Bioscience).

Xenograft tumor model

C57 nude mice aged 5 wk were purchased from Shanghai Laboratory Animal Center of China. SGC7901 cells were transfected with miR-588 inhibitor or negative control, and suspended in saline at a density of 1×10^7 cells/mL. A total of 200 μL of SGC7901 cell suspension was subcutaneously injected to the left back of mice. A week after tumor cell inoculation, the mice were intraperitoneally injected with 15 mg/kg DDP. The mice were euthanized at day 30, and the tumors were isolated, weighted, and processed for subsequent analysis. Tumor size was measured every 5 d and calculated using the following formula: $\text{Width}^2 \times \text{length}/2$.

Statistical analysis

All experiments in this study were performed at least three times independently. All data are presented as the mean ± SD and analyzed with GraphPad Prism 6.0 software. The statistical difference between two groups or multiples groups was analyzed by Student's *t*-test or one-way ANOVA, and was considered significant at $P < 0.05$.

RESULTS

M2 polarized macrophages-derived exosomes can transfer in gastric cancer cells to enhance DDP resistance

To evaluate the effect of M2 polarized macrophages on DDP resistance of gastric cancer cells, M2 polarized macrophages were isolated from murine bone marrow induced with IL-13 and IL-4 and were identified by the M2 specific marker CD206 (Figure 1A). Meanwhile, we found that the expression of M1 polarized marker iNOS was not chanced but the M2 markers, such as Arg1, IL-10, and TGF-β, were enhanced in M2 polarized macrophages compared with inactivated macrophages (Figure 1B). Then, the exosomes were isolated from M2 polarized macrophages and analyzed by TEM and identified by the expression of CD63, CD9, CD81, and HSP70 (Figure 1C and D). Moreover, the delivery of PKH67-labelled exosomes from M2 polarized macrophages was found in SGC7901 cells (Figure 1E). Significantly, M2 macrophages-derived conditioned medium and exosomes enhanced the cell survival of SGC7901 cells exposed to DDP (Figure 1F). The exosomes from M2 polarized macrophages repressed DDP-treated SGC7901 cell apoptosis (Figure 1G).

Co-culture of gastric cancer cells with M2 polarized macrophages promotes DDP resistance

Next, we found that DDP treatment reduced the proliferation of SGC7901 cells in a time-dependent manner (Figure 2A). The co-culture of inactivated macrophages inhibited apoptosis of DDP-treated SGC7901 cells, while the co-culture of M2 polarized macrophages further reduced the cell apoptosis (Figure 2B and C).

Exosomal miR-588 from M2 macrophages contributes to DDP resistance of gastric cancer cells

We then observed that the expression of miR-588 was elevated in the exosomes from M2 macrophages compared with inactivated macrophages (Figure 3A). The miR-588 expression was enhanced in macrophages relative to SGC7901 cells, especially in the M2 polarized macrophages (Figure 3B). Meanwhile, the expression of miR-588 was increased in the DDP-resistant SGC7901 cells co-cultured with M2 macrophages or exosomes from M2 macrophages (Figure 3C). Moreover, we found that the inhibition of miR-588 by inhibitor repressed colony formation of DDP-resistant SGC7901 cells (Figure 3D). The repression of miR-588 induced DDP-resistant SGC7901 cell apoptosis (Figure 3E). The expression of Bax, cleaved caspase-3, and cleaved caspase-9 was enhanced by miR-588 inhibitor in DDP-resistant SGC7901 cells (Figure 3F). Moreover, the IC_{50} of DDP in the inhibition of SGC7901 cell viability was inhibited by miR-588 inhibitor (Figure 4A). Treatment with DDP induced apoptosis of SGC7901 cells, in which miR-588 inhibitor reinforced this effect (Figure 4B and C).

miR-588 can target CYLD in gastric cancer cells

We then identified the binding site for miR-588 in *CYLD* in the bioinformatic analysis (Figure 5A). The luciferase activity and mRNA expression of *CYLD* were significantly repressed by miR-588 mimic in the DDP-resistant SGC7901 cells (Figure 5B and C). Similarly, the protein levels of CYLD were inhibited by miR-588 mimic in DDP-

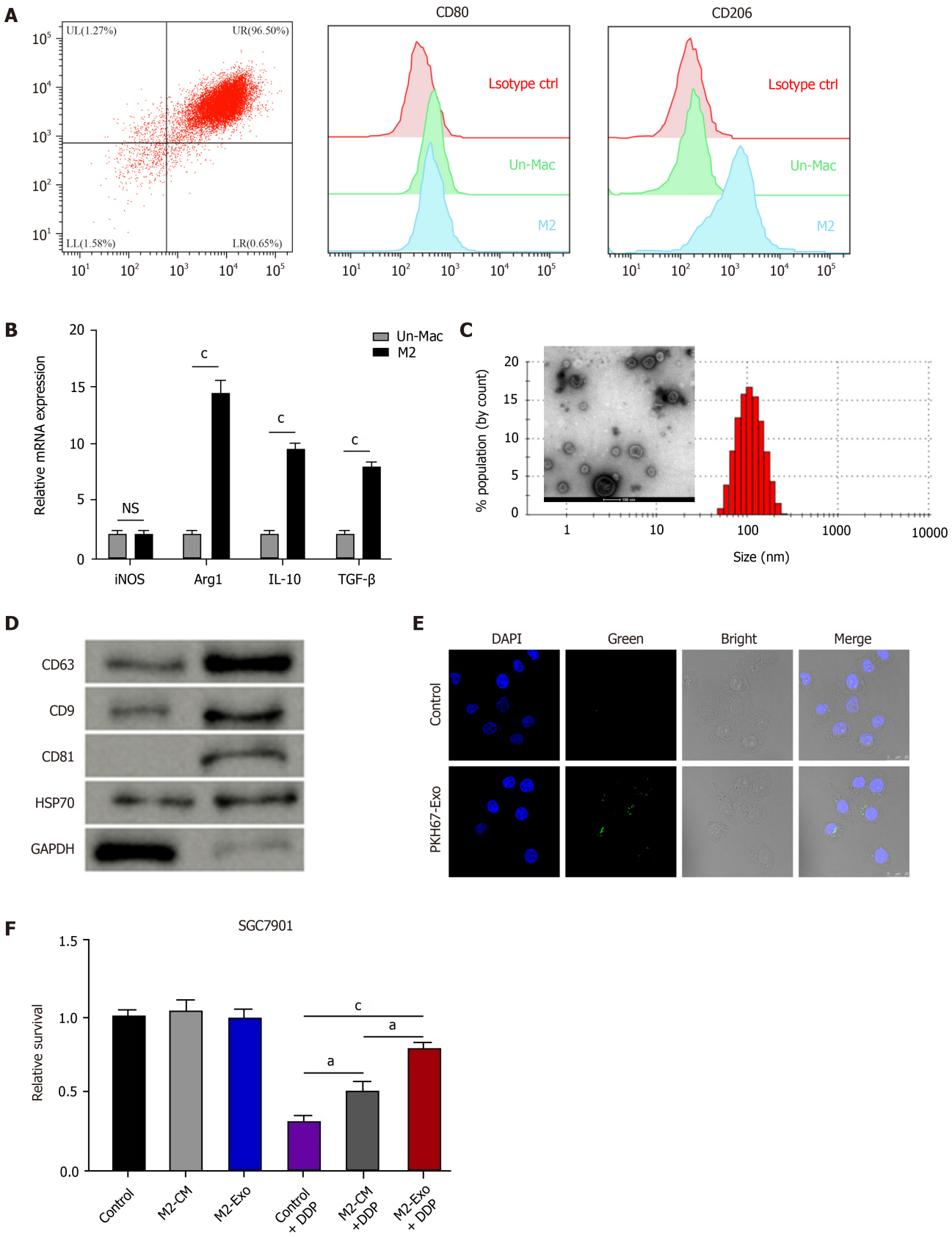
A
UL(1.27%)
UR(96.50%)
LL(1.58%)
LR(0.65%)
CD80
CD206
Lsotype ctrl
Un-Mac
M2
B
Relative mRNA expression
Un-Mac
M2
NS
c
iNOS
Arg1
IL-10
TGF-β
C
% population (by count)
Size (nm)
D
CD63
CD9
CD81
HSP70
GAPDH
E
DAPI
Green
Bright
Merge
Control
PKH67-Exo
F
SGC7901
Relative survival
a
Control
M2-CM
M2-Exo
Control + DDP
M2-CM +DDP
M2-Exo + DDP

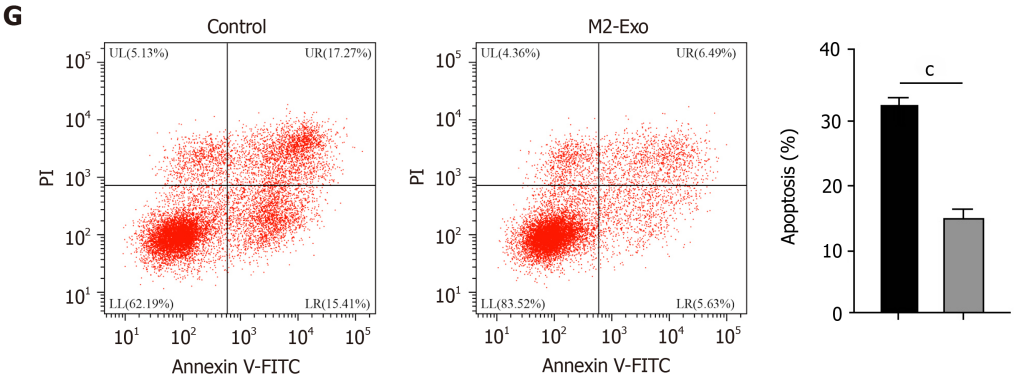

Figure 1 M2 polarized macrophages-derived exosomes can transfer in gastric cancer cells to enhance cisplatin resistance. A and B: Flow cytometry for identifying the M2 polarized macrophages isolated from murine bone marrow induced with interleukin (IL)-13 and IL-4. The M2 specific marker CD206 was identified. Un-Mac represents inactivated macrophages and M2 represents macrophages activated by IL-13 and IL-4. The mRNA expression of *iNOS*, *Arg1*, *IL-10*, and *TGF-β* was detected by qPCR in Un-Mac and M2 macrophages; C: Identification of exosomes from M2 macrophages by transmission electron microscopy; D: Detection of expression of CD63, CD9, CD81, HSP70, and GAPDH by Western blot analysis; E: Detection of uptake of the PKH67-labelled M2 exosomes (M2-Exo) in SGC7901 cells; F: Analysis of cell viability by CCK-8 assay. M2 macrophages-derived conditioned medium and M2-Exo were used to treat SGC7901 cells exposed to cisplatin (DDP) for 48 h; G: Analysis of cell apoptosis by flow cytometry SGC7901 cells were co-treated with DDP and M2-Exo. Data shown are the mean ± SD. ^{a}P <0.05; ^{c}P < 0.001. DDP: Cisplatin; Un-Mac: Inactivated macrophages; M2-Exo: M2 exosomes.

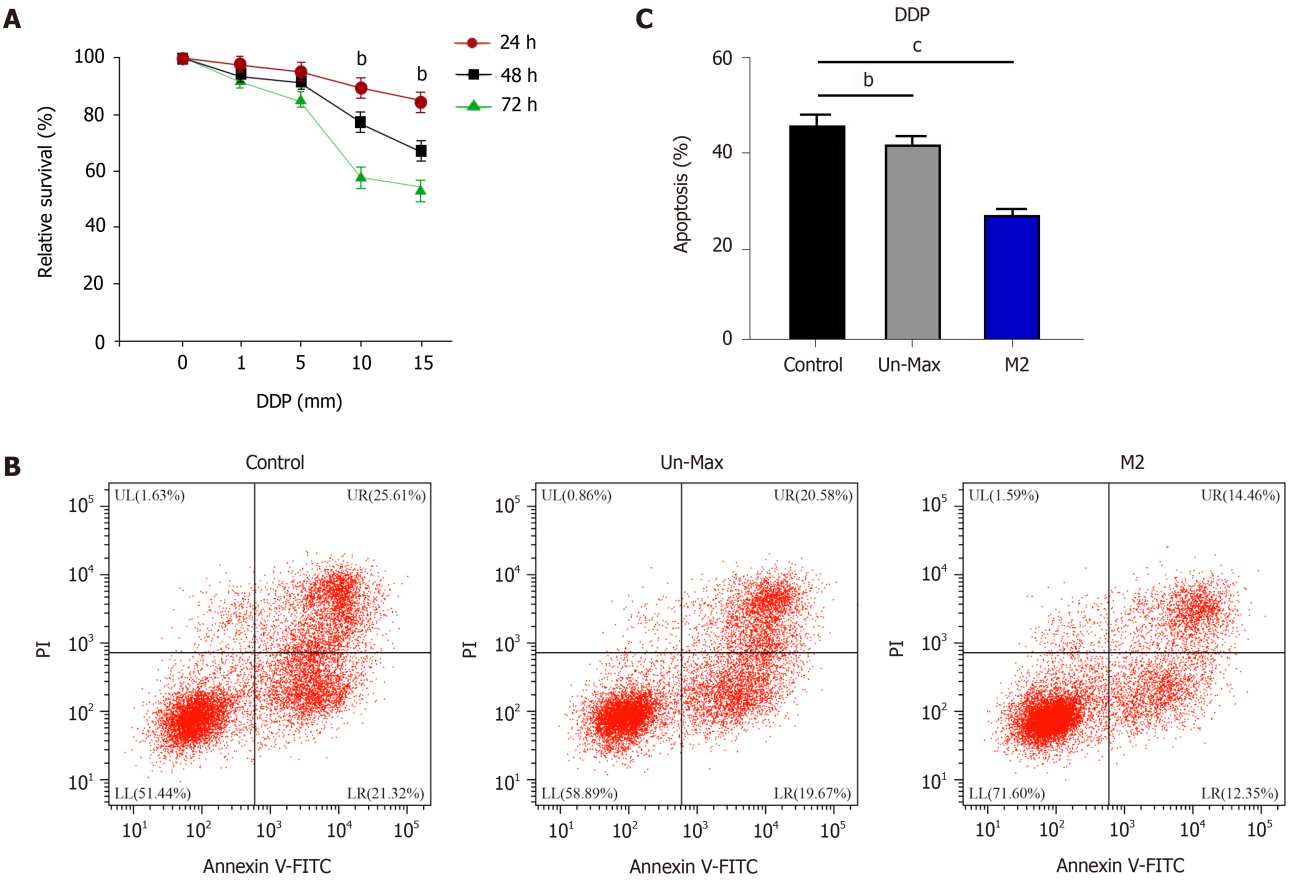

Figure 2 Co-culture of gastric cancer cells with M2 polarized macrophages promotes cisplatin resistance. A: Detection of cell viability by CCK-8 assay in SGC7901 cells treated with cisplatin (DDP); B and C: Analysis of cell apoptosis by flow cytometry in SGC7901 cells co-cultured with inactivated macrophages and M2 macrophages exposed to DDP for 48 h. Data shown are the mean ± SD. ^{b}P < 0.01; ^{c}P <0.001. DDP: Cisplatin.

resistant SGC7901 cells (Figure 5D).

miR-588/CYLD axis regulates DDP resistance of gastric cancer cells

Next, we evaluated the effect of miR-588/CYLD axis on DDP resistance of gastric cancer cells. Our data showed that treatment with DDP inhibited SGC7901 cell proliferation; miR-588 inhibitor enhanced the function of DDP, while the depletion of CYLD

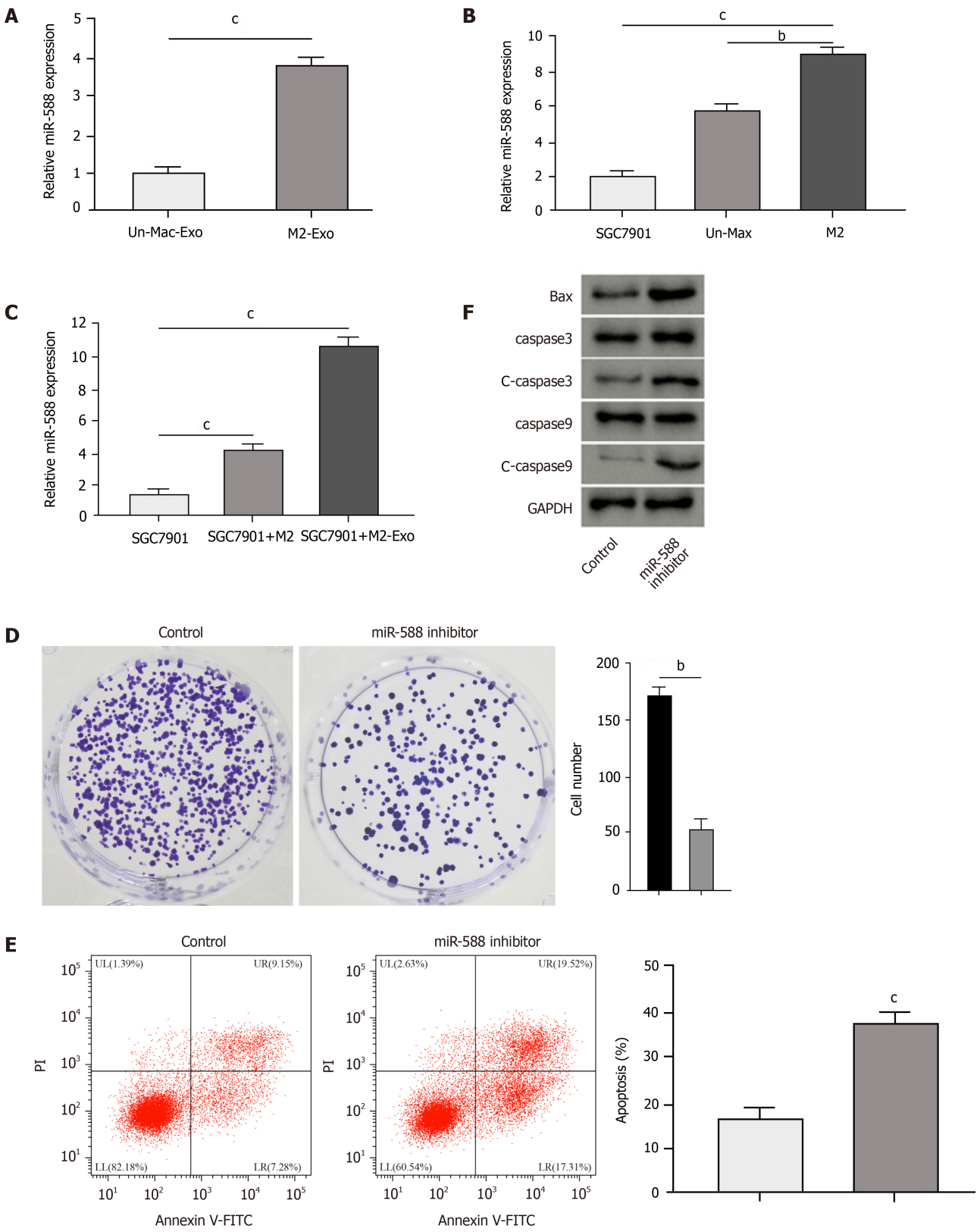

Figure 3 Exosomal miR-588 from M2 macrophages contributes to cisplatin resistance of gastric cancer cells. A: Detection of expression of miR-588 by qPCR in the exosomes from M2 macrophages and inactivated macrophages; B: Detection of expression of miR-588 by qPCR in cisplatin (DDP)-resistant SGC7901 cells, M2 macrophages, and inactivated macrophages; C: Detection of expression of miR-588 by qPCR in DDP-resistant SGC7901 cells co-cultured with M2 macrophages or exosomes from M2 macrophages; D-F: Analysis of cell proliferation by colony formation assay (D), cell apoptosis by flow cytometry (E), and expression of Bax, capase-3, caspase-9, cleaved caspase-3 (c-caspase-3), and cleaved caspase 9 (c-caspase-9) by Western blot analysis (F) in DDP-resistant SGC7901 cells treated with miR-588 inhibitor. Data shown are the mean ± SD, $^{b}P < 0.01$; $^{c}P < 0.001$.

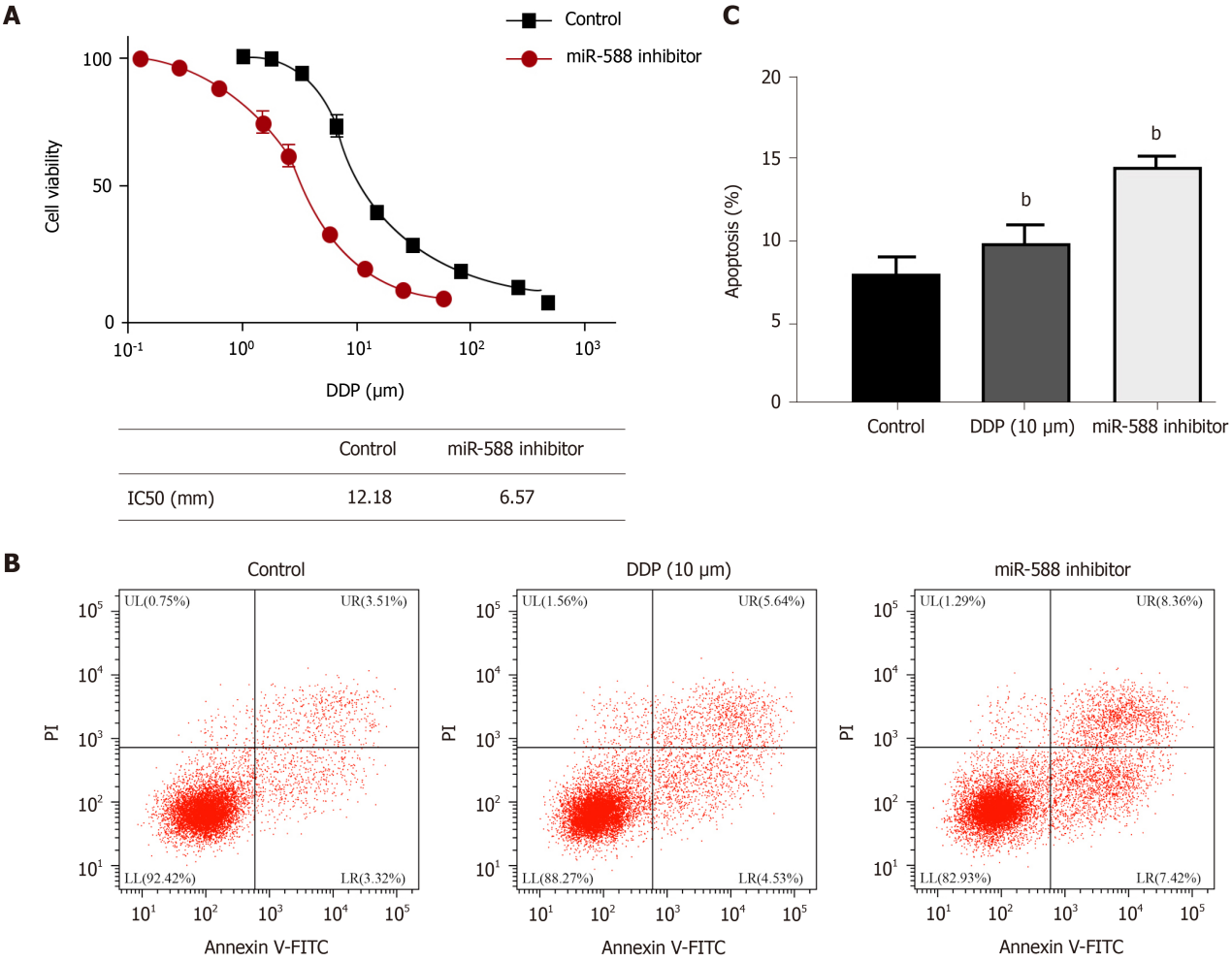

	Control	miR-588 inhibitor
IC50 (mm)	12.18	6.57

Figure 4 miR-588 contributes to cisplatin resistance of gastric cancer cells. A: Detection of cell viability by CCK-8 assay in SGC7901 cells treated with miR-588 inhibitor and exposed to cisplatin (DDP) at the indicated doses; B and C: Detection of cell apoptosis by flow cytometry in DDP-resistant SGC7901 cells co-treated with DDP and miR-588 inhibitor. Data shown are the mean ± SD, $^{b}P < 0.01$. DDP: Cisplatin.

by siRNA reversed the effect of miR-588 inhibition (Figure 6A). Moreover, treatment with DDP induced apoptosis of SGC7901 cells; miR-588 inhibitor further enhanced the cell apoptosis, while CYLD knockdown reversed the effect of miR-588 inhibitor (Figure 6B). Moreover, tumorigenicity analysis in nude mice demonstrated that miR-588 inhibitor suppressed the tumor growth *in vivo* (Figure 7A-D). Meanwhile, we validated that the overexpression of CYLD or treatment with miR-588 inhibitor repressed the tumor growth in nude mice, while the depletion of CYLD rescued miR-588 inhibitor-reduced tumor growth in the model (Figure 7E and F).

DISCUSSION

Gastric cancer is a common malignant cancer with a high death rate and limited therapeutic strategies. DDP is widely applied in the treatment of gastric cancer patients with significant effectiveness, but DDP resistance remains a critical clinical issue. In this study, we identified that M2 polarized macrophages-derived exosomal miR-588 contributes to DDP resistance of gastric cancer cells.

Previous investigations have shown that M2 polarized macrophages-derived exosomes are involved in the modulation of cancer development. It has been reported that tumor-related macrophages-derived exosomes contribute to gastric cancer cell invasion *via* apolipoprotein E[23]. Macrophage-derived exosomal miR-21 regulates DDP resistance of gastric cancer cells[24]. M2 macrophages-derived exosomes promote metastasis of hepatocarcinoma by delivering αMβ2 integrin[25]. These studies have shown the critical function of macrophages-derived exosomal miRNAs in the modulation of cancer development. Meanwhile, miR-588 is a widely reported cancer regulator in previous studies. It has been found that miR-588 is enhanced in prostate

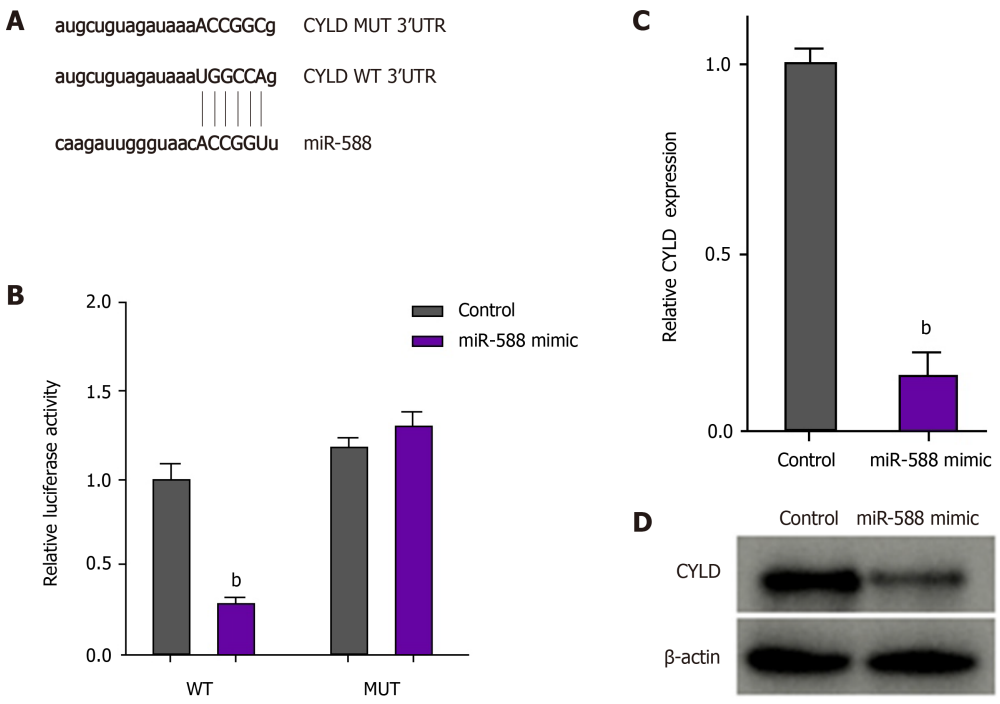

Figure 5 miR-588 can target cylindromatosis in gastric cancer cells. A: The binding site of miR-588 and cylindromatosis (CYLD) was predicted in TargetScan database; B-D: After cisplatin (DDP)-resistant SGC7901 cells were treated with miR-588 mimic, the luciferase activity of CYLD was measured by luciferase reporter assays (B); the expression of CYLD was determined by qPCR (C); and the expression of CYLD was measured by Western blot analysis (D). Data shown are the mean ± SD. $^{b}P < 0.01$. CYLD: Cylindromatosis.

cancer and is correlated with a poor prognosis[15]. miR-588 modulates epithelial-mesenchymal transition, migration, and invasion of gastric cancer cells by targeting EIF5A2 signaling[26]. The PICSAR/miR-588/EIF6 axis contributes to the regulation of hepatocellular carcinoma progression by targeting AKT/mTOR signaling[27]. Moreover, it has been reported that miR-588 serves as a prognosis biomarker for gastric cancer[16]. In previous reports, miR-588 has not been prominently implicated in gastric cancer through interaction between tumor and the surrounding microenvironment. We were interested in the function of M2 macrophages-derived exosomes in cancer development and noticed the potential function of miR-588 in gastric cancer. Therefore, we explored the correlation of M2 macrophage-derived exosomes with miR-588 and their function in gastric cancer. Our data showed that co-cultivation of gastric cancer cells with M2 polarized macrophages promoted DDP resistance. M2 polarized macrophages-derived exosomes could transfer in gastric cancer cells to enhance DDP resistance. Exosomal miR-588 from M2 macrophages contributed to DDP resistance of gastric cancer cells. miR-588 promoted DDP-resistant gastric cancer cell growth *in vivo*. These data not only provide new evidence of the critical function of M2 polarized macrophages-derived exosomes in regulating cancer progression, but also indicate the innovative role of miR-588 in gastric cancer. The correlation of M2 polarized macrophages-derived exosomal miR-588 and miR-588 in the cancer cells in regulating cancer development is an interesting scientific issue, which is needed to explore in the future. Besides, the function of other pivotal miRNAs that have been described as crucial regulators in exosomes-mediated cellular communication should be explored by more investigations. Meanwhile, the mechanisms of miR-588 transfer from macrophage to gastric cancer cells remain unclear. According to previous studies, the communications between macrophages and gastric cancer cells can be mediated by exosomes, which can engulf local tissues immediately or swarm into body fluid to affect distant target organs through endocytosis[7,24,28]. The mechanisms of miR-588 transfer from macrophage to gastric cancer cells should be confirmed by more complicated investigations in future.

Moreover, it has been reported that inhibition of CYLD enhances IFN-γ-regulated PD-L1 expression in thymic epithelial cancer[29]. LINC01260 serves as a tumor inhibitor by regulating the miR-562/CYLD axis in lung cancer[30]. CYLD enhances nasopharyngeal carcinoma cells apoptosis by modulating NDRG1[31]. MiR-454 contributes to oxaliplatin resistance and cell proliferation by targeting CYLD in gastric cancer[32]. These reports have identified the tumor suppressive function of CYLD in

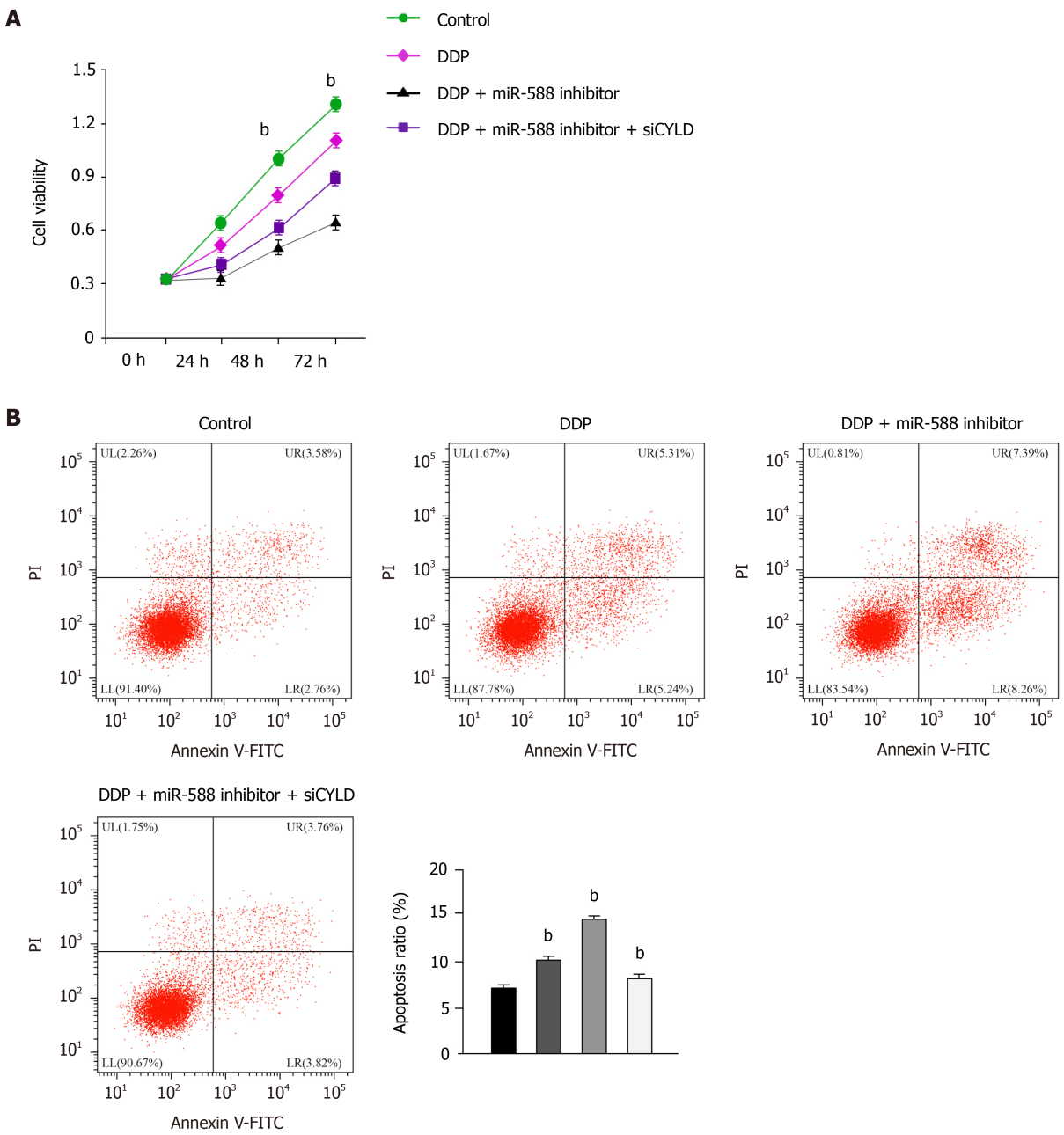

Figure 6 miR-588/cylindromatosis axis regulates cisplatin resistance of gastric cancer cells. A: Cell viability detected by CCK-8 assay; B: Cell apoptosis analyzed by flow cytometry. The SGC7901 cells were treated with cisplatin (DDP), or co-treated with DDP and miR-588 inhibitor with or without cylindromatosis siRNA. Data shown are the mean ± SD. $^{b}P < 0.01$. DDP: Cisplatin; CYLD: Cylindromatosis.

cancer progression. Our mechanical investigation showed that miR-588 targeted CYLD in gastric cancer cells and miR-588/CYLD axis contributed to the progression of gastric cancer. It presents a crucial mechanism underlying miR-588-mediated cancer development. CYLD may not be the only downstream factor underlying miR-588-mediatde tumorigenesis. Other regulators in miR-588-modulated cancer pathogenesis and their crosstalk may be investigated further in future. Targeting exosomal miR-588 from M2 macrophages may be a promising therapeutic strategy for gastric cancer and the clinical translation should be explored in future investigations.

CONCLUSION

In conclusion, we uncovered that exosomal miR-588 from M2 macrophages contributes to DDP resistance of gastric cancer cells by partly targeting CYLD. miR-588 may be applied as a potential therapeutic target for the treatment of gastric cancer.

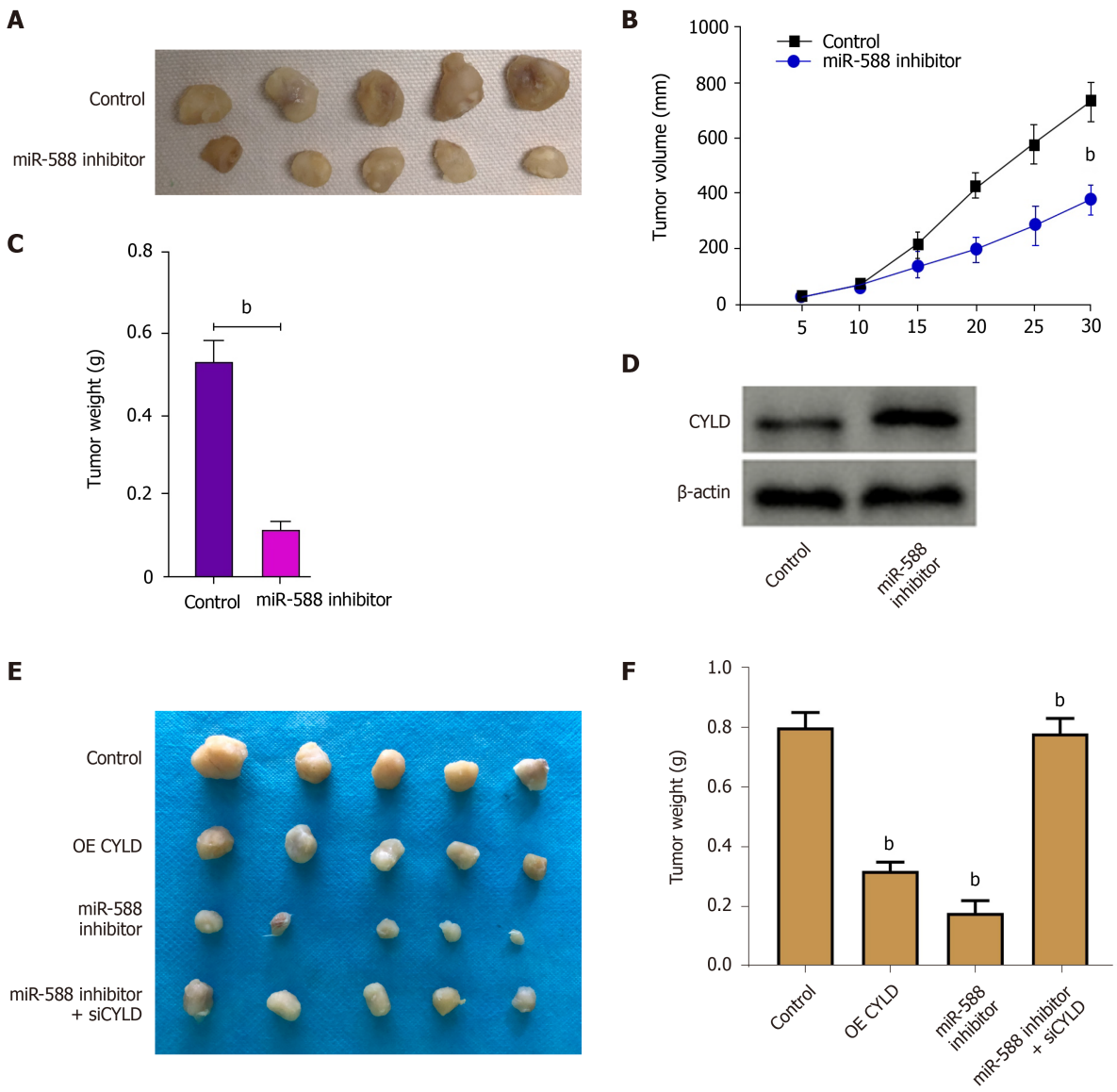

Figure 7 miR-588/cylindromatosis axis modulates cisplatin-resistant gastric cancer cell growth *in vivo*. A-D: The nude mice were injected with SGC7901 cells treated with miR-588 inhibitor, the tumor tissues (A), tumor volume (B), and tumor weight (C) were measured, and the expression of cylindromatosis (CYLD) was detected by Western blot analysis in the tumor tissues (D); E and F: The nude mice were injected with SGC7901 cells treated with CYLD overexpressing plasmid or miR-588 inhibitor, or co-treated with miR-588 inhibitor and CYLD siRNA, and the tumor tissues (E) and tumor weight (F) were measured. Data shown are the mean ± SD (n = 5). $^{b}P < 0.01$. CYLD: Cylindromatosis.

ARTICLE HIGHLIGHTS

Research background

Gastric cancer is a prevalent malignant cancer with a high incidence and significantly affects the health of modern people globally. Cisplatin (DDP) is one of the most common and effective chemotherapies for patients with gastric cancer, but DDP resistance remains a severe clinical challenge.

Research motivation

To identify the function of M2 polarized macrophages-derived exosomal miR-588 in gastric cancer cells.

Research objectives

To explore the effect of M2 polarized macrophages-derived exosomal miR-588 on DDP resistance of gastric cancer cells.

Research methods

M2 polarized macrophages were isolated and identified by specific markers using flow cytometry analysis. The exosomes from M2 macrophages were identified by TEM and related markers. The uptake of the PKH67-labelled M2 macrophages-derived exosomes was detected in SGC7901 cells. The function and mechanism of exosomal miR-588 from M2 macrophages in the modulation of DDP resistance of gastric cancer cell was analyzed by CCK-8 assay, apoptosis analysis, colony formation assay, Western blot analysis, qPCR analysis, and luciferase reporter assay in SGC7901 and SGC7901/DDP cells, and by tumorigenicity analysis in nude mice.

Research results

Polarized macrophages were isolated from mouse bone marrow stimulated with interleukin (IL)-13 and IL-4. Co-culture of gastric cancer cells with M2 polarized macrophages promoted DDP resistance. M2 polarized macrophage-derived exosomes could transfer in gastric cancer cells to enhance DDP resistance. Exosomal miR-588 from M2 macrophages contributed to DDP resistance of gastric cancer cells. miR-588 promoted DDP-resistant gastric cancer cell growth *in vivo*. miR-588 was able to target cylindromatosis (CYLD) in gastric cancer cells. The depletion of CYLD reversed miR-588 inhibition-regulated cell proliferation and apoptosis of gastric cancer cells exposed to DDP.

Research conclusions

In conclusion, we uncovered that exosomal miR-588 from M2 macrophages contributes to DDP resistance of gastric cancer cells by partly targeting CYLD.

Research perspectives

miR-588 may be applied as a potential therapeutic target for the treatment of gastric cancer.

REFERENCES

1 **Smyth EC**, Nilsson M, Grabsch HI, van Grieken NC, Lordick F. Gastric cancer. *Lancet* 2020; **396**: 635-648 [PMID: 32861308 DOI: 10.1016/S0140-6736(20)31288-5]

2 **Johnston FM**, Beckman M. Updates on Management of Gastric Cancer. *Curr Oncol Rep* 2019; **21**: 67 [PMID: 31236716 DOI: 10.1007/s11912-019-0820-4]

3 **Ghosh S**. Cisplatin: The first metal based anticancer drug. *Bioorg Chem* 2019; **88**: 102925 [PMID: 31003078 DOI: 10.1016/j.bioorg.2019.102925]

4 **Shen DW**, Pouliot LM, Hall MD, Gottesman MM. Cisplatin resistance: a cellular self-defense mechanism resulting from multiple epigenetic and genetic changes. *Pharmacol Rev* 2012; **64**: 706-721 [PMID: 22659329 DOI: 10.1124/pr.111.005637]

5 **Ngambenjawong C**, Gustafson HH, Pun SH. Progress in tumor-associated macrophage (TAM)-targeted therapeutics. *Adv Drug Deliv Rev* 2017; **114**: 206-221 [PMID: 28449873 DOI: 10.1016/j.addr.2017.04.010]

6 **Dai E**, Han L, Liu J, Xie Y, Kroemer G, Klionsky DJ, Zeh HJ, Kang R, Wang J, Tang D. Autophagy-dependent ferroptosis drives tumor-associated macrophage polarization *via* release and uptake of oncogenic KRAS protein. *Autophagy* 2020; **16**: 2069-2083 [PMID: 31920150 DOI: 10.1080/15548627.2020.1714209]

7 **Lan J**, Sun L, Xu F, Liu L, Hu F, Song D, Hou Z, Wu W, Luo X, Wang J, Yuan X, Hu J, Wang G. M2 Macrophage-Derived Exosomes Promote Cell Migration and Invasion in Colon Cancer. *Cancer Res* 2019; **79**: 146-158 [PMID: 30401711 DOI: 10.1158/0008-5472.CAN-18-0014]

8 **Kalluri R**. The biology and function of exosomes in cancer. *J Clin Invest* 2016; **126**: 1208-1215 [PMID: 27035812 DOI: 10.1172/JCI81135]

9 **Zhang L**, Yu D. Exosomes in cancer development, metastasis, and immunity. *Biochim Biophys Acta Rev Cancer* 2019; **1871**: 455-468 [PMID: 31047959 DOI: 10.1016/j.bbcan.2019.04.004]

10 **Wortzel I**, Dror S, Kenific CM, Lyden D. Exosome-Mediated Metastasis: Communication from a Distance. *Dev Cell* 2019; **49**: 347-360 [PMID: 31063754 DOI: 10.1016/j.devcel.2019.04.011]

11 **Bartel DP**. MicroRNAs: genomics, biogenesis, mechanism, and function. *Cell* 2004; **116**: 281-297 [PMID: 14744438 DOI: 10.1016/s0092-8674(04)00045-5]

12 **Bach DH**, Hong JY, Park HJ, Lee SK. The role of exosomes and miRNAs in drug-resistance of cancer cells. *Int J Cancer* 2017; **141**: 220-230 [PMID: 28240776 DOI: 10.1002/ijc.30669]

13 **Bayraktar R**, Van Roosbroeck K. miR-155 in cancer drug resistance and as target for miRNA-based therapeutics. *Cancer Metastasis Rev* 2018; **37**: 33-44 [PMID: 29282605 DOI: 10.1007/s10555-017-9724-7]

14 **Gao ZQ**, Wang JF, Chen DH, Ma XS, Yang W, Zhe T, Dang XW. Long non-coding RNA GAS5 antagonizes the chemoresistance of pancreatic cancer cells through down-regulation of miR-181c-5p.

Biomed Pharmacother 2018; **97**: 809-817 [PMID: 29112934 DOI: 10.1016/j.biopha.2017.10.157]

15 **Zhao N**, Lin T, Zhao C, Zhao S, Zhou S, Li Y. MicroRNA-588 is upregulated in human prostate cancer with prognostic and functional implications. *J Cell Biochem* 2017 [PMID: 28980707 DOI: 10.1002/jcb.26417]

16 **Chen Y**, Zhang J, Gong W, Dai W, Xu X, Xu S. miR-588 is a prognostic marker in gastric cancer. *Aging (Albany NY)* 2020; **13**: 2101-2117 [PMID: 33323542 DOI: 10.18632/aging.202212]

17 **Sun SC**. CYLD: a tumor suppressor deubiquitinase regulating NF-kappaB activation and diverse biological processes. *Cell Death Differ* 2010; **17**: 25-34 [PMID: 19373246 DOI: 10.1038/cdd.2009.43]

18 **Lork M**, Verhelst K, Beyaert R. CYLD, A20 and OTULIN deubiquitinases in NF-κB signaling and cell death: so similar, yet so different. *Cell Death Differ* 2017; **24**: 1172-1183 [PMID: 28362430 DOI: 10.1038/cdd.2017.46]

19 **Brummelkamp TR**, Nijman SM, Dirac AM, Bernards R. Loss of the cylindromatosis tumour suppressor inhibits apoptosis by activating NF-kappaB. *Nature* 2003; **424**: 797-801 [PMID: 12917690 DOI: 10.1038/nature01811]

20 **Suenaga N**, Kuramitsu M, Komure K, Kanemaru A, Takano K, Ozeki K, Nishimura Y, Yoshida R, Nakayama H, Shinriki S, Saito H, Jono H. Loss of Tumor Suppressor CYLD Expression Triggers Cisplatin Resistance in Oral Squamous Cell Carcinoma. *Int J Mol Sci* 2019; **20** [PMID: 31635163 DOI: 10.3390/ijms20205194]

21 **Wang Z**, Wang Q, Xu G, Meng N, Huang X, Jiang Z, Chen C, Zhang Y, Chen J, Li A, Li N, Zou X, Zhou J, Ding Q, Wang S. The long noncoding RNA CRAL reverses cisplatin resistance *via* the miR-505/CYLD/AKT axis in human gastric cancer cells. *RNA Biol* 2020; **17**: 1576-1589 [PMID: 31885317 DOI: 10.1080/15476286.2019.1709296]

22 **Xu W**, Chen Q, Wang Q, Sun Y, Wang S, Li A, Xu S, Røe OD, Wang M, Zhang R, Yang L, Zhou J. JWA reverses cisplatin resistance *via* the CK2-XRCC1 pathway in human gastric cancer cells. *Cell Death Dis* 2014; **5**: e1551 [PMID: 25476899 DOI: 10.1038/cddis.2014.517]

23 **Zheng P**, Luo Q, Wang W, Li J, Wang T, Wang P, Chen L, Zhang P, Chen H, Liu Y, Dong P, Xie G, Ma Y, Jiang L, Yuan X, Shen L. Tumor-associated macrophages-derived exosomes promote the migration of gastric cancer cells by transfer of functional Apolipoprotein E. *Cell Death Dis* 2018; **9**: 434 [PMID: 29567987 DOI: 10.1038/s41419-018-0465-5]

24 **Zheng P**, Chen L, Yuan X, Luo Q, Liu Y, Xie G, Ma Y, Shen L. Exosomal transfer of tumor-associated macrophage-derived miR-21 confers cisplatin resistance in gastric cancer cells. *J Exp Clin Cancer Res* 2017; **36**: 53 [PMID: 28407783 DOI: 10.1186/s13046-017-0528-y]

25 **Wu J**, Gao W, Tang Q, Yu Y, You W, Wu Z, Fan Y, Zhang L, Wu C, Han G, Zuo X, Zhang Y, Chen Z, Ding W, Li X, Lin F, Shen H, Tang J, Wang X. M2 Macrophage-Derived Exosomes Facilitate HCC Metastasis by Transferring α_M β_2 Integrin to Tumor Cells. *Hepatology* 2021; **73**: 1365-1380 [PMID: 32594528 DOI: 10.1002/hep.31432]

26 **Zhou X**, Xu M, Guo Y, Ye L, Long L, Wang H, Tan P. MicroRNA-588 regulates invasion, migration and epithelial-mesenchymal transition *via* targeting EIF5A2 pathway in gastric cancer. *Cancer Manag Res* 2018; **10**: 5187-5197 [PMID: 30464616 DOI: 10.2147/CMAR.S176954]

27 **Liu Z**, Mo H, Sun L, Wang L, Chen T, Yao B, Liu R, Niu Y, Tu K, Xu Q, Yang N. Long noncoding RNA PICSAR/miR-588/EIF6 axis regulates tumorigenesis of hepatocellular carcinoma by activating PI3K/AKT/mTOR signaling pathway. *Cancer Sci* 2020; **111**: 4118-4128 [PMID: 32860321 DOI: 10.1111/cas.14631]

28 **Binenbaum Y**, Fridman E, Yaari Z, Milman N, Schroeder A, Ben David G, Shlomi T, Gil Z. Transfer of miRNA in Macrophage-Derived Exosomes Induces Drug Resistance in Pancreatic Adenocarcinoma. *Cancer Res* 2018; **78**: 5287-5299 [PMID: 30042153 DOI: 10.1158/0008-5472.CAN-18-0124]

29 **Umemura S**, Zhu J, Chahine JJ, Kallakury B, Chen V, Kim IK, Zhang YW, Goto K, He Y, Giaccone G. Downregulation of CYLD promotes IFN-γ mediated PD-L1 expression in thymic epithelial tumors. *Lung Cancer* 2020; **147**: 221-228 [PMID: 32738418 DOI: 10.1016/j.lungcan.2020.07.018]

30 **Chen Y**, Lei Y, Lin J, Huang Y, Zhang J, Chen K, Sun S, Lin X. The LINC01260 Functions as a Tumor Suppressor *via* the miR-562/CYLD/NF-κB Pathway in Non-Small Cell Lung Cancer. *Onco Targets Ther* 2020; **13**: 10707-10719 [PMID: 33116647 DOI: 10.2147/OTT.S253730]

31 **Lin Y**, Wang L, Luo W, Zhou X, Chen Y, Yang K, Liao J, Wu D, Cai L. CYLD Promotes Apoptosis of Nasopharyngeal Carcinoma Cells by Regulating NDRG1. *Cancer Manag Res* 2020; **12**: 10639-10649 [PMID: 33149672 DOI: 10.2147/CMAR.S268216]

32 **Huang C**, Liu J, Pan X, Peng C, Xiong B, Feng M, Yang X. miR-454 promotes survival and induces oxaliplatin resistance in gastric carcinoma cells by targeting CYLD. *Exp Ther Med* 2020; **19**: 3604-3610 [PMID: 32346424 DOI: 10.3892/etm.2020.8655]

World Journal of Gastroenterology

Submit a Manuscript: https://www.f6publishing.com

World J Gastroenterol 2021 September 28; 27(36): 6093-6109

DOI: 10.3748/wjg.v27.i36.6093

ISSN 1007-9327 (print) ISSN 2219-2840 (online)

ORIGINAL ARTICLE

Case Control Study

Evaluation of biomarkers, genetic mutations, and epigenetic modifications in early diagnosis of pancreatic cancer

Bilal Rah, Manzoor Ahmad Banday, Gh Rasool Bhat, Omar J Shah, Humira Jeelani, Fizalah Kawoosa, Tahira Yousuf, Dil Afroze

ORCID number: Bilal Rah 0000-0003-3673-5044; Manzoor Ahmad Banday 0000-0002-9495-845X; Gh Rasool Bhat 0000-0002-5223-4875; Omar J Shah 0000-0001-9207-7440; Humira Jeelani 0000-0001-5545-3283; Fizalah Kawoosa 0000-0002-2669-6128; Tahira Yousuf 0000-0002-6983-2716; Dil Afroze 0000-0002-0724-8899.

Author contributions: Rah B performed data analysis and manuscript writing; Banday MA contributed to study design, data analysis and gave directions; Bhat GR contributed to data analysis and proofreading; Shah OJ contributed by providing patient samples; Jeelani H contributed to manuscript writing; Kawoosa F contributed to sample collection and experimentation; Yousuf T contributed to manuscript writing; and Afroze D contributed to study design, data analysis and gave directions; All authors gave the final approval of the current version of the manuscript for publication and agreed to be accountable for the current work.

Institutional review board statement: The study was reviewed and approved by the Institutional Ethics committee (IEC), Sher-i-Kashmir Institute of

Bilal Rah, Gh Rasool Bhat, Humira Jeelani, Tahira Yousuf, Dil Afroze, Advanced Centre for Human Genetics, Sher-i-Kashmir Institute of Medical Sciences, Srinagar 190011, Jammu and Kashmir, India

Manzoor Ahmad Banday, Department of Medical Oncology, Sher-i-Kashmir Institute of Medical Sciences, Srinagar 190011, Jammu and Kashmir, India

Omar J Shah, Department of Surgical Gastroenterology, Sher-i-Kashmir Institute of Medical Sciences, Srinagar 190011, Jammu and Kashmir, India

Fizalah Kawoosa, Department of Immunology and Molecular Medicine, Sher-i-Kashmir Institute of Medical Science, Srinagar 190011, Jammu and Kashmir, India

Corresponding author: Dil Afroze, PhD, Full Professor, Advanced Centre for Human Genetics, Sher-i-Kashmir Institute of Medical Sciences, Main Road, Srinagar 190011, Jammu and Kashmir, India. afrozedil@gmail.com

Abstract

BACKGROUND

Pancreatic cancer (PC) is one of the deadliest malignancies with an alarming mortality rate. Despite significant advancement in diagnostics and therapeutics, early diagnosis remains elusive causing poor prognosis, marred by mutations and epigenetic modifications in key genes which contribute to disease progression.

AIM

To evaluate the various biological tumor markers collectively for early diagnosis which could act as prognostic biomarkers and helps in future therapeutics of PC in Kashmir valley.

METHODS

A total of 50 confirmed PC cases were included in the study to evaluate the levels of carbohydrate antigen 19-9 (CA 19-9), tissue polypeptide specific antigen (TPS), carcinoembryonic antigen (CEA), vascular endothelial growth factor-A (VEGF-A), and epidermal growth factor receptor (EGFR). Mutational analysis was performed to evaluate the mutations in Kirsten rat sarcoma (*KRAS*), Breast cancer type 2 (*BRCA-2*), and deleted in pancreatic cancer-4 (*DPC-4*) genes. However, epigenetic modifications (methylation of CpG islands) were performed in the promoter

Medical Sciences, Srinagar, Jammu and Kashmir, India

Conflict-of-interest statement: The authors declare no conflicts of interest.

Data sharing statement: No additional data are available

STROBE statement: The authors have read the STROBE Statement, and the manuscript was prepared and revised according to the STROBE Statement.

Manuscript source: Unsolicited manuscript

Specialty type: Gastroenterology and hepatology

Country/Territory of origin: India

Peer-review report's scientific quality classification

Grade A (Excellent): 0
Grade B (Very good): 0
Grade C (Good): C
Grade D (Fair): 0
Grade E (Poor): 0

Received: April 7, 2021
Peer-review started: April 7, 2021
First decision: May 27, 2021
Revised: June 10, 2021
Accepted: July 13, 2021
Article in press: July 13, 2021
Published online: September 28, 2021

P-Reviewer: Shafqat S
S-Editor: Ma YJ
L-Editor: Filipodia

regions of cyclin-dependent kinase inhibitor 2A (*p16; CDKN2A*), MutL homolog 1 (*hMLH1*), and Ras association domain-containing protein 1(*RASSF1A*) genes.

RESULTS

We found significantly elevated levels of biological markers CA 19-9 ($P \leq 0.05$), TPS ($P \leq 0.05$), CEA ($P \leq 0.001$), and VEGF ($P \leq 0.001$). Molecular genetic analysis revealed that *KRAS* gene mutation is predominant in codon 12 (16 subjects, $P \leq 0.05$), and 13 (12 subjects, $P \leq 0.05$). However, we did not find a mutation in *DPC-4* (1203G > T) and *BRCA-2* (617delT) genes. Furthermore, epigenetic modification revealed that CpG methylation in 21 ($P \leq 0.05$) and 4 subjects in the promoter regions of the *p16* and *hMLH1* gene, respectively.

CONCLUSION

In conclusion, CA 19-9, TPS, CEA, and VEGF levels were significantly elevated and collectively have potential as diagnostic and prognostic markers in PC. Global data of mutation in the *KRAS* gene commonly in codon 12 and rare in codon 13 could augment the predisposition towards PC. Additionally, methylation of the *p16* gene could also modulate transcription of genes thereby increasing the predisposition and susceptibility towards PC.

Key Words: Pancreatic cancer; Genetic mutations; Epigenetic modifications; Biomarkers; Risk factors; Diagnostics

Core Tip: This study demonstrates that the collective evaluation of genetic mutations, epigenetic modifications in key genes and elevated levels of serum carbohydrate antigen 19-9, tissue polypeptide specific antigen, carcinoembryonic antigen, and vascular endothelial growth factor-A could be used as predictive biomarkers for diagnostics and prognostics in pancreatic cancer patients of the ethnic Kashmiri population. This could be useful to track the disease status of pancreatic cancer patients who are on a different regimen of chemotherapeutic interventions. To validate these results in the ethnic Kashmiri population, future studies need comprehensive, cohort, and replicative studies with large sample size.

Citation: Rah B, Banday MA, Bhat GR, Shah OJ, Jeelani H, Kawoosa F, Yousuf T, Afroze D. Evaluation of biomarkers, genetic mutations, and epigenetic modifications in early diagnosis of pancreatic cancer. *World J Gastroenterol* 2021; 27(36): 6093-6109
URL: https://www.wjgnet.com/1007-9327/full/v27/i36/6093.htm
DOI: https://dx.doi.org/10.3748/wjg.v27.i36.6093

INTRODUCTION

Pancreatic cancer (PC) is one of the deadliest malignancies among several solid malignancies. It is the 15th leading cancer in the world with an overall estimated incidence of 277000 new cases which is being diagnosed every year[1]. In the United States, PC is the fourth leading cause of death with a 5-year survival rate of less than 5%[2]. PC is mostly found in elderly people and has been reported to be associated with several risk factors[3]. The predominant risk factors include age, cigarette smoking, a high-fat diet, decreased serum levels of folate, diabetes mellitus, obesity, and chronic pancreatitis[4,5]. The familial history of pancreatitis increases the probability of developing PC by around 40%[6]. PC has the lowest prognosis among several solid-type tumors, mainly because almost 80% of PC patients are diagnosed when the disease is in the advanced or metastatic stage[7]. Owing to the lack of specific biological biomarkers used in clinical practice for the detection of PC and its nonspecific symptomology at the initial stage of the malignancy, the early diagnosis is extremely critical to detect and analyze disease progression[8]. Therefore, it is vital to identify specific biomarkers that play a key role in early diagnosis thereby improving the management and therapeutic outcome in PC.

P-Editor: Xing YX

Tumor biomarker(s) are the substances that can be examined in body fluids (blood, urine, and other fluids), synthesized and excreted by malignant cells within the tumor tissue besides exceeding the normal level potentiating its use for cancer diagnosis and/or prognosis[9]. Thus, ideally, the tumor markers should have high sensitivity and specificity, however, none of the tumor biomarkers have attained such precision [10]. Recent reports suggest that commonly used biomarkers for various malignancies include carbohydrate antigen 19-9 (CA 19-9), tissue polypeptide specific antigen (TPS), carcinoembryonic antigen (CEA), vascular endothelial growth factor-A (VEGF-A), and epidermal growth factor receptor (EGFR)[11]. The CA 19-9 and CEA are high molecular weight glycoproteins attached to the surface of tumor cells predominantly used in the diagnosis and prognosis of gut-associated cancers. However, marred by low sensitivity and specificity, they far from qualify for the diagnosis of other cancers [12]. The group of intermediate filament proteins to which TPS belongs is mainly used to measure cytokeratin 18 and 19 and expected to reflect the tumor progression. A few studies have examined TPS expression in PC; however, the findings are contentious. Although, individually TPS expression in PC may not provide significant information about the disease progression; in concert with other tumor biological markers it is worthwhile to evaluate its role for early diagnosis, prognosis, and to predict metastatic growth of PC[13]. A predominant dimeric, heparin-associated glycoprotein, VEGF-A has powerful pro-angiogenic and mitogenic activity. Elevated expression of VEGF-A enhances vascular permeability of endothelial cells and is reported to be involved in PC-associated angiogenesis[14], thus potentiates as a predictive biomarker. EGFR is a transmembrane protein that regulates cell growth and development. Mutation or elevated expression of EGFR is a key event in the pathogenesis of various malignancies such as glioblastoma, lung and oral carcinomas. There are reports of EGFR-mediated signaling associated with EGFR mutation in PC patients[15]. Consequently, these reports suggest that evaluation of serum EGFR levels in PC can be a promising putative biomarker for early diagnosis and prognosis to monitor the disease status post-therapeutic interventions. Although, individually the tumor biomarkers could aid in diagnostic and prognostic evaluation to a certain level, however, collectively, they can be more beneficial to track tumor progression and could be more useful to monitor disease status. Therefore, the current study aims to evaluate the collective role of various tumor biomarkers in PC patients for their potential role in early diagnosis and application in prognosis to examine post-treatment disease status in the ethnic Kashmiri population.

Genetic mutations play a pivotal role in tumor progression and genetic markers are critically important for the detection of malignant changes in PC[16]. Approximately, 97% of PC patients have alterations in genes that either follow the germline inheritance mode of transmission or occur sporadically[17]. These mutations could be either oncogenic (gain of function) or diminish tumor suppressor activity (loss of function). Gain-of-function in Kirsten rat sarcoma (*KRAS)* a proto-oncogene that encodes guanosine triphosphatase (GTPase), is one of the prominent mediators in signal transduction pathways that are implicated in neoplastic transformation and inflammation[18]. Approximately 95% of all cancers including PC are reported to harbor a *KRAS* gene mutation which is a key event in early tumorigenesis. The major *KRAS* activating gene mutations reportedly occur at codon 12 and less commonly at codon 13 and codon 61. Therefore, evaluation of genetic mutational analysis at the hotspot regions of the *KRAS* gene could help in early diagnosis and prognosis in PC. Breast cancer type 2 *(BRCA-2)*, a tumor suppressor gene is associated with the maintenance of the genome by enhancing homologous recombination of a double-stranded break. Around 80% of *BRCA-2* mutations are either frameshift or nonsense mutations that result in the formation of premature stop codons to encode non-functional BRCA-2 protein[19]. Almost 7.3% of PC patients have a hereditary mutation in the *BRCA-2* gene which increases the risk of developing PC by approximately 20-fold[20] implicating a critical role of *BRCA-2* in the early diagnosis of PC. Another vital gene, 'deleted in pancreatic cancer-4' *(DPC-4)* also known as SMAD family member 4, mothers against decapentaplegic homolog 4 (*SMAD-4)* is a tumor suppressor gene involved in the regulation of gene transcription. DPC-4 protein a downstream target of transforming growth factor-beta (TGF-β) pathway plays a critical role in the activation of TGF-β signaling thereby promotes neoplastic growth. It is reported that 30% of PC cases develop due to homozygous mutations in the *DPC-4* gene[21,22]. Thus, mutational analysis of the *DPC-4* gene could be a promising factor for the early diagnosis and prognosis of PC.

Besides genetic mutations, recent evidence suggests the epigenetic modifications such as DNA methylation plays a critical role in the pathogenesis of PC. In the recent past, reports suggest that methylation at the promoter regions of key tumor

suppressor genes induces gene silencing and contributes to the development and progression of tumorigenesis[23]. Various tumor suppressor genes were inactivated by epigenetic modifications. Cyclin-dependent kinase inhibitor 2A (*p16; CDKN2A*), a tumor suppressor gene that encodes a member of cyclin-dependent kinase inhibitor which arrests the G_1-S phase of the cell cycle to prevent tumor cell progression. Loss of the *p16* gene is reported in 70% of cancers and around 10%-15% of the loss was due to promoter methylation[24]. Thus, screening of epigenetic modifications at the promoter region of the *p16* gene could help in the early diagnosis of PC. MutL homolog 1 (*hMLH1)* a tumor suppressor gene that belongs to the mismatched repair gene family and prevents DNA damage by radiations and other associated mechanisms. *hMLH1* is also reported to be inactivated epigenetically by promoter methylation which leads to DNA damage. The accumulation of mismatched and damaged DNA promotes tumor cell progression[25]. Ras association domain-containing protein 1*(RASSF1A)* is another tumor suppressor gene inactivated by promoter methylation. It is a component of RAS/PI3K/AKT and RAS/MAPK pathways. Recent reports suggest that epigenetic modifications in the *RASSF1A* promoter region promote tumor progression in various cancers including kidney, breast, lung, prostate, and thyroid[26]. Recent evidence suggests that 64% of pancreatic adenocarcinoma patients have *RASSF1A* hypermethylation at the promoter region, indicating that analysis of hypermethylation of *RASSF1A* at promoter region could be a promising approach for early diagnosis of PC. To summarize, these studies suggest that genetic mutations, epigenetic modulations, and elevated levels of serum biological markers play a critical role in the early diagnosis, therapeutics, and prognosis of various cancer. Therefore, keeping in consideration the documented role of tumor biomarkers, genetic mutations, and DNA methylation of tumor suppressor/protooncogenes in various malignancies including PC. The current study aimed to evaluate the serum levels of various biological tumor markers, genetic mutations, and epigenetic modifications of some key regulatory genes in PC. This would prove immensely helpful in the early diagnosis of PC, which helps in the identification of high-risk PC and may enable their development as biomarkers for future diagnostics, therapeutic interventions, and prognostics in the ethnic Kashmiri population.

MATERIALS AND METHODS

In this study, a total of 50 patients with pancreatic carcinoma and 50 healthy controls were included.

Inclusion criteria

Only the patients with histologically confirmed pancreatic carcinoma were included in this study. Written consent was taken at the very beginning from all the patients and healthy controls that were included in the study.

Exclusion criteria

The patients with a history of other malignancies and those who were not willing to comply with pre-requisite protocol were excluded from the study.

Physical examination and lifestyle habits

The study was designed and approved by the institutional review board of the Sher-i-Kashmir Institute of Medical Sciences (SKIMS), and informed consent was obtained from all participants. A comprehensive physical/clinical examination was performed in the Department of Medical Oncology, SKIMS, and the patients were evaluated for Jaundice (by examining features like yellowing of eyes and skin), pruritis (by examining features like redness, bumps, spots or blisters, dry/cracked skin and leathery/scaly skin), muscle wasting (by evaluating features like weakness or numbness in the limbs, loss of muscle coordination, tingling or weakness of the extremities, impaired balance while walking, fatigue and a general illness, facial weakness, progressive weakness, gradual memory loss and liver enlargement (were examined by features like abdominal pain, nausea/vomiting, fatigue, whitening of eyes and yellowing of the skin).

Besides the physical examination, lifestyle activities of the PC patients were also recorded which included smoking status, salt tea consumption, spicy and non-spicy food intake, dried vegetable consumption, mutton, and beef consumption, fish consumption, oil intake, urine habits, bowel habits, and daily physical activity were also recorded.

Laboratory findings

The basic clinical laboratory findings were performed by using automated analyzers. The laboratory findings are liver function test (like aspartate transaminase-AST, alanine transaminase-ALT, bilirubin, and alkaline phosphatase-ALP), diabetic status (hyperglycemia) by measuring glucose levels, and anemia by measuring red blood cell (RBC) count.

Diagnostic imaging

For any other malignancy PC patients were initially screened by using multiphase multidetector computed tomography (CT) scan, magnetic resonance imaging (MRI), ultrasonography (USG), endoscopic ultrasound (EUS), and chest X-ray (CXR).

Sample collection

A total of 5 mL blood sample was collected in clot activator and Ethylenediaminetetraacetic acid (EDTA) vial from PC patients. The serum was separated from the clot activator vials using centrifugation and was stored at -80 °C for further analysis. EDTA vials contain blood was stored at -20 °C for DNA extraction. A tissue chunk (12-50 µm thick tumor tissue section) was obtained from the PC patient by endoscopy using USG-guided probes for mutational analysis and epigenetic modifications.

Tumor biomarkers

Tumor markers including CA19-9, TPS, CEA, VEGF-A, and EGFR were estimated in the serum obtained from blood collected from the PC patients. Measurement of CA 19-9, CEA, VEGF-A, and EGFR levels in serum were performed by using a modular E-170 analyzer. However, TPS levels in the serum were measured by using an Immulite instrument.

Genetic mutation analysis

Genomic DNA was extracted by the phenol-chloroform method from mononuclear cells. Hypaque density gradient centrifugation was performed to extract leucocytes from blood and tissue samples obtained from PC patients. The quantity and quality control analysis of genomic DNA was performed by carrying out UV spectrophotometer (Eppendorf Biospectrometer®, Hamburg Germany) analysis and Gel electrophoresis, respectively. However, polymerase chain reaction (PCR) was carried out with a different set of primers for *KRAS*, *DPC-4*, and *BRACA-2* genes under different PCR conditions. The PCR products obtained were subjected to Restriction Fragment Length Polymorphism (RFLP) using restriction enzymes BstN1 and BglI for mutational analysis of *KRAS* codon 12 and 13, respectively. GGA→TGA in exon 8, codon 358 of *DPC-4* gene was analyzed by using MnlI restriction enzyme. 6174delT of *BRCA-2* was analyzed by using allele-specific PCR technique and polyacrylamide gel electrophoresis (PAGE) was carried out to study any change in the *BRCA-2* gene.

Epigenetic analysis

The epigenetic analysis was performed by examining the methylation status of the promoter and exon regions of genes including *p16*, *RASSF1A*, and *hMLH1*. The methylation status of *p16*, *RASSF1A*, and *hMLH1* genes was determined by methylation-specific (MSP) PCR. Briefly, DNA extracted from tissue samples was first subjected to bisulfite conversion using EZ direct methylation kit. The bisulfite-converted DNA was then subjected to PCR using methylated and unmethylated primers specific for the respective genes. The results were analyzed on 2% agarose gel.

Statistical analysis

Numerical data collected from experiments for statistical analysis were performed by using non-parametrical statistical analysis tools which are the Kruskal-Wallis test and Mann-Whitney *U* test.

RESULTS

The current study included 50 PC patients with a mean age of 47.82 years at the time of diagnosis for the evaluation of various tumor biological markers for the PC diagnosis. Radio-diagnostics such as USG and CT, confirmed that all 50 patients had PC. Further, histopathological analysis supported the radio-diagnostic results and revealed that out of 50 confirmed PC patients, 47 PC patients had characterized to

have adenocarcinoma whereas the remaining 3 PC patients have neuroendocrine carcinoma in the pancreas as shown in Figure 1. The other demographic parameters and daily activities of all confirmed 50 PC patients are presented in Table 1.

Owing to have relative ease in blood collection and non-invasive, it is preferred to evaluate the biological tumor markers in serum. Therefore, we also intended to evaluate the biological tumor markers which included CA 19-9, TPS, CEA, VEGF-A, and EGFR levels in the blood collected from PC patients. Our results demonstrated that the levels of serum biological tumor markers CA 19-9, CEA, VEGF-A, TPS, EGFR of PC patients were significantly raised in 33 (66%), 32 (64%), 48 (96%), 48 (96%) and 0 out of 50 PC patients, respectively (Table 2) and Figure 2.

Although the PC progression is a heterogeneous and complex process that includes cell proliferation of intraepithelial and dysplasia to form a mass of cells, followed by an invasion of cells to neighboring tissues. Subsequently, one of the important driving factors of PC progression is genetic mutations of protooncogenes (gain-of-function) and tumor suppressor genes (loss-of-function). Among genetic mutations, *KRAS* mutation is the key point mutation followed by deletion mutation in tumor suppressor genes *BRCA-2, DPC-4,* and *p16* in PC. To evaluate whether the PC patients in our study harbor these mutations, we sought to perform mutational analysis of *KRAS* hotspot codons (codon 12 and codon 13), *DPC-4* (1203G>T), and *BRCA-2* mutation (6174delT) in our PC subjects. Our mutational analysis results revealed that out of 50 PC patients, 16 and 12 PC patients had *KRAS* mutation at codons 12 and 13, respectively. However, we could not find mutation(s) at codons 12 and 13 of the *KRAS* gene in the remaining 34 and 38 PC patients, respectively Figure 3. The representative agarose gel picture of the amplification product of codons 12 and 13 of the *KRAS* gene and their RFLP pattern is shown in Figures 4 and 5. Subsequently, the mutational analysis of tumor suppressor gene *DPC-4* (1203G>T) and *BRCA-2* (6174delT) were also evaluated in all PC subjects. Interestingly, we did not find any mutations in *DPC-4* and *BRCA-2* mutation at (1203G>T) (6174delT) sites, respectively Figure 3. The representative agarose gel picture of *DPC-4* (1203G>T) amplification and RFLP pattern is shown in Figure 6, respectively, and that of amplification and RFLP pattern of *BRCA-2* (6174delT) is shown in Figure 7. The results obtained from the genetic mutation analysis are summarized in Table 3.

Epigenetic alterations have been documented to play a crucial role in PC progression. The *p16, RASSF1A,* and *hMLH1* are key tumor suppressor genes regulating mismatch repair to minimize DNA damage and are frequently inactivated by epigenetic modification in various malignancies. Therefore, we intended to investigate the epigenetic modification (methylation of CpG islands) of *p16, RASSF1A,* and *hMLH1* genes by determining the methylation in their respective promoter regions in all PC subjects. Our epigenetic modification results demonstrated that 21 out of 50 PC subjects were found methylated in the CpG islands of the promoter region of the *p16* gene while the remaining 29 were unmethylated. However, the CpG islands in the promoter region of *RASSF1A* were found to be unmethylated in all 50 PC patients. Additionally, we observed that 4 out of 50 PC patients showed methylation patterns in the promoter region of the *hMLH1* gene, whereas the remaining 46 PC patients had the *hMLH1* gene unmethylated in their promoter regions. The representative agarose gel pic of MS-PCR for *hMLH1* and *RASSF1A* is shown in Figure 8. The methylation and unmethylation status as observed in the present study for *p16, hMLH1,* and *RASSF1A* are summarized in Table 4 and Figure 9.

DISCUSSION

Despite new therapeutic approaches to improve the outcome of PC patients by the introduction of molecular target approaches and combinatorial therapy, there is an unmet need to find the prospective biomarkers for early diagnosis of PC[27]. Therefore, the aim of the current study was to collective evaluation of tumor biological markers, mutational status, and epigenetic modulations in PC patients of the ethnic Kashmiri population for early diagnosis. Our findings revealed the elevated levels of serum biomarkers CA 19-9, TPS, CEA, and VEGF-A, in the blood samples of PC patients, however, EGFR levels were found to be in the normal range. The mutational analysis demonstrated that the *KRAS* gene mutation which is the major driver in PC progression was found in codons 12 (16 subjects) and 13 (12 subjects). Furthermore, DNA of CpG islands of 21 subjects was found significantly methylated in the promoter regions of the *p16* gene. Collectively, these results suggest that in combination with mutational analysis and epigenetic modulations (CpG methylation), the biological

Table 1 Characteristics and clinical presentations of cases in the present study, *n* (%)

Patient characteristics	Cases, *n* = 50	*P* value
Age in yr		
≤ 50	28 (56.0)	0.0377
> 50	22 (44.0)	
Gender		
Male	29 (58.0)	0.031
Female	21 (42.0)	
Family history		
Smoker		
Yes	22 (44.0)	0.034
No	28 (56.0)	
Lifestyle		
Active	44 (88.0)	0.001
Sedentary	06 (12.0)	
Residence		
Rural	40 (80.0)	0.01
Urban	10 (20.0)	
Dietary habits		
Salt tea		
Yes	47 (94.0)	0.01
No	03 (06.0)	
Spicy food		
Yes	28 (56.0)	0.043
No	22 (44.0)	
Appetite		
Yes	25 (50.0)	0.05
No	25 (50.0)	
Vegetables		
Yes	48 (100.0)	0.001
No	02 (00.0)	
Non-veg.		
Yes	47 (100.0)	0.001
No	03 (00.0)	
Edible oil		
Saturated	43 (86.0)	0.01
Unsaturated	07 (17.0)	
Urine habits		
Normal	28 (56.0)	0.05
Disturbed	22 (44.0)	
Bowel habits		
Normal	30 (60.0)	0.05
Disturbed	20 (40.0)	

Table 2 Analysis of tumor biological marker in the serum of pancreatic cancer patients

Tumor marker	Normal level	PC patients with elevated levels of tumor markers	PC patients with normal levels of tumor markers	*P* value for PC patients with elevated levels *vs* normal levels
CA19-9	< 37 U/mL	33	17	0.05
TPS	< 80 U/L	32	18	0.05
CEA	< 5 ng/mL	48	02	0.003
VEGF-A	31.2-2000 pg/mL	48	02	0.003
EGFR	62.5-4000 pg/mL	0	50	0.001

PC: Pancreatic cancer; CA19-9: Carbohydrate antigen 19-9; TPS: Tissue polypeptide specific antigen; CEA: Carcinoembryonic antigen; VEGF-A: Vascular endothelial growth factor-A; EGFR: Epidermal growth factor receptor.

Table 3 Mutational analysis of *KRAS* (Codon 12 and 13), *DPC-4*, and *BRCA-2* gene mutations within pancreatic cancer subjects

Key genes in PC patients evaluated for mutational analysis	Mutation's present	Mutation's absent	*P* value for mutations present *vs* absent
KRAS mutation (codon 12)	16	34	0.05
KRAS mutation (codon 13)	12	38	0.05
DPC-4 mutation (1203G>T)	0	50	0.001
BRCA-2 mutation (6174delT)	0	50	0.001

KRAS: Kirsten rat sarcoma; *DPC-4*: Deleted in pancreatic cancer-4; *BRCA-2*: Breast cancer type 2.

Table 4 Methylation and unmethylation status in the promoter region of *p16*, *RASSF1A*, and *hMLH1*within pancreatic cancer subjects

Genes	Promoter methylation analysis status	Promoter unmethylation analysis status	*P* value for promoter methylation *vs* ummethylation
p16	21	29	0.05
RASSF1A	0	50	0.001
hMLH1	4	46	0.165

tumor markers evaluated in PC subjects could be valuable for early diagnostics and could strongly predict the PC prognostics. Additionally, these types of studies could further strengthen the validation of biological tumor markers and have a promising perspective for the predisposition and susceptibility towards PC.

A biological tumor marker is an entity in the body that gives information about a diagnosis, prognosis, and therapeutic modalities for a particular disease. The preferred entity to be eligible as a biomarker should be available in body fluids and non-invasive [28]. One of the important tumor biomarkers used in various malignancies is a high molecular weight glycoprotein CA 19-9. Biochemically, a carbohydrate antigen, CA19-9 is mainly expressed by the cells of the pancreaticobiliary system. Previous studies suggest that CA 19-9 levels were elevated in gut-associated malignancies such as gastric, bile duct, colorectal, and ovarian cancers. Owing to its relatively higher sensitivity and specificity among other biomarkers in PC patients, CA 19-9 is an important and valuable biomarker in the diagnostics of PC[29]. Although reports suggest a significant progress in overall survival and reduction in CA19-9 levels in PC, however, a recent study by Hess *et al*[30] did not support these findings. O'Brien *et al* [31] reported that CA 19-9 levels were raised in PC patients and may act as a better biomarker for the early diagnosis of PC. Besides, the levels of CA 19-9 were found directly associated with tumor size, tumor burden, and stage of tumorigenesis in PC, the pre-and post-operative levels of CA 19-9 in PC patients could be used as a prognosticator. Consistent with these findings, our results revealed that out of 50 PC

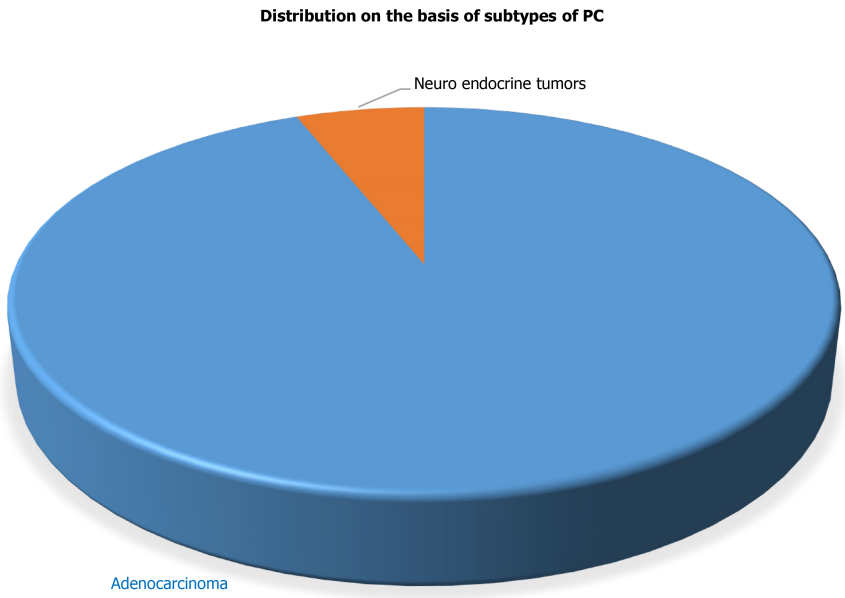

Figure 1 Distribution of samples (cases) based on subtypes of pancreatic cancer. PC: Pancreatic cancer.

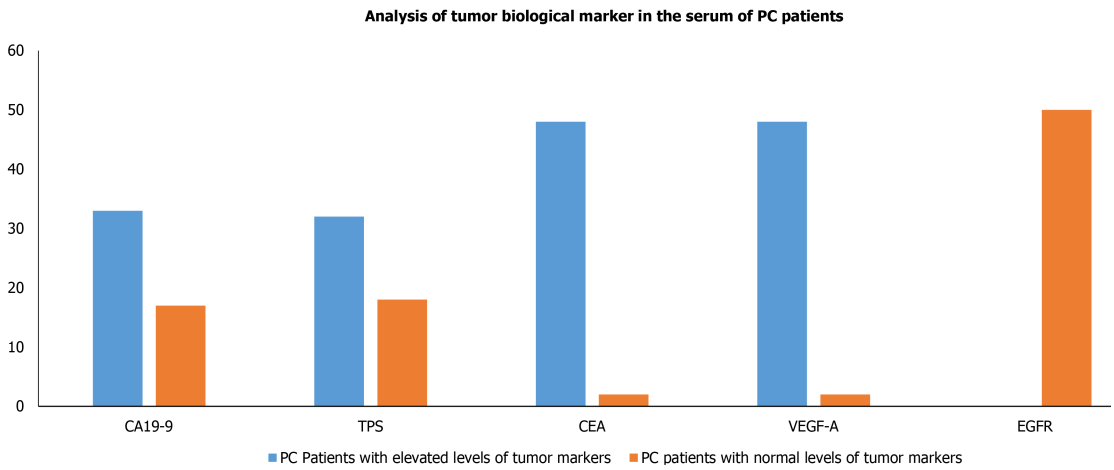

Figure 2 Analysis of tumor biological marker (carbohydrate antigen 19-9, tissue polypeptide specific antigen, carcinoembryonic antigen, vascular endothelial growth factor-A, and epidermal growth factor receptor) in the serum of pancreatic cancer patients. PC: Pancreatic cancer; CA19-9: Carbohydrate antigen 19-9; TPS: Tissue polypeptide specific antigen; CEA: Carcinoembryonic antigen; VEGF-A: Vascular endothelial growth factor-A; EGFR: Epidermal growth factor receptor.

patients 33 had significantly elevated levels of CA 19-9 in their blood samples, which indicates that more studies with a large cohort size are needed in the future to validate CA 19-9 as a better early diagnostic biomarker in PC.

Another valuable biomarker used in the diagnosis of various malignancies is TPS. It is essentially an antigen that binds to the epitope of soluble cytokeratin 18 fragments. The striking feature of TPS is to differentiate between PC and chronic pancreatitis and it is a better marker than CA 19-9 for differentiating PC and pancreatitis[32]. Previous studies suggested that serum TPS levels have a better correlation with gastric, colorectal, and pancreatic cancer than CA 19-9, CA 195, or CEA biomarkers[33,34]. Consistent with the previous studies, our results revealed that 48 out of 50 confirmed PC patients had significantly elevated levels of TPS, which suggests that elevated levels of serum TPS are better correlated with PC than CA 19-9 and could act as a better diagnostic and prognostic biomarker in PC. CEA, a glycoprotein, first identified in 1965, is present normally in the fetal pancreas, gastrointestinal tract, and liver. In the adolescent stage, it is found in lesser quantity in endodermal tissue and colon. CEA was used as a diagnostic marker of PC decades before and is now replaced by markers that have greater sensitivity for the detection of PC[35]. Elevated serum levels of CEA

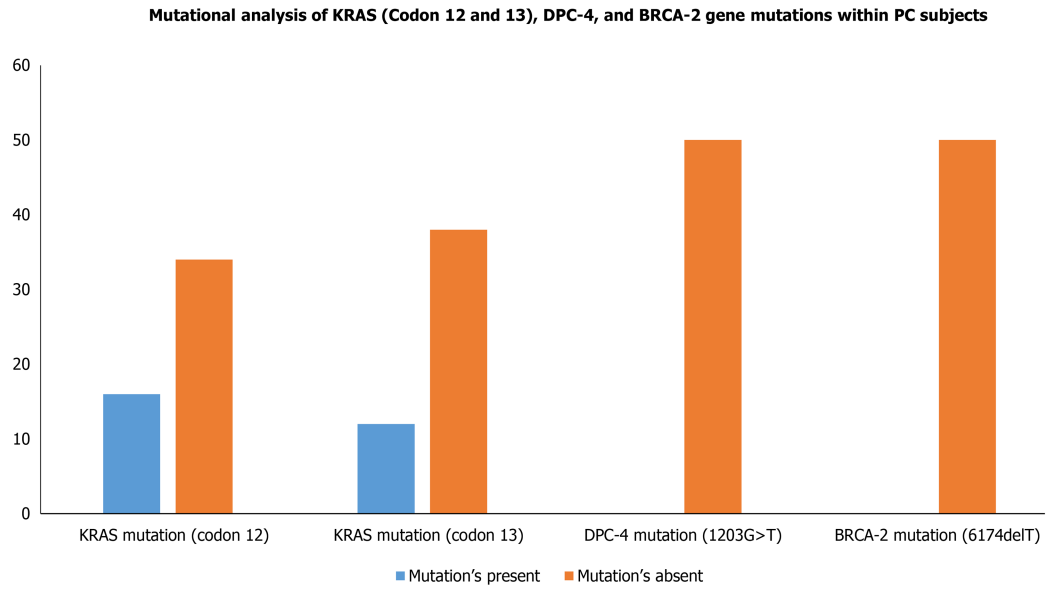

Figure 3 Mutational analysis of *KRAS* (Codon 12 and 13), *DPC-4*, and *BRCA-2* gene mutations within pancreatic cancer cases. KRAS: Kirsten rat sarcoma; DPC-4: Deleted in pancreatic cancer-4; BRCA-2: Breast cancer type 2.

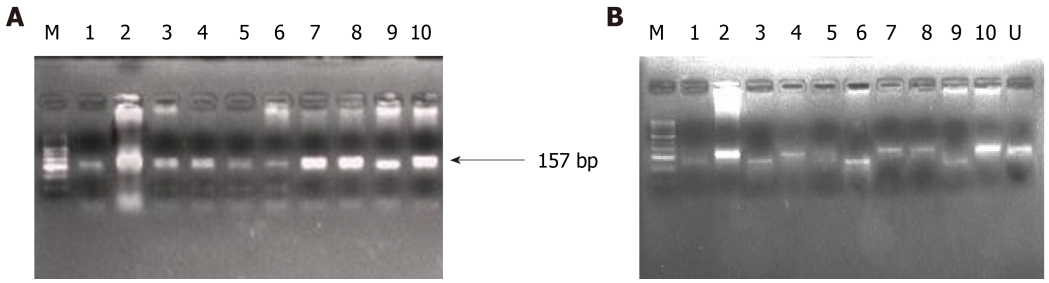

Figure 4 Representative agarose gel picture of polymerase chain reaction amplification (A) and restriction fragment length polymorphism using BstN1 (B) for *KRAS* codon 12. The arrow represents the 157 bp amplicon and M denotes the DNA marker (50 bp). Lane M represents a DNA marker (50 bp). Lanes 2, 4, 7, 8, and 10 represent the mutant band (undigested) of 157 bp. Lane 1, 3, 6, and 9 represent the wild band (digested) of 128 bp. U represents the undigested band used as mutant control.

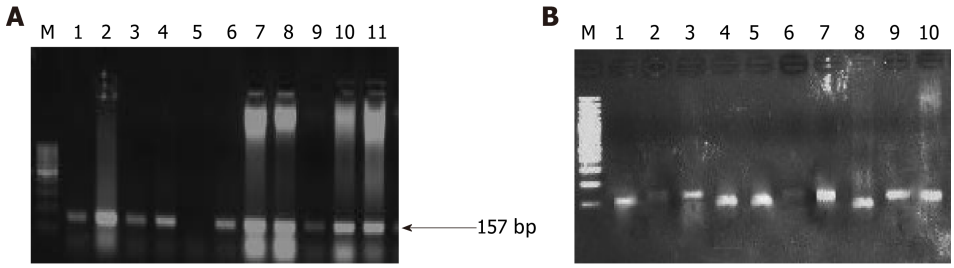

Figure 5 Representative gel picture of polymerase chain reaction amplification (A) and restriction fragment length polymorphism using BglI (B) for *K-RAS* codon 13. The arrow represents the 157 bp amplicon and M denotes the DNA marker (100 bp). Lane M represents a DNA marker (100 bp). Lanes 2, 3, 6, 7, 8, 9, 10, and 11 represent the mutant band (undigested) of 157 bp. Lanes 1, 4, 5, and 8 represent a wild band (digested) of 125 bp.

have been documented in more than 60% of cases of PC. Consistent with previous findings, our results demonstrated that 64% of patients (32 out of 50 confirmed PC) had elevated levels of serum CEA. However, if used with other biomarkers for early diagnostics, CEA could be adding up great value to early diagnostics of PC[36]. High expression of VEGF-A is associated with tumor size and progression. Overexpression of VEGF-A has been reported in head and neck, non-small cell lung, ovarian, endometrial, osteosarcoma, bladder, B cell lymphoma, ocular adnexal lymphoma, papillary renal cell carcinoma, and pancreatic cancers. VEGF-A is reported to have an

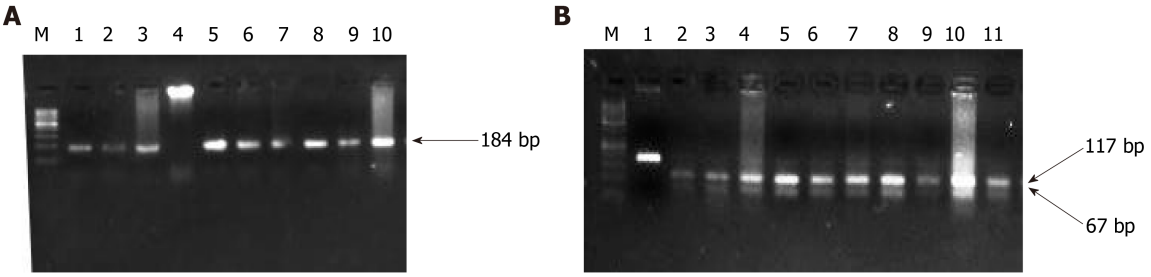

Figure 6 Representative gel picture of polymerase chain reaction amplification and restriction fragment length polymorphism using MnlI of *DPC-4*. The arrow represents the 184bp amplicon and M denotes the DNA marker (100 bp). Lane M represents a DNA marker (50 bp). 117 bp and 67 bp represent the wild bands (digested). U represents the mutant control band of 184 bp (undigested).

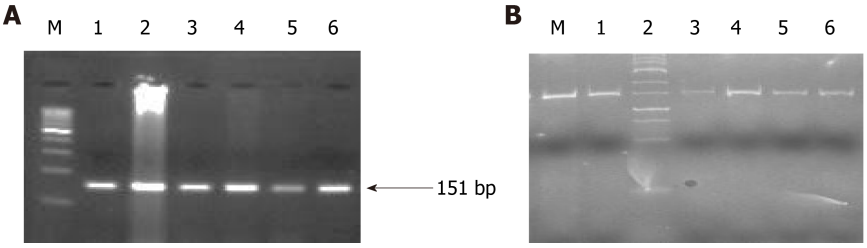

Figure 7 Representative agarose gel picture of AS-polymerase chain reaction amplification (A) and gel picture representing polyacrylamide gel electrophoresis (20% gel) (B) of *BRCA-2*. All the lanes show 151 bp amplicon which is the wild band and M denotes the DNA marker (100 bp). M is the marker lane (25 bp). Here also, the only wild band (151 bp) is observed in all the lanes.

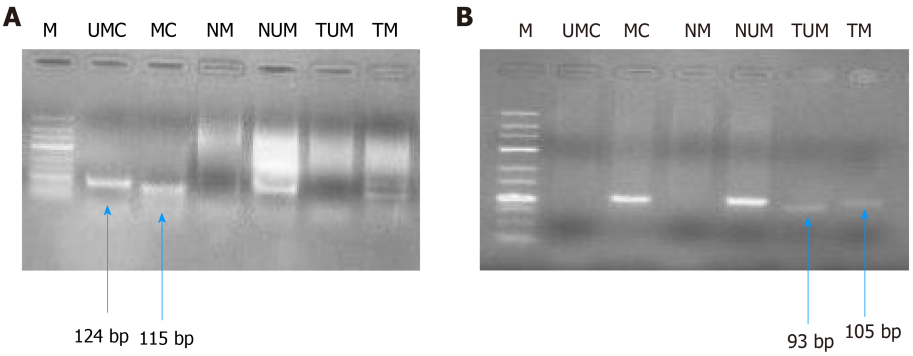

Figure 8 Gel picture representing MS-polymerase chain reaction for *hMLH1* (A, 100 bp) and *RASSF1A* (B, 25 bp). M represents DNA marker; UMC represents unmethylated control; MC represents methylated control; NM represents normal methylated; NUM represents normal unmethylated; TUM represents tumor unmethylated; TM represents tumor methylation.

80 gene loci whose alterations are reported in hepatocarcinoma, lung, pancreatic, and endometrial cancers[36]. A study conducted by Seo *et al*[37] demonstrated that 93% of ductal pancreatic adenocarcinomas showed high expression of VEGF-A protein. In the recent past, around 77% of VEGF-A expression was observed in PC tissues whereas only 15% of VEGF-A expression was found in the normal range[38]. Consistent with these findings, our results showed that out of 50 confirmed PC subjects, 48 cases had elevated levels of VEGF-A expression, which indicates that VEGF-A plays a critical role and had a strong causal association with PC progression, thus could act as a valuable tumor biomarker in combination with other biomarkers for early diagnosis of PC.

Besides, the currently available biomarkers for PC diagnostics, it is worthy to introduce genetic markers to develop more sophisticated tools for early detection of PC. PC is a disease that harbors somatic as well as hereditary mutations. Approximately, 5%-10% of the familial PC is caused by a mutation in a myriad of genes and surges the predisposition to PC by several-fold[24]. Previous studies reported that several genes showed a strong causal association with PC progression, among these most important are *KRAS*, *DPC-4*, and *BRCA-2* which in turn are associated with

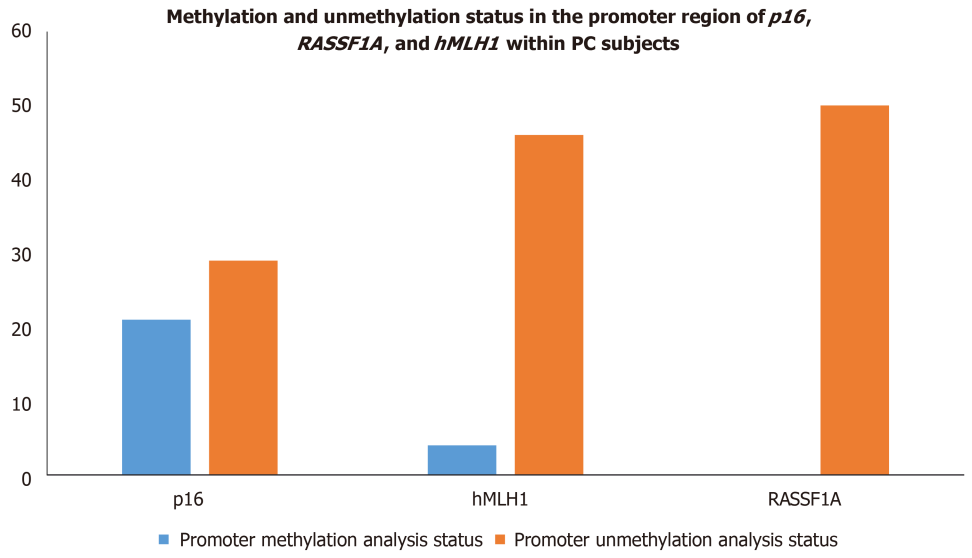

Figure 9 Methylation and unmethylation status in the promoter region of *p16*, *RASSF1A*, and *hMLH1* within pancreatic cancer subjects. PC: Pancreatic cancer.

different other genes using different interactions like physical interaction, genetic interaction, shared protein interaction, *etc.* as depicted in Figure 10[39]. The most common mutation reported in PC is *KRAS* mutation and is the earliest recognizable event in its pathogenesis. Studies have reported that mutations in the *KRAS* gene are mainly limited to codon 12 and rarely on codon 13[40,41]. The pathological mutation in *KRAS* encodes constitutive Ras protein which belongs to GTP binding protein family. The constitute Ras protein facilitates the oncogenic signaling pathway which leads to inflammation, deregulated cellular growth, cell motility, and remodeling of the cytoskeletal elements. *KRAS* gene mutations are known to be driver mutations that occur sporadically. It accounts for 30% of early neoplasms of the pancreas and nearly 100% in pancreatic adenocarcinomas. Besides PC, a mutation in the *KRAS* gene is adequate to promote lung cancer, colon cancer, breast cancer, and other cancers as well [42,43]. Recent clinical data suggest that *KRAS* mutations act as significant prognostic biomarker to predict therapeutic intervention for PC management. Kim *et al*[44] demonstrated that out of 136 PC patients, 70 PC patients harbored point mutation in codon 12 of the *KRAS* gene, and these patients have shown dismal response to gemcitabine-based chemotherapy compared to those who had wild type allele for *KRAS* gene[44]. Another study revealed that out of 173 PC patients, 121 were found to harbor point mutations in codon 12 of the *KRAS* gene, and among them are nonresponders to erlotinib. However, patients with wild-type alleles displayed a promising overall survival rate[45]. Consistent with these studies, our mutational analysis results revealed that 16 PC patients had *KRAS* point mutation at codon 12, interestingly we observe point mutation in the *KRAS* gene at codon 13. These findings suggest that further studies are needed to validate the high frequency of point mutation in codon 13 of the *KRAS gene. BRCA-1 and BRCA-2* germline mutations substantially increase the lifetime risk of breast cancer tumorigenesis. Recent reports suggest that the mutations in these genes also have a strong causal association with other cancers including PC[46]. The primary role of the *BRCA-2* gene is the maintenance of the genome by enhancing homologous recombination of a double-stranded break. Approximately, 80% of *BRCA-2* mutations are either frameshift or non-sense mutations which result in the formation of premature stop codons to encode non-functional BRCA-2 protein. *BRCA-2* mutations have been found in 7.3% of familial PC patients which indicates an increased risk of cancers by about 20-fold[47]. *DPC-4* (*SMAD-4)* is a tumor suppressor gene intricated in the regulatory mechanisms of gene transcription. Approximately, 30% of PC cases have been reported to harbor homozygous mutations in the *DPC-4* gene[21]. The mutated *DPC-4* gene-encoded hyperactivated Smad-4 protein leads to the activation of TGF-β pathways thereby promote cell proliferation and tumor growth. Mutations in the *DPC-4* gene have been reported in approximately 50% of PCs and serves as a leading cause of protein inactivation[48]. Inconsistent with previous studies, our mutational analysis of *BRCA-2* and *DPC-4* genes revealed a zero frequency of *DPC-4* 1203 G>T and *BRCA-2* 6174 deletion in PC patients. Collectively, these findings suggest that a larger sample size is

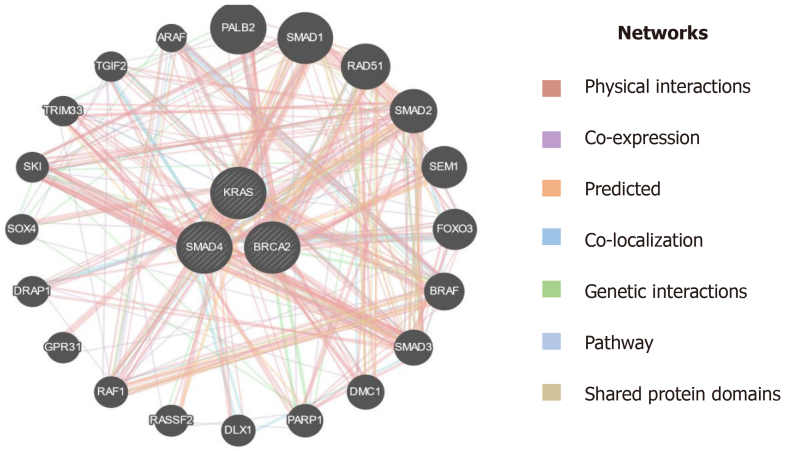

Figure 10 Interaction of *KRAS*, *SMAD4* (*DPC4*), and *BRCA2* with other genes based on various parameters. KRAS: Kirsten rat sarcoma; DPC-4: Deleted in pancreatic cancer-4; BRCA-2: Breast cancer type 2.

needed to validate our results in the ethnic Kashmiri population.

Epigenetic modulations play a critical role in tumorigenesis. Change in DNA methylation of tumor suppressor genes has indispensable importance in therapeutics and could serve as biomarkers for diagnostics and prognostics in various cancers[49]. *p16* is a tumor suppressor gene that encodes cyclin-dependent kinase inhibitors to arrest the cellular growth of malignant cells. Besides point mutations and homozygous deletions in the *p16* gene, recent evidence suggests that methylation of CpG islands in the promoter regions of *p16* stimulates transcriptional silencing of the *p16* gene and contributes to PC progression. In the recent past, hypermethylation in the promoter region of *p16* is significantly raised in chronic pancreatitis compared to normal; suggesting that hypermethylation in the promoter region of the *p16* gene might deregulate cell cycle kinetics and could promote PC progression. Further, reports demonstrated that *p16* hypermethylation in chronic pancreatitis might increase the risk of PC development many-fold[48]. Moore *et al*[50] demonstrated the role of *p16* promoter hypermethylation and associated molecular pathways involved in exocrine and endocrine development of PC. Further, studies suggest that the reduction in overall survival rate associated with *p16* alterations signifies the fact that *p16* could act as an important diagnostic and prognostic biomarker in resected ductal PC patients [51]. *RASSF1A* is another tumor suppressor and an important component of RAS/PI3K/AKT and RAS/RAF/MEK/ERK pathways that have been epigenetically inactivated in various sporadic human malignancies. A higher frequency of promoter methylation status of *RASSF1A* has been implicated in several cancers. The highest frequency of *RASSF1A* promoter hypermethylation was reported in prostate cancer (99%), followed by lung cancer (95%) and breast cancer (88%)[52]. Recent reports suggest that a low frequency of *hMLH1* hypermethylation was detected in PC. The loss of the *hMLH1* gene which encodes for Mut L protein homology 1 is common in various cancers. Further, whole-genome sequencing revealed that somatic *hMLH1* mutations are rare in cancers with an observed frequency of < 1%[53]. In the present study, we carried out epigenetic modifications (CpG methylation) of promoter regions of *p16*, *RASSF1A*, and *hMLH1* genes. Our results demonstrate that significant hypermethylation (CpG islands) was reported in the promoter regions of the *p16* gene in PC patients. However, we observed an extremely low frequency of methylation in the promoter region of the *hMLH1* gene in PC patients. Interestingly, the CpG methylation in the promoter region of the *RASSF1A* gene was completely absent in PC patients. Additionally, *in-silico* analysis suggest that plethora of genes are associated through various interactions with the key genes (*hMLH1*, *RASSF1A*, and *CDKN2A*) as in Figure 11, which could play a key role in the progression of PC[39]. Together, these results suggest that a cohort and comprehensive study with larger sample size is needed to document our findings in the ethnic Kashmiri population.

CONCLUSION

In conclusion, the present study strongly suggests that the elevated levels of serum CA

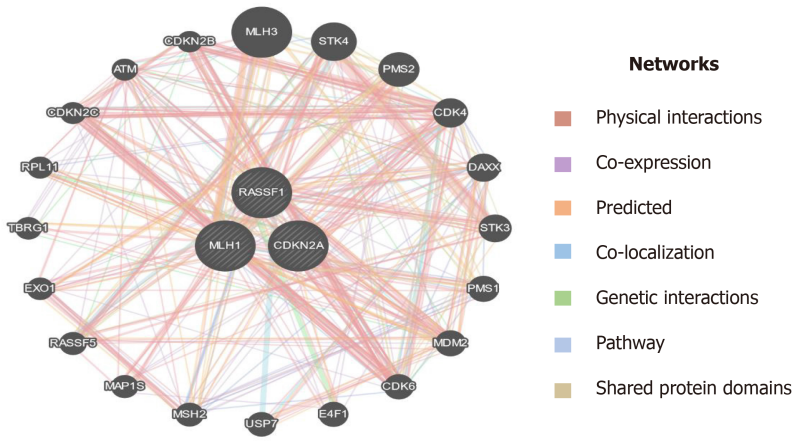

Figure 11 Interaction of *MLH1*, *RASSF1*, and *CDKN2A* (*p16*) with other important genes which have a role in the progression of pancreatic cancer.

19-9, TPS, CEA, and VEGF-A can be used as predictive biomarkers in PC patients of the ethnic Kashmiri population and may act as prognostic biomarkers to benefit the patients who are on a different regimen of chemotherapeutic interventions. Further, mutational analysis data suggest that besides harboring point mutation in codon 12 of *KRAS* gene, the PC patients of the current study significantly harbored codon 13-point mutation as well, which is very rarely reported in the previous studies. This may act as a genetic risk predictor in the development of PC. Additionally, considerable hypermethylation (CpG islands) in the promoter region of the *p16* gene in the current study may lead to silencing of the *p16* gene and could also increase the predisposition towards PC. However, we could not find the association of *DPC*-4G>T and *BRCA*-2 6174 deletion mutations and hypermethylation of CpG islands in the promoter region of *RASSF1A* and *hMLH1* gene towards the risk of PC. To validate these results in the Kashmiri population the future studies need to be comprehensive and with larger sample sizes.

ARTICLE HIGHLIGHTS

Research background

Pancreatic cancer (PC) is one of the deadliest malignancies with an alarming mortality rate. Despite significant advancement in diagnostics and therapeutics, early diagnosis remains elusive causing poor prognosis, marred by mutations and epigenetic modifications in key genes which contribute to disease progression.

Research motivation

To explore the various biological tumor markers collectively and mutational analysis of key regulatory genes for early diagnosis and prognosis of PC.

Research objectives

To evaluate various biological tumor markers collectively in PC and their association with genetic mutation and epigenetic modification of key regulatory genes that could act as early diagnostic and prognostic biomarkers and will help in future therapeutics of PC in Kashmir valley.

Research methods

The current study includes 50 confirmed PC cases to evaluate the levels of carbohydrate antigen 19-9 (CA 19-9), tissue polypeptide specific antigen (TPS), carcinoembryonic antigen (CEA), vascular endothelial growth factor-A (VEGF-A), and epidermal growth factor receptor (EGFR) by enzyme-linked immunosorbent assay (ELISA) method. Mutational analysis of key genes Kirsten rat sarcoma (*KRAS*), Breast cancer type 2 (*BRCA*-2), and deleted in pancreatic cancer-4 (*DPC*-4) genes was performed to evaluate the mutations at hotspot regions. Furthermore, epigenetic modifications were performed in the promoter regions of cyclin-dependent kinase

inhibitor 2A (*p16; CDKN2A*), MutL homolog 1 (*hMLH1*), and Ras association domain-containing protein 1 (*RASSF1A*) genes.

Research results

Besides significant elevation in levels of tumor markers CA 19-9 ($P \leq 0.05$), TPS ($P \leq 0.05$), CEA ($P \leq 0.001$), and VEGF ($P \leq 0.001$), our mutational analysis observed that *KRAS* gene mutation is predominant in codon 12 (16 subjects, $P \leq 0.05$), and 13 (12 subjects, $P \leq 0.05$). Additionally, epigenetic modification analysis suggests that CpG methylation was observed in 21 ($P \leq 0.05$) and 4 subjects in the promoter regions of the *p16* and *hMLH1* gene, respectively.

Research conclusions

The study revealed the significant elevation of serum biological markers in PC patients and the causal association of hotspot mutations and epigenetic modification of key with PC pathogenesis thus indicates the potential of biological markers, mutational status, and epigenetic modifications of key genes collectively for predisposition, susceptibility as well as diagnostics and prognostics of PC.

Research perspectives

The study strongly suggests that the elevated levels of serum CA 19-9, TPS, CEA, and VEGF-A can be used as predictive biomarkers in PC subjects. Additionally, mutational analysis epigenetic modifications in the promoter region of key genes may act as prognostic biomarkers to benefit the patients who are on a different regimen of chemotherapeutic interventions. Further to validate these results, future studies need comprehensive, cohort, and explicative studies with large sample sizes.

ACKNOWLEDGEMENTS

The authors extend their appreciation to the State Department of Science and Technology, Jammu and Kashmir, India.

REFERENCES

1 **Hadden M**, Mittal A, Samra J, Zreiqat H, Sahni S, Ramaswamy Y. Mechanically stressed cancer microenvironment: Role in pancreatic cancer progression. *BiochimBiophysActa Rev Cancer* 2020; **1874**: 188418 [PMID: 32827581 DOI: 10.1016/j.bbcan.2020.188418]

2 **Saad AM**, Turk T, Al-Husseini MJ, Abdel-Rahman O. Trends in pancreatic adenocarcinoma incidence and mortality in the United States in the last four decades; a SEER-based study. *BMC Cancer* 2018; **18**: 688 [PMID: 29940910 DOI: 10.1186/s12885-018-4610-4]

3 **Rawla P**, Sunkara T, Gaduputi V. Epidemiology of Pancreatic Cancer: Global Trends, Etiology and Risk Factors. *World J Oncol* 2019; **10**: 10-27 [PMID: 30834048 DOI: 10.14740/wjon1166]

4 **Midha S**, Chawla S, Garg PK. Modifiable and non-modifiable risk factors for pancreatic cancer: A review. *Cancer Lett* 2016; **381**: 269-277 [PMID: 27461582 DOI: 10.1016/j.canlet.2016.07.022]

5 **Avgerinos KI**, Spyrou N, Mantzoros CS, Dalamaga M. Obesity and cancer risk: Emerging biological mechanisms and perspectives. *Metabolism* 2019; **92**: 121-135 [PMID: 30445141 DOI: 10.1016/j.metabol.2018.11.001]

6 **Wang W**, Chen S, Brune KA, Hruban RH, Parmigiani G, Klein AP. PancPRO: risk assessment for individuals with a family history of pancreatic cancer. *J ClinOncol* 2007; **25**: 1417-1422 [PMID: 17416862 DOI: 10.1200/JCO.2006.09.2452]

7 **Stathis A**, Moore MJ. Advanced pancreatic carcinoma: current treatment and future challenges. *Nat Rev ClinOncol* 2010; **7**: 163-172 [PMID: 20101258 DOI: 10.1038/nrclinonc.2009.236]

8 **McGuigan A**, Kelly P, Turkington RC, Jones C, Coleman HG, McCain RS. Pancreatic cancer: A review of clinical diagnosis, epidemiology, treatment and outcomes. *World J Gastroenterol* 2018; **24**: 4846-4861 [PMID: 30487695 DOI: 10.3748/wjg.v24.i43.4846]

9 **Marrugo-Ramírez J**, Mir M, Samitier J. Blood-Based Cancer Biomarkers in Liquid Biopsy: A Promising Non-Invasive Alternative to Tissue Biopsy. *Int J MolSci* 2018; **19** [PMID: 30248975 DOI: 10.3390/ijms19102877]

10 **Kumar S**, Mohan A, Guleria R. Biomarkers in cancer screening, research and detection: present and future: a review. *Biomarkers* 2006; **11**: 385-405 [PMID: 16966157 DOI: 10.1080/13547500600775011]

11 **Brase JC**, Wuttig D, Kuner R, Sültmann H. Serum microRNAs as non-invasive biomarkers for cancer. *Mol Cancer* 2010; **9**: 306 [PMID: 21110877 DOI: 10.1186/1476-4598-9-306]

12 **Rückert F**, Pilarsky C, Grützmann R. Serum tumor markers in pancreatic cancer-recent discoveries.

Cancers (Basel) 2010; **2**: 1107-1124 [PMID: 24281109 DOI: 10.3390/cancers2021107]

13 **Barak V**, Goike H, Panaretakis KW, Einarsson R. Clinical utility of cytokeratins as tumor markers. *ClinBiochem* 2004; **37**: 529-540 [PMID: 15234234 DOI: 10.1016/j.clinbiochem.2004.05.009]

14 **van der Bilt AR**, Terwisscha van ScheltingaAG, Timmer-Bosscha H, Schröder CP, Pot L, Kosterink JG, van der Zee AG, Lub-de Hooge MN, de Jong S, de Vries EG, Reyners AK. Measurement of tumor VEGF-A levels with 89Zr-bevacizumab PET as an early biomarker for the antiangiogenic effect of everolimus treatment in an ovarian cancer xenograft model. *Clin Cancer Res* 2012; **18**: 6306-6314 [PMID: 23014526 DOI: 10.1158/1078-0432.CCR-12-0406]

15 **Lassman AB**, Roberts-Rapp L, Sokolova I, Song M, Pestova E, Kular R, Mullen C, Zha Z, Lu X, Gomez E, Bhathena A, Maag D, Kumthekar P, Gan HK, Scott AM, Guseva M, Holen KD, Ansell PJ, van den Bent MJ. Comparison of Biomarker Assays for *EGFR*: Implications for Precision Medicine in Patients with Glioblastoma. *Clin Cancer Res* 2019; **25**: 3259-3265 [PMID: 30796037 DOI: 10.1158/1078-0432.CCR-18-3034]

16 **Iacobuzio-Donahue CA**. Genetic evolution of pancreatic cancer: lessons learnt from the pancreatic cancer genome sequencing project. *Gut* 2012; **61**: 1085-1094 [PMID: 21749982 DOI: 10.1136/gut.2010.236026]

17 **Ducreux M**, Cuhna AS, CaramellaC, Hollebecque A, Burtin P, Goéré D, Seufferlein T, Haustermans K, Van Laethem JL, Conroy T, Arnold D; ESMO Guidelines Committee. Cancer of the pancreas: ESMO Clinical Practice Guidelines for diagnosis, treatment and follow-up. *Ann Oncol* 2015; **26** Suppl 5: v56-v68 [PMID: 26314780 DOI: 10.1093/annonc/mdv295]

18 **Matikas A**, Mistriotis D, Georgoulias V, Kotsakis A. Targeting KRAS mutated non-small cell lung cancer: A history of failures and a future of hope for a diverse entity. *Crit Rev OncolHematol* 2017; **110**: 1-12 [PMID: 28109399 DOI: 10.1016/j.critrevonc.2016.12.005]

19 **Blackford A**, Parmigiani G, Kensler TW, Wolfgang C, Jones S, Zhang X, Parsons DW, Lin JC, Leary RJ, Eshleman JR, Goggins M, Jaffee EM, Iacobuzio-Donahue CA, Maitra A, Klein A, Cameron JL, Olino K, Schulick R, Winter J, Vogelstein B, Velculescu VE, Kinzler KW, Hruban RH. Genetic mutations associated with cigarette smoking in pancreatic cancer. *Cancer Res* 2009; **69**: 3681-3688 [PMID: 19351817 DOI: 10.1158/0008-5472.CAN-09-0015]

20 **Reznik R**, Hendifar AE, Tuli R. Genetic determinants and potential therapeutic targets for pancreatic adenocarcinoma. *Front Physiol* 2014; **5**: 87 [PMID: 24624093 DOI: 10.3389/fphys.2014.00087]

21 **Cicenas J**, Kvederaviciute K, Meskinyte I, Meskinyte-Kausiliene E, Skeberdyte A, Cicenas J. KRAS, TP53, CDKN2A, SMAD4, BRCA1, and BRCA2 Mutations in Pancreatic Cancer. *Cancers (Basel)* 2017; **9** [PMID: 28452926 DOI: 10.3390/cancers9050042]

22 **Buscail L**, Bournet B, Cordelier P. Role of oncogenic KRAS in the diagnosis, prognosis and treatment of pancreatic cancer. *Nat Rev GastroenterolHepatol* 2020; **17**: 153-168 [PMID: 32005945 DOI: 10.1038/s41575-019-0245-4]

23 **Mishra NK**, Guda C. Genome-wide DNA methylation analysis reveals molecular subtypes of pancreatic cancer. *Oncotarget* 2017; **8**: 28990-29012 [PMID: 28423671 DOI: 10.18632/oncotarget.15993]

24 **Maitra A**, Hruban RH. Pancreatic cancer. *Annu Rev Pathol* 2008; **3**: 157-188 [PMID: 18039136 DOI: 10.1146/annurev.pathmechdis.3.121806.154305]

25 **Smith L**, Anti S, White N, Saldanha SN. The Genetics and Epigenetics of Colorectal Cancer Health Disparity. In: Epigenetic Mechanisms in Cancer. Elsevier, 2018: 87-115

26 **Wang G**, Zhao D, Spring DJ, DePinho RA. Genetics and biology of prostate cancer. *Genes Dev* 2018; **32**: 1105-1140 [PMID: 30181359 DOI: 10.1101/gad.315739.118]

27 **Herreros-Villanueva M**, Bujanda L. Non-invasive biomarkers in pancreatic cancer diagnosis: what we need *vs* what we have. *Ann Transl Med* 2016; **4**: 134 [PMID: 27162784 DOI: 10.21037/atm.2016.03.44]

28 **D'Costa JJ**, Goldsmith JC, Wilson JS, Bryan RT, Ward DG. A Systematic Review of the Diagnostic and Prognostic Value of Urinary Protein Biomarkers in Urothelial Bladder Cancer. *Bladder Cancer* 2016; **2**: 301-317 [PMID: 27500198 DOI: 10.3233/BLC-160054]

29 **Sattar Z**, Ali S, Hussain I, Sattar F, Hussain S, Ahmad S. Diagnosis of pancreatic cancer. In: Theranostic Approach for Pancreatic Cancer. Elsevier, 2019: 51-68

30 **Hess V**, Glimelius B, Grawe P, Dietrich D, Bodoky G, Ruhstaller T, Bajetta E, Saletti P, Figer A, Scheithauer W, Herrmann R. CA 19-9 tumour-marker response to chemotherapy in patients with advanced pancreatic cancer enrolled in a randomised controlled trial. *Lancet Oncol* 2008; **9**: 132-138 [PMID: 18249033 DOI: 10.1016/S1470-2045(08)70001-9]

31 **O'Brien DP**, Sandanayake NS, Jenkinson C, Gentry-Maharaj A, Apostolidou S, Fourkala EO, Camuzeaux S, Blyuss O, Gunu R, Dawnay A, Zaikin A, Smith RC, Jacobs IJ, Menon U, Costello E, Pereira SP, Timms JF. Serum CA19-9 is significantly upregulated up to 2 years before diagnosis with pancreatic cancer: implications for early disease detection. *Clin Cancer Res* 2015; **21**: 622-631 [PMID: 24938522 DOI: 10.1158/1078-0432.CCR-14-0365]

32 **Slesak B**, Harlozinska-Szmyrka A, Knast W, Sedlaczek P, van Dalen A, Einarsson R. Tissue polypeptide specific antigen (TPS), a marker for differentiation between pancreatic carcinoma and chronic pancreatitis. A comparative study with CA 19-9. *Cancer* 2000; **89**: 83-88 [PMID: 10897004 DOI: 10.1002/1097-0142(20000701)89:1<83::aid-cncr12>3.0.co;2-j]

33 **Kornek G**, Schenk T, Raderer M, Djavarnmad M, Scheithauer W. Tissue polypeptide-specific antigen (TPS) in monitoring palliative treatment response of patients with gastrointestinal tumours. *Br J Cancer* 1995; **71**: 182-185 [PMID: 7529527 DOI: 10.1038/bjc.1995.37]

34 **Jelski W**, Mroczko B. Biochemical Markers of Colorectal Cancer - Present and Future. *Cancer Manag Res* 2020; **12**: 4789-4797 [PMID: 32606968 DOI: 10.2147/CMAR.S253369]

35 **Hammarstrom S**, Shively JE, Paxton RJ, Beatty BG, Larsson A, Ghosh R, Bormer O, Buchegger F, Mach JP, Burtin P. Antigenic sites in carcinoembryonic antigen. *Cancer Res* 1989; **49**: 4852-4858 [PMID: 2474375]

36 **Wu FT**, Stefanini MO, Mac Gabhann F, Kontos CD, Annex BH, Popel AS. A systems biology perspective on sVEGFR1: its biological function, pathogenic role and therapeutic use. *J Cell Mol Med* 2010; **14**: 528-552 [PMID: 19840194 DOI: 10.1111/j.1582-4934.2009.00941.x]

37 **Seo Y**, Baba H, Fukuda T, Takashima M, Sugimachi K. High expression of vascular endothelial growth factor is associated with liver metastasis and a poor prognosis for patients with ductal pancreatic adenocarcinoma. *Cancer* 2000; **88**: 2239-2245 [PMID: 10820344 DOI: 10.1002/(sici)1097-0142(20000515)88:10<2239::aid-cncr6>3.0.co;2-v]

38 **Stacker SA**, Achen MG. The VEGF signaling pathway in cancer: the road ahead. *Chin J Cancer* 2013; **32**: 297-302 [PMID: 23419196 DOI: 10.5732/cjc.012.10319]

39 **Warde-Farley D**, Donaldson SL, Comes O, Zuberi K, Badrawi R, Chao P, Franz M, Grouios C, Kazi F, Lopes CT, Maitland A, Mostafavi S, Montojo J, Shao Q, Wright G, Bader GD, Morris Q. The GeneMANIA prediction server: biological network integration for gene prioritization and predicting gene function. *Nucleic Acids Res* 2010; **38**: W214-W220 [PMID: 20576703 DOI: 10.1093/nar/gkq537]

40 **Kim ST**, Lim DH, Jang KT, Lim T, Lee J, Choi YL, Jang HL, Yi JH, Baek KK, Park SH, Park YS, Lim HY, Kang WK, Park JO. Impact of KRAS mutations on clinical outcomes in pancreatic cancer patients treated with first-line gemcitabine-based chemotherapy. *Mol Cancer Ther* 2011; **10**: 1993-1999 [PMID: 21862683 DOI: 10.1158/1535-7163.MCT-11-0269]

41 **Ghimessy A**, Radeczky P, Laszlo V, Hegedus B, Renyi-Vamos F, Fillinger J, Klepetko W, Lang C, Dome B, Megyesfalvi Z. Current therapy of KRAS-mutant lung cancer. *Cancer Metastasis Rev* 2020; **39**: 1159-1177 [PMID: 32548736 DOI: 10.1007/s10555-020-09903-9]

42 **Hezel AF**, Kimmelman AC, Stanger BZ, Bardeesy N, Depinho RA. Genetics and biology of pancreatic ductal adenocarcinoma. *Genes Dev* 2006; **20**: 1218-1249 [PMID: 16702400 DOI: 10.1101/gad.1415606]

43 **Kodaz H**, Kostek O, Hacioglu MB, Erdogan B, Kodaz CE, Hacibekiroglu I, Turkmen E, Uzunoglu S, Cicin I. Frequency of RAS mutations (KRAS, NRAS, HRAS) in human solid cancer. *Breast Cancer* 2017; 7 [DOI: 10.14744/ejmo.2017.22931]

44 **Kim D**, Xue JY, Lito P. Targeting KRAS(G12C): From Inhibitory Mechanism to Modulation of Antitumor Effects in Patients. *Cell* 2020; **183**: 850-859 [PMID: 33065029 DOI: 10.1016/j.cell.2020.09.044]

45 **Boeck S**, Ormanns S, Haas M, Bächmann S, Laubender RP, Siveke JT, Jung A, Kirchner T, Heinemann V. Translational research in pancreatic cancer: KRAS and beyond. *Pancreas* 2014; **43**: 150-152 [PMID: 24326376 DOI: 10.1097/MPA.0b013e31829629f6]

46 **Wong W**, Raufi AG, Safyan RA, Bates SE, Manji GA. BRCA Mutations in Pancreas Cancer: Spectrum, Current Management, Challenges and Future Prospects. *Cancer Manag Res* 2020; **12**: 2731-2742 [PMID: 32368150 DOI: 10.2147/CMAR.S211151]

47 **Goggins M**, Schutte M, Lu J, Moskaluk CA, Weinstein CL, Petersen GM, Yeo CJ, Jackson CE, Lynch HT, Hruban RH, Kern SE. Germline BRCA2 gene mutations in patients with apparently sporadic pancreatic carcinomas. *Cancer Res* 1996; **56**: 5360-5364 [PMID: 8968085]

48 **Maitra A**, Kern SE, Hruban RH. Molecular pathogenesis of pancreatic cancer. *Best Pract Res ClinGastroenterol* 2006; **20**: 211-226 [PMID: 16549325 DOI: 10.1016/j.bpg.2005.10.002]

49 **van Kampen JG**, Marijnissen-van Zanten MA, Simmer F, van der Graaf WT, Ligtenberg MJ, Nagtegaal ID. Epigenetic targeting in pancreatic cancer. *Cancer Treat Rev* 2014; **40**: 656-664 [PMID: 24433955 DOI: 10.1016/j.ctrv.2013.12.002]

50 **Moore PS**, Orlandini S, Zamboni G, Capelli P, Rigaud G, Falconi M, Bassi C, Lemoine NR, Scarpa A. Pancreatic tumours: molecular pathways implicated in ductal cancer are involved in ampullary but not in exocrine nonductal or endocrine tumorigenesis. *Br J Cancer* 2001; **84**: 253-262 [PMID: 11161385 DOI: 10.1054/bjoc.2000.1567]

51 **Gerdes B**, Ramaswamy A, Ziegler A, Lang SA, Kersting M, Baumann R, Wild A, Moll R, Rothmund M, Bartsch DK. p16INK4a is a prognostic marker in resected ductal pancreatic cancer: an analysis of p16INK4a, p53, MDM2, an Rb. *Ann Surg* 2002; **235**: 51-59 [PMID: 11753042 DOI: 10.1097/00000658-200201000-00007]

52 **Dammann R**, Schagdarsurengin U, Liu L, Otto N, Gimm O, Dralle H, Boehm BO, Pfeifer GP, Hoang-Vu C. Frequent RASSF1A promoter hypermethylation and K-ras mutations in pancreatic carcinoma. *Oncogene* 2003; **22**: 3806-3812 [PMID: 12802288 DOI: 10.1038/sj.onc.1206582]

53 **Lawrence YR**, Moughan J, Magliocco AM, Klimowicz AC, Regine WF, Mowat RB, DiPetrillo TA, Small W Jr, Simko JP, Golan T, Winter KA, Guha C, Crane CH, Dicker AP. Expression of the DNA repair gene MLH1 correlates with survival in patients who have resected pancreatic cancer and have received adjuvant chemoradiation: NRG Oncology RTOG Study 9704. *Cancer* 2018; **124**: 491-498 [PMID: 29053185 DOI: 10.1002/cncr.31058]

World Journal of Gastroenterology

Submit a Manuscript: https://www.f6publishing.com

World J Gastroenterol 2021 September 28; 27(36): 6110-6127

DOI: 10.3748/wjg.v27.i36.6110

ISSN 1007-9327 (print) ISSN 2219-2840 (online)

ORIGINAL ARTICLE

Retrospective Study

Impact of radiogenomics in esophageal cancer on clinical outcomes: A pilot study

Valentina Brancato, Nunzia Garbino, Lorenzo Mannelli, Marco Aiello, Marco Salvatore, Monica Franzese, Carlo Cavaliere

ORCID number: Valentina Brancato 0000-0002-6232-7645; Nunzia Garbino 0000-0001-6863-7313; Lorenzo Mannelli 0000-0002-9102-4176; Marco Aiello 0000-0002-3676-0664; Marco Salvatore 0000-0001-9734-7702; Monica Franzese 0000-0002-6490-7694; Carlo Cavaliere 0000-0002-3297-2213.

Author contributions: Brancato V performed the research and wrote the manuscript; Franzese M, Mannelli L and Aiello M contributed to the conception and design of the study and to the acquisition and interpretation of the data; Garbino N, Franzese M and Brancato V contributed to the data curation and processing; Franzese M, Salvatore M, Aiello M and Mannelli L revised the article; Cavaliere C designed the research and approved the final version for publication.

Institutional review board statement: The study was conducted in accordance with the Declaration of Helsinki, and the study protocol was approved by the Ethics Committee of the Istituto Nazionale Tumori "Fondazione G. Pascale (protocol number 1/20).

Informed consent statement: Patients were not required to give informed consent to the study

Valentina Brancato, Nunzia Garbino, Lorenzo Mannelli, Marco Aiello, Marco Salvatore, Monica Franzese, Carlo Cavaliere, IRCCS SDN, Naples 80143, Italy

Corresponding author: Lorenzo Mannelli, MD, PhD, Professor, IRCCS SDN, Via E. Gianturco, Naples 80143, Italy. mannellilorenzo@yahoo.it

Abstract

BACKGROUND

Esophageal cancer (ESCA) is the sixth most common malignancy in the world, and its incidence is rapidly increasing. Recently, several microRNAs (miRNAs) and messenger RNA (mRNA) targets were evaluated as potential biomarkers and regulators of epigenetic mechanisms involved in early diagnosis. In addition, computed tomography (CT) radiomic studies on ESCA improved the early stage identification and the prediction of response to treatment. Radiogenomics provides clinically useful prognostic predictions by linking molecular characteristics such as gene mutations and gene expression patterns of malignant tumors with medical images and could provide more opportunities in the management of patients with ESCA.

AIM

To explore the combination of CT radiomic features and molecular targets associated with clinical outcomes for characterization of ESCA patients.

METHODS

Of 15 patients with diagnosed ESCA were included in this study and their CT imaging and transcriptomic data were extracted from The Cancer Imaging Archive and gene expression data from The Cancer Genome Atlas, respectively. Cancer stage, history of significant alcohol consumption and body mass index (BMI) were considered as clinical outcomes. Radiomic analysis was performed on CT images acquired after injection of contrast medium. In total, 1302 radiomics features were extracted from three-dimensional regions of interest by using PyRadiomics. Feature selection was performed using a correlation filter based on Spearman's correlation (ρ) and Wilcoxon-rank sum test respect to clinical outcomes. Radiogenomic analysis involved ρ analysis between radiomic features associated with clinical outcomes and transcriptomic signatures consisting of eight N6-methyladenosine RNA methylation regulators and five up-regulated

miRNA. The significance level was set at $P < 0.05$.

RESULTS

Of 25, five and 29 radiomic features survived after feature selection, considering stage, alcohol history and BMI as clinical outcomes, respectively. Radiogenomic analysis with stage as clinical outcome revealed that six of the eight mRNA regulators and two of the five up-regulated miRNA were significantly correlated with ten and three of the 25 selected radiomic features, respectively ($-0.61 < \rho < -0.60$ and $0.53 < \rho < 0.69$, $P < 0.05$). Assuming alcohol history as clinical outcome, no correlation was found between the five selected radiomic features and mRNA regulators, while a significant correlation was found between one radiomic feature and three up-regulated miRNAs ($\rho = -0.56$, $\rho = -0.64$ and $\rho = 0.61$, $P < 0.05$). Radiogenomic analysis with BMI as clinical outcome revealed that four mRNA regulators and one up-regulated miRNA were significantly correlated with 10 and two radiomic features, respectively ($-0.67 < \rho < -0.54$ and $0.53 < \rho < 0.71$, $P < 0.05$).

CONCLUSION

Our study revealed interesting relationships between the expression of eight N6-methyladenosine RNA regulators, as well as five up-regulated miRNAs, and CT radiomic features associated with clinical outcomes of ESCA patients.

Key Words: Esophageal cancer; Radiogenomics; Computed tomography; Radiomics; MicroRNAs; N6-methyladenosine

Core Tip: This is a retrospective study aiming at investigating the relationship between the expression levels of transcriptomic features (eight N6-methyladenosine RNA methylation regulators and five up-regulated microRNAs) and radiomic features extracted from computed tomography images that were significantly associated to clinical outcomes (stage, alcohol history, body mass index) in patients with esophageal cancer . Radiogenomic analysis revealed significant correlations between the expression of the N6-methyladenosine RNA regulators, as well as five up-regulated microRNAs, and several computed tomography radiomic features associated with three investigated clinical outcomes of esophageal cancer patients.

Citation: Brancato V, Garbino N, Mannelli L, Aiello M, Salvatore M, Franzese M, Cavaliere C. Impact of radiogenomics in esophageal cancer on clinical outcomes: A pilot study. *World J Gastroenterol* 2021; 27(36): 6110-6127
URL: https://www.wjgnet.com/1007-9327/full/v27/i36/6110.htm
DOI: https://dx.doi.org/10.3748/wjg.v27.i36.6110

INTRODUCTION

Esophageal cancer (ESCA) is one of the most common malignancies and ranks sixth as a cause of lethal cancer worldwide[1]. Despite the different types of treatment, ESCA remains a devastating pathology with an overall 5-year survival rate of 15%–25%. The main issue related to ESCA is that, given the late symptoms manifestation, most patients are diagnosed with advanced-stage ESCA characterized by unresectability or metastatic disease, for which the best treatment choices are palliative interventions such as concurrent chemoradiotherapy and combination chemotherapy[2,3]. The majority of ESCAs fall into two main histologic subtypes: Esophageal adenocarcinoma and esophageal squamous cell carcinoma (ESCC)[4]. Imaging plays a key role in each step of the management of ESCA. Computed tomography (CT) plays an important role in the diagnosis, staging and treatment guidance of ESCA. This imaging technique allows to evaluate the loco-regional extension of ESCA by showing the extent of involvement of the esophageal wall by tumor, as well as the tumor invasion of the peri-esophageal fat[5]. Moreover, it is also useful to detect the presence of distant

because the analysis used anonymous clinical data that were obtained after each patient agreed to treatment by written consent.

Conflict-of-interest statement: The authors declare that there is no conflict of interest in this study.

Data sharing statement: No additional data are available.

Manuscript source: Unsolicited manuscript

Specialty type: Oncology

Country/Territory of origin: Italy

Peer-review report's scientific quality classification
Grade A (Excellent): A
Grade B (Very good): 0
Grade C (Good): C, C
Grade D (Fair): 0
Grade E (Poor): E

Received: March 2, 2021
Peer-review started: March 2, 2021
First decision: June 3, 2021
Revised: June 16, 2021
Accepted: July 30, 2021
Article in press: July 30, 2021
Published online: September 28, 2021

P-Reviewer: Barad AK, Endo S, Hamaya Y
S-Editor: Zhang H
L-Editor: Filipodia
P-Editor: Xing YX

metastases[6,7]. However, CT has several limitations associated with the ability to evaluate the intra-tumor heterogeneity of the ESCA, as well as in visually distinguishing the post-treatment residual tumor[8,9].

Therefore, since it is well-recognized that information arising from images may be substantially enhanced by quantitative imaging analysis, the radiomics role has rapidly increased in the last decade for cancer applications, including those related to ESCA[10-12]. Radiomics is evolving as medical technology and is currently one of the most interesting research fields. Through radiomics, quantitative data can be extrapolated from diagnostic images, and these extracted parameters (radiomic features) have the potential to identify tumor characteristics[10,11,13]. The innovative field of radiomics could provide opportunities in the management of ESCA patients for improvements in every step of ESCA management[12,14]. Recent studies on CT radiomics in ESCA analyzed CT radiomics features for several steps of ESCA management, such as preoperative stage identification[15] and prediction of response to treatment[3,16].

On the other hand, the emerging clinical relevance of genomics in cancer medicine by applying the next generation sequencing technologies has provided unprecedented opportunities to understand the biological basis of different cancer types, identify genomic biomarkers in carcinogenesis, identify potential bio-molecular targets for drug response and resistance and to guide clinical decision-making regarding the personalized medicine and the clinical practice[17,18].

Gene expression profiling can improve knowledge about the molecular alterations during carcinogenesis. Biomarkers of these molecular alterations, in turn, may be useful in diagnosing cancers, particularly early, curable cancers. Recently, results from gene expression data analyses have made it possible to investigate the complex pathological mechanisms involved in ESCA, with the aim to discover novel molecular markers for tumor diagnosis and to customize therapy based on an individual tumor genetic composition[19-21]. Several microRNA (miRNA), such as miR-93, miR-21, miR-4746 and miR-196a, were evaluated as potential biomarkers for the early diagnosis of cancer, highlighting their diagnostic values[22]. Recently, several studies also suggested that N6-methyladenosine (m6A) methylation can play a crucial role in cancer progression by regulating biological functions that affect noncoding RNA expression[23,24] In particular, a recent study[25] highlighted the role of m6A methylation regulators aberrantly expressed in ESCA to predict clinical outcomes.

Combining radiomic features with molecular and genomic characteristics can provide insights to characterize tumor phenotype[26]. In this direction, radiogenomics, as a new field that provides clinically useful prognostic predictions by linking molecular characteristics such as gene mutations and gene expression patterns of malignant tumors with medical images, could provide more opportunities in the management of patients with ESCA for improvements in staging, predicting treatment response and survival[7,21]. Based on promising results obtained from preliminary CT-based radiomics studies on ESCA[16,27] and considering the capability of miRNAs as potential biomarkers able to characterize differential expression of different cancer tissues, as well as the critical role of m6A as epigenetic regulator in cancer biology, we aimed to combine these findings in a radiogenomic study, using appropriate variables as clinical endpoints. Specifically, we used the preoperative ESCA stage as a clinical outcome, since the survival of ESCA patients with early stage (stage I−II) could be up to 85%[28]. Additionally, surgical resection, chemoradiation or other optimal therapeutic approaches depend on accurate preoperative staging. Therefore, accurate preoperative staging is important for predicting prognosis and choosing a suitable therapeutic strategy for patients with ESCA[15]. We also used the history of significant alcohol consumption as a clinical outcome, since this is considered as one of the major risk factors for ESCA[29]. Lastly, we evaluated body mass index (BMI) as a clinical outcome, due to its association with increased risk of ESCA[30,31].

Using publicly available integrated ESCA cohort from The Cancer Genome Atlas (TCGA) and The Cancer Imaging Archive (TCIA)[32,33], we aimed at investigating possible relationships between CT-radiomic features associated with the three above-mentioned clinical outcomes and correlated with esophageal up-regulated miRNAs, which were *in silic*o-validated from Zeng *et al*[22], in order to evaluate potential biomarkers for the early diagnosis of ESCA. Furthermore, we evaluated if the same CT-radiomics features could be associated with epigenetic signatures, considering m6A RNA methylation regulators-based prognostic signature for ESCA from Xu *et al* [25] in order to support important information for developing diagnostic and therapeutic strategies.

MATERIALS AND METHODS

Patient population and definition of clinical outcomes

The study was conducted in accordance with the Declaration of Helsinki, and the study protocol was approved by the Ethics Committee of the Istituto Nazionale Tumori "Fondazione G. Pascale (protocol number 1/20). Sixteen patients with diagnosed ESCA were extrapolated by combining the public databases TCIA-TCGA and included in this study[32,33]. All subjects performed CT investigation with iodized contrast medium injection. Of 16 patients, one was excluded due to the presence of artifacts on acquired images. Due to their availability for all 15 patients, the transcriptome profiling and the following clinical variables were extracted and considered as outcomes for this study: Cancer stage, history of significant alcohol consumption and BMI value. We did not perform analyses on smoking measurements (tobacco history, age at starting smoking, pack-year smoked) due to the incompleteness of these data. To perform radiogenomic analyses, we divided patients into two groups according to stages I−II or III−IV, making stage outcome binary. Refer to Table 1 for clinical characteristics and outcomes of included patients.

Image acquisition and processing

CT examinations were acquired on GE Medical Systems (9 patients) and Siemens (6 patients) CT scanner, with slice thickness ranging from 1.25 mm to 2.5 mm and pixel size varying from 0.67 to 0.9. three-dimensional (3D) regions of interest (ROIs) encompassing the tumor were manually delineated slice-by-slice by using ITK-SNAP (version 3.6.0, http://www.itksnap.org) on the post-administration of contrast agents CT images. The tumor localization was divided into three regions: 7 patients presented lesions at the middle level, 2 subjects in the middle/distal area and 6 patients in the distal esophagus.

Gray-levels normalization was not performed, since CT gray values reflect absolute world values (Hounsfield units) and should be comparable between scanners. To correct variability from parameters related to voxel size and so unify voxel size across the cohort, radiomics data were extracted from images resampled to isotropic voxels of $1 \times 1 \times 1$ mm^3 using B Spline interpolator.

Radiomic analysis

Radiomic features extraction: A total of 1302 radiomics features were extracted from segmented ROIs by using the open source Python package PyRadiomics (https://pyradiomics.readthedocs.io/en/Latest/). The extracted radiomics features were categorized into five groups: (1) Shape features (n = 14); (2) First-order features including 18 intensity statistics; (3) 74 multi-dimensional texture features including 23 gray level co-occurrence matrix (GLCM), 16 gray level size zone matrix (GLSZM), 16 gray level run length matrix (GLRLM), 14 gray level dependence matrix (GLDM) and 5 neighboring gray tone difference matrix (NGTDM) features; 1196 transformed first-order and textural features including; (4) 736 wavelet features in frequency channels LHL, LLH, HHH, HLH, HLL,HHL, LHH and LLL, where L and H are low- and high-pass filters, respectively; and (5) 460 LoG filtered features with sigma ranging from 1.0 and 5.0, with step size = 1. Features of groups (2) and (3) were grouped together and, from now on, this group will be referred to as "original features". The extracted radiomics features grouped by similarity in four categories are listed in the Supplementary Table 1. The computing algorithms can be found at www.radiomics.io and the image biomarker standardization initiative presented a document to standardize the nomenclature and definition of radiomic features[34].

Radiomic features selection: Features selection was performed separately for shape features, original features, wavelet features and LoG filtered features in two steps, followed by a third step involving the whole set of features passed through the step I and II. In the first step, a correlation filter based on the absolute values of pairwise Spearman's correlation (ρ) coefficient was used to reduce feature redundancy. Threshold for ρ was set to 0.8. Briefly, if two features had $\rho > 0.8$, the function looks at the mean absolute correlation of each variable and the variable with the largest mean absolute correlation is removed. The second step varied according to the type of outcome variables. For binary outcomes, a further feature restriction through a univariate analysis was performed by using non-parametric Wilcoxon rank-sum test to investigate the statistical significance with respect to the outcome. Statistical significance was set to $P < 0.05$. The significantly different features were then selected and further reduced in the third step. For continuous outcomes, the second step

Table 1 Characteristics of included patients

Clinical characteristic	Value
Age (mean ± SD)	56.8 ± 8.65
Sex, *n* (%)	
Male	12 (20)
Female	3 (80)
Histologic diagnosis, *n* (%)	
EAC	2 (13.3)
ESCC	13 (86.7)
Cancer stage, *n* (%)	
I-II	4 (26.7)
III-IV	11 (73.3)
TNM staging	
Primary tumor (T)	
T1	3 (20)
T2	2 (13.3)
T3	8 (53.4)
T4	2 (13.3)
Regional lymph nodes (N)	
N0	4 (26.7)
N1	6 (40)
N2	3 (20)
N3	2 (13.3)
Distant metastases (M)	
M0	12 (80)
M1	3 (20)
Alcohol history, *n* (%)	
Yes	8 (53)
No	7 (47)
Smoking history, *n* (%)	
Lifelong non-smoker	1 (6.6)
Current smoker	7 (46.6)
Current reformed smoker	2 (13.3)
Current reformed smoker for > 15 yr	1 (6.6)
NA	4 (26.6)
Age at starting smoking	
Under 18 yr old	6 (40)
Over 18 yr old	3 (20)
NA	6 (40)
Pack-year smoked	
Under 10	6 (40)
Over 10	3 (20)
NA	6 (40)

BMI (mean ± SD)	20.8 ± 3.55

BMI: Body mass index; EAC: Esophagus adenocarcinoma; ESCC: Esophagus squamous cell carcinoma; TNM: tumor, node, and metastasis classification (classification of malignant tumors).

consisted of computing ρ between each feature selected through the step I and the reference outcome. Then, all features with a significant ρ > 0.5 and *P* value < 0.05 were considered. In order to check for redundancies among features belonging to the different four groups, the third step consisted in applying the correlation filter described in step I to the whole feature set passed through step II. All steps were implemented using Matlab R2020a (The MathWorks Inc., Natick, MA, United States).

Predictive models building and analysis for stage assessment: In order to evaluate the predictive power of CT radiomic features taken by them for ESCA staging, a fourth step of feature selection was performed for features that were associated with stage. The latter step consisted in ranking the remaining features based on the mutual information (MI) between the distribution of the values of a certain feature and the membership to a particular class. Features were evaluated independently, and the final feature selection occurred by aggregating the five top ranked ones[35-37]. For the binary stage I-II/stage III-IV classification task, the reduced feature set was used to build logistic regression models of order from 1 to 5 that would best predict ESCA stage by using an imbalanced-adjusted bootstrap resampling (IABR) approach on 1000 bootstrap samples[38]. Specifically, the training set was made up 1000 bootstrap samples randomly drawn with replacement from the available dataset. The testing set consisted of the instances that did not belong to the bootstrap sample. Then, application of the imbalance-adjustment step made the probability of picking a positive and a negative instance in the bootstrap sample the same[39-41].

For each model order, the combination of features maximizing the 0.632+ area under the receiver operating characteristic curve (AUC) within 1000 bootstrap training and testing samples was identified. Finally, IABR on 1000 samples was performed again for all models to assess prediction performances[38,42].

Additional analyses were performed starting from the first two, three and four features surviving after the MI-based feature selection step (which was used to build logistic regression models of order from 1 to 2, 1 to 3 and 1 to 4, respectively) that would best predict ESCA stage. Moreover, given that the overall stage is determined after the cancer is assigned categories describing the tumor (T), node (N) and metastasis (M) categories, we tested the capability of these features for predicting T and N status. Analyses assuming M status as clinical outcome were not performed due to the extremely unbalanced sample. Patients were divided into two groups according to T1-T2 or T3−T4 tumor status, making T stage outcome binary. Similarly, we evaluated if CT radiomic features could assess N status by dividing patients into two groups according to the absence (N0) or presence (N1-N2-N3) lymph node status[43].

Transcriptomic data collection

RNA-Seq and miRNA-Seq data of esophageal carcinoma of tumor tissues were downloaded from the GDC Data Portal (https://gdc-portal.nci.nih.gov/) considering for TCGA-ESCA project only patients with associated imaging data from TCIA database (see Supplementary Tables 2 and 3 for Clinical and Transcriptomic data, respectively). The mRNAs expression levels were considered as read count based on gene length and the total number of mapped reads (FPKM values). Moreover, miRNA expression quantification was downloaded and normalized counts in reads-per-million-miRNA-mapped were considered.

Radiogenomic analysis

An integrative study design was defined (see Figure 1 for the flowchart reporting the organization of data and analyses in the study) and reported as radiogenomic workflow in Figure 2 in order to evaluate potential association between significant radiomic features according to selected clinical variables (stage, history of significant alcohol consumption and BMI) with biomarkers and RNA regulators characterizing esophageal cancer. For this purpose, a Spearman's correlation analysis was investigated between radiomic features selected after the three features selection steps described above and transcriptomic signatures suggested by Zeng *et al*[22] and Xu *et al*[25]. Specifically, we calculated ρ between the whole selected feature set and the eight

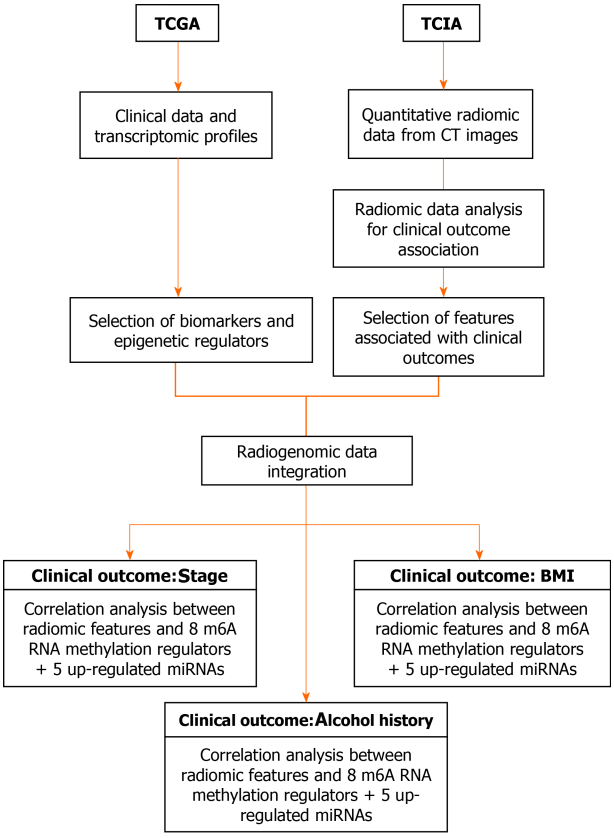

Figure 1 Flowchart reporting the organization of data and analyses in the study. BMI: Body mass index; CT: Computed tomography; TCGA: The Cancer Genome Atlas; TCIA: The Cancer Imaging Archive.

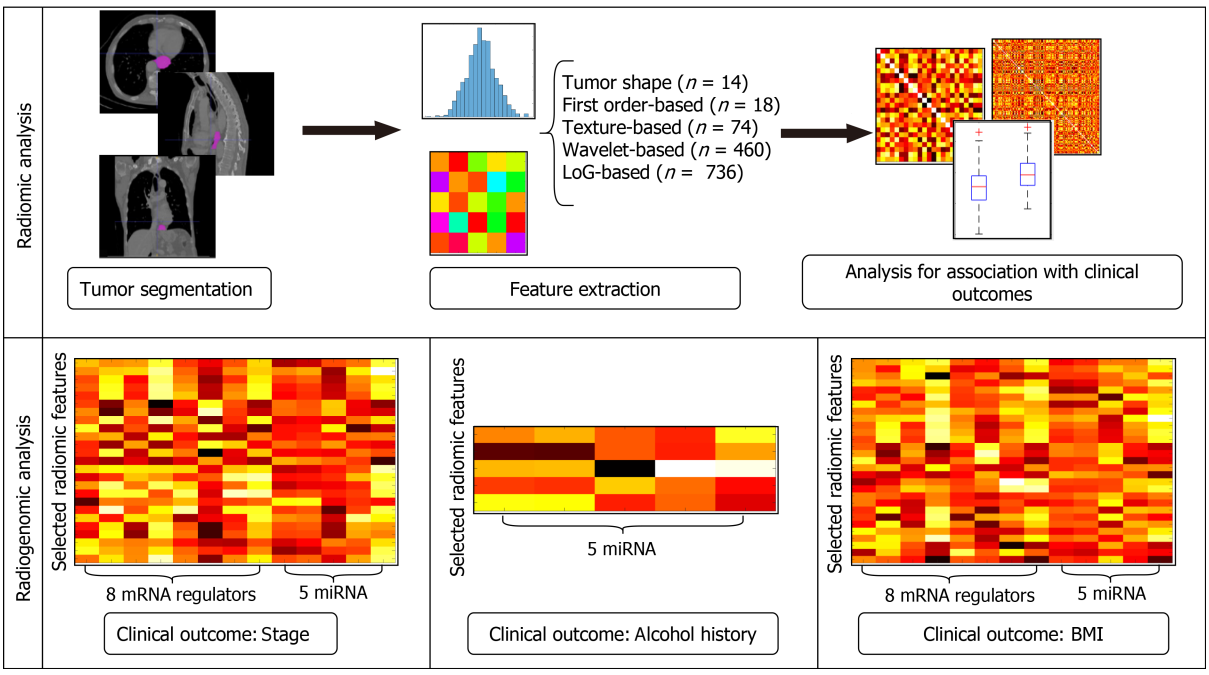

Figure 2 Workflow of radiogenomic analysis implemented in the study. On the first row the radiomic analysis steps. On the second row the radiogenomic analysis for each clinical outcome. BMI: Body mass index; miRNA: MicroRNA; mRNA: Messenger RNA.

m6A RNA methylation regulators (KIAA1429, HNRNPC, RBM15, METTL3, WTAP, YTHDF1, YTHDC1, YTHDF2), as well as ρ between the whole selected feature set and the five up-regulated miRNAs (miRNA-93, miRNA-21, miRNA-4746, miRNA-196a-1, miRNA-196a-2). The significance level was set to 0.05. All analyses were performed

using Matlab R2020a. The statistical methods of this study were reviewed by our bioinformatics and biostatistics group of our research support center.

RESULTS

Radiomic analysis

Radiomic feature selection: None of the 14 shape features passed the step II of features selection, both considering binary outcomes (namely stage and alcohol history) and BMI. So, radiogenomic analysis was not performed for this feature group. Concerning original, wavelet and Log sigma feature groups, the step I of feature selection reduced the feature sets from 92, 736 and 460 to 23, 127 and 65, respectively. Concerning stage analysis, Wilcoxon rank-sum test used in step II of feature selection revealed significant results for 26 radiomic features, of which 25 belonging to the wavelet feature set and the remaining one was the original first order maximum value. However, the latter feature did not pass the second correlation filter of step III (refer to Table 2). Considering the presence of alcoholic history as clinical outcome, Wilcoxon rank-sum test revealed significant results for five features, of which one belonging to original feature set (Kurtosis) and the remaining ones to wavelet feature set. These five features passed step III, since Kurtosis showed a correlation lower than 0.8 with all four wavelet features (refer to Table 2). Lastly, considering BMI as the clinical outcome, 26 wavelet and three LoG sigma features were selected due to a significant $\rho > 0.5$ ($P < 0.05$) with BMI. In total, 29 radiomic features (see Table 3) survived after the second correlation filter and were associated with the three examined clinical outcomes.

Predictive models building and analysis for stage assessment: The top five features selected after the MI-based feature selection step were wavelet LLH GLDM high gray level emphasis, LLH NGTDM complexity, HHH GLCM joint entropy, HLH entropy and HLL GLCM cluster prominence. Prediction performances of multivariable logistic regression models for the stage I-II/stage III-IV classification task were very high for both five model orders. However, by inspecting prediction performances values in Table 4, we determined that the simplest multivariable model with the best prediction performances were reached by the second order model (AUC = 87%, sensitivity = 64%, specificity = 83% and accuracy = 79%), which was based on wavelet LLH NGTDM complexity and HHH GLCM joint entropy. These results were also confirmed by additional analyses (Supplementary Tables 4-6). The top five features were also found to be able to predict T and N staging, with best AUCs (0.79 and 0.80, respectively) reached by second order models (see Supplementary Tables 7 and 8 for analyses involving five features). Results of additional analyses for T and N prediction by using two, three and four features are reported in Supplementary Tables 9-11 (T staging) and Supplementary Tables 12-14 (N staging).

Radiogenomic analysis

Stage: Overall, radiogenomic analysis revealed that six of the eight mRNA regulators were significantly correlated with 10 of the 25 selected radiomic features, which were all belonging to the wavelet group. In particular, HRNPC and WTAP were positively correlated with wavelet HHL NGTDM strength ($\rho = 0.61$, $\rho = 0.61$, $P < 0.05$, respectively); METTL3 was positively correlated with wavelet LHL GLDM high gray level emphasis, HLL GLRLM gray level variance, HLL GLDM dependence entropy and LLL GLDM small dependence high gray level emphasis ($\rho = 0.54$, $\rho = 0.53$, $\rho = 0.56$, $\rho = 0.6$, $P < 0.05$, respectively) and negatively correlated with wavelet HLL GLCM inverse variance ($\rho = -0.6$, $P < 0.05$); YTHDF1 reported a positive and significant correlation with the wavelet feature HLL GLCM maximum probability ($\rho = 0.6$, $P < 0.05$) and a negative correlation with HLL 90th percentile ($\rho = -0.61$, $P < 0.05$); YTHDF2 was positively correlated with the wavelet feature HHH GLCM contrast and HHH GLSZM zone percentage ($\rho = 0.57$, $\rho = 0.56$, $P < 0.05$, respectively); the latter feature was also positively correlated with YTHDC1 ($\rho = 0.6$, $P < 0.05$). Moreover, correlation analysis with the five up-regulated miRNA revealed a significant positive correlation between miRNA-93 and two radiomic features, namely wavelet LHL GLDM high gray level emphasis ($\rho = 0.69$, $P < 0.05$) and HHH GLCM joint entropy ($\rho = 0.58$, $P < 0.05$). Notably, HHH GLCM joint entropy contributed to building the best predictive models for stage assessment, as well as T and N assessment. Finally, a positive correlation between miRNA-4746 and HHL GLCM cluster shade was found ($\rho = 0.53$, $P < 0.05$). The radiogenomic results for stage are shown through a heatmap in the Figure 3.

Table 2 Selected radiomic features after the three feature selection steps for binary outcomes

Selected radiomic features, stage	Stage I-II, mean ± SD	Stage III-IV, mean ± SD	*P* value
Wavelet-HLH first order entropy	0.62 ± 0.13	0.21 ± 0.31	0.031
Wavelet-LHL GLDM high gray level emphasis	0.59 ± 0.32	0.21 ± 0.21	0.044
Wavelet-HLL GLDM high gray level run emphasis	0.67 ± 0.37	0.2 ± 0.18	0.019
Wavelet-HLL GLDM gray level variance	0.74 ± 0.29	0.22 ± 0.29	0.007
Wavelet-HLL GLDM cluster prominence	0.59 ± 0.36	0.14 ± 0.3	0.019
Wavelet-HLL GLDM inverse variance	0.27 ± 0.3	0.68 ± 0.23	0.028
Wavelet-HLL GLDM maximum probability	0.14 ± 0.17	0.58 ± 0.32	0.042
Wavelet-HLL GLDM dependence entropy	0.78 ± 0.18	0.42 ± 0.25	0.028
Wavelet-HLL GLDM dependence variance	0.2 ± 0.21	0.48 ± 0.26	0.044
Wavelet-HLL GLSZM size zone non uniformity	0.69 ± 0.39	0.15 ± 0.15	0.028
Wavelet-HLL GLSZM small area low gray level emphasis	0.02 ± 0.03	0.24 ± 0.33	0.041
Wavelet-HLL first order 90 percentile	0.55 ± 0.39	0.17 ± 0.16	0.029
Wavelet-HHH GLRLM gray level non uniformity normalized	0.39 ± 0.27	0.87 ± 0.19	0.007
Wavelet-HHH GLCM joint entropy	0.68 ± 0.22	0.2 ± 0.27	0.021
Wavelet-HHH GLCM Contrast	0.78 ± 0.19	0.45 ± 0.25	0.021
Wavelet-HHH GLSZM gray level variance	0.91 ± 0.11	0.3 ± 0.39	0.021
Wavelet-HHH GLSZM zone percentage	0.83 ± 0.13	0.35 ± 0.34	0.029
Wavelet-HHH first order 10 percentile	0.11 ± 0.08	0.46 ± 0.35	0.029
Wavelet-HHL NGTDM strength	0.66 ± 0.3	0.28 ± 0.3	0.044
Wavelet-HHL GLCM cluster shade	0.51 ± 0.49	0.04 ± 0.03	0.007
Wavelet-HHL first order Entropy	0.68 ± 0.33	0.27 ± 0.21	0.029
Wavelet-HHL first order mean absolute deviation	0.66 ± 0.35	0.25 ± 0.18	0.029
Wavelet-LLH NGTDM complexity	0.23 ± 0.13	0.13 ± 0.29	0.044
Wavelet-LLH GLDM high gray level emphasis	0.34 ± 0.23	0.14 ± 0.29	0.044
Wavelet-LLL GLDM small dependence high gray level emphasis	0.67 ± 0.32	0.25 ± 0.22	0.029
Selected radiomic features (alcohol history)	**No alcohol history (mean ± SD)**	**Alcohol history (mean ± SD)**	***P* value**
Original first order kurtosis	0.37 ± 0.32	0.12 ± 0.12	0.037
Wavelet-LHH first order interquartile range	0.24 ± 0.24	0.5 ± 0.25	0.049
Wavelet-LHH first order mean	0.94 ± 0.04	0.75 ± 0.31	0.013
Wavelet-HHL first order median	0.62 ± 0.2	0.37 ± 0.19	0.026
Wavelet-LLH first order uniformity	0.68 ± 0.27	0.41 ± 0.26	0.037

The first column includes the two binary clinical outcomes investigated in this study (stage, alcohol history). GLCM: Gray level co-occurrence matrix; GLDM: Gray level dependence matrix; GLRLM: Gray level run length matrix; GLSZM: Gray level size zone matrix; H: High-pass filter; L: Low-pass filter; NGTDM: Neighboring gray tone difference matrix; SD: Standard deviation.

Alcohol history: From the integrated analysis, none of the five selected radiomic features was significantly correlated with any of eight RNA regulators (data not shown). Conversely, correlation analysis with the five up-regulated miRNA revealed a significant correlation between the wavelet feature LHH first order Mean and three up-regulated miRNA, namely miRNA-21 (ρ = -0.56, P < 0.05), miRNA-4746 (ρ = 0.64, P < 0.05) and miRNA-93 (ρ = 0.61, P < 0.05), as reported in the heatmap in Figure 4.

Table 3 Selected radiomic features after the three feature selection steps for body mass index

Selected radiomic features	mean ± SD	ρ	*P* value
Wavelet-HLH GLCM IMC2	0.46 ± 0.31	0.6	0.017
Wavelet-HLH GLCM MCC	0.33 ± 0.27	0.67	0.006
Wavelet-HLH first order median	0.59 ± 0.28	-0.56	0.029
Wavelet-HLH first order entropy	0.32 ± 0.33	0.63	0.013
Wavelet-HLH first order root mean squared	0.44 ± 0.31	0.71	0.003
Wavelet-HLH first order skewness	0.5 ± 0.33	0.52	0.049
Wavelet-HLH first order mean absolute deviation	0.54 ± 0.29	0.62	0.013
Wavelet-LHL GLCM IDN	0.77 ± 0.29	0.58	0.023
Wavelet-LHL GLDM high gray level emphasis	0.31 ± 0.29	0.54	0.039
Wavelet-HLL GLRLM high gray level run emphasis	0.32 ± 0.32	0.54	0.038
Wavelet-HLL GLRLM gray level variance	0.36 ± 0.37	0.62	0.014
Wavelet-HLL GLCM cluster prominence	0.26 ± 0.36	0.6	0.018
Wavelet-HLL GLCM inverse variance	0.57 ± 0.3	-0.58	0.022
Wavelet-HLL GLCM maximum probability	0.47 ± 0.35	-0.53	0.043
Wavelet-HLL GLDM dependence variance	0.41 ± 0.27	-0.6	0.018
Wavelet-HLL GLSZM size zone non uniformity	0.29 ± 0.33	0.57	0.028
Wavelet-HHH GLRLM gray level non uniformity normalized	0.74 ± 0.3	-0.54	0.039
Wavelet-HHH GLCM difference average	0.64 ± 0.31	0.56	0.03
Wavelet-HHH GLCM contrast	0.53 ± 0.28	0.64	0.009
Wavelet-HHH GLSZM small area emphasis	0.55 ± 0.33	0.69	0.005
Wavelet-HHH GLSZM small area low gray level emphasis	0.55 ± 0.33	0.59	0.022
Wavelet-HHL first order entropy	0.38 ± 0.3	0.57	0.025
Wavelet-HHL first order mean	0.64 ± 0.28	0.59	0.02
Wavelet-HHL first order mean absolute deviation	0.36 ± 0.29	0.55	0.032
Wavelet-LLH NGTDM complexity	0.16 ± 0.26	0.53	0.044
Wavelet-LLL GLDM small dependence high gray level emphasis	0.36 ± 0.3	0.56	0.031
Log-sigma-1-0-mm-3D first order root mean squared	0.43 ± 0.26	-0.51	0.049
Log-sigma-5-0-mm-3D GLRLM short run low gray level emphasis	0.22 ± 0.25	-0.52	0.047
Log-sigma-5-0-mm-3D first order 10 percentile	0.48 ± 0.39	-0.59	0.02

GLCM: Gray level co-occurrence matrix; GLDM: Gray level dependence matrix; GLRLM: Gray level run length matrix; GLSZM: Gray level size zone matrix; H: High-pass filter; L: Low-pass filter; NGTDM: Neighboring gray tone difference matrix; SD: Standard deviation.

BMI: Overall, radiogenomic analysis revealed that four of the eight mRNA regulators were significantly correlated with 10 of the 29 selected radiomic features, of which five belonging to wavelet group and three belonging to LoG sigma group as reported in Figure 5. In particular, METTL3 was positively correlated with HLH median, LHL GLDM high gray level emphasis, HLL GLRLM gray level variance and LLL GLDM small dependence high gray level emphasis (ρ = 0.71, ρ = 0.54, ρ = 0.53, ρ = 0.6, P < 0.05, respectively) and negatively correlated with HLL GLCM inverse variance and LoG sigma 10th percentile calculated with sigma = 5.0 (ρ = -0.6, ρ = -0.66, P < 0.05, respectively); YTHDF1 was positively correlated with wavelet feature HLL GLCM maximum probability (ρ = 0.6, P < 0.05), whereas YTHDC1 was positively correlated with the wavelet HHH GLCM difference average (ρ = 0.67, P < 0.05) and inversely

Table 4 Results of multivariate analysis for the stage I-II/stage III-IV classification task

Model order	Features involved	AUC ± SE	Sens ± SE	Spec ± SE	ACC ± SE
1	Wavelet-HHH GLCM joint entropy	0.896 ± 0.005	0.513 ± 0.021	0.865 ± 0.007	0.77 ± 0.006
2	Wavelet-LLH NGTDM complexity; Wavelet-HHH GLCM joint entropy	0.869 ± 0.008	0.643 ± 0.021	0.834 ± 0.008	0.79 ± 0.006
3	Wavelet-LLH NGTDM complexity; Wavelet-HHH GLCM joint entropy; Wavelet-HLH first order entropy	0.826 ± 0.009	0.523 ± 0.023	0.815 ± 0.009	0.744 ± 0.006
4	Wavelet-HLL GLCM cluster prominence; Wavelet-HHH GLCM joint entropy; Wavelet-LLH NGTDM complexity; Wavelet-HLH first order entropy	0.799 ± 0.009	0.668 ± 0.022	0.766 ± 0.009	0.752 ± 0.007
5	Wavelet-LLH GLDM high gray level emphasis; Wavelet-HHH GLCM joint entropy; Wavelet HLL GLCM cluster prominence; Wavelet HLH entropy; Wavelet LLH NGTDM complexity	0.724 ± 0.011	0.516 ± 0.025	0.762 ± 0.01	0.708 ± 0.008

For each model (from order 1 to 5), area under the receiver operating characteristic curve, sensitivity, specificity and accuracy were reported with the standard error on a 95%CI over all bootstrap sample. AUC: Area under the receiver operating characteristic curve; GLCM: Gray level co-occurrence matrix; GLDM: Gray level dependence matrix; GLRLM: Gray level run length matrix; GLSZM: Gray level size zone matrix; H: High-pass filter; L: Low-pass filter; NGTDM: Neighboring gray tone difference matrix; SE: Standard error.

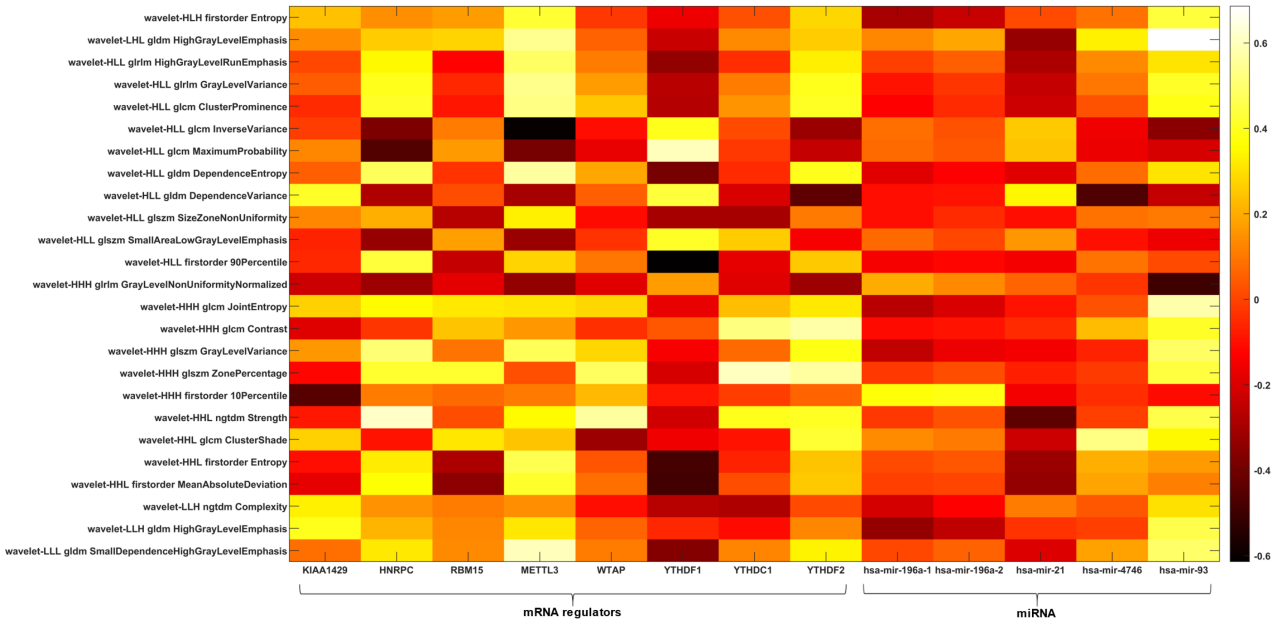

Figure 3 Radiogenomic analysis using stage as clinical outcome. Heatmap depicting the correlation matrix between transcriptomic features and radiomic features significantly associated with stage. GLCM: Gray level co-occurrence matrix; GLDM: Gray level dependence matrix; GLRLM: Gray level run length matrix; GLSZM: Gray level size zone matrix; H: High-pass filter; L: Low-pass filter; NGTDM: Neighboring gray tone difference matrix.

correlated with and LoG sigma root mean squared calculated with sigma = 1.0 (ρ = -0.67, P < 0.05); similarly, YTHDF2 was positively correlated with the wavelet HHH GLCM contrast (ρ = 0.57, P < 0.05) and inversely with the LoG sigma 10th percentile calculated with sigma = 5.0 (ρ = -0.56, P < 0.05). Moreover, correlation analysis with the five up-regulated miRNA revealed a significant correlation only between miRNA-93 and two radiomic features as reported in Figure 5 and in particular with the wavelet feature LHL GLRLM high gray level run emphasis (ρ = 0.69, P < 0.05) and the LoG sigma 10th percentile calculated with sigma = 5.0 (ρ = -0.54, P < 0.05).

DISCUSSION

Several studies reported that some miRNAs, such as miR-21, miR-183, miR-574-5p and miR-601, can regulate the pathways in esophageal carcinogenesis by their altered

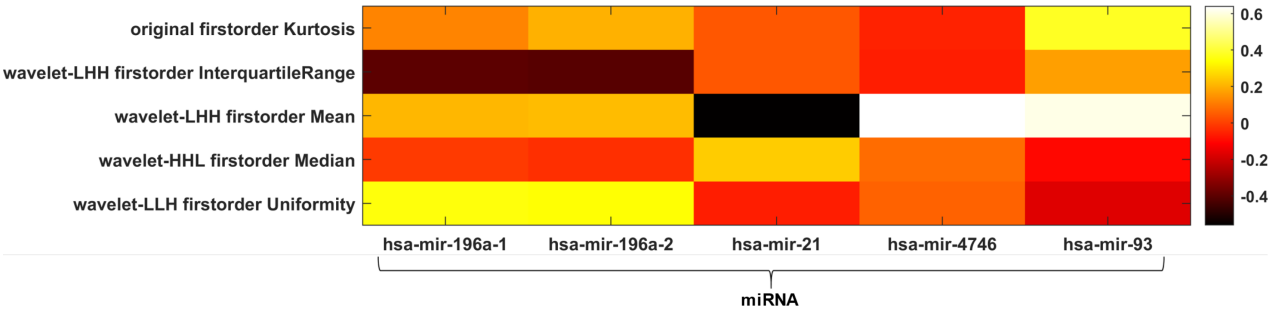

Figure 4 Radiogenomic analysis using alcohol history as clinical outcome. Heatmap depicting the correlation matrix between transcriptomic features and radiomic features significantly associated with alcohol history. H: High-pass filter; L: Low-pass filter; miRNA: MicroRNA.

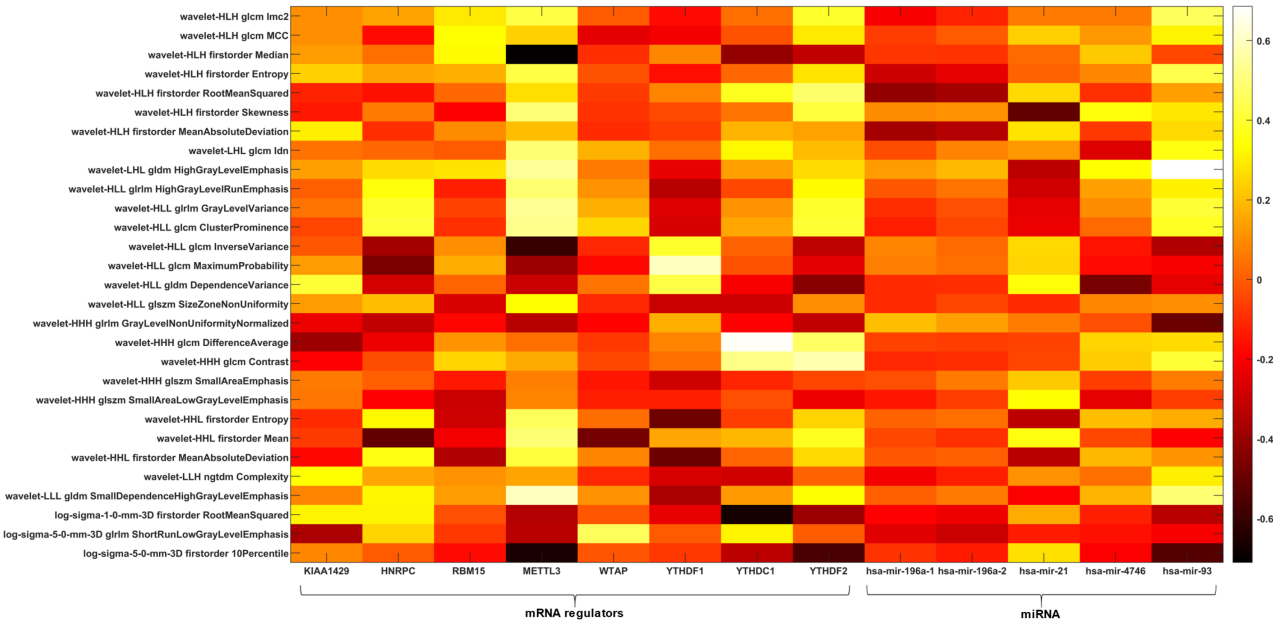

Figure 5 Radiogenomic analysis using body mass index as clinical outcome. Heatmap depicting the correlation matrix between transcriptomic features and radiomic features significantly associated with body mass index. GLCM: Gray level co-occurrence matrix; GLDM: Gray level dependence matrix; GLRLM: Gray level run length matrix; GLSZM: Gray level size zone matrix; H: High-pass filter; L: Low-pass filter; miRNA: MicroRNA; mRNA: Messenger RNA; NGTDM: Neighboring gray tone difference matrix.

expression associated with the increasing of risks factors, including dietary, smoking and drinking habits[44]. Moreover, a recent study, through an integrated approach, evaluated how dysregulated miRNAs by regulating RNA targets changed the relative miRNA-mRNA expression to survival and clinical characteristics[45]. In addition, miRNAs, more generally noncoding RNAs, have the ability to regulate m6A modifications, thereby affecting gene expression in cancer progression. Previous studies highlighted a strong relation between RNA methylation and breast cancer. In particular, Zhang *et al*[46] reported significant difference in expression levels and prognostic value of five m6RNA regulators (YTHDF3, ZC3H13, LRPPRC, METTL16, RBM15B) in breast cancer. Furthermore, in a recent study, Zhao *et al*[47] showed that m6A regulator genomic aberration is associated with prognosis of ESCA patients.

It is recognized that the use of CT radiomics is rapidly increasing in the field of ESCA management, playing an important role in preoperative nodal staging, diagnosis and prognosis and for predicting treatment response to chemoradiotherapy [3,48-52]. Wu *et al*[15] showed that CT radiomic features were able to discriminate between stage I-II and III-IV ESCA. In a study by Yang *et al*[45], predictive models based on CT radiomic features were able to predict complete pathologic response after neoadjuvant chemoradiotherapy of ESCA patients. CT texture features were also found to be independent predictors of survival[48], while CT wavelet features were associated with the 3-year overall survival after chemoradiotherapy in a study involving 165 patients performed by Larue *et al*[51].

In our pilot study, we examined the relationship between the expression levels of eight m6A RNA methylation regulators (KIAA1429, HNRNPC, RBM15, METTL3, WTAP, YTHDF1, YTHDC1, YTHDF2), as well as five up-regulated miRNAs (miRNA-93, miRNA-21, miRNA-4746, miRNA-196a-1 and miRNA-196a-2) and radiomic features extracted from CT images that were significantly associated to clinical outcomes (stage, alcohol history, BMI) in patients with ESCA belonging to the public integrated datasets TCGA/TCIA. We decided to evaluate by combining radiomic and transcriptomic data the above-mentioned m6A RNA methylation regulators and up-regulated miRNA since previous studies on gene expression in ESCA found interesting results on specific mRNAs associated with tumor stage through epigenetic regulation and miRNAs signature as a prognostic biomarker[22,25].

Interestingly, both considering binary clinical outcomes (namely stage and alcohol history) and BMI, CT radiomic features that survived after radiomic feature selection were mostly belonging to the wavelet group, while only histogram Kurtosis and three LoG sigma features (one textural and two histogram features) survived after feature selection for alcohol history and BMI analysis, respectively. Wavelet features were also able to differentiate between stage I-II and III-IV ESCA, with an AUC superior to 80%. Similar performances were achieved when using the same features for predicting T and N, and this could be because T and N assignments contribute to determine the overall ESCA stage[43]. These results are in line with those found by Liu *et al*[53], even if they did not include textural features from wavelet CT images.

These results were in line with previous radiomics studies, in which CT imaging features describing tumor heterogeneity also were shown to have prognostic value in esophageal cancer[51,54]. Wavelet radiomic features from pretreatment CT were found to be useful to predict overall survival of ESCA patients after chemoradiotherapy in a study by Larue *et al*[51]. Moreover, in the work by Qiu *et al*[54], wavelet features resulted predominant in the radiomic-based predictive model developed to estimate recurrence-free survival in ESCA patients achieving a pathologic complete response.

Radiogenomic analysis performed for stage assessment revealed significant correlations between 10 wavelet textural features and six of the eight m6A RNA methylation regulators (HRNPC, WTAP, METTL3, YTHDF1, YTHDF2, YTHDC1). Moreover, correlation analysis with the five up-regulated miRNA revealed a significant positive correlation between miRNA-93 and two radiomic wavelet features, namely LHL GLDM high gray level emphasis and HHH GLCM joint entropy. It is worth to note that the wavelet feature HHH GLCM joint entropy was positively correlated with miRNA-93 and contributed to building the best predictive models for the overall stage assessment and for the assessment of the T and N categories. From the literature, miR-93 is reported to be associated in various tumors and it is recently found to regulate mechanisms of drug resistance in triple negative breast cancer[55]. Moreover, Ansari *et al*[56] evaluated miR-93 as potential deregulated biomarker for early detection of ESCA. Based on these considerations, combining genomic features with radiomic ones might be of further added value for ESCA staging, thereby influencing the personalized medicine workflow in the field of ESCA. Concerning radiogenomic analysis performed using alcohol history as clinical outcome, there were no significant associations between selected CT features and the eight m6A RNA methylation regulators, while the correlation analysis with the five up-regulated miRNA revealed a significant correlation between the wavelet feature LHH first order mean and three up-regulated miRNA, namely miRNA-21, miRNA-4746 and miRNA-93. Finally, the radiogenomic analysis on BMI revealed a significant correlation between wavelet and LoG sigma features and METTL3, YTHDF1, YTHDC1 and YTHDF2. Wavelet and LoG sigma features were also associated with miRNA-93 in radiogenomic analysis involving the five up-regulated miRNAs.

In addition, a recent study has experimentally verified that overexpression of METTL3 in tumor tissues of ESCA patients compared with normal condition from adjacent tissues is associated with metabolic status, highlighting a significant correlation with tumor size and histological differentiation; this result suggests that MTLL3 may become a possible pathological index for diagnosis and a potential therapeutic target[57].

However, to our knowledge, this is the first ESCA radiogenomic study investigating the association with clinical staging and potential risk factors. Although previous radiogenomic studies were performed on ESCA[21,49,58], the strength of our study was that this is the first radiogenomic study investigating the association with stage, alcohol history, and BMI. Moreover, is not to be neglected that it is a radiogenomic study on an unexplored cancer type such as ESCA.

However, several limitations are worth noting. First, due to the extremely small sample size and the retrospective nature of the study, our results remain to be validated with a larger and prospective patient sample in the future. Second, the small sample size may have affected also prediction model performances. Therefore, a larger and more balanced study group is needed to conduct better a radiomic analysis and build more robust prediction models. In particular, although the IABR strategy we used for model building is a common reliable approach in case of small and imbalanced datasets, a larger sample size would allow using part of the dataset for the training and part for testing and validating the performance of the classifier with external datasets. In addition, it should be considered that the availability of the eight m6A RNA methylation regulators and the five up-regulated miRNAs only for a small population has prevented us from investigating other clinical outcomes, which were missing for the investigated patients. It would have been interesting to perform similar analyses considering smoking variables as clinical outcomes. In fact, in addition to alcohol, tobacco is an established risk factor for ESCA and has been proven to act synergically with alcohol to increase the risk of ESCA[59,60]. However, we could not perform analyses involving outcomes associated with smoking due to the incompleteness of these data for the included patients' cohort.

CONCLUSION

In conclusion, our preliminary study revealed interesting relationships between the expression levels of eight m6A RNA methylation regulators, as well as the five up-regulated miRNAs, and CT radiomic features that were significantly associated with clinical outcomes. Our results strengthen the role of miRNA overexpression and the possible characterization of biomarkers from liquid biopsy for ESCA assessment and staging, introducing new insights for omics integration toward a personalized medicine approach. Further prospective and retrospective studies involving larger groups of patients are essential to validate obtained results and perform in-depth analyses.

ARTICLE HIGHLIGHTS

Research background

Esophageal cancer (ESCA) is the sixth most common malignancy in the world, and its incidence is rapidly increasing. Radiogenomics provides clinically useful prognostic predictions by linking molecular characteristics such as gene mutations and gene expression patterns of malignant tumors with medical images and could provide more opportunities in the management of patients with ESCA.

Research motivation

Recently, several microRNAs (miRNAs) and messenger (RNA) targets were evaluated as potential biomarkers and regulators of epigenetic mechanisms involved in ESCA. In addition, the use of computed tomography (CT) radiomics is rapidly increasing in the field of ESCA and plays an important role in different ESCA management steps. Moreover, there are no previous radiogenomic studies on ESCA investigating the association with clinical staging and potential risk factors. This has motivated us to investigate on the relationship between the expression levels of eight N6-methyl-adenosine (m6A) RNA methylation regulators, as well as the five up-regulated miRNAs, and radiomic features extracted from CT images that were significantly associated to clinical outcomes.

Research objectives

To explore the combination of CT radiomic features and molecular targets associated with clinical outcomes for characterization of ESCA patients.

Research methods

Fifteen patients with diagnosed ESCA were included in this study, and their CT imaging and transcriptomic data were extracted from The Cancer Imaging Archive and gene expression data from The Cancer Genome Atlas, respectively. Cancer stage, history of significant alcohol consumption and body mass index (BMI) were

considered as clinical outcomes. Radiomic analysis was performed on CT images acquired after injection of contrast medium. In total, 1302 radiomics features were extracted from three-dimensional regions of interest by using PyRadiomics. Radiogenomic analysis involved Spearman's correlation (ρ) analysis between radiomic features associated with clinical outcomes and transcriptomic signatures consisting in eight m6A RNA methylation regulators and five up-regulated miRNA.

Research results

Radiogenomic analysis with stage as clinical outcome revealed that six of the eight mRNA regulators and two of the five up-regulated miRNA were significantly correlated with 10 and three of the 25 selected radiomic features, respectively. Assuming alcohol history as clinical outcome, no correlation was found between the five selected radiomic features and mRNA regulators, while a significant correlation was found between one radiomic feature and three up-regulated miRNA. Radiogenomic analysis with BMI as clinical outcome revealed that four mRNA regulators and one up-regulated miRNA were significantly correlated with 10 and two radiomic features, respectively.

Research conclusions

Our study revealed interesting relationships between the expression of eight m6a RNA regulators, as well as five up-regulated miRNAs, and CT radiomic features associated with clinical outcomes of ESCA patients.

Research perspectives

This preliminary study revealed interesting associations between m6a RNA regulators, as well as miRNAs, and CT radiomic features associated with clinical outcomes of ESCA patients. Further investigations on different ESCA omics data are required. Moreover, multimodal data combined with artificial intelligence techniques characteristics are desirable.

ACKNOWLEDGEMENTS

All results shown here are in whole or part based upon data generated by the TCGA Research Network: https://www.cancer.gov/tcga.

REFERENCES

1 **Bray F**, Ferlay J, Soerjomataram I, Siegel RL, Torre LA, Jemal A. Global cancer statistics 2018: GLOBOCAN estimates of incidence and mortality worldwide for 36 cancers in 185 countries. *CA Cancer J Clin* 2018; **68**: 394-424 [PMID: 30207593 DOI: 10.3322/caac.21492]

2 **Ahmad NR**, Goosenberg EB, Frucht H, Coia LR. Palliative Treatment of Esophageal Cancer. *Semin Radiat Oncol* 1994; **4**: 202-214 [PMID: 10717108 DOI: 10.1053/SRAO00400192]

3 **Yang Z**, He B, Zhuang X, Gao X, Wang D, Li M, Lin Z, Luo R. CT-based radiomic signatures for prediction of pathologic complete response in esophageal squamous cell carcinoma after neoadjuvant chemoradiotherapy. *J Radiat Res* 2019; **60**: 538-545 [PMID: 31111948 DOI: 10.1093/jrr/rrz027]

4 **Napier KJ**, Scheerer M, Misra S. Esophageal cancer: A Review of epidemiology, pathogenesis, staging workup and treatment modalities. *World J Gastrointest Oncol* 2014; **6**: 112-120 [PMID: 24834141 DOI: 10.4251/wjgo.v6.i5.112]

5 **Milsom JW**, Senagore A, Walshaw RK, Mostosky UV, Wang P, Johnson W, Chaudry IH. Preoperative radiation therapy produces an early and persistent reduction in colorectal anastomotic blood flow. *J Surg Res* 1992; **53**: 464-469 [PMID: 1434596 DOI: 10.1016/0022-4804(92)90091-d]

6 **Tirumani H**, Rosenthal MH, Tirumani SH, Shinagare AB, Krajewski KM, Ramaiya NH. Esophageal Carcinoma: Current Concepts in the Role of Imaging in Staging and Management. *Can Assoc Radiol J* 2015; **66**: 130-139 [PMID: 25770628 DOI: 10.1016/j.carj.2014.08.006]

7 **Elsherif SB**, Andreou S, Virarkar M, Soule E, Gopireddy DR, Bhosale PR, Lall C. Role of precision imaging in esophageal cancer. *J Thorac Dis* 2020; **12**: 5159-5176 [PMID: 33145093 DOI: 10.21037/jtd.2019.08.15]

8 **Umeoka S**, Koyama T, Togashi K, Saga T, Watanabe G, Shimada Y, Imamura M. Esophageal cancer: evaluation with triple-phase dynamic CT--initial experience. *Radiology* 2006; **239**: 777-783 [PMID: 16621930 DOI: 10.1148/radiol.2393050222]

9 **Sultan R**, Haider Z, Chawla TU. Diagnostic accuracy of CT scan in staging resectable esophageal cancer. *J Pak Med Assoc* 2016; **66**: 90-92 [PMID: 26712189]

10 **Lambin P**, Rios-Velazquez E, Leijenaar R, Carvalho S, van Stiphout RG, Granton P, Zegers CM,

Gillies R, Boellard R, Dekker A, Aerts HJ. Radiomics: extracting more information from medical images using advanced feature analysis. *Eur J Cancer* 2012; **48**: 441-446 [PMID: 22257792 DOI: 10.1016/j.ejca.2011.11.036]

11 **Gillies RJ**, Kinahan PE, Hricak H. Radiomics: Images Are More than Pictures, They Are Data. *Radiology* 2016; **278**: 563-577 [PMID: 26579733 DOI: 10.1148/radiol.2015151169]

12 **van Rossum PSN**, Xu C, Fried DV, Goense L, Court LE, Lin SH. The emerging field of radiomics in esophageal cancer: current evidence and future potential. *Transl Cancer Res* 2016; **5**: 410-423 [PMID: 30687593 DOI: 10.21037/tcr.2016.06.19]

13 **Rizzo S**, Botta F, Raimondi S, Origgi D, Fanciullo C, Morganti AG, Bellomi M. Radiomics: the facts and the challenges of image analysis. *Eur Radiol Exp* 2018; **2**: 36 [PMID: 30426318 DOI: 10.1186/s41747-018-0068-z]

14 **Hou T-C**, Huang W-C, Tai H-C, Chen Y-J. Integrated radiomic model for predicting the prognosis of esophageal squamous cell carcinoma patients undergoing neoadjuvant chemoradiation. *Ther Radiol Oncol* 2019; **3**: 28 [DOI: 10.21037/tro.2019.07.03]

15 **Wu L**, Wang C, Tan X, Cheng Z, Zhao K, Yan L, Liang Y, Liu Z, Liang C. Radiomics approach for preoperative identification of stages I-II and III-IV of esophageal cancer. *Chin J Cancer Res* 2018; **30**: 396-405 [PMID: 30210219 DOI: 10.21147/j.issn.1000-9604.2018.04.02]

16 **Jin X**, Zheng X, Chen D, Jin J, Zhu G, Deng X, Han C, Gong C, Zhou Y, Liu C, Xie C. Prediction of response after chemoradiation for esophageal cancer using a combination of dosimetry and CT radiomics. *Eur Radiol* 2019; **29**: 6080-6088 [PMID: 31028447 DOI: 10.1007/s00330-019-06193-w]

17 **Hyman DM**, Taylor BS, Baselga J. Implementing Genome-Driven Oncology. *Cell* 2017; **168**: 584-599 [PMID: 28187282 DOI: 10.1016/j.cell.2016.12.015]

18 **Berger MF**, Mardis ER. The emerging clinical relevance of genomics in cancer medicine. *Nat Rev Clin Oncol* 2018; **15**: 353-365 [PMID: 29599476 DOI: 10.1038/s41571-018-0002-6]

19 **Guo W**, Jiang YG. Current gene expression studies in esophageal carcinoma. *Curr Genomics* 2009; **10**: 534-539 [PMID: 20514215 DOI: 10.2174/138920209789503888]

20 **Visser E**, Franken IA, Brosens LA, Ruurda JP, van Hillegersberg R. Prognostic gene expression profiling in esophageal cancer: a systematic review. *Oncotarget* 2017; **8**: 5566-5577 [PMID: 27852047 DOI: 10.18632/oncotarget.13328]

21 **Hoshino I**, Yokota H, Ishige F, Iwatate Y, Takeshita N, Nagase H, Uno T, Matsubara H. Radiogenomics predicts the expression of microRNA-1246 in the serum of esophageal cancer patients. *Sci Rep* 2020; **10**: 2532 [PMID: 32054931 DOI: 10.1038/s41598-020-59500-7]

22 **Zeng JH**, Xiong DD, Pang YY, Zhang Y, Tang RX, Luo DZ, Chen G. Identification of molecular targets for esophageal carcinoma diagnosis using miRNA-seq and RNA-seq data from The Cancer Genome Atlas: a study of 187 cases. *Oncotarget* 2017; **8**: 35681-35699 [PMID: 28415685 DOI: 10.18632/oncotarget.16051]

23 **Ma S**, Chen C, Ji X, Liu J, Zhou Q, Wang G, Yuan W, Kan Q, Sun Z. The interplay between m6A RNA methylation and noncoding RNA in cancer. *J Hematol Oncol* 2019; **12**: 121 [PMID: 31757221 DOI: 10.1186/s13045-019-0805-7]

24 **Lan Q**, Liu PY, Haase J, Bell JL, Hüttelmaier S, Liu T. The Critical Role of RNA m^6A Methylation in Cancer. *Cancer Res* 2019; **79**: 1285-1292 [PMID: 30894375 DOI: 10.1158/0008-5472.CAN-18-2965]

25 **Xu LC**, Pan JX, Pan HD. Construction and Validation of an m6A RNA Methylation Regulators-Based Prognostic Signature for Esophageal Cancer. *Cancer Manag Res* 2020; **12**: 5385-5394 [PMID: 32753956 DOI: 10.2147/CMAR.S254870]

26 **Sah BR**, Owczarczyk K, Siddique M, Cook GJR, Goh V. Radiomics in esophageal and gastric cancer. *Abdom Radiol (NY)* 2019; **44**: 2048-2058 [PMID: 30116873 DOI: 10.1007/s00261-018-1724-8]

27 **Klaassen R**, Larue RTHM, Mearadji B, van der Woude SO, Stoker J, Lambin P, van Laarhoven HWM. Feasibility of CT radiomics to predict treatment response of individual liver metastases in esophagogastric cancer patients. *PLoS One* 2018; **13**: e0207362 [PMID: 30440002 DOI: 10.1371/journal.pone.0207362]

28 **Wu R**, Zhuang H, Mei YK, Sun JY, Dong T, Zhao LL, Fan ZN, Liu L. Systematic identification of key functional modules and genes in esophageal cancer. *Cancer Cell Int* 2021; **21**: 134 [PMID: 33632229 DOI: 10.1186/s12935-021-01826-x]

29 **Peng Q**, Chen H, Huo JR. Alcohol consumption and corresponding factors: A novel perspective on the risk factors of esophageal cancer. *Oncol Lett* 2016; **11**: 3231-3239 [PMID: 27123096 DOI: 10.3892/ol.2016.4401]

30 **Long E**, Beales IL. The role of obesity in oesophageal cancer development. *Therap Adv Gastroenterol* 2014; **7**: 247-268 [PMID: 25364384 DOI: 10.1177/1756283X14538689]

31 **Turati F**, Tramacere I, La Vecchia C, Negri E. A meta-analysis of body mass index and esophageal and gastric cardia adenocarcinoma. *Ann Oncol* 2013; **24**: 609-617 [PMID: 22898040 DOI: 10.1093/annonc/mds244]

32 **Lucchesi FR**, Aredes ND. Radiology Data from The Cancer Genome Atlas Esophageal Carcinoma [TCGA-ESCA] collection. *The Cancer Imaging Archive* 2016 [DOI: 10.7937/K9/TCIA.2016.VPTNRGFY]

33 **Clark K**, Vendt B, Smith K, Freymann J, Kirby J, Koppel P, Moore S, Phillips S, Maffitt D, Pringle M, Tarbox L, Prior F. The Cancer Imaging Archive (TCIA): maintaining and operating a public information repository. *J Digit Imaging* 2013; **26**: 1045-1057 [PMID: 23884657 DOI: 10.1007/s10278-013-9622-7]

34 **Zwanenburg A**, Vallières M, Abdalah MA, Aerts HJWL, Andrearczyk V, Apte A, Ashrafinia S, Bakas S, Beukinga RJ, Boellaard R, Bogowicz M, Boldrini L, Buvat I, Cook GJR, Davatzikos C, Depeursinge A, Desseroit MC, Dinapoli N, Dinh CV, Echegaray S, El Naqa I, Fedorov AY, Gatta R, Gillies RJ, Goh V, Götz M, Guckenberger M, Ha SM, Hatt M, Isensee F, Lambin P, Leger S, Leijenaar RTH, Lenkowicz J, Lippert F, Losnegård A, Maier-Hein KH, Morin O, Müller H, Napel S, Nioche C, Orlhac F, Pati S, Pfaehler EAG, Rahmim A, Rao AUK, Scherer J, Siddique MM, Sijtsema NM, Socarras Fernandez J, Spezi E, Steenbakkers RJHM, Tanadini-Lang S, Thorwarth D, Troost EGC, Upadhaya T, Valentini V, van Dijk LV, van Griethuysen J, van Velden FHP, Whybra P, Richter C, Löck S. The Image Biomarker Standardization Initiative: Standardized Quantitative Radiomics for High-Throughput Image-based Phenotyping. *Radiology* 2020; **295**: 328-338 [PMID: 32154773 DOI: 10.1148/radiol.2020191145]

35 **Vergara JR**, Estévez PA. A review of feature selection methods based on mutual information. *Neural Comput Applic* 2014; **24**: 175-186 [DOI: 10.1007/s00521-013-1368-0]

36 **Zaffalon M**, Hutter M. Robust Feature Selection by Mutual Information Distributions. 2014 Preprint. Available from: arXiv: 1408.1487v1

37 **Roffo G**. Feature Selection Library (MATLAB Toolbox). 2018 Preprint. Available from: arXiv: 1607.01327v5

38 **Vallières M**, Freeman CR, Skamene SR, El Naqa I. A radiomics model from joint FDG-PET and MRI texture features for the prediction of lung metastases in soft-tissue sarcomas of the extremities. *Phys Med Biol* 2015; **60**: 5471-5496 [PMID: 26119045 DOI: 10.1088/0031-9155/60/14/5471]

39 **Efron B**. Bootstrap Methods: Another Look at the Jackknife. *Ann Statist* 1979; **7**: 1-26 [DOI: 10.1214/aos/1176344552]

40 **Efron B**, Tibshirani R. Improvements on Cross-Validation: The .632+ Bootstrap Method. *J Am Stat Assoc* 1997; **92**: 548 [DOI: 10.2307/2965703]

41 **Brancato V**, Aiello M, Basso L, Monti S, Palumbo L, Di Costanzo G, Salvatore M, Ragozzino A, Cavaliere C. Evaluation of a multiparametric MRI radiomic-based approach for stratification of equivocal PI-RADS 3 and upgraded PI-RADS 4 prostatic lesions. *Sci Rep* 2021; **11**: 643 [PMID: 33436929 DOI: 10.1038/s41598-020-80749-5]

42 **Sahiner B**, Chan HP, Hadjiiski L. Classifier performance prediction for computer-aided diagnosis using a limited dataset. *Med Phys* 2008; **35**: 1559-1570 [PMID: 18491550 DOI: 10.1118/1.2868757]

43 **Berry MF**. Esophageal cancer: staging system and guidelines for staging and treatment. *J Thorac Dis* 2014; **6** Suppl 3: S289-S297 [PMID: 24876933 DOI: 10.3978/j.issn.2072-1439.2014.03.11]

44 **Stánitz É**, Juhász K, Gombos K, Gőcze K, Tóth C, Kiss I. Alteration of miRNA expression correlates with lifestyle, social and environmental determinants in esophageal carcinoma. *Anticancer Res* 2015; **35**: 1091-1097 [PMID: 25667498]

45 **Yang H**, Su H, Hu N, Wang C, Wang L, Giffen C, Goldstein AM, Lee MP, Taylor PR. Integrated analysis of genome-wide miRNAs and targeted gene expression in esophageal squamous cell carcinoma (ESCC) and relation to prognosis. *BMC Cancer* 2020; **20**: 388 [PMID: 32375686 DOI: 10.1186/s12885-020-06901-6]

46 **Zhang B**, Gu Y, Jiang G. Expression and Prognostic Characteristics of m^6 A RNA Methylation Regulators in Breast Cancer. *Front Genet* 2020; **11**: 604597 [PMID: 33362863 DOI: 10.3389/fgene.2020.604597]

47 **Zhao H**, Xu Y, Xie Y, Zhang L, Gao M, Li S, Wang F. m6A Regulators Is Differently Expressed and Correlated With Immune Response of Esophageal Cancer. *Front Cell Dev Biol* 2021; **9**: 650023 [PMID: 33748145 DOI: 10.3389/fcell.2021.650023]

48 **Ganeshan B**, Skogen K, Pressney I, Coutroubis D, Miles K. Tumour heterogeneity in oesophageal cancer assessed by CT texture analysis: preliminary evidence of an association with tumour metabolism, stage, and survival. *Clin Radiol* 2012; **67**: 157-164 [PMID: 21943720 DOI: 10.1016/j.crad.2011.08.012]

49 **Hu Y**, Xie C, Yang H, Ho JWK, Wen J, Han L, Chiu KWH, Fu J, Vardhanabhuti V. Assessment of Intratumoral and Peritumoral Computed Tomography Radiomics for Predicting Pathological Complete Response to Neoadjuvant Chemoradiation in Patients With Esophageal Squamous Cell Carcinoma. *JAMA Netw Open* 2020; **3**: e2015927 [PMID: 32910196 DOI: 10.1001/jamanetworkopen.2020.15927]

50 **Piazzese C**, Foley K, Whybra P, Hurt C, Crosby T, Spezi E. Discovery of stable and prognostic CT-based radiomic features independent of contrast administration and dimensionality in oesophageal cancer. *PLoS One* 2019; **14**: e0225550 [PMID: 31756181 DOI: 10.1371/journal.pone.0225550]

51 **Larue RTHM**, Klaassen R, Jochems A, Leijenaar RTH, Hulshof MCCM, van Berge Henegouwen MI, Schreurs WMJ, Sosef MN, van Elmpt W, van Laarhoven HWM, Lambin P. Pre-treatment CT radiomics to predict 3-year overall survival following chemoradiotherapy of esophageal cancer. *Acta Oncol* 2018; **57**: 1475-1481 [PMID: 30067421 DOI: 10.1080/0284186X.2018.1486039]

52 **Hou Z**, Yang Y, Li S, Yan J, Ren W, Liu J, Wang K, Liu B, Wan S. Radiomic analysis using contrast-enhanced CT: predict treatment response to pulsed low dose rate radiotherapy in gastric carcinoma with abdominal cavity metastasis. *Quant Imaging Med Surg* 2018; **8**: 410-420 [PMID: 29928606 DOI: 10.21037/qims.2018.05.01]

53 **Liu S**, Zheng H, Pan X, Chen L, Shi M, Guan Y, Ge Y, He J, Zhou Z. Texture analysis of CT imaging for assessment of esophageal squamous cancer aggressiveness. *J Thorac Dis* 2017; **9**: 4724-4732 [DOI: 10.21037/jtd.2017.06.46]

54 **Qiu Q**, Duan J, Deng H, Han Z, Gu J, Yue NJ, Yin Y. Development and Validation of a Radiomics

Nomogram Model for Predicting Postoperative Recurrence in Patients With Esophageal Squamous Cell Cancer Who Achieved pCR After Neoadjuvant Chemoradiotherapy Followed by Surgery. *Front Oncol* 2020; **10**: 1398 [PMID: 32850451 DOI: 10.3389/fonc.2020.01398]

55 **Qattan A**, Al-Tweigeri T, Alkhayal W, Suleman K, Tulbah A, Amer S. Clinical Identification of Dysregulated Circulating microRNAs and Their Implication in Drug Response in Triple Negative Breast Cancer (TNBC) by Target Gene Network and Meta-Analysis. *Genes* 2021; **12**: 549 [DOI: 10.3390/genes12040549]

56 **Ansari MH**, Irani S, Edalat H, Amin R, Mohammadi Roushandeh A. Deregulation of miR-93 and miR-143 in human esophageal cancer. *Tumor Biol* 2016; **37**: 3097-3103 [DOI: 10.1007/s13277-015-3987-9]

57 **Liu XS**, Yuan LL, Gao Y, Zhou LM, Yang JW, Pei ZJ. Overexpression of METTL3 associated with the metabolic status on ^{18}F-FDG PET/CT in patients with Esophageal Carcinoma. *J Cancer* 2020; **11**: 4851-4860 [PMID: 32626532 DOI: 10.7150/jca.44754]

58 **Hu Y**, Xie C, Yang H, Ho JWK, Wen J, Han L, Lam KO, Wong IYH, Law SYK, Chiu KWH, Vardhanabhuti V, Fu J. Computed tomography-based deep-learning prediction of neoadjuvant chemoradiotherapy treatment response in esophageal squamous cell carcinoma. *Radiother Oncol* 2021; **154**: 6-13 [PMID: 32941954 DOI: 10.1016/j.radonc.2020.09.014]

59 **Prabhu A**, Obi KO, Rubenstein JH. The synergistic effects of alcohol and tobacco consumption on the risk of esophageal squamous cell carcinoma: a meta-analysis. *Am J Gastroenterol* 2014; **109**: 822-827 [PMID: 24751582 DOI: 10.1038/ajg.2014.71]

60 **Dong J**, Thrift AP. Alcohol, smoking and risk of oesophago-gastric cancer. *Best Pract Res Clin Gastroenterol* 2017; **31**: 509-517 [PMID: 29195670 DOI: 10.1016/j.bpg.2017.09.002]

World Journal of Gastroenterology

Submit a Manuscript: https://www.f6publishing.com

World J Gastroenterol 2021 September 28; 27(36): 6128-6141

DOI: 10.3748/wjg.v27.i36.6128

ISSN 1007-9327 (print) ISSN 2219-2840 (online)

ORIGINAL ARTICLE

Retrospective Study

Clinicopathological characteristics and longterm survival of patients with synchronous multiple primary gastrointestinal stromal tumors: A propensity score matching analysis

Hao Wu, Chen Li, Han Li, Liang Shang, Hai-Yan Jing, Jin Liu, Zhen Fang, Feng-Ying Du, Yang Liu, Meng-Di Fu, Ke-Wei Jiang, Le-Ping Li

ORCID number: Hao Wu 0000-0001-9222-2521; Chen Li 0000-0003-3556-2719; Han Li 0000-0002-0699-673X; Liang Shang 0000-0002-9542-7650; Hai-Yan Jing 0000-0003-0913-6898; Jin Liu 0000-0001-7959-1541; Zhen Fang 0000-0002-7073-8997; Feng-Ying Du 0000-0002-2767-1301; Yang Liu 0000-0001-7167-7439; Meng-Di Fu 0000-0002-4172-6794; Ke-Wei Jiang 0000-0002-6706-4741; Le-Ping Li 0000-0003-2329-6791.

Author contributions: All authors helped to perform the research; Wu H and Li C were involved equally in the conception and design; Li H provided clinical advice; Fu MD was involved in the follow-up of patients; Fang Z was involved in preliminary medical record screening and entry; Liu Y was involved in the verification of the included data; Du FY was involved in the drafting of the paper or revising it critically for intellectual content; Jing HY and Jiang KW provided pathology images and supervised the report; Shang L and Li LP were involved in the final approval of the version to be published; All authors agreed to be accountable for all aspects of the work.

Supported by Key Research and

Hao Wu, Liang Shang, Zhen Fang, Feng-Ying Du, Yang Liu, Le-Ping Li, Department of Gastroenterological Surgery, Shandong Provincial Hospital, Cheeloo College of Medicine, Shandong University, Jinan 250021, Shandong Province, China

Chen Li, Ke-Wei Jiang, Department of Gastroenterological Surgery, Peking University People's Hospital, Beijing 100044, China

Han Li, Department of General Surgery, The First Affiliated Hospital of Shandong First Medical University, Jinan 250021, Shandong Province, China

Liang Shang, Le-Ping Li, Department of Digestive Tumor Translational Medicine, Engineering Laboratory of Shandong Province, Shandong Provincial Hospital, Jinan 250021, Shandong Province, China

Liang Shang, Le-Ping Li, Medical Science and Technology Innovation Center, Shandong First Medical University & Shandong Academy of Medical Sciences, Jinan 250021, Shandong Province, China

Hai-Yan Jing, Department of Pathology, Shandong Provincial Hospital, Cheeloo College of Medicine, Shandong University, Jinan 250021, Shandong Province, China

Jin Liu, Department of Gastroenterology, Shandong Provincial Hospital, Cheeloo College of Medicine, Shandong University, Jinan 250021, Shandong Province, China

Meng-Di Fu, Department of Clinical Medicine, Cheeloo College of Medicine, Shandong University, Jinan 250021, Shandong Province, China

Corresponding author: Le-Ping Li, MD, Full Professor, Department of Gastroenterological Surgery, Shandong Provincial Hospital, Cheeloo College of Medicine, Shandong University, No. 324 Jingwuweiqi road, Huaiyin District, Jinan 250021, Shandong Province, China. lileping@sdu.edu.cn

Abstract

BACKGROUND

Multiple gastrointestinal stromal tumors (MGISTs) are specific and rare. Little is

Development Program of Shandong Province, No. 2019JZZY010104 and No. 2019GSF108146; Special Foundation for Taishan Scholars Program of Shandong Province, No. ts20190978; and Academic Promotion Programme of Shandong First Medical University, No. 2019QL021.

Institutional review board statement: This study was designed in compliance with the Helsinki Declaration and approved by the Ethics Committee of Shandong Provincial Hospital (SWYX: No. 2021-035).

Informed consent statement: Patients were not required to give informed consent to the study because the analysis used anonymous clinical data that were obtained after each patient agreed to treatment by written consent.

Conflict-of-interest statement: We have no financial relationships to disclose.

Manuscript source: Unsolicited manuscript

Specialty type: Gastroenterology and hepatology

Country/Territory of origin: China

Peer-review report's scientific quality classification

Grade A (Excellent): 0
Grade B (Very good): B
Grade C (Good): 0
Grade D (Fair): 0

known about the impact of MGISTs on the survival of patients with gastrointestinal stromal tumors (GIST). The diagnosis, treatment and follow-up strategies of MGISTs is not specifically described in guidelines.

AIM

To compare the clinicopathological characteristics and prognosis of MGISTs and solitary GISTs (SGISTs)

METHODS

Patients diagnosed with primary GISTs from March 2010 to January 2020 were included. Due to the inhomogeneous distribution of several baseline characteristics and uneven MGIST and SGIST group sizes, propensity score matching was performed according to comorbidities, body mass index, tumor location, mitotic index, sex, age and American Society of Anesthesiologists score. Differences in clinicopathological characteristics and prognosis between patients with MGISTs and patients with SGISTs were compared.

RESULTS

Among the entire cohort of 983 patients, the incidence of MGISTs was 4.17%. Before matching, patients with MGISTs and those with SGISTs had disparities in body mass index, surgical approach, tumor size and mitotic index. After 1:4 ratio matching, the clinical baseline data were comparable. The 5-year progression-free survival rate was 52.17% in the MGIST group and 75.00% in the SGIST group (P = 0.031). On multivariate analysis, tumor location, tumor size, mitotic index, imatinib treatment and MGISTs (hazard ratio = 2.431, 95% confidence interval = 1.097-5.386, P = 0.029) were identified as independent prognostic factors of progression-free survival. However, overall survival was similar between the SGIST and MGIST groups.

CONCLUSION

Patients with MGISTs had poorer progression-free survival than patients with SGISTs. Risk criteria and diagnostic and treatment strategies should be developed to achieve personalized precision therapy and maximize the survival benefit.

Key Words: Gastrointestinal stromal tumors; Synchronous; Multiple tumors; Solitary tumor; Propensity score matching; Prognosis

Core Tip: Whether the clinicopathological characteristics and long-term survival of patients with multiple gastrointestinal stromal tumors are different from those of patients with solitary gastrointestinal stromal tumors is unclear. This is the first study to compare and describe these features. For accuracy and clarity, propensity score matching was used to balance the differences to explore the prognostic factors for patients with multiple gastrointestinal stromal tumors. To date, this study has the most detailed data and the largest number of patients, which may bring new insight to the diagnosis and treatment of multiple gastrointestinal stromal tumors.

Citation: Wu H, Li C, Li H, Shang L, Jing HY, Liu J, Fang Z, Du FY, Liu Y, Fu MD, Jiang KW, Li LP. Clinicopathological characteristics and longterm survival of patients with synchronous multiple primary gastrointestinal stromal tumors: A propensity score matching analysis. *World J Gastroenterol* 2021; 27(36): 6128-6141
URL: https://www.wjgnet.com/1007-9327/full/v27/i36/6128.htm
DOI: https://dx.doi.org/10.3748/wjg.v27.i36.6128

INTRODUCTION

As one of the most common mesenchymal tumors with an incidence of approximately 10 per million population, gastrointestinal stromal tumors (GISTs) are receiving

Grade E (Poor): 0

Received: June 19, 2021
Peer-review started: June 19, 2021
First decision: July 14, 2021
Revised: July 26, 2021
Accepted: August 13, 2021
Article in press: August 13, 2021
Published online: September 28, 2021

P-Reviewer: Vij M
S-Editor: Yan JP
L-Editor: Filipodia
P-Editor: Li JH

increasing attention[1-3]. GISTs are commonly located in the stomach and small intestine and rarely found in the esophagus, colon and rectum[4].

Multiple GISTs (MGISTs) refer to GISTs with two or more synchronous tumors in the gastrointestinal tract[5]. With the rapid advancement of precise diagnostic techniques and detailed pathological examinations, the detection and reporting of MGISTs have increased gradually. MGISTs accounted for nearly 2% of all GISTs in a multicenter study in China from 2001 to 2014[6]. However, due to the low incidence, there is currently no large-scale demographic survey showing the incidence of MGISTs.

Whether the clinical and pathological features of MGISTs are different from those of solitary GISTs (SGISTs) also remains unclear. Additionally, little is known about the impact of MGISTs on the survival of patients with GISTs. The diagnosis, treatment and follow-up strategies for MGISTs are not specifically described in the guidelines from the National Comprehensive Cancer Network, European Society for Medical Oncology and other academic institutions. Thus, we analyzed the clinicopathological characteristics and long-term survival of a large cohort of patients with MGISTs. It is urgent to gain insight into these questions to achieve personalized precision therapy in the future.

MATERIALS AND METHODS

Study design and approval

This retrospective cohort study was performed based on a prospectively collected database of GISTs at our hospital. All relevant procedures were approved by the Institutional Review Board. This study was designed in compliance with the Declaration of Helsinki and approved by the Ethics Committee of our hospital. The Reporting and Guidelines in propensity score analysis were also followed[7].

Patients

A total of 1163 consecutive patients diagnosed with GISTs and undergoing resection at our hospital between March 2010 and January 2020 were initially pooled; of whom, 1054 were classified as having primary GISTs (Figure 1). All oncological resections with curative intent were performed by senior surgeons specialized in achieving the rigorous standard at our institution. The inclusion criteria were: (1) Age > 18 years; (2) Pathological diagnosis of GIST; (3) No evidence of recurrent GIST or distant metastasis before treatment; and (4) Physiological status based on an Eastern Cooperative Oncology Group score < 3 points. The exclusion criteria were: (1) Any previous or concurrent malignancies; (2) First operation performed in other institutions; (3) Missing or illegible baseline information; and (4) Missing follow-up data. Finally, 983 patients with regular follow-up were included and analyzed. The follow-up was performed every 3 mo for the first 3 years, then every 6 mo up to 5 years, and then every year or until death in the following years. The latest follow-up date was December 2020.

Data collection

The following clinicopathological characteristics were routinely collected from the GIST database: Age, sex, tobacco and alcohol use, body mass index (BMI), comorbidities, chief complaint, tumor location, tumor size, mitotic index (per 50 high power fields), American Society of Anesthesiologists score, modified National Institutes of Health risk category, surgical approach, intraoperative blood transfusion, operation time, postoperative complications, hospitalization time, postoperative imatinib, immunohistochemistry results and hematological indices. BMI was classified into the following categories: < 18.5, 18.5-24.9 and ≥ 25 kg/m2, based on the World Health Organization classification. The comorbidities analyzed comprised hypertension, diabetes mellitus, anemia, pulmonary disease (asthma, pneumonia, chronic obstructive pulmonary disease, *etc.*), heart disease (arrhythmia, coronary atherosclerotic heart disease, *etc.*), liver disease (hepatitis, cirrhosis, *etc.*), renal disease (nephritis, chronic kidney disease, *etc.*) and central nervous system disease (cerebrovascular disease, neurodegenerative disease, *etc.*).

The primary outcome was progression-free survival (PFS), which was defined as the interval between the date of resection and the date of confirmed disease progression or death. The secondary outcome was overall survival (OS), which was calculated from the date of surgery until the date of death. Patients were censored at the date of the last follow-up without the above event.

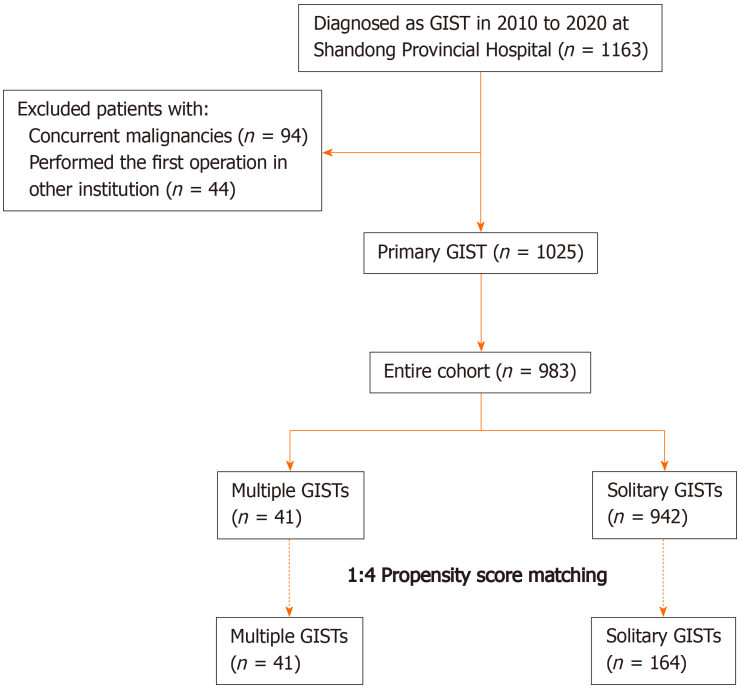

Figure 1 Flow chart of the of this study. GIST: Gastrointestinal stromal tumors; MGIST: Multiple gastrointestinal stromal tumors.

Definition of MGISTs

There is currently no authoritative and recognized definition of MGISTs. With reference to the criteria for multiple other cancers[8-11], especially multiple gastric cancers[12], we defined MGISTs as follows: (1) Each lesion must be pathologically proven; (2) All lesions must be separated microscopically; and (3) The possibility that one of the lesions represents a local extension of a metastatic tumor must be ruled out beyond reasonable doubt. It is because of the above criteria that all patients with any GIST outside the digestive tract (such as the omentum) were excluded. We defined MGISTs as two or more GISTs in the digestive tract. When MGISTs were different in size and mitotic index, the tumor was recorded according to the most advanced tumor. Similarly, in clinical practice, a modified National Institutes of Health risk category was also defined and assessed according to the most advanced tumor.

Statistical analysis

Categorical variables were analyzed using Pearson's χ^2 test or Fisher's exact test, according to the expected values. The Mann–Whitney U test was utilized to compare continuous variables, which are presented as medians and interquartile ranges and as the mean ± SD. The Kaplan–Meier method and log-rank test were performed to conduct survival analyses and evaluate differences in survival time, respectively. Univariate and multivariate analyses were performed using the Cox proportional hazards model. Univariate analysis was primarily performed, and variables with $P < 0.2$ were subsequently input into the multivariate analysis to determine the independent prognostic factors. Hazard ratios with their 95% confidence intervals were also derived. Statistical significance was defined as $P < 0.05$. SPSS version 26.0 (IBM, Armonk, NY, United States) and R version 3.5.3 (The R Foundation for Statistical Computing, Vienna, Austria) were used for statistical analysis.

Propensity score matching

Due to the inhomogeneous distribution of several baseline characteristics and uneven group sizes between patients with MGISTs and SGISTs, propensity score matching was performed. First, a propensity score was calculated using a logistic regression model in which the MGIST group was regressed as a dependent variable on relevant baseline parameters. The propensity score matching ratio was set to a 1:4 ratio to minimize the differences due to comorbidities, BMI, tumor location, mitotic index, sex, age and American Society of Anesthesiologist score with the nearest neighbor method. The assessment of propensity score matching is shown in Supplementary Figure 1.

RESULTS

Patient characteristics

The flow chart for the study is shown in Figure 1. Of the 983 consecutive patients who were pooled into the entire cohort between March 2010 and January 2020 at our institution, 41 (4.17%) with MGISTs were identified.

The preoperative clinical characteristics are described in Table 1. Before matching, most of the baseline characteristics were similar between the two groups, with significant differences only in BMI (P = 0.010). Regarding surgical and postoperative pathological characteristics and treatment of the SGISTs and MGISTs (Table 2), there were significant differences in surgical approach (P = 0.028), tumor size (P = 0.007), mitotic index (P = 0.009) and modified National Institutes of Health risk category (P = 0.044).

After propensity score matching at a 1:4 ratio, all baseline characteristics of the 41 patients in the MGIST group were compared with those of the 164 patients in the SGIST group (Tables 1 and 2). Supplementary pathological characteristics and blood indicators are shown in Supplementary Table 1. We also listed the clinical characteristics of patients with multiple tumors in detail (Supplementary Table 2) and showed several pathological images from these patients (Supplementary Figure 2).

Impact of MGISTs on PFS and OS

The median follow-up time of the entire matched cohort was 1468 d (IQR, 938-2225 d), and the 1-, 3- and 5-year PFS rates were 96.06%, 83.66% and 70.09%, respectively. For the patients with MGISTs, the 1-, 3- and 5-year PFS rates were 90.00%, 74.19% and 52.17%, respectively and compared with the 1-, 3- and 5-year PFS rates of 97.55%, 86.78% and 75.00% for the patients with SGISTs (P = 0.031) (Figure 2). We continued to explore the impact of MGISTs on OS. The 1-, 3- and 5-year OS rates were 98.16%, 92.50% and 83.75% for patients with SGISTs compared with 100%, 86.67% and 60.00% for patients with MGISTs, respectively, with no significant differences (P = 0.085) (Figure 3).

Univariate and multivariate analyses

Univariate analysis identified the following prognostic factors for PFS: age (P = 0.069), tumor location (P < 0.001), tumor size (P = 0.001), mitotic index (P < 0.001), blood transfusion (P = 0.018), intraoperative tumor rupture (P = 0.011), imatinib treatment (P = 0.133) and MGISTs (P = 0.035). On multivariate analysis, tumor location (P = 0.002), tumor size (P = 0.035), mitotic index (P = 0.001), imatinib treatment (P < 0.001) and MGISTs (P = 0.029) were eventually identified as independent prognostic factors for PFS (Table 3).

Univariate analysis revealed that tumor location (P < 0.001), tumor size (P = 0.021), mitotic index (P < 0.001), blood transfusion (P = 0.008), intraoperative tumor rupture (P = 0.113), imatinib treatment (P = 0.030) and MGISTs (P = 0.092) were correlated with OS. Subsequent multivariate analysis showed that tumor location (P = 0.003), mitotic index (P= 0.015) and imatinib treatment (P < 0.001) could be identified as independent risk factors for OS (Table 4). OS of patients with MGISTs (P = 0.106) was similar to that of patients with a single GIST.

DISCUSSION

MGISTs are often found in clinical treatment but ignored or misinterpreted as recurrence or metastasis. With the current lack of convincing results from large-scale studies based on demographics or clinicopathological characteristics, this is the first study to analyze the clinicopathological differences between patients with MGISTs and those with SGISTs. For accuracy and clarity, propensity score matching was used to balance the differences to explore the prognostic factors for patients with MGISTs.

A total of 983 patients were included in the cohort, including 41 with MGISTs. MGISTs accounted for approximately 4.17% of all GISTs in our study. With a median age of 60 years, patients with MGISTs had a similar age at initial diagnosis as patients with SGISTs. The incidence of GISTs is almost equal in men and women[13]; however, in our study, a male predisposition (M/F=27/14) was observed.

The BMI of patients with MGISTs was significantly lower than that of patients with SGISTs, which was pointed out for the first time, but the reason for this finding is not clear. Smoking and alcohol consumption did not affect the occurrence of MGISTs. There were no significant differences in American Society of Anesthesiologists classi-

Table 1 Preoperative clinical characteristics of solitary gastrointestinal stromal tumors and multiple gastrointestinal stromal tumors in the entire cohort and after propensity score matching

Parameters	Entire cohort, before matching		*P* value	Propensity score matched cohort		*P* value
	SGIST, *n* (%)	MGIST, *n* (%)		SGIST, *n* (%)	MGIST, *n* (%)	
All cases	942	41		164	41	
Age (yr)			0.450			0.889
≤ 60	516 (54.78)	20 (48.78)		82 (50.00)	20 (48.78)	
> 60	426 (45.22)	21 (51.22)		82 (50.00)	21 (51.22)	
Gender			0.060			0.596
Male	479 (50.85)	27 (65.85)		115 (70.12)	27 (65.85)	
Female	463 (49.15)	14 (34.15)		49 (29.88)	14 (34.15)	
BMI (kg/m^2)			**0.010**			0.193
BMI < 18.5	41 (4.35)	6 (14.63)		11 (6.71)	6 (14.63)	
18.5 ≤ BMI < 25	501 (53.18)	19 (46.34)		94 (57.32)	19 (46.34)	
BMI ≥ 25	400 (42.46)	16 (39.02)		59 (35.98)	16 (39.02)	
Tobacco use			0.899			0.093
No	704 (74.73)	31 (75.61)		101 (61.59)	31 (75.61)	
Yes	238 (25.27)	10 (24.39)		63 (38.41)	10 (24.39)	
Alcohol use			0.514			0.768
No	687 (72.93)	28 (60.98)		108 (65.85)	28 (60.98)	
Yes	255 (27.07)	13 (31.71)		56 (34.15)	13 (31.71)	
ASA score			0.443			0.868
I/II	779 (82.70)	32 (78.05)		126 (74.83)	32 (78.05)	
III/IV	163 (17.30)	9 (21.95)		38 (23.17)	9 (21.85)	
Comorbidities[1]			0.236			1.000
Present	417 (44.27)	22 (53.66)		88 (53.66)	22 (53.66)	
Absent	525 (55.73)	19 (46.34)		76 (46.34)	19 (46.34)	
Location			0.450			0.884
Gastric	650 (69.00)	26 (63.41)		106 (64.63)	26 (63.41)	
Non-gastric	292 (31.00)	15 (36.58)		58 (35.37)	15 (36.58)	
Chief complaint						
Abdominal pain	303 (32.17)	15 (36.58)	0.554	54 (32.93)	15 (36.58)	0.657
Abdominal distention	149 (15.82)	9 (21.95)	0.295	23 (14.02)	9 (21.95)	0.211
Hematemesis	42 (4.46)	3 (7.32)	0.429	9 (5.49)	3 (7.32)	0.710
Hematochezia	167 (17.72)	9 (21.95)	0.490	34 (20.73)	9 (21.95)	0.864
Medical examination	275 (29.19)	11 (26.83)	0.744	42 (25.61)	11 (26.83)	0.906
Other	96 (10.19)	2 (4.88)	0.266	17 (10.37)	2 (4.88)	0.278

[1]Comorbidities: comprised of hypertension, diabetes mellitus, anemia, pulmonary disease (asthma, pneumonia, chronic obstructive pulmonary disease, *etc.*), heart disease (arrhythmia, coronary atherosclerotic heart disease, *etc.*), liver disease (hepatitis, cirrhosis, *etc.*), renal disease (nephritis, chronic kidney disease, *etc.*) and central nervous system disease (cerebrovascular disease, neurodegenerative disease, *etc.*). Bold values indicate $P < 0.05$. ASA: American Society of Anesthesiologists; BMI: Body mass index; MGIST: Multiple gastrointestinal stromal tumors; SGIST: Solitary gastrointestinal stromal tumors.

fication or comorbidities, which means that the patients were in similar physical conditions at the time of diagnosis.

Table 2 Surgical and postoperative pathological characteristics and treatment of the solitary gastrointestinal stromal tumors and multiple gastrointestinal stromal tumors of the entire cohort and after propensity score matching

Parameters	Entire cohort, before matching		*P* value	Propensity score matched cohort		*P* value
	SGIST, *n* (%)	MGIST, *n* (%)		SGIST, *n* (%)	MGIST, *n* (%)	
All cases	942	41		164	41	
Surgical approach			**0.028**			0.361
Open	458 (48.62)	27 (65.85)		94 (57.32)	27 (65.85)	
Laparoscopic	255 (27.07)	11 (26.83)		43 (26.22)	11 (26.83)	
Endoscopic	229 (24.31)	3 (7.32)		27 (14.63)	3 (7.32)	
Blood transfusion			0.161			1.000
Yes	171 (18.15)	11 (26.83)		44 (26.83)	11 (26.83)	
No	771 (81.85)	30 (73.17)		120 (73.17)	30 (73.17)	
Tumor size (cm)			**0.007**			0.200
Length ≤ 5	575 (61.04)	15 (36.59)		74 (45.12)	15 (36.59)	
5 < Length ≤ 10	239 (25.37)	16 (39.02)		41 (25.00)	16 (39.02)	
Length > 10	128 (13.59)	10 (24.39)		49 (29.88)	10 (24.39)	
Mitotic index (per 50 HPF)			**0.009**			0.715
0-5	724 (76.86)	27 (65.85)		101 (61.59)	27 (65.85)	
6-10	127 (13.48)	4 (9.76)		24 (14.63)	4 (9.76)	
> 10	91 (9.66)	10 (24.39)		39 (23.78)	10 (24.39)	
Modified NIH risk			**0.044**			0.486
Very low	210 (22.29)	4 (9.76)		29 (17.68)	4 (9.76)	
Low	291 (30.89)	9 (21.95)		30 (18.29)	9 (21.95)	
Intermediate	147 (15.61)	8 (19.51)		22 (13.41)	8 (19.51)	
High	294 (31.21)	20 (48.78)		83 (50.61)	20 (48.78)	
Operate time (min)			0.336			0.627
mean ± SD	139 ± 78	151 ± 63		145 ± 67	151 ± 63	
Median (IQR)	120 (80-180)	150 (120-180)		140 (90-190)	150 (120-180)	
Intraoperative tumor rupture			0.376			0.490
Yes	10 (1.06)	1 (2.44)		2 (1.22)	1 (2.44)	
No	932 (98.94)	40 (97.56)		162 (98.78)	40 (97.56)	
Hospitalization time in d			0.226			0.442
mean ± SD	13.55 ± 6.32	14.78 ± 7.66		13.96 ± 5.69	14.78 ± 7.66	
Median (IQR)	12 (10-15)	14 (9-16)		13 (11-16)	14 (9-16)	
Postoperative complications			0.391			0.610
Present	179 (19.00)	10 (24.39)		34 (20.73)	10 (24.39)	
Absent	763 (81.00)	31 (73.61)		130 (79.27)	31 (73.61)	
Imatinib treatment			0.187			0.832
Yes	298 (31.63)	17 (41.46)		71 (43.29)	17 (41.46)	
No	644 (68.37)	24 (58.54)		93 (56.71)	24 (58.54)	

Bold values indicate $P < 0.05$. HPF: High power field; IQR: Interquartile range; MGIST: Multiple gastrointestinal stromal tumors; NIH: National Institutes of Health; SD: SD; SGIST: Solitary gastrointestinal stromal tumors.

There was no significant difference in the chief complaint, which also implies

Table 3 Univariate and multivariate of the clinicopathological factors for progression-free survival

Characteristics	Univariate analysis		Multivariate analysis	
	HR (95%CI)	*P* value	HR (95%CI)	*P* value
Age in yr				
≤ 60	Reference		Reference	
> 60	1.845 (0.953-3.571)	0.069	1.525 (0.740-3.143)	0.252
Sex				
Female	Reference			
Male	0.913 (0.460-1.809)	0.793		
Comorbidities				
Absent	Reference			
Present	1.147 (0.606-2.172)	0.673		
Tumor location				
Gastric	Reference		Reference	
Non-gastric	3.548 (1.847-6.818)	**< 0.001**	3.176 (1.526-6.607)	**0.002**
Tumor size in cm		**0.001**		**0.035**
Length ≤ 5	Reference		Reference	
5 < Length ≤ 10	3.022 (1.117-8.179)	**0.029**	2.180 (0.716-6.642)	0.170
Length > 10	5.848 (2.359-14.499)	**< 0.001**	4.071 (1.375-12.052)	**0.011**
Mitotic index, per 50 HPF		**< 0.001**		**0.001**
0-5	Reference		Reference	
6-10	4.094 (1.555-10.777)	**0.004**	4.108 (1.309-12.897)	**0.015**
> 10	7.859 (3.676-16.799)	**< 0.001**	6.577 (2.540-17.029)	**< 0.001**
Surgical approach		0.251		
Open	Reference			
Laparoscopic	0.449 (0.174-1.154)	0.096		
Endoscopic	0 (0-1.006E+230)	0.961		
Blood transfusion				
No	Reference		Reference	
Yes	2.176 (1.143-4.145)	**0.018**	1.569 (0.739-3.332)	0.241
Intraoperative tumor rupture				
No	Reference		Reference	
Yes	6.383 (1.524-26.726)	**0.011**	4.458 (0.863-23.015)	0.074
Imatinib treatment				
Yes	Reference		Reference	
No	0.584 (0.290-1.178)	0.133	4.608 (2.030-10.461)	**< 0.001**
MGIST				
Absent	Reference		Reference	
Present	2.091 (1.055-4.145)	**0.035**	2.431 (1.097-5.386)	**0.029**

Bold values indicate $P < 0.05$. CI: Confidence interval; HPF: High power field; HR: Hazard ratio; MGIST: Multiple gastrointestinal stromal tumors.

difficulty in clinical diagnosis. MGISTs are often reported to be associated with type 1 neurofibromatosis[14], the Carney triad[15] and Carney–Stratakis syndrome[16]. In the records of our medical center, there was only one patient with neurofibromatosis, who

Table 4 Univariate and multivariate analysis of the clinicopathological factors for overall survival

Characteristics	Univariate analysis		Multivariate analysis	
	HR (95%CI)	*P* value	HR (95%CI)	*P* value
Age in yr				
≤ 65	Reference			
> 65	1.665 (0.754-3.676)	0.207		
Gender				
Female	Reference			
Male	1.099 (0.461-2.616)	0.832		
Comorbidities				
Absent	Reference			
Present	1.061 (0.491-2.291)	0.881		
Tumor location				
Gastric	Reference		Reference	
Non-gastric	4.428 (1.967-9.965)	**< 0.001**	3.812 (1.577-9.213)	**0.003**
Tumor size in cm		**0.021**		0.556
Length ≤ 5	Reference		Reference	
5 < Length ≤ 10	2.279 (0.722-7.189)	0.160	1.381 (0.346-5.519)	0.648
Length > 10	4.159 (1.498-11.549)	**0.006**	2.070 (0.539-7.959)	0.290
Mitotic index, per 50 HPF		**< 0.001**		**0.015**
0-5	Reference		Reference	
6-10	3.120 (0.913-10.669)	0.070	4.129 (0.963-17.707)	0.056
> 10	7.515 (3.045-18.548)	**< 0.001**	6.051 (1.762-20.778)	**0.004**
Surgical approach		0.684		
Open	Reference			
Laparoscopic	0.621 (0.213-1.815)	0.384		
Endoscopic	0 (0-3.609E+275)	0.968		
Blood transfusion				
No	Reference		Reference	
Yes	2.832 (1.312-6.113)	**0.008**	1.298 (0.547-3.082)	0.554
Intraoperative tumor rupture				
No	Reference		Reference	
Yes	5.094 (0.682-38.043)	0.113	3.264 (0.355-30.022)	0.296
Imatinib treatment				
Yes	Reference		Reference	
No	2.952 (1.113-7.831)	**0.030**	7.841 (2.677-22.693)	**< 0.001**
MGIST				
Absent	Reference		Reference	
Present	2.050 (0.889-4.726)	0.092	2.404 (0.830-6.966)	0.106

Bold values indicate $P < 0.05$. CI: Confidence interval; HPF: High power field; HR: Hazard ratio; MGIST: Multiple gastrointestinal stromal tumors.

has been reported in our previous study[17]. However, this patient was not included in this cohort because of concurrent colon cancer. Familial and pediatric GISTs are also associated with multicentric risk[18]. However, these types of MGISTs were not found

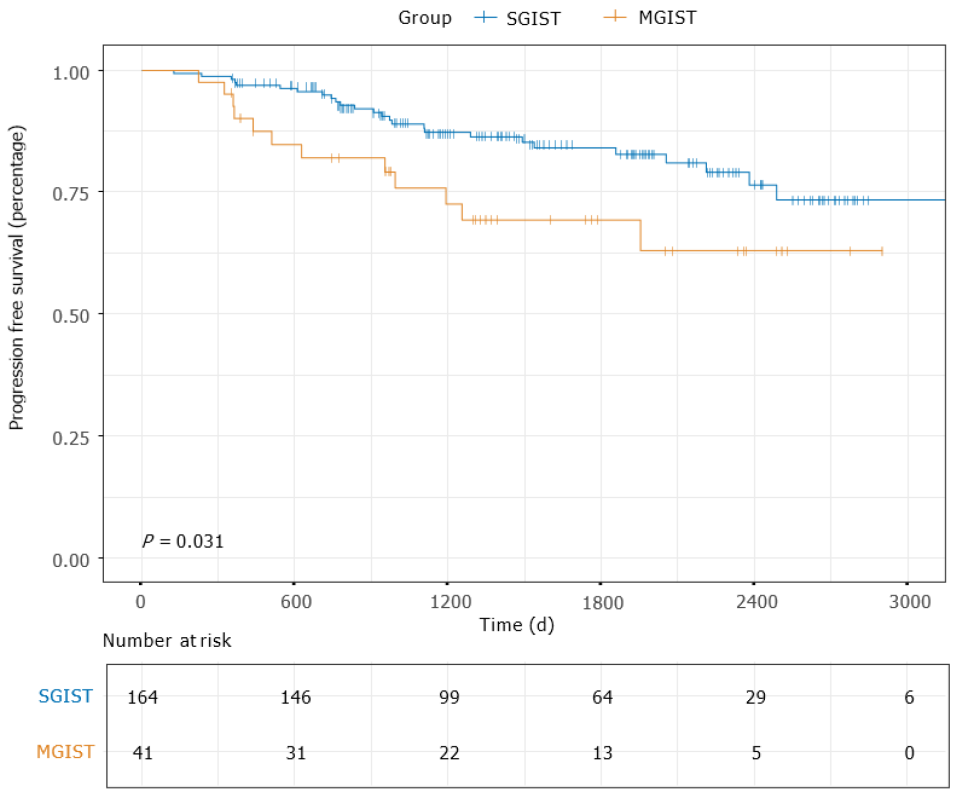

Figure 2 Kaplan–Meier survival analysis of progression-free survival. MGIST: Multiple gastrointestinal stromal tumors; SGIST: Solitary gastrointestinal stromal tumors.

in our study. This may be due to bias in the publication of case reports on these particular patients or the fact that the examination strategy has not been perfected so that such patients are missed by our colleagues. In addition, all cases of GISTs predominantly affected a single organ, and we should still pay attention to patients with multiorgan involvement to prevent misdiagnosis.

Imaging examination is an important basis for diagnosis[19]. Computed tomography or enhanced computed tomography is currently recommended but does not play an adequate role in the diagnosis of MGISTs. Of the 41 MGIST patients in our hospital, 38 underwent computed tomography examination, but only four were diagnosed accordingly. None of the MGISTs < 1 cm were detected, but this may be due to the large size of the major tumor or insufficient imaging evidence to diagnose the small tumor. For endoscopic examination, 8 of the 26 patients were suspected to have MGISTs before surgery, but endoscopy only revealed the tumor growing into the intestinal cavity, and none of the 15 cases of small intestinal MGISTs was detected. No case of MGISTs was diagnosed by B-ultrasonography or upper digestive tract radiography. Magnetic resonance imaging might be useful for diagnosis but is seldom used in ordinary examinations. Micro-GISTs, with low or no mitotic activity and little clinical significance, are common in the stomach (20%-35%)[20,21] and can transform to clinical GISTs by unknown mechanisms. Therefore, the development or modification of an examination method for preoperative screening of MGISTs can develop a more appropriate treatment plan for patients and obtain a greater survival benefit.

Heterogeneous morphology could be observed and the common growth patterns of MGISTs manifest a satellite phenomenon, that is, one or more main tumors surrounded by several small tumors. Of course, homogeneous morphology was still present in some tumors of MGISTs. Almost all gastric MGISTs consisted of two tumors and grew inside. On the contrary, small intestinal GISTs, especially in the jejunum, almost always had more than two tumors, and most of them grew outside. Unfortunately, the phenomenon has rarely been described in other studies, and it is difficult to determine whether it is a general finding. It is possible that MGISTs have different growth patterns and prognoses from SGISTs, and further research is needed.

The cellular types of the tumors were similar. Before propensity score matching, there was a significant difference in tumor necrosis. In addition, the proportion of calcification and cystic degeneration of MGISTs was higher than that of SGISTs, but

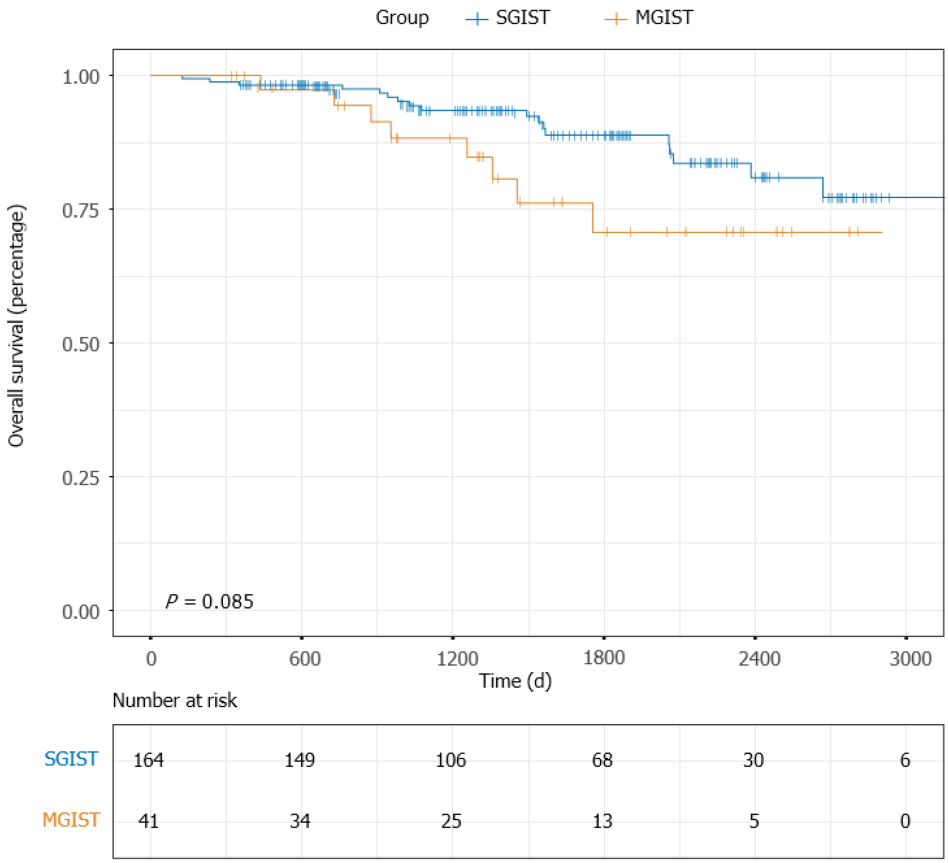

Figure 3 Kaplan–Meier survival analysis of overall survival. MGIST: Multiple gastrointestinal stromal tumors; SGIST: Solitary gastrointestinal stromal tumors.

the difference was not significant. In the propensity score matched cohort, all the above characteristics of MGISTs were compared with those of SGISTs.

For blood parameters, except for prealbumin, no significant differences were found. Immunohistochemical staining for Ki-67 antigen is often used, although this score is relatively subjective[22]. With regard to immunohistochemical markers, KIT (CD117) and ANO1 (DOG1) are two of the most sensitive and specific for GISTs[23]. S-100 and CD34 can also be used as auxiliary diagnostic indicators[24]. Unfortunately, there was no significant difference in these indicators between the patients with MGISTs and those with SGISTs.

The tumor mitotic rate is the most significant independent prognostic factor for GIST recurrence after surgery for both the stomach[25] and small intestine[26]. In our cohort, patients with MGISTs had larger tumors and a higher mitotic index, which also contributed to more advanced tumor stages.

The main treatment strategy for GISTs > 2 cm is surgical resection, and this is also the case for MGISTs. R0 resection, minimally invasive surgery and regular imaging surveillance are required to ensure perioperative and postoperative safety of patients. MGISTs may involve many segments of the gastrointestinal tract, so extensive resection is more common than with SGISTs. Therefore, consultation with experienced specialists is required to assess surgical extension and perioperative adjuvant therapy. In the practice of our medical center, the rate of open surgery for MGISTs is significantly higher than that for SGISTs. Imatinib was used for KIT/PDGFRA mutated GISTs[27] and is usually recommended for high-risk patients after surgery.

Of the 41 patients evaluated, 11 received intraoperative blood transfusions, which is higher than the rate for other operations and should compel surgeons to conduct a thorough preoperative evaluation and develop appropriate protocols. However, there was only a slight increase in operation time, intraoperative tumor rupture, postoperative hospital stays and postoperative complications in patients with MGISTs, and the difference was not significant.

After propensity score matching, all the above parameters were well balanced. We then tried to evaluate the clinical, perioperative and therapeutic factors associated with OS through Cox univariate and multivariate hazard ratio models.

There have been few studies related to the prognosis of patients with MGISTs[28]. Our study demonstrated that PFS of patients with MGISTs was significantly poorer than that of patients with SGISTs and that MGISTs were an independent risk factor for poor PFS. However, OS was similar between patients with SGISTs and those with MGISTs. This may be related to the characteristics of patients with MGISTs, suggesting that clinicians should closely monitor the condition of these patients, and it may be necessary to improve the risk classification of MGIST patients.

Given the lack of clinical trials, SGIST therapy has conflicting results in MGIST patients with regard to factors such as surgical excision and perioperative adjuvant therapy. This study suggests that more attention should be paid to such patients to explore more suitable treatment strategies. Gene detection and molecular biological experiments are also needed to explain specific manifestations[29,30].

There were some shortcomings in our research. First, as a single-center design with a small sample size, the statistical power of our findings might have been weakened. Moreover, due to the high cost, few of these patients had undergone gene detection. Last, there may have been a possibility of missed diagnoses, which could have led to an underestimation of the incidence of MGISTs.

To date, this study has the most detailed data and the largest number of patients, which may bring new insight to the diagnosis and treatment of MGISTs.

CONCLUSION

Patients with MGISTs may have demographic characteristics and immunohistochemical markers that are similar to those of patients with SGISTs, but MGIST patients also have unique tumor features. In this study, we found that MGISTs were an independent factor for PFS after propensity score matching analysis; however, OS was similar. The perioperative and long-term prognosis of patients remains of concern and requires multicenter, large sample, long-term follow-up, prospective studies. Most importantly, risk criteria, diagnostic strategies and treatment procedures suitable for this disease of lower morbidity should be developed to achieve personalized precision therapy and maximize the survival benefit of these patients.

ARTICLE HIGHLIGHTS

Research background

Synchronous primary multiple gastrointestinal stromal tumors (MGISTs) are specific and rare. The diagnosis, treatment and follow-up strategies of MGISTs are not specifically described in guidelines.

Research motivation

Due to the low incidence, there is currently no large-scale demographic survey showing the incidence of MGISTs. Additionally, little is known about the impact of MGISTs on the survival of patients with gastrointestinal stromal tumors (GISTs).

Research objectives

This study aimed to compare the clinicopathological characteristics and prognoses of patients with MGISTs and patients with solitary GISTs (SGISTs).

Research methods

Due to the inhomogeneous distribution of several baseline characteristics and uneven MGIST and SGIST group sizes, propensity score matching was performed according to comorbidities, body mass index, tumor location, mitotic index, sex, age and American Society of Anesthesiologists score.

Research results

Among the entire cohort, the incidence of MGISTs was 4.17%. Patients with MGISTs and those with SGISTs had disparities in body mass index, surgical approach, tumor size and mitotic index. Tumor location, tumor size, mitotic index, imatinib treatment and MGISTs were identified as independent prognostic factors of progression-free survival. However, overall survival was similar between the SGIST and MGIST groups.

Research conclusions

Patients with MGISTs may have demographic characteristics and immunohistochemical markers that are similar to those of patients with SGISTs, but MGIST patients also have unique tumor features. Without specific diagnostic indicators and symptoms, patients with MGISTs were identified as having a poorer progression-free survival than patients with SGISTs.

Research perspectives

Risk criteria, diagnostic strategies and treatment procedures suitable for these tumors of lower morbidity should be developed to achieve personalized precision therapy and maximize the survival benefit of these patients.

ACKNOWLEDGEMENTS

We extend our thanks to all patients involved in the study. We would also like to thank the Medical Records Department of Shandong Provincial Hospital for providing data support and the efforts of medical workers over the past decades.

REFERENCES

1 **Joensuu H**, Hohenberger P, Corless CL. Gastrointestinal stromal tumour. *Lancet* 2013; **382**: 973-983 [PMID: 23623056 DOI: 10.1016/S0140-6736(13)60106-3]

2 **Ma GL**, Murphy JD, Martinez ME, Sicklick JK. Epidemiology of gastrointestinal stromal tumors in the era of histology codes: results of a population-based study. *Cancer Epidemiol Biomarkers Prev* 2015; **24**: 298-302 [PMID: 25277795 DOI: 10.1158/1055-9965.EPI-14-1002]

3 **Serrano C**, George S. Gastrointestinal Stromal Tumor: Challenges and Opportunities for a New Decade. *Clin Cancer Res* 2020; **26**: 5078-5085 [PMID: 32601076 DOI: 10.1158/1078-0432.CCR-20-1706]

4 **Nilsson B**, Bümming P, Meis-Kindblom JM, Odén A, Dortok A, Gustavsson B, Sablinska K, Kindblom LG. Gastrointestinal stromal tumors: the incidence, prevalence, clinical course, and prognostication in the preimatinib mesylate era--a population-based study in western Sweden. *Cancer* 2005; **103**: 821-829 [PMID: 15648083 DOI: 10.1002/cncr.20862]

5 **Gasparotto D**, Rossi S, Bearzi I, Doglioni C, Marzotto A, Hornick JL, Grizzo A, Sartor C, Mandolesi A, Sciot R, Debiec-Rychter M, Dei Tos AP, Maestro R. Multiple primary sporadic gastrointestinal stromal tumors in the adult: an underestimated entity. *Clin Cancer Res* 2008; **14**: 5715-5721 [PMID: 18779314 DOI: 10.1158/1078-0432.CCR-08-0622]

6 **Zhang X**, Ning L, Hu Y, Zhao S, Li Z, Li L, Dai Y, Jiang L, Wang A, Chu X, Li Y, Yang D, Lu C, Yao L, Cui G, Lin H, Chen G, Cui Q, Guo H, Zhang H, Lun Z, Xia L, Su Y, Han G, Hui X, Wei Z, Sun Z, Shen S, Zhou Y. Prognostic Factors for Primary Localized Gastrointestinal Stromal Tumors After Radical Resection: Shandong Gastrointestinal Surgery Study Group, Study 1201. *Ann Surg Oncol* 2020; **27**: 2812-2821 [PMID: 32040699 DOI: 10.1245/s10434-020-08244-9]

7 **Yao XI**, Wang X, Speicher PJ, Hwang ES, Cheng P, Harpole DH, Berry MF, Schrag D, Pang HH. Reporting and Guidelines in Propensity Score Analysis: A Systematic Review of Cancer and Cancer Surgical Studies. *J Natl Cancer Inst* 2017; **109** [PMID: 28376195 DOI: 10.1093/jnci/djw323]

8 **He W**, Zheng C, Wang Y, Dan J, Zhu M, Wei M, Wang J, Wang Z. Prognosis of synchronous colorectal carcinoma compared to solitary colorectal carcinoma: a matched pair analysis. *Eur J Gastroenterol Hepatol* 2019; **31**: 1489-1495 [PMID: 31441800 DOI: 10.1097/MEG.0000000000001487]

9 **Bos ACRK**, Matthijsen RA, van Erning FN, van Oijen MGH, Rutten HJT, Lemmens VEPP. Treatment and Outcome of Synchronous Colorectal Carcinomas: A Nationwide Study. *Ann Surg Oncol* 2018; **25**: 414-421 [PMID: 29159744 DOI: 10.1245/s10434-017-6255-y]

10 **Otowa Y**, Nakamura T, Takiguchi G, Yamamoto M, Kanaji S, Imanishi T, Oshikiri T, Suzuki S, Tanaka K, Kakeji Y. Safety and benefit of curative surgical resection for esophageal squamous cell cancer associated with multiple primary cancers. *Eur J Surg Oncol* 2016; **42**: 407-411 [PMID: 26733367 DOI: 10.1016/j.ejso.2015.11.012]

11 **Yu YC**, Hsu PK, Yeh YC, Huang CS, Hsieh CC, Chou TY, Hsu HS, Wu YC, Huang BS, Hsu WH. Surgical results of synchronous multiple primary lung cancers: similar to the stage-matched solitary primary lung cancers? *Ann Thorac Surg* 2013; **96**: 1966-1974 [PMID: 24021769 DOI: 10.1016/j.athoracsur.2013.04.142]

12 **Moertel CG**, Bargen JA, Soule EH. Multiple gastric cancers; review of the literature and study of 42 cases. *Gastroenterology* 1957; **32**: 1095-1103 [PMID: 13438166]

13 **Rubin BP**, Heinrich MC, Corless CL. Gastrointestinal stromal tumour. *Lancet* 2007; **369**: 1731-1741 [PMID: 17512858 DOI: 10.1016/s0140-6736(07)60780-6]

14 **Miettinen M**, Fetsch JF, Sobin LH, Lasota J. Gastrointestinal stromal tumors in patients with

neurofibromatosis 1: a clinicopathologic and molecular genetic study of 45 cases. *Am J Surg Pathol* 2006; **30**: 90-96 [PMID: 16330947 DOI: 10.1097/01.pas.0000176433.81079.bd]

15 **Zhang L**, Smyrk TC, Young WF Jr, Stratakis CA, Carney JA. Gastric stromal tumors in Carney triad are different clinically, pathologically, and behaviorally from sporadic gastric gastrointestinal stromal tumors: findings in 104 cases. *Am J Surg Pathol* 2010; **34**: 53-64 [PMID: 19935059 DOI: 10.1097/PAS.0b013e3181c20f4f]

16 **Pasini B**, McWhinney SR, Bei T, Matyakhina L, Stergiopoulos S, Muchow M, Boikos SA, Ferrando B, Pacak K, Assie G, Baudin E, Chompret A, Ellison JW, Briere JJ, Rustin P, Gimenez-Roqueplo AP, Eng C, Carney JA, Stratakis CA. Clinical and molecular genetics of patients with the Carney-Stratakis syndrome and germline mutations of the genes coding for the succinate dehydrogenase subunits SDHB, SDHC, and SDHD. *Eur J Hum Genet* 2008; **16**: 79-88 [PMID: 17667967 DOI: 10.1038/sj.ejhg.5201904]

17 **Shang L**, Fang Z, Liu J, Du F, Jing H, Xu Y, Dong K, Zhang X, Wu H, Jing C, Li L. Case report of ascending colon cancer and multiple jejunal GISTs in a patient with neurofibromatosis type 1 (NF1). *BMC Cancer* 2019; **19**: 1196 [PMID: 31805970 DOI: 10.1186/s12885-019-6375-9]

18 **Haller F**, Schulten HJ, Armbrust T, Langer C, Gunawan B, Füzesi L. Multicentric sporadic gastrointestinal stromal tumors (GISTs) of the stomach with distinct clonal origin: differential diagnosis to familial and syndromal GIST variants and peritoneal metastasis. *Am J Surg Pathol* 2007; **31**: 933-937 [PMID: 17527083 DOI: 10.1097/01.pas.0000213440.78407.27]

19 **Vernuccio F**, Taibbi A, Picone D, LA Grutta L, Midiri M, Lagalla R, Lo Re G, Bartolotta TV. Imaging of Gastrointestinal Stromal Tumors: From Diagnosis to Evaluation of Therapeutic Response. *Anticancer Res* 2016; **36**: 2639-2648 [PMID: 27272772]

20 **Kawanowa K**, Sakuma Y, Sakurai S, Hishima T, Iwasaki Y, Saito K, Hosoya Y, Nakajima T, Funata N. High incidence of microscopic gastrointestinal stromal tumors in the stomach. *Hum Pathol* 2006; **37**: 1527-1535 [PMID: 16996566 DOI: 10.1016/j.humpath.2006.07.002]

21 **Agaimy A**, Wünsch PH, Hofstaedter F, Blaszyk H, Rümmele P, Gaumann A, Dietmaier W, Hartmann A. Minute gastric sclerosing stromal tumors (GIST tumorlets) are common in adults and frequently show c-KIT mutations. *Am J Surg Pathol* 2007; **31**: 113-120 [PMID: 17197927 DOI: 10.1097/01.pas.0000213307.05811.f0]

22 **Liang YM**, Li XH, Li WM, Lu YY. Prognostic significance of PTEN, Ki-67 and CD44s expression patterns in gastrointestinal stromal tumors. *World J Gastroenterol* 2012; **18**: 1664-1671 [PMID: 22529697 DOI: 10.3748/wjg.v18.i14.1664]

23 **Novelli M**, Rossi S, Rodriguez-Justo M, Taniere P, Seddon B, Toffolatti L, Sartor C, Hogendoorn PC, Sciot R, Van Glabbeke M, Verweij J, Blay JY, Hohenberger P, Flanagan A, Dei Tos AP. DOG1 and CD117 are the antibodies of choice in the diagnosis of gastrointestinal stromal tumours. *Histopathology* 2010; **57**: 259-270 [PMID: 20716168 DOI: 10.1111/j.1365-2559.2010.03624.x]

24 **Riddle ND**, Gonzalez RJ, Bridge JA, Antonia S, Bui MM. A CD117 and CD34 immunoreactive sarcoma masquerading as a gastrointestinal stromal tumor: diagnostic pitfalls of ancillary studies in sarcoma. *Cancer Control* 2011; **18**: 152-159 [PMID: 21666577 DOI: 10.1177/107327481101800302]

25 **Miettinen M**, Sobin LH, Lasota J. Gastrointestinal stromal tumors of the stomach: a clinicopathologic, immunohistochemical, and molecular genetic study of 1765 cases with long-term follow-up. *Am J Surg Pathol* 2005; **29**: 52-68 [PMID: 15613856 DOI: 10.1097/01.pas.0000146010.92933.de]

26 **Miettinen M**, Makhlouf H, Sobin LH, Lasota J. Gastrointestinal stromal tumors of the jejunum and ileum: a clinicopathologic, immunohistochemical, and molecular genetic study of 906 cases before imatinib with long-term follow-up. *Am J Surg Pathol* 2006; **30**: 477-489 [PMID: 16625094 DOI: 10.1097/00000478-200604000-00008]

27 **Li K**, Tjhoi W, Shou C, Yang W, Zhang Q, Liu X, Yu J. Multiple gastrointestinal stromal tumors: analysis of clinicopathologic characteristics and prognosis of 20 patients. *Cancer Manag Res* 2019; **11**: 7031-7038 [PMID: 31413638 DOI: 10.2147/CMAR.S197560]

28 **Li C**, Yang KL, Wang Q, Tian JH, Li Y, Gao ZD, Yang XD, Ye YJ, Jiang KW. Clinical features of multiple gastrointestinal stromal tumors: A pooling analysis combined with evidence and gap map. *World J Gastroenterol* 2020; **26**: 7550-7567 [PMID: 33384554 DOI: 10.3748/wjg.v26.i47.7550]

29 **Nguyen V**, Banerjee S, Sicklick JK. Moving gastrointestinal stromal tumours towards truly personalised precision therapy. *Lancet Oncol* 2020; **21**: 865-867 [PMID: 32615099 DOI: 10.1016/S1470-2045(20)30335-1]

30 **Li J**, Shen L. The current status of and prospects in research regarding gastrointestinal stromal tumors in China. *Cancer* 2020; **126** Suppl 9: 2048-2053 [PMID: 32293728 DOI: 10.1002/cncr.32684]

World Journal of Gastroenterology

Submit a Manuscript: https://www.f6publishing.com

World J Gastroenterol 2021 September 28; 27(36): 6142-6153

DOI: 10.3748/wjg.v27.i36.6142

ISSN 1007-9327 (print) ISSN 2219-2840 (online)

ORIGINAL ARTICLE

Observational Study

Urotensin II levels in patients with inflammatory bowel disease

Damir Alicic, Dinko Martinovic, Doris Rusic, Piero Marin Zivkovic, Ivana Tadin Hadjina, Marino Vilovic, Marko Kumric, Daria Tokic, Daniela Supe-Domic, Slaven Lupi-Ferandin, Josko Bozic

ORCID number: Damir Alicic 0000-0002-5354-6299; Dinko Martinovic 0000-0003-2060-5130; Doris Rusic 0000-0002-7018-4947; Piero Marin Zivkovic 0000-0001-5649-698X; Ivana Tadin Hadjina 0000-0002-4443-5896; Marino Vilovic 0000-0002-5433-5063; Marko Kumric 0000-0002-9696-3359; Daria Tokic 0000-0001-9508-4160; Daniela Supe-Domic 0000-0002-5584-3182; Slaven Lupi-Ferandin 0000-0003-0220-5256; Josko Bozic 0000-0003-1634-0635.

Author contributions: Bozic J was the guarantor and designed the study; Alicic D, Martinovic D, Rusic D, Zivkovic PM, Tadin Hadjina I, Vilovic M, Kumric M, Tokic D, Lupi-Ferandin S and Supe-Domic D participated in the acquisition, analysis, and interpretation of the data and drafted the initial manuscript; Bozic J, Alicic D and Martinovic D revised the article critically for important intellectual content.

Institutional review board statement: The study was approved by the Ethics Committee of University Hospital of Split, No. 500-03/17-01/86.

Informed consent statement: All study participants, or their legal guardian, provided informed written consent prior to study enrollment.

Damir Alicic, Piero Marin Zivkovic, Ivana Tadin Hadjina, Department of Gastroenterology, University Hospital of Split, Split 21000, Croatia

Dinko Martinovic, Marino Vilovic, Marko Kumric, Josko Bozic, Department of Pathophysiology, University of Split School of Medicine, Split 21000, Croatia

Doris Rusic, Department of Pharmacy, University of Split School of Medicine, Split 21000, Croatia

Daria Tokic, Department of Anesthesiology and Intensive care, University Hospital of Split, Split 21000, Croatia

Daniela Supe-Domic, Department of Health Studies, University of Split, Split 21000, Croatia

Slaven Lupi-Ferandin, Department of Maxillofacial Surgery, University Hospital of Split, Split 21000, Croatia

Corresponding author: Josko Bozic, MD, PhD, Associate Professor, Department of Pathophysiology, University of Split School of Medicine, Soltanska 2, Split 21000, Croatia. josko.bozic@mefst.hr

Abstract

BACKGROUND

Patients with inflammatory bowel disease (IBD) are associated with increased cardiovascular risk and have increased overall cardiovascular burden. On the other hand, urotensin II (UII) is one of the most potent vascular constrictors with immunomodulatory effect that is connected with a number of different cardiometabolic disorders as well. Furthermore, patients with ulcerative colitis have shown increased expression of urotensin II receptor in comparison to healthy controls. Since the features of IBD includes chronic inflammation and endothelial dysfunction as well, it is plausible to assume that there is connection between increased cardiac risk in IBD and UII.

AIM

To determine serum UII levels in patients with IBD and to compare them to control subjects, as well as investigate possible associations with relevant clinical and biochemical parameters.

METHODS

This cross sectional study consecutively enrolled 50 adult IBD patients (26 with

Conflict-of-interest statement: There are no conflict of interest to report.

Data sharing statement: No additional data are available.

STROBE statement: The authors have read the STROBE Statement-checklist of items, and the manuscript was prepared and revised according to the STROBE Statement-checklist of items.

Manuscript source: Invited manuscript

Specialty type: Gastroenterology and hepatology

Country/Territory of origin: Croatia

Peer-review report's scientific quality classification

Grade A (Excellent): 0
Grade B (Very good): B
Grade C (Good): 0
Grade D (Fair): 0
Grade E (Poor): 0

Received: April 27, 2021
Peer-review started: April 27, 2021
First decision: June 13, 2021
Revised: June 17, 2021
Accepted: August 19, 2021
Article in press: August 19, 2021
Published online: September 28, 2021

P-Reviewer: Sassaki LY
S-Editor: Wu YXJ
L-Editor: Filipodia
P-Editor: Yuan YY

Crohn's disease and 24 with ulcerative colitis) and 50 age and gender matched controls. Clinical assessment was performed by the same experienced gastroenterologist according to the latest guidelines. Ulcerative Colitis Endoscopic Index of Severity and Simple Endoscopic Score for Crohn's Disease were used for endoscopic evaluation. Serum levels of UII were determined using the enzyme immunoassay kit for human UII, according to the manufacturer's instructions.

RESULTS

IBD patients have significantly higher concentrations of UII when compared to control subjects (7.57 ± 1.41 *vs* 1.98 ± 0.69 ng/mL, $P < 0.001$), while there were no significant differences between Crohn's disease and ulcerative colitis patients (7.49 ± 1.42 *vs* 7.65 ± 1.41 ng/mL, $P = 0.689$). There was a significant positive correlation between serum UII levels and high sensitivity C reactive peptide levels ($r = 0.491$, $P < 0.001$) and a significant negative correlation between serum UII levels and total proteins ($r = -0.306$, $P = 0.032$). Additionally, there was a significant positive correlation between serum UII levels with both systolic ($r = 0.387$, $P = 0.005$) and diastolic ($r = 0.352$, $P = 0.012$) blood pressure. Moreover, serum UII levels had a significant positive correlation with Ulcerative Colitis Endoscopic Index of Severity ($r = 0.425$, $P = 0.048$) and Simple Endoscopic Score for Crohn's Disease ($r = 0.466$, $P = 0.028$) scores. Multiple linear regression analysis showed that serum UII levels retained significant association with high sensitivity C reactive peptide (β ± standard error, 0.262 ± 0.076, $P < 0.001$) and systolic blood pressure (0.040 ± 0.017, $P = 0.030$).

CONCLUSION

It is possible that UII is involved in the complex pathophysiology of cardiovascular complications in IBD patients, and its purpose should be investigated in further studies.

Key Words: Inflammatory bowel disease; Crohn's disease; Ulcerative colitis; Urotensin II; Cardiovascular risk; Endoscopic activity

Core Tip: Urotensin II (UII) is a potent vasoconstrictor with an immunomodulatory effect that is connected to various cardiovascular disorders. On the other hand, patients with inflammatory bowel disease (IBD) have increased cardiovascular burden as well as increased expression of UII receptors. It is plausible that UII is involved in the complex pathophysiology of IBD complications. In the current study, we investigated UII levels in the IBD population and compared it to matched control subjects, as well as connection of UII with relevant clinical and biochemical parameters. The results of this study showed that serum UII levels are higher in IBD patients in comparison with the control group.

Citation: Alicic D, Martinovic D, Rusic D, Zivkovic PM, Tadin Hadjina I, Vilovic M, Kumric M, Tokic D, Supe-Domic D, Lupi-Ferandin S, Bozic J. Urotensin II levels in patients with inflammatory bowel disease. *World J Gastroenterol* 2021; 27(36): 6142-6153
URL: https://www.wjgnet.com/1007-9327/full/v27/i36/6142.htm
DOI: https://dx.doi.org/10.3748/wjg.v27.i36.6142

INTRODUCTION

Inflammatory bowel disease (IBD) is a relapsing chronic inflammation of the gastrointestinal tract with an unpredictable course[1]. It can be divided into two disorders: Crohn's disease (CD) and ulcerative colitis (UC). Although the two disorders have a similar clinical manifestation, they differ in the location and the depth of the inflammation. The etiology of the disease is considered to be multifactorial as a complex interrelation between extrinsic factors, genetic predisposition, immunological

imbalance and microbiota disturbances. Furthermore, IBD can exhibit a wide range of extraintestinal manifestations that affect the kidneys, eyes, joints, liver, skin, heart and blood circulation[2-6].

Urotensin II (UII) is a pleotropic peptide originally found 40 years ago in the neurosecretory system of the teleost fish, while in the meantime its activity was also found in humans. UII is considered to be the most potent vasoconstrictor discovered so far, with the effect 10-fold stronger than that of endothelin-1[7]. Furthermore, its expression was found distributed in most organs and tissues, including both the central nervous and cardiovascular systems, as well as the lungs, kidneys, spleen, hypophysis, adrenal glands, stomach, pancreas, ovaries and liver[8,9]. UII activity is regulated through the urotensin receptor (UTR), which after activation induces calcium mobilization in cellular plasma, smooth muscle cells proliferation and collagen synthesis[10]. Due to the wide range of functions, UII has an extensive effect on most of the organ systems in the body, and consequently it is also associated with numerous diseases and disorders[11-13]. Moreover, recent studies are pointing to possible UII immunomodulatory effects, as it was shown that UII is involved in the regulation of the inflammation process[14,15].

In the last few decades, the extraintestinal manifestations and complications of IBD are a major issue that is increasingly investigated for an improvement of both diagnostic and treatment criteria. It is well-established that patients with IBD are associated with a high cardiovascular risk, and it was shown that they have a higher prevalence cardiovascular diseases[16-18]. However, a Danish cohort study showed that patients with IBD have a lower prevalence of the traditional cardiovascular risk factors in comparison to the general population, while on the other hand they had a higher cardiovascular burden[19]. This ambiguity is well-established, yet it is unclear what are the factors that contribute to high cardiovascular risk in patients with IBD. Since UII is one of the most potent vasoconstrictors known, and it is well-known that it is associated with cardiovascular diseases, it is reasonable to presume that there is a possible connection between cardiovascular risk in IBD patients and UII[20,21]. Moreover, seeing that recent studies are pointing to UII immunomodulatory effect and since the hallmark of IBD is the chronic inflammation, this further suggests the need to investigate clinically the possible association between them[14,15]. Additionally, a recent study conducted on patients with UC showed that they have an increased expression of UTR compared to healthy controls[22]. Moreover, that expression was found to be increased in both disease lesions and healthy tissue biopsies.

Hence, the aim of this study was to evaluate serum UII levels in patients with IBD and to compare them with healthy, gender and age matched controls. Moreover, we further investigated the possible association between UII levels and the relevant clinical and biochemical parameters.

MATERIALS AND METHODS

Study design and ethical considerations

This cross-sectional study was conducted at the University Hospital of Split and the University of Split School of Medicine during the period from January 2018 to March 2019.

Before the start of the study, every participant was informed about the aim, course and procedures involved, and they all signed an informed written consent. The study was conducted in accordance with all ethical principles of the Seventh Revision of the Helsinki Declaration, and it was approved by the Ethics Committee of University Hospital of Split (date of approval: November 23, 2017).

Subjects

This study included 50 adult patients with pre-diagnosed IBD (24 patients with UC and 26 patients with CD) and 50 healthy, age and gender matched controls. The diagnosis of UC and CD was established on clinical, radiological, endoscopic and histological traits in accordance with the European Consensus on Crohn's Disease and Ulcerative Colitis[23]. Inclusion criteria were: Disease duration of at least 1 year, stable disease activity in the past 3 mo and age between 18 and 65 years. Exclusion criteria were: Diabetes, obesity, arterial hypertension, use of statins, cardiovascular disorders, therapy with corticosteroids during 3 mo prior to study onset, substance abuse and consumption of alcohol more than 40 g/d.

Additionally, we checked medical records of the control subjects regarding gastrointestinal conditions, and additionally we performed screening for abdominal pain presence, symptoms related to defecation and change in frequency and form of stool according to the Rome IV criteria for irritable bowel syndrome[24], as well as any other symptoms that could suggest gluten and lactose intolerance. If any of these conditions were present, we excluded the subject from the control group. Furthermore, all potential control group subjects underwent detailed physical examination along with laboratory analysis of the complete blood count and biochemical parameters. We excluded all participants who showed any sign of inflammation in any of these steps.

Disease severity assessment

Disease activity evaluation was performed using clinical and endoscopic indices. The assessment was conducted by the same experienced gastroenterologist according to the latest guidelines, and the colonoscopy needed for the evaluation of the disease activity was performed within 2 wk of blood sampling. We used endoscopic indices for the evaluation of the disease activity since they have an advantage before clinical indices according to the European Consensus on Crohn's Disease and Ulcerative Colitis guidelines[25]. Moreover, all IBD patients had their high sensitivity C reactive peptide (hsCRP) and fecal calprotectin evaluated to assess further the activity of the disease.

Ulcerative Colitis Endoscopic Index of Severity (UCEIS) is a quantitative grading system used for the evaluation of UC activity. Depending on the score, there are four possible grades for disease activity: (0-1)–remission; (2-4)–mild; (5-6)–moderate and (7-8)–severe activity[26].

Simple Endoscopic Score for CD (SES-CD) is a quantitative grading system used for the evaluation of CD activity. According to the majority of studies, the threshold values for interpretation of the results are: (0-2)–remission; (3-6)–mild activity; (7-15)–moderate activity and (≥ 16)–severe disease[27].

Blood sampling and laboratory analysis

All blood samples were taken from the cubital vein after 12-h fasting. After extraction, all samples were processed in the same day except for the UII samples, which were centrifuged and stored at -80 °C for further analysis. All the procedures were conducted according to the international standards, in the same laboratory and by the same experienced medical biochemist who was blinded to the subjects group in the study. Serum levels of UII were determined using the enzyme immunoassay kit for human UII (Phoenix Pharmaceuticals, Burlingame, CA, United States), according to the manufacturer's instructions. Concentration of the analyzed quality control sample that arrived from the manufacturer was within predefined acceptable deviation. The linear range of the assay was 0.06-8.2 ng/mL, and sensitivity was 0.06 ng/mL. Coefficient of variation within the probe was less than 10% and between probes was less than 15%. Other biochemical parameters were analyzed according to standard laboratory procedures.

Stool samples were received by a trained laboratory technician in sterile containers within 3 d of sampling. Fecal extraction and analyses were performed by an experienced medical biochemist.

Anthropometric and clinical assessment

All participants were subjected to detailed anamnesis, physical examination and measurements of anthropometric characteristics - body weight, body height and body mass index (BMI). For measurement of body weight and height, a calibrated medical scale with built-in heights (Seca, Birmingham, United Kingdom) was used. BMI was calculated according to the formula = [body weight (kg)]/[height per square (m^2)].

Statistical analysis

Collected data were analyzed with statistical software MedCalc (version 17.4.1; MedCalc Software, Ostend, Belgium,). Quantitative data were expressed as mean ± SD or median and interquartile range, while qualitative data were expressed as whole number and percentage. Kolmogorov-Smirnov test was used to estimate the normality of data distribution. Comparison of serum UII levels and other parameters between patients with IBD and control subjects was done by Student *t*-test for independent samples or Mann-Whitney *U* test. For comparison of qualitative variables, Chi-squared test was used. Pearson's correlation or Spearman's correlation was used to estimate the correlation between biochemical, anthropometric and clinical parameters with serum UII levels. Furthermore, multiple linear regression analysis was used to determine

significant independent predictors of serum UII levels, with reporting corresponding *P* values with unstandardized β-coefficients, standard error and t-values. The level of statistical significance was set at $P < 0.05$.

RESULTS

Baseline characteristics of the study population

There were no statistically significant differences regarding age, gender and anthropometric features between the IBD patients and healthy controls (Table 1). Laboratory analyses showed that the IBD group compared to the control group had significantly lower erythrocytes (4.7 ± 0.5 *vs* 5.0 ± 0.4 × 10^{12}/L, $P = 0.020$), hemoglobin (140.4 ± 17.3 *vs* 148.1 ± 13.7 g/L, $P = 0.015$) and albumins (39.5 ± 5.1 *vs* 43.7 ± 2.4 g/L, $P < 0.001$), while they had significantly higher hsCRP levels (3.4 ± 2.6 *vs* 1.2 ± 1.1 mg/L, $P < 0.001$) (Table 2).

Serum urotensin II levels

Serum UII levels were significantly higher in the IBD group compared to the control group (7.26 ± 1.67 *vs* 1.98 ± 0.68 ng/mL, $P < 0.001$) (Figure 1A). Furthermore, there were no statistically significant differences in serum UII levels between the patients with UC and patients with CD (7.15 ± 1.63 *vs* 7.36 ± 1.73 ng/mL, $P = 0.672$) (Figure 1B).

Correlations between urotensin II and other biochemical, anthropometric and clinical parameters

There was a significant positive correlation between serum UII levels and hsCRP levels ($r = 0.491$, $P < 0.001$) and a significant negative correlation between serum UII levels and total proteins ($r = -0.306$, $P = 0.032$). There were no significant correlations with other biochemical parameters (Table 3).

There was a significant positive correlation between serum UII levels with both systolic ($r = 0.387$, $P = 0.005$) and diastolic ($r = 0.352$, $P = 0.012$) blood pressure. Moreover, serum UII levels had a significant positive correlation with UCEIS ($r = 0.425$, $P = 0.048$) and SES-CD ($r = 0.466$, $P = 0.028$) scores (Table 3).

Multiple linear regression

Multiple linear regression analysis showed that serum UII levels retained significant association with hsCRP (β ± standard error, 0.262 ± 0.076, $P < 0.001$) and systolic blood pressure (0.040 ± 0.017, $P = 0.030$) after model adjustment for age, gender, BMI and diastolic blood pressure, with serum UII levels as a dependent variable (Table 4).

DISCUSSION

The results of this study showed that serum UII levels are higher in patients with IBD compared to the healthy controls, while there was no significant difference between patients with UC and patients with CD. To the best of our knowledge, this is the first clinical study to investigate serum UII levels in both UC and CD.

Association between UII and IBD was only explored in a recent experimental pilot study that investigated expression of the UII receptor UTR in patients with UC[22]. They measured UTR expression from biopsies of the UC lesions and healthy colon tissue, and their outcomes determined that UTR expression was significantly higher in both the UC lesions and healthy tissue of the UC patients compared to the control group biopsies. Furthermore, a Chinese animal study conducted on mice with dextran sulfate sodium induced colitis explored the mechanisms of UTR in colonic inflammation[28]. They administrated the mice with urantide, a special antagonist of UTR that consequently alleviated rectal bleeding, tissue injury and production of interleukin (IL)-17 and tumor necrosis factor alpha (TNF-α). Furthermore, they showed that the inhibition of UTR reduced the activation of the nuclear factor-κB both *in vitro* and *in vivo*. Similarly, a study conducted on mice with induced acute liver failure assessed UTR expression and mechanisms involved[15]. They found that mice treated with urantide and consequent UTR downregulation expressed prevention of pro-inflammatory cytokines increase. TNF-α, IL-1β and interferon-γ were significantly lower compared to the mice with induced acute liver failure that were not treated with urantide. Additionally, a recent study explored UTR effects in acute liver failure by using Kupffer cells as a model system[29]. They found that UTR mediates production

Table 1 Baseline characteristics of the inflammatory bowel disease group and the control group

Parameter	IBD group (*n* = 50)	Control group (*n* = 50)	*P* value[1]
Male gender, *n* (%)	31 (62)	29 (58)	0.838
Age (yr)	44.3 ± 14.8	40.6 ± 12.3	0.181
Body weight (kg)	78.4 ± 14.0	81.1 ± 15.0	0.356
Body height (cm)	176.9 ± 9.8	179.6 ± 7.9	0.130
Body mass index (kg/m^2)	23.9 ± 3.7	24.9 ± 3.4	0.136
SBP (mmHg)	119.5 ± 11.2	116.6 ± 9.2	0.156
DBP (mmHg)	77.7 ± 8.3	75.0 ± 8.6	0.112
Smoking, *n* (%)	12 (24.0)	9 (18.4)	0.660
Disease duration (yr)[2]	6.0 (3.0-11.0)	-	-
UCEIS (score)	6.0 (5.0-7.0)	-	-
SES-CD (score)	9.2 (6.6-12.0)	-	-
Aminosalycilates	32 (64.0%)	-	-
DMARD	15 (30.0%)	-	-
Monoclonal antibodies	29 (58.0%)	-	-

[1]Chi-square test or t-test for independent samples.
[2]Time period since the initial diagnosis.
DBP: Diastolic blood pressure; DMARD: Disease-modifying antirheumatic drug; SBP: Systolic blood pressure; SES-CD: Simple endoscopic score for Crohn's disease; UCEIS: Ulcerative colitis index of severity. Data are presented as whole number (percentage), mean ± SD or median (interquartile range).

Table 2 Laboratory parameters of the inflammatory bowel disease group and the control group

Parameter	IBD group (*n* = 50)	Control group (*n* = 50)	*P* value[1]
Erythrocytes (× 10^{12}/L)	4.7 ± 0.5	5.0 ± 0.4	0.020
Hemoglobin (g/L)	140.4 ± 17.3	148.1 ± 13.7	0.015
Fasting glucose (mmol/L)	5.1 ± 0.9	5.0 ± 0.6	0.653
Urea (mmol/L)	4.7 ± 1.5	5.6 ± 1.6	0.004
Creatinine (μmol/L)	71.4 ± 15.3	75.9 ± 14.7	0.134
Total proteins (g/L)	71.2 ± 6.6	72.1 ± 3.9	0.394
Albumins (g/L)	39.5 ± 5.1	43.7 ± 2.4	< 0.001
hsCRP (mg/L)	3.4 ± 2.6	1.2 ± 1.1	< 0.001
Triglycerides (mmol/L)	1.3 ± 0.9	1.1 ± 0.6	0.311
Total cholesterol (mmol/L)	4.8 ± 1.3	5.2 ± 1.2	0.091
HDL cholesterol (mmol/L)	1.3 ± 0.4	1.4 ± 0.3	0.447
LDL cholesterol (mmol/L)	2.6 (2.1-3.4)	3.2 (2.4-3.9)	0.018
FC (μg/g)	231 (61.5-619.2)	-	-

[1]*t*-test for independent samples or Mann-Whitney *U* test.
FC: Fecal calprotectin; HDL: High-density lipoprotein; HsCRP: High sensitivity C-reactive protein; LDL: Low-density lipoprotein. Data are presented as mean ± SD and median (interquartile range).

and release of proinflammatory cytokines TNF-α, IL-1β and interferon-γ by using the inflammatory pathway nuclear factor-κB. All of these aforementioned studies point to the possibility that UII, besides the already well-established vasoconstriction, is also involved in the development and enhancement of the inflammatory response.

Table 3 Correlation analysis between serum urotensin II levels and different biochemical, anthropometric and clinical parameters in the inflammatory bowel disease group (*n* = 50)

Parameter	*r*[1]	*P* value
hsCRP (mg/L)	0.491	< 0.001
Total proteins (g/L)	-0.306	0.032
Albumins (g/L)	-0.182	0.210
Triglycerides (mmol/L)	0.057	0.698
Total cholesterol (mmol/L)	-0.114	0.439
HDL (mmol/L)	-0.153	0.298
LDL (mmol/L)	-0.103[3]	0.487
Urea (mmol/L)	0.013	0.928
Creatinine (μmol/L)	0.133	0.356
Age (yr)	-0.072	0.614
Body mass index (kg/m^2)	-0.037	0.800
SBP (mmHg)	0.387	0.005
DBP (mmHg)	0.352	0.012
IBD duration (yr)[2]	0.045[3]	0.751
FC (μg/g)	0.048[3]	0.812
UCEIS (score)	0.425[3]	0.048
SES-CD (score)	0.466[3]	0.028

[1]Pearson's correlation coefficient.
[2]Time period before the initial diagnosis.
[3]Spearman's rank correlation coefficient.
DBP: Diastolic blood pressure; FC: Fecal calprotectin; hsCRP: High sensitivity C-reactive protein; SBP: Systolic blood pressure; SES-CD: Simple endoscopic score for Crohn's disease; UCEIS: Ulcerative colitis index of severity.

Table 4 Multiple linear regression model of independent predictors for serum urotensin II levels

Variable	B[1]	SE	*t* value	*P* value
Age	0.009	0.015	0.570	0.571
Gender	-0.740	0.405	-1.825	0.075
BMI	-0.106	0.059	-1.793	0.080
SBP	0.040	0.017	2.243	0.030
DBP	0.039	0.025	1.535	0.132
hsCRP	0.262	0.076	3.469	< 0.001

[1]Unstandardized coefficient β.
BMI: Body mass index; DBP: Diastolic blood pressure; hsCRP: High sensitivity C-reactive protein; SBP: Systolic blood pressure; SE: Standard error.

According to these results, it could be hypothesized that in IBD, among other mechanisms, higher UII levels and consequently greater UTR activity can be associated with elevated TNF-α concentrations, which cause the development of the aberrant inflammatory response[30]. It is well established that IBD is linked with elevated TNF-α levels in the mucosa of the gastrointestinal tract and consequently an abnormal inflammatory response that is associated with the dysregulation of mucosal immune cells and tissue injury[31]. Moreover, TNF-α contributes to inflammation through disruption of the epithelial barrier, stimulation of villous epithelial cells apoptosis and secretion of chemokines from intestinal epithelium[32]. This possibility is further supported by our results that UII is in a significant positive association with

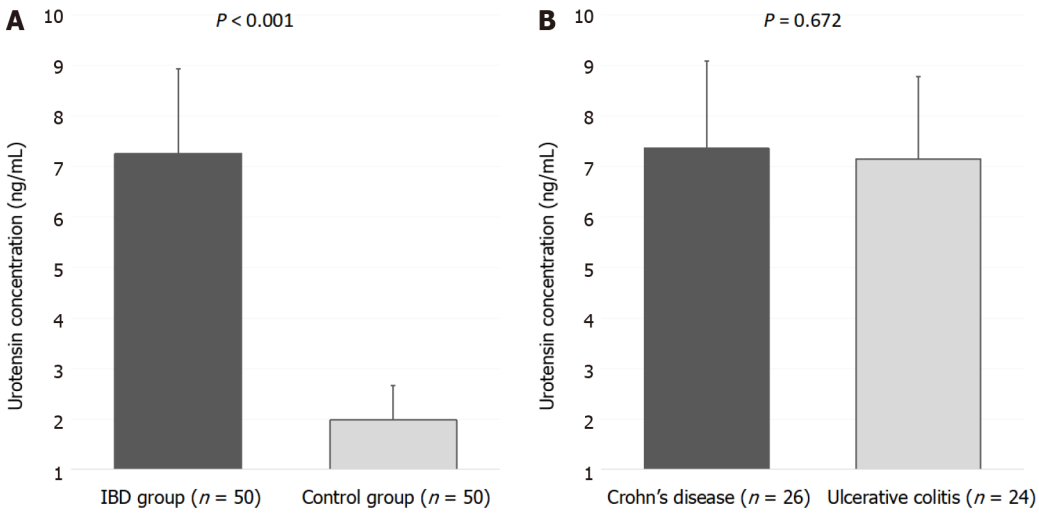

Figure 1 Serum urotensin II levels. A: Comparison between the inflammatory bowel disease group and the control group. B: Comparison between patients with Crohn's disease and patients with ulcerative colitis.

hsCRP, which was additionally supported with multiple linear regression, and clinical indices of IBD activity as well. These results implicate that disease activity could be closely related to UII levels.

Moreover, it is important to highlight that the previous studies have shown that high TNF-α levels play a major role in the disruption of macro and microvascular circulation[33]. It induces the production of reactive oxygen species, which results in endothelial dysfunction, while several studies presented that the administration of anti-TNF-α therapy to patients with IBD results in a significant improvement of endothelial dysfunction[32,34]. It is possible that functional and structural changes of the vascular endothelium due to chronic inflammation consequently results in higher cardiovascular risk in IBD patients[35]. Furthermore, with more severe disease activity and consequent greater inflammation, the resulting endothelial dysfunction that accompanies these changes is more advanced. It was presented by two recent studies that heart dysfunction, as well as fibrosis and cell hypertrophy, were significantly decreased in experimental heart models treated with UTR antagonists[36,37]. Moreover, a recent study showed that elevated UII levels are associated with the severity of cardiovascular risk factors[38].

In the last 2 decades, it has become clear that chronic systemic inflammation plays a major part in the initiation and progression of atherosclerosis[39,40]. Circulating UII was reported to promote increase of reactive oxygen species levels, which are important molecules in the initiation of atherosclerosis[41]. In a Chinese animal study, urantide administration reduced the proportion of the macrophage lesion area as well as improved the plaque characteristics in hyperlipidemic rabbits by increasing the collagen content[42]. Even though UTR antagonist downregulated proinflammatory cytokines, it did not significantly change the lipid profile. In summary, although the UTR antagonist did not change the progression of atherosclerosis, it significantly affected composition of atherosclerotic plaque. These results imply that UII is associated with the process of atherosclerosis, but the downregulation of its receptor UTR only affects the properties of the atherosclerotic plaque, while it does not stop its actual progression.

Our results also determined a significant positive correlation between serum UII levels with systolic and diastolic blood pressure. This is in alignment with several other clinical and experimental studies that have found an association between UII and arterial pressure, probably present due to its established vasoconstrictive effect[43,44]. Moreover, studies have shown that IBD patients have a lower incidence of some of the traditional risk factors for cardiovascular diseases, including hypertension[19]. In a current scenario, it is still questionable why IBD patients have lower incidence of hypertension, although UII levels are elevated in comparison with healthy subjects. It is hard to hypothesize from our results what are the possible reasons for this ambiguity, and further studies are needed to elaborate this issue. However, it is possible that UII vasoconstriction effect is diminished by other factors that are present in IBD patients.

This study had several limitations. It was a single center study with a cross-sectional design. Moreover, our sample size was relatively low, and we were not able to eliminate completely all possible confounding effects.

CONCLUSION

In conclusion, this study showed that patients with IBD have a higher serum level of UII compared to the control group. This implied association with IBD was further supported with the positive correlation between UII and hsCRP, UCEIS and SES-CD. All of these results suggest that UII could be involved in the pathophysiology of IBD, especially in the inflammation severity and disease activity. However, future studies need to clarify these connections.

ARTICLE HIGHLIGHTS

Research background

Patients with inflammatory bowel disease (IBD) are associated with increased cardiovascular risk and have increased overall cardiovascular burden. On the other hand, urotensin II (UII) is one of the most potent vascular constrictors with immunomodulatory effect that is connected with a number of different cardiometabolic disorders as well. Since the features of IBD includes chronic inflammation and endothelial dysfunction, it is plausible to assume that there is connection between increased cardiac risk in IBD and UII.

Research motivation

While a recent study showed that patients with ulcerative colitis (UC) have increased expression of urotensin II receptor in comparison to healthy controls, a larger clinical study regarding UII serum levels in patients with IBD is still missing.

Research objectives

The aim of this study was to compare serum levels of UII between patients with IBD and healthy controls. The additional goal was to investigate the association of serum UII levels with the anthropometric, clinical and biochemical parameters.

Research methods

This study included 50 adult patients with pre-diagnosed IBD (24 patients with UC and 26 patients with Crohn's disease (CD) and 50 healthy, age and gender matched controls. Serum levels of UII were determined using the enzyme immunoassay kit for human UII, according to the manufacturer's instructions. Other parameters were analyzed according to the standard laboratory procedures.

Research results

Analysis has shown that IBD patients have significantly higher concentrations of UII when compared to control subjects (7.57 ± 1.41 *vs* 1.98 ± 0.69 ng/mL, $P < 0.001$), while there were no significant differences between CD and UC patients (7.49 ± 1.42 *vs* 7.65 ± 1.41 ng/mL, $P = 0.689$). There was a significant positive correlation between serum UII levels and high sensitivity C reactive peptide levels ($r = 0.491$, $P < 0.001$), UC Endoscopic Index of Severity ($r = 0.425$, $P = 0.048$) and Simple Endoscopic Score for CD ($r = 0.466$, $P = 0.028$) scores.

Research conclusions

Our clinical results suggest that UII could be involved in the pathophysiology of IBD, especially in the inflammation severity and disease activity.

Research perspectives

Future larger scale multicenter studies need to clarify the connection between UII and IBD.

ACKNOWLEDGEMENTS

The authors would like to thank to Behmen D, MA for her careful language assistance.

REFERENCES

1 **Zhang YZ**, Li YY. Inflammatory bowel disease: pathogenesis. *World J Gastroenterol* 2014; **20**: 91-99 [PMID: 24415861 DOI: 10.3748/wjg.v20.i1.91]

2 **Brnic D**, Martinovic D, Zivkovic PM, Tokic D, Vilovic M, Rusic D, Tadin Hadjina I, Libers C, Glumac S, Supe-Domic D, Tonkic A, Bozic J. Inactive matrix Gla protein is elevated in patients with inflammatory bowel disease. *World J Gastroenterol* 2020; **26**: 4866-4877 [PMID: 32921963 DOI: 10.3748/wjg.v26.i32.4866]

3 **Brnić D**, Martinovic D, Zivkovic PM, Tokic D, Tadin Hadjina I, Rusic D, Vilovic M, Supe-Domic D, Tonkic A, Bozic J. Serum adropin levels are reduced in patients with inflammatory bowel diseases. *Sci Rep* 2020; **10**: 9264 [PMID: 32518265 DOI: 10.1038/s41598-020-66254-9]

4 **Fragoulis GE**, Liava C, Daoussis D, Akriviadis E, Garyfallos A, Dimitroulas T. Inflammatory bowel diseases and spondyloarthropathies: From pathogenesis to treatment. *World J Gastroenterol* 2019; **25**: 2162-2176 [PMID: 31143068 DOI: 10.3748/wjg.v25.i18.2162]

5 **Filimon AM**, Negreanu L, Doca M, Ciobanu A, Preda CM, Vinereanu D. Cardiovascular involvement in inflammatory bowel disease: Dangerous liaisons. *World J Gastroenterol* 2015; **21**: 9688-9692 [PMID: 26361415 DOI: 10.3748/wjg.v21.i33.9688]

6 **Cheng K**, Faye AS. Venous thromboembolism in inflammatory bowel disease. *World J Gastroenterol* 2020; **26**: 1231-1241 [PMID: 32256013 DOI: 10.3748/wjg.v26.i12.1231]

7 **Svistunov AA**, Tarasov VV, Shakhmardanova SA, Sologova SS, Bagaturiya ET, Chubarev VN, Galenko-Yaroshevsky PA, Avila-Rodriguez MF, Barreto GE, Aliev G. Urotensin II: Molecular Mechanisms of Biological Activity. *Curr Protein Pept Sci* 2018; **19**: 924-934 [PMID: 28875851 DOI: 10.2174/1389203718666170829162335]

8 **Federico A**, Zappavigna S, Dallio M, Misso G, Merlino F, Loguercio C, Novellino E, Grieco P, Caraglia M. Urotensin-II Receptor: A Double Identity Receptor Involved in Vasoconstriction and in the Development of Digestive Tract Cancers and other Tumors. *Curr Cancer Drug Targets* 2017; **17**: 109-121 [PMID: 27338741 DOI: 10.2174/1568009616666160621101248]

9 **Pereira-Castro J**, Brás-Silva C, Fontes-Sousa AP. Novel insights into the role of urotensin II in cardiovascular disease. *Drug Discov Today* 2019; **24**: 2170-2180 [PMID: 31430542 DOI: 10.1016/j.drudis.2019.08.005]

10 **Castel H**, Desrues L, Joubert JE, Tonon MC, Prézeau L, Chabbert M, Morin F, Gandolfo P. The G Protein-Coupled Receptor UT of the Neuropeptide Urotensin II Displays Structural and Functional Chemokine Features. *Front Endocrinol (Lausanne)* 2017; **8**: 76 [PMID: 28487672 DOI: 10.3389/fendo.2017.00076]

11 **Eyre HJ**, Speight T, Glazier JD, Smith DM, Ashton N. Urotensin II in the development and progression of chronic kidney disease following ⅝ nephrectomy in the rat. *Exp Physiol* 2019; **104**: 421-433 [PMID: 30575177 DOI: 10.1113/EP087366]

12 **Khan K**, Albanese I, Yu B, Shalal Y, Al-Kindi H, Alaws H, Tardif JC, Gourgas O, Cerutti M, Schwertani A. Urotensin II, urotensin-related peptide, and their receptor in aortic valve stenosis. *J Thorac Cardiovasc Surg* 2019 [PMID: 31679703 DOI: 10.1016/j.jtcvs.2019.09.029]

13 **Chen X**, Yin L, Jia WH, Wang NQ, Xu CY, Hou BY, Li N, Zhang L, Qiang GF, Yang XY, Du GH. Chronic Urotensin-II Administration Improves Whole-Body Glucose Tolerance in High-Fat Diet-Fed Mice. *Front Endocrinol (Lausanne)* 2019; **10**: 453 [PMID: 31379736 DOI: 10.3389/fendo.2019.00453]

14 **Sun SL**, Liu LM. Urotensin II: an inflammatory cytokine. *J Endocrinol* 2019 [PMID: 30601760 DOI: 10.1530/joe-18-0505]

15 **Liang DY**, Liu LM, Ye CG, Zhao L, Yu FP, Gao DY, Wang YY, Yang ZW. Inhibition of UII/UTR system relieves acute inflammation of liver through preventing activation of NF-κB pathway in ALF mice. *PLoS One* 2014; **8**: e64895 [PMID: 23755157 DOI: 10.1371/journal.pone.0064895]

16 **Bigeh A**, Sanchez A, Maestas C, Gulati M. Inflammatory bowel disease and the risk for cardiovascular disease: Does all inflammation lead to heart disease? *Trends Cardiovasc Med* 2020; **30**: 463-469 [PMID: 31653485 DOI: 10.1016/j.tcm.2019.10.001]

17 **Singh S**, Kullo IJ, Pardi DS, Loftus EV Jr. Epidemiology, risk factors and management of cardiovascular diseases in IBD. *Nat Rev Gastroenterol Hepatol* 2015; **12**: 26-35 [PMID: 25446727 DOI: 10.1038/nrgastro.2014.202]

18 **Zivkovic PM**, Matetic A, Tadin Hadjina I, Rusic D, Vilovic M, Supe-Domic D, Borovac JA, Mudnic I, Tonkic A, Bozic J. Serum Catestatin Levels and Arterial Stiffness Parameters Are Increased in Patients with Inflammatory Bowel Disease. *J Clin Med* 2020; **9** [PMID: 32110996 DOI: 10.3390/jcm9030628]

19 **Kristensen SL**, Ahlehoff O, Lindhardsen J, Erichsen R, Jensen GV, Torp-Pedersen C, Nielsen OH, Gislason GH, Hansen PR. Disease activity in inflammatory bowel disease is associated with increased risk of myocardial infarction, stroke and cardiovascular death--a Danish nationwide cohort study. *PLoS One* 2013; **8**: e56944 [PMID: 23457642 DOI: 10.1371/journal.pone.0056944]

20 **Ahmed AH**, Maulood IM. Endothelin-1 and angiotensin-II modulate urotensin-II vasoconstriction in rat aorta exposed to mercury. *Bratisl Lek Listy* 2018; **119**: 444-449 [PMID: 30160135 DOI: 10.4149/BLL_2018_081]

21 **Jumaah S**, Çelekli A, Sucu M. The role of human urotensin-II in patients with hypertrophic cardiomyopathy. *J Immunoassay Immunochem* 2018; **39**: 150-162 [PMID: 28686108 DOI: 10.1080/15321819.2017.1344130]

22 **Gravina AG**, Dallio M, Tuccillo C, Martorano M, Abenavoli L, Luzza F, Stiuso P, Lama S, Grieco P, Merlino F, Caraglia M, Loguercio C, Federico A. Urotensin II receptor expression in patients with ulcerative colitis: a pilot study. *Minerva Gastroenterol Dietol* 2020; **66**: 23-28 [PMID: 31293119 DOI: 10.23736/S1121-421X.19.02602-3]

23 **Magro F**, Gionchetti P, Eliakim R, Ardizzone S, Armuzzi A, Barreiro-de Acosta M, Burisch J, Gecse KB, Hart AL, Hindryckx P, Langner C, Limdi JK, Pellino G, Zagórowicz E, Raine T, Harbord M, Rieder F; European Crohn's and Colitis Organisation [ECCO]. Third European Evidence-based Consensus on Diagnosis and Management of Ulcerative Colitis. Part 1: Definitions, Diagnosis, Extra-intestinal Manifestations, Pregnancy, Cancer Surveillance, Surgery, and Ileo-anal Pouch Disorders. *J Crohns Colitis* 2017; **11**: 649-670 [PMID: 28158501 DOI: 10.1093/ecco-jcc/jjx008]

24 **Schmulson MJ**, Drossman DA. What Is New in Rome IV. *J Neurogastroenterol Motil* 2017; **23**: 151-163 [PMID: 28274109 DOI: 10.5056/jnm16214]

25 **Sturm A**, Maaser C, Calabrese E, Annese V, Fiorino G, Kucharzik T, Vavricka SR, Verstockt B, van Rheenen P, Tolan D, Taylor SA, Rimola J, Rieder F, Limdi JK, Laghi A, Krustiņš E, Kotze PG, Kopylov U, Katsanos K, Halligan S, Gordon H, González Lama Y, Ellul P, Eliakim R, Castiglione F, Burisch J, Borralho Nunes P, Bettenworth D, Baumgart DC, Stoker J; European Crohn's and Colitis Organisation [ECCO] and the European Society of Gastrointestinal and Abdominal Radiology [ESGAR]. ECCO-ESGAR Guideline for Diagnostic Assessment in IBD Part 2: IBD scores and general principles and technical aspects. *J Crohns Colitis* 2019; **13**: 273-284 [PMID: 30137278 DOI: 10.1093/ecco-jcc/jjy114]

26 **Travis SP**, Schnell D, Krzeski P, Abreu MT, Altman DG, Colombel JF, Feagan BG, Hanauer SB, Lichtenstein GR, Marteau PR, Reinisch W, Sands BE, Yacyshyn BR, Schnell P, Bernhardt CA, Mary JY, Sandborn WJ. Reliability and initial validation of the ulcerative colitis endoscopic index of severity. *Gastroenterology* 2013; **145**: 987-995 [PMID: 23891974 DOI: 10.1053/j.gastro.2013.07.024]

27 **Daperno M**, D'Haens G, Van Assche G, Baert F, Bulois P, Maunoury V, Sostegni R, Rocca R, Pera A, Gevers A, Mary JY, Colombel JF, Rutgeerts P. Development and validation of a new, simplified endoscopic activity score for Crohn's disease: the SES-CD. *Gastrointest Endosc* 2004; **60**: 505-512 [PMID: 15472670 DOI: 10.1016/s0016-5107(04)01878-4]

28 **Yang Y**, Zhang J, Chen X, Wu T, Xu X, Cao G, Li H, Li Y. UII/GPR14 is involved in NF-κB-mediated colonic inflammation *in vivo* and in vitro. *Oncol Rep* 2016; **36**: 2800-2806 [PMID: 27600191 DOI: 10.3892/or.2016.5069]

29 **Liu LM**, Liang DY, Ye CG, Tu WJ, Zhu T. The UII/UT system mediates upregulation of proinflammatory cytokines through p38 MAPK and NF-κB pathways in LPS-stimulated Kupffer cells. *PLoS One* 2015; **10**: e0121383 [PMID: 25803040 DOI: 10.1371/journal.pone.0121383]

30 **Lichtenstein GR**. Comprehensive review: antitumor necrosis factor agents in inflammatory bowel disease and factors implicated in treatment response. *Therap Adv Gastroenterol* 2013; **6**: 269-293 [PMID: 23814608 DOI: 10.1177/1756283X13479826]

31 **Friedrich M**, Pohin M, Powrie F. Cytokine Networks in the Pathophysiology of Inflammatory Bowel Disease. *Immunity* 2019; **50**: 992-1006 [PMID: 30995511 DOI: 10.1016/j.immuni.2019.03.017]

32 **Schinzari F**, Armuzzi A, De Pascalis B, Mores N, Tesauro M, Melina D, Cardillo C. Tumor necrosis factor-alpha antagonism improves endothelial dysfunction in patients with Crohn's disease. *Clin Pharmacol Ther* 2008; **83**: 70-76 [PMID: 17507924 DOI: 10.1038/sj.clpt.6100229]

33 **Zhang H**, Park Y, Wu J, Chen Xp, Lee S, Yang J, Dellsperger KC, Zhang C. Role of TNF-alpha in vascular dysfunction. *Clin Sci (Lond)* 2009; **116**: 219-230 [PMID: 19118493 DOI: 10.1042/CS20080196]

34 **Zanoli L**, Inserra G, Cappello M, Ozturk K, Castellino P. Aortic Stiffness in Patients With Inflammatory Bowel Disease Reduced After Anti-Tumor Necrosis Factor Therapy. *J Am Coll Cardiol* 2019; **73**: 981-982 [PMID: 30819367 DOI: 10.1016/j.jacc.2018.12.032]

35 **Cibor D**, Domagala-Rodacka R, Rodacki T, Jurczyszyn A, Mach T, Owczarek D. Endothelial dysfunction in inflammatory bowel diseases: Pathogenesis, assessment and implications. *World J Gastroenterol* 2016; **22**: 1067-1077 [PMID: 26811647 DOI: 10.3748/wjg.v22.i3.1067]

36 **Park CH**, Lee JH, Lee MY, Lee BH, Oh KS. A novel role of G protein-coupled receptor kinase 5 in urotensin II-stimulated cellular hypertrophy in H9c2$_{UT}$ cells. *Mol Cell Biochem* 2016; **422**: 151-160 [PMID: 27613164 DOI: 10.1007/s11010-016-2814-y]

37 **Oh KS**, Lee JH, Yi KY, Lim CJ, Park BK, Seo HW, Lee BH. A novel urotensin II receptor antagonist, KR-36996, improved cardiac function and attenuated cardiac hypertrophy in experimental heart failure. *Eur J Pharmacol* 2017; **799**: 94-102 [PMID: 28163023 DOI: 10.1016/j.ejphar.2017.02.003]

38 **Demirpence M**, Guler A, Yilmaz H, Sayin A, Pekcevik Y, Turkon H, Colak A, Ari EM, Aslanipour B, Kocabas GU, Calan M. Is elevated urotensin II level a predictor for increased cardiovascular risk in subjects with acromegaly? *J Endocrinol Invest* 2019; **42**: 207-215 [PMID: 29804270 DOI: 10.1007/s40618-018-0905-1]

39 **Chistiakov DA**, Grechko AV, Myasoedova VA, Melnichenko AA, Orekhov AN. The role of monocytosis and neutrophilia in atherosclerosis. *J Cell Mol Med* 2018; **22**: 1366-1382 [PMID: 29364567 DOI: 10.1111/jcmm.13462]

40 **Koelwyn GJ**, Corr EM, Erbay E, Moore KJ. Regulation of macrophage immunometabolism in atherosclerosis. *Nat Immunol* 2018; **19**: 526-537 [PMID: 29777212 DOI: 10.1038/s41590-018-0113-3]

41 **Mohammadi A**, Najar AG, Khoshi A. Effect of urotensin II on apolipoprotein B100 and apolipoprotein A-I expression in HepG2 cell line. *Adv Biomed Res* 2014; **3**: 22 [PMID: 24600602 DOI: 10.4103/2277-9175.124661]

42 **Yu QQ**, Cheng DX, Xu LR, Li YK, Zheng XY, Liu Y, Li YF, Liu HL, Bai L, Wang R, Fan JL, Liu EQ, Zhao SH. Urotensin II and urantide exert opposite effects on the cellular components of atherosclerotic plaque in hypercholesterolemic rabbits. *Acta Pharmacol Sin* 2020; **41**: 546-553 [PMID: 31685976 DOI: 10.1038/s41401-019-0315-8]

43 **Watanabe T**, Kanome T, Miyazaki A, Katagiri T. Human urotensin II as a link between hypertension and coronary artery disease. *Hypertens Res* 2006; **29**: 375-387 [PMID: 16940699 DOI: 10.1291/hypres.29.375]

44 **Debiec R**, Christofidou P, Denniff M, Bloomer LD, Bogdanski P, Wojnar L, Musialik K, Charchar FJ, Thompson JR, Waterworth D, Song K, Vollenweider P, Waeber G, Zukowska-Szczechowska E, Samani NJ, Lambert D, Tomaszewski M. Urotensin-II system in genetic control of blood pressure and renal function. *PLoS One* 2013; **8**: e83137 [PMID: 24391740 DOI: 10.1371/journal.pone.0083137]

World Journal of Gastroenterology

Submit a Manuscript: https://www.f6publishing.com

World J Gastroenterol 2021 September 28; 27(36): 6154-6160

DOI: 10.3748/wjg.v27.i36.6154

ISSN 1007-9327 (print) ISSN 2219-2840 (online)

CASE REPORT

Inverted Meckel's diverticulum diagnosed using capsule endoscopy: A case report

Ismael El Hajra Martínez, Marta Calvo, José Luis Martínez-Porras, Lucia Gomez-Pimpollo Garcia, Jose L Rodriguez, Carmen Leon, José Luis Calleja Panero

ORCID number: Ismael El Hajra Martínez 0000-0002-7802-0920; Marta Calvo 0000-0003-0744-8636; José Luis Martínez-Porras 0000-0003-0560-9213; Lucia Gomez-Pimpollo Garcia 0000-0001-8914-8500; Jose L Rodriguez 0000-0003-0513-1707; Carmen Leon 0000-0003-1971-9253; José Luis Calleja Panero 0000-0002-2265-6591.

Author contributions: El Hajra Martínez I and Calvo M contributed to the manuscript design and drafting, and reviewed the literature; Martínez-Porras JL performed capsule endoscopy, and interpretation and revision of the manuscript; Gomez-Pimpollo Garcia L contributed to analysis and interpretation of the imaging findings, and revision of the manuscript; Rodriguez JL contributed to pathological examination and revision of the manuscript; Leon C performed laparoscopic surgery and manuscript drafting; Calleja Panero JL and Calvo M were responsible for revision of the manuscript for important intellectual content; All authors issued final approval for the version to be submitted.

Informed consent statement: The patient provided informed written consent prior to treatment.

Ismael El Hajra Martínez, Marta Calvo, José Luis Martínez-Porras, Department of Gastroenterology, Hospital Universitario Puerta de Hierro, Madrid 28222, Spain

Lucia Gomez-Pimpollo Garcia, Department of Radiology, Hospital Universitario Puerta de Hierro, Madrid 28222, Spain

Jose L Rodriguez, Department of Diagnostic Pathology, Hospital Universitario Puerta de Hierro, Madrid 28222, Spain

Carmen Leon, Department of Surgery, Hospital Universitario Puerta de Hierro, Madrid 28222, Spain

José Luis Calleja Panero, Department of Gastroenterology, Hospital Universitario Puerta de Hierro, Madrid 28222, Spain

Corresponding author: Marta Calvo, PhD, Doctor, Department of Gastroenterology, Hospital Universitario Puerta de Hierro, Calle Joaquín Rodrigo, 1, Majadahonda, Madrid 28222, Spain. calvo.marta@gmail.com

Abstract

BACKGROUND

Meckel's diverticulum is a common asymptomatic congenital gastrointestinal anomaly. However, its presentation as an inverted Meckel's diverticulum is a rare complication, of which few cases have been reported in the literature.

CASE SUMMARY

Here, we report the case of a 33-year-old man with iron deficiency anemia without manifestation of gastrointestinal bleeding. An upper gastrointestinal endoscopy and total colonoscopy were performed, but no abnormalities were found within the observed area. Finally, a capsule endoscopy was performed and offered us a clue to subsequently confirm the diagnosis of inverted Meckel's diverticulum *via* computed tomography scan. Laparoscopic intestinal resection surgery was performed. The final pathology report described a Meckel's diverticulum.

CONCLUSION

Since inverted Meckel's diverticulum is an uncommon disease and its clinical presentation is not specific, it may go undetected by capsule endoscopy.

Conflict-of-interest statement: The authors declare having no conflicts of interest.

CARE Checklist (2016) statement: The authors have read the CARE Checklist (2016), and the manuscript was prepared and revised according to the CARE Checklist (2016).

Manuscript source: Unsolicited manuscript

Specialty type: Gastroenterology and hepatology

Country/Territory of origin: Spain

Peer-review report's scientific quality classification

Grade A (Excellent): 0
Grade B (Very good): B, B, B
Grade C (Good): 0
Grade D (Fair): 0
Grade E (Poor): 0

Received: February 25, 2021
Peer-review started: February 25, 2021
First decision: April 29, 2021
Revised: May 13, 2021
Accepted: August 16, 2021
Article in press: August 16, 2021
Published online: September 28, 2021

P-Reviewer: Camí MM, Racz I, Sulbaran MN
S-Editor: Wang JL
L-Editor: Filipodia
P-Editor: Li JH

Successful diagnosis and treatment of this disease requires a high index of clinical suspicion.

Key Words: Inverted Meckel's diverticulum; Capsule endoscopy; Anemia study; Small bowel tumor; Case report

Core Tip: Inverted Meckel's diverticulum is an uncommon disease with a wide spectrum of accompanying nonspecific symptoms. We present, here, a case of iron deficiency anemia with negative endoscopic study, in which capsule endoscopy played a key role in confirming the diagnosis. Since inverted Meckel's diverticulum is an uncommon disease with few cases described in the literature, this report aims to contribute more information concerning the clinical characteristics as well as radiological and capsule endoscopy findings of inverted Meckel's diverticulum that can help clinicians make the correct diagnosis.

Citation: El Hajra Martínez I, Calvo M, Martínez-Porras JL, Gomez-Pimpollo Garcia L, Rodriguez JL, Leon C, Calleja Panero JL. Inverted Meckel's diverticulum diagnosed using capsule endoscopy: A case report. *World J Gastroenterol* 2021; 27(36): 6154-6160
URL: https://www.wjgnet.com/1007-9327/full/v27/i36/6154.htm
DOI: https://dx.doi.org/10.3748/wjg.v27.i36.6154

INTRODUCTION

Meckel's diverticulum is a common congenital gastrointestinal anomaly which is a remanent of the omphalomesenteric duct[1]. It is often within 100 cm of the ileocecal valve and located in the antimesenteric surface of the ileum[2]. According to autopsy studies, this condition is found in 0.3%-2% of the general population[3,4].

Patients with Meckel's diverticulum are usually asymptomatic. However, up to 6.4% develop complications that require surgery[5]. The most common complications are gastrointestinal bleeding in association with ectopic gastric and/or pancreatic mucosa, intestinal obstruction, intussusceptions, diverticulitis or volvulus. The inversion of Meckel's diverticulum is a rare complication with a pathophysiology not clearly understood, that can be a clinical challenge given its diagnostic difficulty. Moreover, the clinical presentation is nonspecific, the most frequent mode of presentation being intussusception, abdominal pain, anemia or gastrointestinal bleeding[6].

Although Meckel's diverticulum is the most common congenital anomaly of the small bowel, inversion or invagination of the diverticulum is a rare occurrence. To date, there are only around 100 cases in the literature that demonstrate the presence of inverted Meckel's diverticulum.

Herein, we present the case of iron deficiency anemia without manifestation of gastrointestinal bleeding, in which capsule endoscopy played a key role in the final diagnosis of inverted Meckel's diverticulum.

CASE PRESENTATION

Chief complaints

A 33-year-old male with no significant medical history presented to the emergency room with progressive weakness, easy fatigability and headache. He had no evidence of lower or upper gastrointestinal bleeding and he reported no abdominal pain, nausea, vomiting, anorexia, fever or weight loss.

History of present illness

The patient's symptoms started 3 wk prior and had worsened over the last 4 d.

History of past illness
There was no significant medical history.

Personal and family history
There was no significant medical history.

Physical examination
In the emergency room, the patient was clinically stable, with a normal temperature (36.7 °C). The patient exhibited an oxygen saturation level of 97% while he was breathing ambient air. His blood pressure was 102/61 mmHg and his heart rate was 91 beats per minute. The patient was awake, alert, and fully oriented. Physical examination revealed signs of pallor and an absence of lymphadenopathy, hepatosplenomegaly, bone tenderness or jaundice. Examination of the rectum revealed a few external hemorrhoids, but there was no blood or melena in the rectal vault; there were no skin tags, fissures or palpable masses.

Laboratory examinations
The initial laboratory findings showed low hemoglobin levels (7 g/dL), a white blood cell count of 11250 per mm^3, a platelet count of 221000 per mm^3 and a C-reactive protein of 1.31 mg/dL. Two pints of packed red blood cells were therefore transfused and the patient was admitted to the gastroenterology department. Electrocardiography (ECG) showed sinus rhythm at 93 beats per minute and the results of the patient's chest radiography were normal.

The patient's next blood test, showed a mean corpuscular volume of 72.5 fl, a mean corpuscular hemoglobin of 25.6 pg, and a reticulocyte count of 1%. The patient's iron level was 38 μg/dL, his ferritin level was 17 ng/mL, and his transferrin saturation was 9%. The hemolysis study was negative. Hence, the patient's anemia was classified as iron deficiency anemia.

Imaging examinations
During this period, an upper gastrointestinal endoscopy and a colonoscopy were performed to study the patient's anemia. The colonoscopy revealed internal hemorrhoids without any other relevant findings while the upper gastrointestinal endoscopy showed no abnormalities. The patient remained stable and was discharged and the study was completed on an outpatient basis with oral iron treatment.

During his visit to the outpatient clinic 3 wk later, the patient remained anemic, with a hemoglobin level of 8.8 g/dL. The anemia study was completed with a capsule endoscopy, which revealed a lifted erosion and mild bulge in the ileum of approximately 8-9 mm in size (Figure 1). These findings of appearance of a subepithelial bulge in the ileum suggested an inverted Meckel diverticulum. Normal intestinal mucosa was seen on the surface of the tumor with a longer small intestine transit time suggestive of Meckel's diverticulum. A technetium-99m pertechnetate radioisotope scintigraphy (Meckel's scan) was performed and was negative. The patient subsequently underwent an ultrasound examination, which revealed no pathological findings. Finally, an abdominal computed tomography (CT) was performed and showed a central area of fat attenuation surrounded by a thick collar of soft tissue attenuation (Figure 2) suggestive of inverted Meckel's diverticulum.

FINAL DIAGNOSIS
The patient was diagnosed with an inverted Meckel's diverticulum and underwent a laparoscopic surgery. A large intraluminal polyp-like mass in the mid-ileum was observed. The remainder of the small bowel was normal to the level of the ligament of Treitz. A segmentary resection of the small bowel with adequate margin was performed and side-to-side anastomosis was carried out using a stapling device.

On gross examination, the specimen consisted of a segmental resection of the small bowel of 8 cm × 4 cm × 2.6 cm with a sausage-shaped polypoid lesion.

Histological examination (Figure 3) showed a polypoid lesion, with a central fatty and collagenous core lined with an intestinal type mucosa. A central area of ulceration was seen, with no presence of gastric or pancreatic heterotopia. The final pathology report described a Meckel's diverticulum.

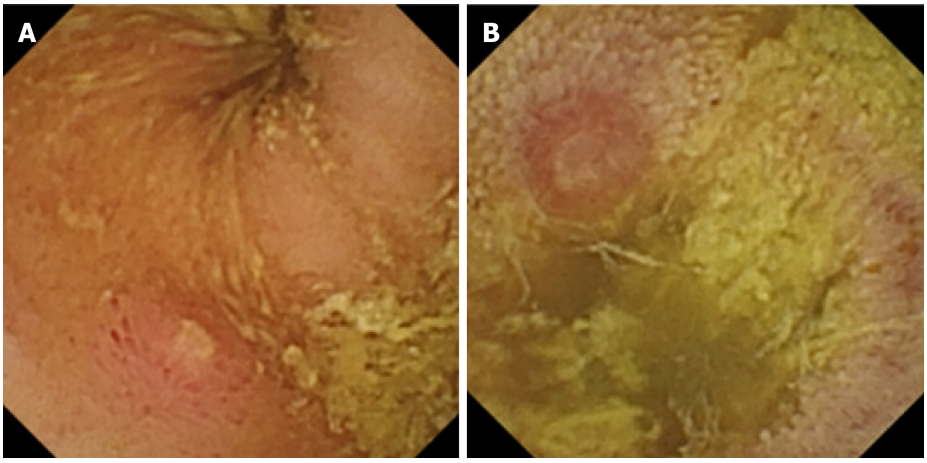

Figure 1 Capsule endoscopy with protruding lesion. A: Capsule endoscopy with protruding lesion, with a depressed erosion at the tip suggestive of Meckel's diverticulum; B: Capsule endoscopy with protruding lesion suggestive of Meckel's diverticulum.

Figure 2 Abdominal computed tomography scan revealed a central area of fat attenuation surrounded by a thick collar of soft tissue attenuation suggestive of Meckel's diverticulum.

TREATMENT

The patient was diagnosed with an inverted Meckel's diverticulum and underwent a laparoscopic surgery. A large intraluminal polyp-like mass in the mid-ileum was observed. The remainder of the small bowel was normal to the level of the ligament of Treitz. A segmentary resection of the small bowel with adequate margin was performed and side-to-side anastomosis was carried out using a stapling device.

OUTCOME AND FOLLOW-UP

The patient had an uneventful postoperative course and was discharged 4 d after surgery.

DISCUSSION

Meckel's diverticulum is the most common congenital anomaly in the gastrointestinal tract[1] and is often incidentally discovered during evaluations performed for other reasons, as it is usually an asymptomatic condition. However, complications can occur in up to 6.4% of patients[7]. These are more frequent in the pediatric population and mainly involve bowel obstruction with or without intussusception, gastrointestinal hemorrhage, diverticulitis and inflammation, and Littre hernia (hernia involving the

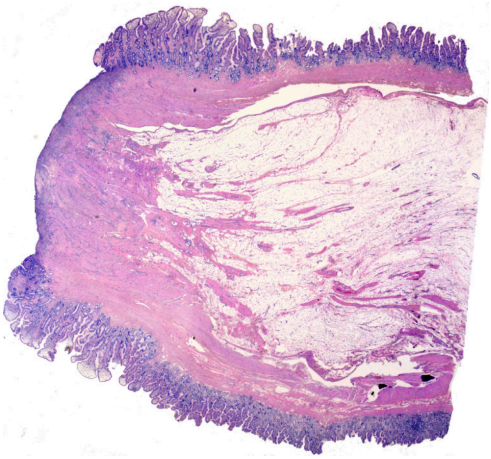

Figure 3 Low power histologic examination of a polypoid lesion lined by an intestinal type mucosa with a central ulcerated area. No gastric or pancreatic heterotopic tissue can be found.

bowel segment bearing Meckel's)[4,7].

Inverted Meckel's diverticulum is an unusual condition that is not yet clearly understood and there are no more than 100 cases reported in literature.

It has been proposed that the mechanism that could produce the inversion is an abnormal peristaltic movement around an ulceration or ectopic tissue. Nevertheless, no ectopic tissue was found in 41% of patients with inverted Meckel's diverticulum[6]. In this regard, tc-99m pertechnetate scintigraphy can help detect ectopic gastric mucosa and has been used for years as a diagnostic method for Meckel's diverticulum, especially in children, with a sensitivity of 92.1% and a specificity of 95.4%[8]. In adults, the sensitivity of this method is significantly less (54%)[9]. No cases of diagnosis of inverted Meckel's diverticulum by scintigraphy have been described, while there is only 1 case with gastric and pancreatic mucosa in the histopathological sample where the scintigraphy was negative[10]. Our patient's scintigraphy was negative. Therefore, this suggests that a negative scan does not preclude the presence of ectopic mucosa and the diagnosis of possible inverted Meckel's diverticulum.

This inversion of the Meckel's diverticulum can lead to a complete intussusception of the bowel or compromise blood flow to that bowel, ulceration and then gastrointestinal bleeding. The bleeding can also be explained by repetitive mechanical trauma to the mucosa from the reversible intussusception.

As in our patient, anemia or gastrointestinal bleeding are the most frequent clinical manifestations, found in up to 80% of patients[6]. This usually leads to an upper and lower gastrointestinal endoscopy, where the cause of the bleeding cannot be found.

Other clinical manifestations which can occur are abdominal pain (68%) and intussusception (39%). The median age of presentation is 27.7 years, younger than that reported for Meckel's diverticulum, which has been 33, with a male to female ratio of approximately 2.33:1[6].

Regarding the diagnostic tools, abdominal ultrasonography can contribute to the diagnosis, but often shows nonspecific findings such as thickened intestinal wall, fluid fille target or distended loops of bowel[11,12]. In our case, abdominal ultrasonography revealed no pathological findings.

One of the most useful tools is a CT scan. It usually shows a thickened small intestinal wall, with an elongated, intraluminal, fat-attenuating lesion[13], as in our case. In the case of intussusceptions, a CT scan is especially useful as it can reveal the characteristic "target sign". Inverted Meckel's diverticulum is sometimes confused with a lipoma on CT scans because it also consists of macroscopic fatty tissue. However, in most cases, abdominal CT scans provide useful information for the diagnosis and treatment of inverted Meckel's diverticulum[6].

Capsule endoscopy has recently been considered a useful diagnostic tool for diagnosing Meckel's diverticulum[9,14,15]. However, the role of capsule endoscopy in the identification of Meckel's diverticulum is not yet clear, with only a few case reports and case series available. Furthermore, in the case of inverted Meckel's diverticulum, the information is very limited, represented by only 2 case reports[16,17]. The capsule findings compatible with inverted Meckel's diverticulum were described as an elevated lesion with normal mucosa[16] or as pedunculated polyp[17].

In our case, the capsule endoscopy images were similar (a subepithelial protruding lesion in the ileum with the presence of blood, hematin, ulcer or erosion) and offered us a clue to subsequently confirm the diagnosis of inverted Meckel's diverticulum. In addition, the clinical suspicion due to the clinical characteristics (such as the fact that the patient was a young man with anemia) and a negative endoscopic study was of great importance for the diagnosis of inverted Meckel's diverticulum.

Regarding the risk of possible intestinal obstruction of the endoscopic capsule due to Meckel's diverticulum, no events have been described.

Surgery is the treatment of choice for symptomatic Meckel's diverticulum. The general consensus is that it should be treated with resection. In the case of asymptomatic Meckel's diverticulum, there is some debate. Resection is generally recommended for patients younger than 40-years-old, with diverticulum longer than 2 cm, diverticula with narrow necks, fibrous bands, and/or ectopic gastric tissue, and/or when the diverticulum appears thickened and inflamed[4,6,18].

It is important to note that in cases of anemia without abdominal pain, like that of our patient, it may take a long time for the patient to be diagnosed with inverted Meckel's diverticulum, given that it is an unusual condition with a nonspecific clinical presentation. Capsule endoscopy is usually performed in those patients with anemia with a normal upper and lower gastrointestinal endoscopy. However, if clinicians are unaware of the characteristics of this lesion, it may go undetected since it is an uncommon disease. Therefore, this report aims to contribute more information concerning the clinical characteristics, radiological findings and especially, the capsule endoscopy findings of inverted Meckel's diverticulum that can help clinicians suspect that this disease is present and enable them to establish a definitive diagnosis.

CONCLUSION

To date, inverted Meckel's diverticulum is a pathology that is still not completely well known, with few cases described in the literature. Its clinical presentation is not specific, its most frequent symptoms being anemia or lower gastrointestinal bleeding. Patients are often given an upper and lower gastrointestinal endoscopy which reveals no abnormalities and a subsequent capsule endoscopy. Therefore, increased awareness of the disease and a greater understanding of the features of this lesion in capsule endoscopy findings could ultimately help clinicians make the correct diagnosis.

REFERENCES

1 **Sagar J**, Kumar V, Shah DK. Meckel's diverticulum: a systematic review. *J R Soc Med* 2006; **99**: 501-505 [PMID: 17021300 DOI: 10.1258/jrsm.99.10.501]

2 **Karadeniz Cakmak G**, Emre AU, Tascilar O, Bektaş S, Uçan BH, Irkorucu O, Karakaya K, Ustundag Y, Comert M. Lipoma within inverted Meckel's diverticulum as a cause of recurrent partial intestinal obstruction and hemorrhage: a case report and review of literature. *World J Gastroenterol* 2007; **13**: 1141-1143 [PMID: 17373755 DOI: 10.3748/wjg.v13.i7.1141]

3 **WEINSTEIN EC**, CAIN JC, REMINE WH. Meckel's diverticulum: 55 years of clinical and surgical experience. *JAMA* 1962; **182**: 251-253 [PMID: 13999637 DOI: 10.1001/jama.1962.03050420027007]

4 **Park JJ**, Wolff BG, Tollefson MK, Walsh EE, Larson DR. Meckel diverticulum: the Mayo Clinic experience with 1476 patients (1950-2002). *Ann Surg* 2005; **241**: 529-533 [PMID: 15729078 DOI: 10.1097/01.sla.0000154270.14308.5f]

5 **Cullen JJ**, Kelly KA, Moir CR, Hodge DO, Zinsmeister AR, Melton LJ 3rd. Surgical management of Meckel's diverticulum. An epidemiologic, population-based study. *Ann Surg* 1994; **220**: 564-8; discussion 568 [PMID: 7944666 DOI: 10.1097/00000658-199410000-00014]

6 **Rashid OM**, Ku JK, Nagahashi M, Yamada A, Takabe K. Inverted Meckel's diverticulum as a cause of occult lower gastrointestinal hemorrhage. *World J Gastroenterol* 2012; **18**: 6155-6159 [PMID: 23155346 DOI: 10.3748/wjg.v18.i42.6155]

7 **Hansen CC**, Søreide K. Systematic review of epidemiology, presentation, and management of Meckel's diverticulum in the 21st century. *Medicine (Baltimore)* 2018; **97**: e12154 [PMID: 30170459 DOI: 10.1097/MD.0000000000012154]

8 **Hosseinnezhad T**, Shariati F, Treglia G, Kakhki VR, Sadri K, Kianifar HR, Sadeghi R. 99mTc-Pertechnetate imaging for detection of ectopic gastric mucosa: a systematic review and meta-analysis of the pertinent literature. *Acta Gastroenterol Belg* 2014; **77**: 318-327 [PMID: 25509203]

9 **Krstic SN**, Martinov JB, Sokic-Milutinovic AD, Milosavljevic TN, Krstic MN. Capsule endoscopy is useful diagnostic tool for diagnosing Meckel's diverticulum. *Eur J Gastroenterol Hepatol* 2016; **28**: 702-707 [PMID: 26854797 DOI: 10.1097/MEG.0000000000000603]

10 **Dujardin M**, de Beeck BO, Osteaux M. Inverted Meckel's diverticulum as a leading point for

ileoileal intussusception in an adult: case report. *Abdom Imaging* 2002; **27**: 563-565 [PMID: 12172999 DOI: 10.1007/s00261-001-0070-3]

11 **El-Dhuwaib Y**, O'Shea S, Ammori BJ. Laparoscopic reduction of an ileoileal intussusception and resection of an inverted Meckel's diverticulum in an adult. *Surg Endosc* 2003; **17**: 1157 [PMID: 12728389 DOI: 10.1007/s00464-002-4284-4]

12 **Karahasanoglu T**, Memisoglu K, Korman U, Tunckale A, Curgunlu A, Karter Y. Adult intussusception due to inverted Meckel's diverticulum: laparoscopic approach. *Surg Laparosc Endosc Percutan Tech* 2003; **13**: 39-41 [PMID: 12598757 DOI: 10.1097/00129689-200302000-00009]

13 **Takagaki K**, Osawa S, Ito T, Iwaizumi M, Hamaya Y, Tsukui H, Furuta T, Wada H, Baba S, Sugimoto K. Inverted Meckel's diverticulum preoperatively diagnosed using double-balloon enteroscopy. *World J Gastroenterol* 2016; **22**: 4416-4420 [PMID: 27158212 DOI: 10.3748/wjg.v22.i17.4416]

14 **Wu J**, Huang Z, Wang Y, Tang Z, Lai L, Xue A, Huang Y. Clinical features of capsule endoscopy in 825 children: A single-center, retrospective cohort study. *Medicine (Baltimore)* 2020; **99**: e22864 [PMID: 33120825 DOI: 10.1097/MD.0000000000022864]

15 **Lin L**, Liu K, Liu H, Wu J, Zhang Y. Capsule endoscopy as a diagnostic test for Meckel's diverticulum. *Scand J Gastroenterol* 2019; **54**: 122-127 [PMID: 30638099 DOI: 10.1080/00365521.2018.1553353]

16 **Ibuka T**, Araki H, Sugiyama T, Takada J, Kubota M, Shirakami Y, Shiraki M, Shimizu M, Suzui N, Miyazaki T. [A case of an elderly patient with inverted Meckel's diverticulum with small intestinal bleeding detected using capsule and double-balloon endoscopies]. *Nihon Shokakibyo Gakkai Zasshi* 2017; **114**: 2005-2011 [PMID: 29109349 DOI: 10.11405/nisshoshi.114.2005]

17 **Payeras Capó MA**, Ambrona Zafra D, Garrido Durán C. Inverted Meckel's diverticulum in an adult patient diagnosed *via* capsule endoscopy. *Rev Esp Enferm Dig* 2018; **110**: 210-211 [PMID: 29368940 DOI: 10.17235/reed.2018.5347/2017]

18 **Lequet J**, Menahem B, Alves A, Fohlen A, Mulliri A. Meckel's diverticulum in the adult. *J Visc Surg* 2017; **154**: 253-259 [PMID: 28698005 DOI: 10.1016/j.jviscsurg.2017.06.006]

Published by **Baishideng Publishing Group Inc**
7041 Koll Center Parkway, Suite 160, Pleasanton, CA 94566, USA
Telephone: +1-925-3991568
E-mail: bpgoffice@wjgnet.com
Help Desk: https://www.f6publishing.com/helpdesk
https://www.wjgnet.com